



Brunel
University
London

μ ECM process investigation and sustainability assessment

A thesis submitted for the degree of
Doctor of Philosophy

By

Mina Mortazavi Nasiri

College of Engineering, Design and Physical Sciences
Department of Mechanical and Aerospace Engineering
London Brunel University

Abstract

Micro electro chemical machining (μ ECM) as an alternative machining process gains more attraction in micro and nano industries and gradually finds its place among other non-conventional manufacturing methods. μ ECM same as ECM aimed at electrically conductive materials; μ ECM process is based on anodic dissolution of the materials at atomic level.

Current progress in μ ECM has presented valuable improvement in the process control and monitoring, shaping accuracy, simplifying the tool design and the process stability. This makes the μ ECM an outstanding alternative technology to produce accurate and complex 3-dimensional micro components. However, there is still a gap in application of μ ECM at research level and industrial level; development and commercialisation of the μ ECM require huge industrial investment which still needs justification to be attractive for investors.

Despite worldwide attempts to investigate and demonstrate the μ ECM process in full details and develop the μ ECM technology for the industrial applications, there is still a need for further investigation and research due to the complex and multidisciplinary nature of this process. Currently, this process is very much dependent on operator experience and trial and error approach. The lack of trained knowledgeable operators in addition to the lack of a comprehensive database (combination of materials, electrolytes and machining parameters) have increased the time and the cost of the commercialised development of this technology.

A comprehensive analytical literature review highlighted three areas of knowledge gap which can be further investigated and developed.

One of the main challenges in current state of this technology is initial set up for machining parameters. Current records show that the initial parameters have been set up using trial and error approach or simulation data; and there is still ongoing effort to find a better solution to set up the initial parameters.

The electrode-electrolyte interface was recognised as one of the main effective parameters on μ ECM machining performance. The complex nature of the reaction which

happens at this interface, in addition to the electrode-electrolyte structure need further investigation and analysis in order to improve the μ ECM machining performance.

Finally, the ever increasing demand to optimise all manufacturing processes and products, has increased the need to assess the sustainability of the machining process including new developed technologies; but there is very little information available in the area of micro and nano machining sustainability assessment including μ ECM.

Therefore, in this research it has been tried to address these three knowledge gaps and to suggest new methodologies to overcome them using a new practice consisting of laboratory experiments, mathematical analysis and simulation to investigate the initial machining parameters' values, explore the electrode-electrolyte interface structure for stainless steel workpiece and tungsten and nickel tool electrodes. Also, to introduce a series of indicators and measures to assess the sustainability of the μ ECM process to justify its initial high cost in comparison with any other machining process.

Laboratory experiments carried out using potentiostat (iviumstat) and mathematical analysis and simulation took place using Matlab and Simulink; and a few experiments carried out using in house built μ ECM machine to examine the obtained results through the laboratory and simulation works.

The results suggested that combination of 6.5 to 7.5 volts, electrolyte concentration between 0.4 and 0.7 mole/L and inter-electrode gap between 22 and 27 μ m generates optimum process results.

Additionally, electrode-electrolyte interface structure is a useful parameter to set up the pulse on time.

Finally, introduced sustainability assessment indicators and measures provides the opportunity to assess the μ ECM process for further optimisation.

As a result, μ ECM is a valuable process and in claim for current manufacturing industries especially in micro and nano products which demand higher accuracy and quality, better production life cycle and lower cost. So, it is very worthy to invest for further development to bring this technology to the industrial level.

Keywords- Micro electrochemical machining (μ ECM); Electric double layer (EDL); Inter-electrode gap (IEG); Sustainability assessment; Sustainable μ ECM

“If you be aware of a truth,
If ye possess a jewel, of which others are deprived,
Share it with them in a language of utmost kindness and good-will.”
Baha’u’llah

Acknowledgment

I would like to express my gratitude and appreciation to those who kindly and willingly helped me throughout this journey and supported me to achieve the aim of this journey.

I would like to thank my supervisor, Dr. Atanas Ivanov for his guidance, encouragement and patience during all up and downs I was facing to make this project a success. Also, I would like to thank my research advisor Dr. Nadarajah Manivannan (Mani), Prof David Harrison and other academic members of the university who helped me to achieve valuable experiences alongside my research project.

I would like to express my sincere gratitude and love to my family and loved ones for their ongoing support, encouragement and never-ended love; without their support, I would not be able to do what I have achieved so far.

Finally, I would like to thank all technicians and technical support team and also Faraday motion controls who always supported me especially when I was facing any obstacles.

This work is dedicated to my parents.

TABLE OF CONTENTS

LIST OF FIGURES	X
LIST OF TABLES	XVII
LIST OF ABBREVIATIONS	XIX
CHAPTER 1 INTRODUCTION.....	1
1.1 μ ECM history	1
1.1.1 Examples of μ ECM applications	2
1.2 Justification, Aims and Objectives	4
1.2.1 Justification	4
1.2.2 Aims and objectives	5
1.3 Methodology	6
1.4 Description of chapters.....	7
CHAPTER 2 LITERATURE REVIEW.....	9
2.1 Introduction	9
2.1.1 Electro Discharge Machining:.....	10
2.1.2 Chemical Machining (CM):	11
2.1.3 ECM:.....	12
2.2 Introduction to ECM and μ ECM.....	13
2.2.1 μ ECM process fundamental.....	16
2.3 μ ECM process investigation	20
2.3.1 IEG	23
2.3.2 Tool feed rate	25

2.3.3	Power (pulse) supply unit.....	26
2.3.4	Electrolyte	29
2.3.5	Micro tool.....	32
2.3.6	Workpiece	34
2.3.7	Mechanical features.....	35
2.3.8	Electric Double Layer (EDL).....	36
2.4	Initial machining parameters setup.....	36
2.4.1	Interrelation between predominant machining parameters	38
2.5	Modelling and simulation.....	40
2.5.1	Mathematical and numerical simulation	41
2.5.2	COMSOL simulation	45
2.6	Sustainability assessment	46
2.6.1	μ ECM process sustainability assessment: current state	47
2.7	Summary and conclusion	50
 CHAPTER 3 ELECTROCHEMICAL INVESTIGATION AND		
MATHEMATICAL ANALYSIS..... 55		
3.1	Introduction to electrochemical cell	56
3.1.1	Electrode-electrolyte interface	63
3.2	Electrochemical impedance spectroscopy (EIS).....	71
3.2.1	EIS and μ ECM	74
3.2.2	Experimental consideration.....	76
3.2.3	Design of Experiment.....	77

3.3	Machinability evaluation for stainless steel 304	85
3.3.1	NaNO ₃ electrolyte (0.3 mole/L), variable voltage, variable gap size.....	88
3.3.2	NaNO ₃ electrolyte (0.5 mole/L), variable voltage, variable gap size.....	98
3.3.3	NaNO ₃ electrolyte (1.0 mole/L), variable voltage, variable gap size.....	107
3.4	Response surface methodology using MATLAB toolbox	115
3.4.1	Voltage & gap parameters, MRR & overcut (OC) criteria	117
3.4.2	Voltage & electrolyte concentration parameters, MRR & OC criteria.....	119
3.4.3	Gap size & electrolyte concentration parameters, MRR & OC criteria.....	121
3.5	Tungsten tool electrode assessment	124
3.6	Conclusion.....	126
CHAPTER 4 EDL EQUIVALENT RC CIRCUIT AND SIMULATION.....		128
4.1	Equivalent circuit for μ ECM electrode-electrolyte interface	129
4.1.1	Equivalent circuit electrode-electrolyte interface – Tungsten tool electrode	130
4.1.2	Equivalent circuit electrode-electrolyte interface – Nickel tool electrode..	144
4.2	Impedance experiment tool assessment	148
4.2.1	Tungsten tool electrode assessment (impedance experiment)	148
4.2.2	Nickel tool electrode assessment (impedance experiment).....	149
4.3	Matlab Simulation.....	151
4.3.1	μ ECM electrode-electrolyte interface model (0.5 mole/L electrolyte concentration) - Tungsten tool electrode	152

4.3.2	μ ECM electrode-electrolyte interface model (0.6 mole/L electrolyte concentration) - Tungsten tool electrode	161
4.3.3	μ ECM electrode-electrolyte interface model (0.5 & 0.6 mole/L electrolyte concentration) - Nickel tool electrode	164
4.4	Performance assessment based on Impedance results (Tungsten tool electrode) and initial parameters.....	168
4.5	μ ECM machine	172
4.5.1	In house- built μ ECM machine	172
4.5.2	Micro-hole machining using Tungsten tool electrode.....	174
4.5.3	Micro-hole machining using Nickel tool electrode.....	176
4.6	Conclusion.....	177
CHAPTER 5 SUSTAINABLE μECM PROCESS, INDICATORS AND ASSESSMENT		181
5.1	Introduction	182
5.2	Dimensions of the sustainability	183
5.3	Sustainability indicators	186
5.3.1	Energy consumption.....	189
5.3.2	Waste management	191
5.3.3	Environment impact	193
5.3.4	Health and safety	195
5.3.5	Cost management	196
5.4	Discussion	199

5.5 Conclusion.....	204
CHAPTER 6 CONCLUSIONS AND FUTURE WORKS	206
6.1 Conclusion:.....	206
6.2 Key contribution and publications	207
6.3 Recommendation for the future work	209
APPENDIX A	211
APPENDIX B	212
APPENDIX C	215
APPENDIX D	216
APPENDIX E	217
APPENDIX F	220
APPENDIX G	223
REFERENCES.....	224

LIST OF FIGURES

Figure 1-1: SEM image of micro ECM 3D sharpened needle (Left), SEM image of sterile medical needle (Right).....	3
Figure 2-1: EDM process demonstration (Qin, 2015)	11
Figure 2-2: Chemical machining process demonstration (Cakir, 2007).....	12
Figure 2-3: Schematic Diagram of ECM process (Bai, 2019).....	12
Figure 2-4: μ ECM sub methods (Bhattacharyya, 2015).....	16
Figure 2-5: General μ ECM set up.....	18
Figure 2-6: Some of effective factors in the μ ECM machining	19
Figure 2-7 Taper schematic	22
Figure 2-8: Distribution of 25 publications between different non-traditional machining methods.....	49
Figure 2-9: Comparison between ECM, PECM, μ ECM in terms of IEG and resolution	51
Figure 3-1: Current-Voltage curve for ideally polarised electrode, A and B present departure from ideal behaviour.....	57
Figure 3-2: Electrolyte resistance and double layer capacitance model	58
Figure 3-3: Schematic equivalent circuit	61
Figure 3-4: Schematic of Randles model.....	62
Figure 3-5: EDL schematic diagram A) Helmholtz B) Gouy-Chapman C) Stern model.	66
Figure 3-6: EDL equivalent electrical model in μ ECM (Bhattacharyya, 2015).....	67
Figure 3-7: EDL equivalent electrical model in μ ECM presenting tool longitudinal surface (Bhattacharyya, 2015).....	68

Figure 3-8: Pseudo-linearity for very small section of the curve.....	76
Figure 3-9: Experiment setup diagram	78
Figure 3-10: Analysis and assessment diagram	79
Figure 3-11: Iviumstat device, Faraday cage, standard cable.....	80
Figure 3-12: Tool- workpiece cell	81
Figure 3-13: JCM-6000Plus Versatile Benchtop SEM.....	81
Figure 3-14: EDS spectrum of stainless steel – AISI 304 (Fe/Cr18/Ni10).....	82
Figure 3-15: Workpiece surface image using SEM.....	83
Figure 3-16: EDS spectrum of tool electrode- Tungsten (9.95% purity)	84
Figure 3-17: Tool surface image using SEM.....	84
Figure 3-18 Transient mode (left) – Linearsweep mode (right)	87
Figure 3-19: Polarisation graph & related SEM image (5V, 20, 25, 30 μm)	91
Figure 3-20: Polarisation graph for 0.3 mole/L NaNO_3 , 5 volts and 40 μm gap.....	92
Figure 3-21: Polarisation graph & related SEM image (6 V, 20, 25, 30 μm)	92
Figure 3-22: Polarisation graph & related SEM image (6 V, 40 μm)	93
Figure 3-23: Polarisation graph & related SEM image (7 V, 20, 25, 30 μm)	93
Figure 3-24: Polarisation graph & related SEM image (7 V, 40 μm)	94
Figure 3-25: Polarisation graph & related SEM image (8V, 20, 25, 30 μm)	94
Figure 3-26: Polarisation graph & related SEM image (8 V, 40 μm)	95
Figure 3-27: Polarisation graph & related SEM image (9V, 20, 25, 30 μm)	96
Figure 3-28: Polarisation graph & related SEM image (9 V, 40 μm)	96
Figure 3-29: MRR (0.3 mole/L NaNO_3).....	97

Figure 3-30: Overcut (0.3 mole/L NaNO ₃)	98
Figure 3-31: Polarisation graph & related SEM image (5V, 20, 25 & 30 μm)	101
Figure 3-32: Polarisation graph (5V, 40 μm)	101
Figure 3-33: Polarisation graph & related SEM image (6V, 20, 25, 30 μm)	102
Figure 3-34: Polarisation graph & related SEM image (6V, 40 μm)	102
Figure 3-35: Polarisation graph & related SEM image (7V, 20, 25, 30 μm)	103
Figure 3-36: Polarisation graph & related SEM image (7V, 40 μm)	103
Figure 3-37: Polarisation graph & related SEM image (8volts)	104
Figure 3-38: Polarisation graph & related SEM images (9 volts)	105
Figure 3-39: MRR (0.5 mole/L NaNO ₃ electrolyte)	106
Figure 3-40: Overcut (0.5 mole/L NaNO ₃ electrolyte)	106
Figure 3-41: Polarisation graph & related SEM image (5 volts)	109
Figure 3-42: Polarisation graph & related SEM image (6 volts)	110
Figure 3-43: Polarisation graph & related SEM image (7 volts)	111
Figure 3-44: Polarisation graph & related SEM image (8 volts)	112
Figure 3-45: Polarisation graph & related SEM image (9 volts)	113
Figure 3-46: MRR (1.0 mole/L NaNO ₃ electrolyte)	114
Figure 3-47: Overcut (1.0 mole/L NaNO ₃ electrolyte)	114
Figure 3-48: Curve fit for Voltage & Gap parameters and MRR	118
Figure 3-49: Curve fit for Voltage & Gap parameters and OC	118
Figure 3-50: Curve fit for Voltage & electrolyte concentration parameters and MRR ..	120
Figure 3-51: Curve fit for Voltage & electrolyte concentration parameters and OC	121

Figure 3-52: Curve fit for gap & electrolyte concentration parameters and MRR.....	122
Figure 3-53: Curve fit for gap & electrolyte concentration parameters and OC	123
Figure 3-54: Used Tungsten tool surface SEM image.....	125
Figure 3-55: Used Tungsten EDS spectrum	125
Figure 4-1: Voltage and current signals' phase shift	130
Figure 4-2: Impedance mode on ivium stat (left) & selection of frequencies (right)	131
Figure 4-3: Bode plot for a two time constant cell, a) Impedance vs Frequency, b) Phase angle vs Frequency	133
Figure 4-4: Frequency response from Impedance method on iviumstat.....	135
Figure 4-5: Impedance results- frequency response at 251 KHz.....	135
Figure 4-6: Impedance results- frequency response at 500 KHz.....	136
Figure 4-7: Impedance results: Kramers Kronig test.....	136
Figure 4-8: Impedance result: Equivalent circuit fit and components values.....	137
Figure 4-9: Frequency response from Impedance method on iviumstat (0.6 mole/L) ...	139
Figure 4-10: Impedance results- frequency response at 99.1 KHz.....	140
Figure 4-11: Impedance results- frequency response 998.2 KHz.....	140
Figure 4-12: Kramers Kronig test (0.6 mole/L, 7.5 volts, 26 μ m).....	141
Figure 4-13: Impedance result: Equivalent circuit fit and components values.....	141
Figure 4-14: Impedance experiment marks on workpiece (Nickel tool electrode, 0.5 mole/L electrolyte concentration).....	145
Figure 4-15: Impedance experiment marks on workpiece (Nickel tool electrode, 0.6 mole/L electrolyte concentration).....	147

Figure 4-16: Tungsten tool surface SEM image at the end of the impedance experiment	
.....	148
Figure 4-17: Tungsten tool surface EDS spectrum at the end of the impedance experiment	
.....	149
Figure 4-18- SEM image Nickel tool electrode before impedance experiments.....	150
Figure 4-19: EDS spectrum- Nickel tool electrode before impedance experiments	150
Figure 4-20: SEM image - Nickel tool electrode after impedance experiments.....	151
Figure 4-21: EDS spectrum- Nickel tool electrode after impedance experiments	151
Figure 4-22: Matlab constant RC model.....	154
Figure 4-23: Voltage signal across EDL capacitor (Anode side)	157
Figure 4-24: Current signals through charge transfer resistor and EDL capacitor	158
Figure 4-25: Current signals through electrolyte resistor	159
Figure 4-26: Current signal: charge transfer (Left), electrolyte (Right)	160
Figure 4-27: Flat faradic current timing (duty cycle = 50%).....	160
Figure 4-28: Flat faradic current timing (duty cycle = 75%).....	161
Figure 4-29: Frequency response for equivalent circuit (7.5 V, 0.5 mole/L, 25 μ m gap)- from 1KHz.....	166
Figure 4-30: Frequency response for equivalent RC circuit (7.5 V, 0.5 mole/L, 25 μ m gap)- up to 1MHz	166
Figure 4-31: Current signals for pulse on time= 1.92 μ s (Red: R-CT current, Yellow: C- DL current & pink: R-EL current signals).....	168

Figure 4-32: Voltage – MR & OC graph for 0.5 mole/L electrolyte concentration & Tungsten tool electrode	169
Figure 4-33: Voltage- MR & OC graph for 0.6 mole/L electrolyte concentration & Tungsten tool electrode	169
Figure 4-34: Voltage – MR & OC graph for 0.5 mole/L electrolyte concentration & Nickel tool electrode.....	171
Figure 4-35: Voltage – MR & OC graph for 0.6 mole/L electrolyte concentration & Nickel tool electrode.....	171
Figure 4-36: 3D view of the assembled machine (more details- Appendix G)	173
Figure 4-37: Developed μ ECM machine with initial power supply unit	173
Figure 4-38: Micro hole on stainless steel (1.01 mm thickness), Tungsten tool electrode, OCP=1A	175
Figure 4-39: Micro hole on stainless steel (3.1 mm thickness), Tungsten tool electrode, OCP= 3A	175
Figure 4-40: Micro hole on stainless steel (1.01 mm thickness), Nickel tool electrode, OCP= 3A	176
Figure 4-41: Micro hole on stainless steel (3.1 mm thickness), Nickel tool electrode, OCP= 3A	177
Figure 5-1: Sustainable manufacturing: System, process and production	182
Figure 5-2: Elements of machining process sustainability	184
Figure 5-3: Basic model for μ ECM process to identify indicators and metrics	188

Figure 5-4: Brief presentation of μ ECM sustainability indicators and their dependency	198
Figure 5-5: μ ECM sustainability assessment flowchart	203

LIST OF TABLES

Table 2-1 ECM & μ ECM parameters and features summary (Li and Niu, 2008)	15
Table 2-2: Most used electrolyte for a range of metals	31
Table 2-3: Interrelation between machining parameters and machining performance criteria (Left), Resources for the information (Right) (Full details- Appendix A)...	39
Table 3-1: Predominant parameters' range in iviumstat experiment.....	86
Table 3-2: Experimental data for 0.3 mole/L NaNO_3	89
Table 3-3: Measured and calculated values (0.3 mole/L).....	90
Table 3-4: Experimental data for 0.5 mole/L NaNO_3	99
Table 3-5: Measured and calculated values (0.5 mole/L).....	100
Table 3-6: Experimental data for 1.0 mole/L NaNO_3	107
Table 3-7: Measured and calculated values (1.0 mole/L).....	108
Table 3-8: Input data for Matlab curve fitting toolbox	116
Table 3-9: Table of fits - Voltage & Gap parameters, MRR & overcut (OC) criteria....	117
Table 3-10: Table of fits - Voltage & electrolyte concentration parameters, MRR & OC criteria.....	119
Table 3-11: Table of fits - gap & electrolyte concentration parameters, MRR & OC criteria.....	122
Table 3-12: Optimum values for voltage, electrolyte concentration and IEG size.....	124
Table 4-1: Optimum values for voltage, electrolyte concentration and IEG size.....	129

Table 4-2: Equivalent circuit components values (0.5 mole/L).....	134
Table 4-3: Equivalent circuit components values (0.6 mole/L).....	138
Table 4-4: Conductivity and removed material measurement during impedance experiment	143
Table 4-5 Equivalent circuit values (Nickel tool electrode, 0.5 mole/L electrolyte concentration)	144
Table 4-6: Equivalent circuit values (Nickel tool electrode, 0.6 mole/L electrolyte concentration)	146
Table 4-7: Equivalent circuit's components' value for Matlab model	153
Table 4-8 Time constant and capacitor charging percentage.....	156
Table 4-9: Applied pulse time, measured currents and voltages details.....	157
Table 4-10: Max faradic current period as %pulse on time.....	159
Table 4-11: Equivalent circuit's components' values (0.6 mole/L)	162
Table 4-12: Applied pulse time, measured currents and voltages	163
Table 4-13: Max faradic current period as pulse on time%- Tungsten tool electrode....	164
Table 4-14: Equivalent RC component's values for impedance test (7.5 V, 0.5 mole/L, 25 μm gap)	165
Table 4-15: Max faradic current period as pulse on time%- Nickel tool electrode	167
Table 5-1: Effective factors in energy consumption indicator.....	190
Table 5-2: Health and Safety indicators in μECM operation	196
Table 5-3: μECM sustainability metrics and indicators	200

LIST of ABBREVIATIONS

μECM	Micro Electro-Chemical Machining
μPECM	Micro Precise Electro-Chemical Machining
τ	Time constant
ASMC	American Small Manufacturing Coalition
C	Capacitor
CE	Counter Electrode
CF	Correction Factor
CM	Chemical Machining
C O₂	Carbon Dioxide
CR	Chrome
DL	Double Layer
EBM	Electron Beam Machining
ECM	Electro-Chemical Machining
ECMM	Electro-Chemical Micromachining
EDL	Electrical Double Layer
EDM	Electro Discharge Machining
EDS (EDX)	Energy-Dispersive X-ray Spectroscopy
EDWM	Electro Discharge Wire Machining
EI	Environmental Impact
EIS	Electrochemical Impedance Spectroscopy
EMM	Electrochemical Micro Machining
Fe	Iron

GDP	Gross Domestic Product
GND	Ground
GRI	Global Reporting Initiative
IEG	Inter Electrode Gap
InSb	Indium Antimonide
IPE	Ideal Polarised Electrode
K-K	Kramers-Kronig
M	Molar concentration
MEMS	Micro Electro-Mechanical Systems
MRR	Material Removal Rate
MLQ	Minimum Quantity Lubrication
MQCL	Minimum Quantity Cooling Lubrication
NaCl	Sodium Chloride
NaClO₃	Sodium Chlorate
NaNO₃	Sodium Nitrate
NaOH	Sodium Hydroxide
NCM	Non-Conventional Machining
Ni	Nickel
NIST	National Institute of Standards and Technology
OC	Overcut
OCP	Over Current Protector
OECD	Organisation for Economic Co-operation and Development
PECM	Precise Electro-Chemical Machining
PECMM	Pulsed Electro-Chemical Micro Machining

R	Resistor
RE	Reference Electrode
RM	Removed Material
RSM	Response Surface Methodology
SE	Sense Electrode
SEM	Scanning Electron Microscopy
SiC	Silicon Carbide
Si₃N₄	Silicon Nitrate
Ti	Titanium
WE	Working Electrode
WC-Co	Tungsten Carbide with Cobalt binder

CHAPTER 1

Introduction

μ ECM is a non-conventional machining (NCM) process which is based on anodic dissolution of materials at atomic level and it is suitable for conductive materials. μ ECM has based on similar foundation as ECM but it is a younger technology and it has been used for micro and nano dimensions products and recently has attracted more attention at the academic and industrial research and development levels.

This process is referred to as ECM and PECM (Precise Electro-Chemical Machining), PECEM (Pulse Electro-Chemical Machining) at macro level and is referred as μ ECM, μ PECEM (Micro Pulse Electro-Chemical Machining), EMM (Electrochemical Micro Machining) and PECEMM (Pulse Electro-Chemical Micro Machining) at micro and nano levels.

In this research the term of μ ECM will be used for micro electrochemical machining at micro level and the term of ECM will be used for electrochemical machining at macro level.

1.1 μ ECM history

Michael Faraday made great discoveries in the field of electrochemistry and his early metallurgical research from 1818 to 1824 has been regarded as the origin of the electrochemical machining. He discovered the principles of anodic metal dissolution and his laws of electrochemistry have created a solid foundation for the electrochemical processes.

Early in 20th century, Russian chemists, Shpitalsky used electrolytic polishing method in 1911 which was in a way the origin of the ECM. Later, in 1928, Russian engineer, Gusev patent was recorded as the actual origin of the ECM as he was the first who machined metal using anodic dissolution (Kumar, 2016).

In 1941, the first ECM publication presented to the electrochemical society on ECM and later in 1950s the most significant development happened. This point can be considered as the starting point of the commercial development of the ECM technologies

by companies. During 60s and 70s, ECM technology was growing steadily and the leading companies in development of this technology were mainly active in the aerospace and tool manufacturing industries (Kumar, 2016).

The development of EDM (Electro Discharge Machining) and its speedy growth at the same period overtook the ECM technology due to the simplicity of the process control in EDM. But EDM technology was not allowed in aerospace production because of the recast layer which can cause unexpected fatigue effect on the parts. ECM continued to be viable process because did not create recast layer and there is no wear of the electrode, but mostly found its place in research and development institutes due to the complexity of the technological process.

Between 1980s and 2000, the pulsed ECM was introduced, and ECM made significant progress towards commercialisation. The demand for machining hard and newly developed materials was sharply increasing between 1998 and 2011 including production of micro-parts from non-silicon materials. At that time appeared microsecond pulse ECM with great potential to machine micro parts from any electrically conductive materials over conventional machining processes including μ ECM. In short time numerous applications were found to be possible only if μ ECM is used and its undoubtable advantages over conventional machining found to be the solution and began to find ever-increasing applications.

Since then, μ ECM technique has been constantly developed further and has showed an astonishing progress. Newly increased demand in micro and nano manufacturing has opened new horizon for μ ECM to be developed and expanded at industrial level (Bhattacharyya, 2004; Ghoshal and Bhattacharyya, 2013). μ ECM process capabilities now open new horizon for designing micro parts to the level of nanoscale accuracy.

1.1.1 Examples of μ ECM applications

ECM has been successfully used in cutting, deburring, drilling industries and shaping workpiece; it has been applied in many industrial applications including turbine blades, engine castings, bearing cages, gears, dies and molds and surgical implants

(Rajurkar, 2013). The success of the ECM process has motivated the researchers and technology developers to adjust and apply the process in micro and nano production.

μ ECM has been successfully tested for different industrial applications including but not limited to the following examples (Ivanov and Mortazavi, 2016):

- Drilling holes in the fuel injector nozzles: The requirement is to drill a complex shaped hole in 18NiCr6 alloy. The shape of the hole is like inverted funnel to improve the fuel burning and efficiency. Currently, the holes are drilled using micro EDM to drill a straight hole and abrasive flow machining to round the edges of the inlet of the hole. Using μ ECM in this application can avoid abrasive flow machining; also applying a variable pulse on-time can create the hole with the shape of the funnel.

- Drilling cooling holes for turbine blades: At present, the cooling holes are drilled using micro EDM process which creates 20 to 40 micrometres defective layer; by replacing micro EDM with μ ECM, the defective layer was disappeared and a smooth transition between the central hole of the blade and each individual cooling hole was achieved.

- 3D sharpening of medical needles: Medical needles are made of extruded stainless-steel tubing. Currently, needles are sharpened using grinding process which increases the temperature of the contact point up to 600 degree Celsius. The direct effect of this extreme heat is the burning of the materials and bending the tip of the needle. Using μ ECM process has improved the surface roughness to Ra10 nm and decreased the machining time to 10 s per needle.

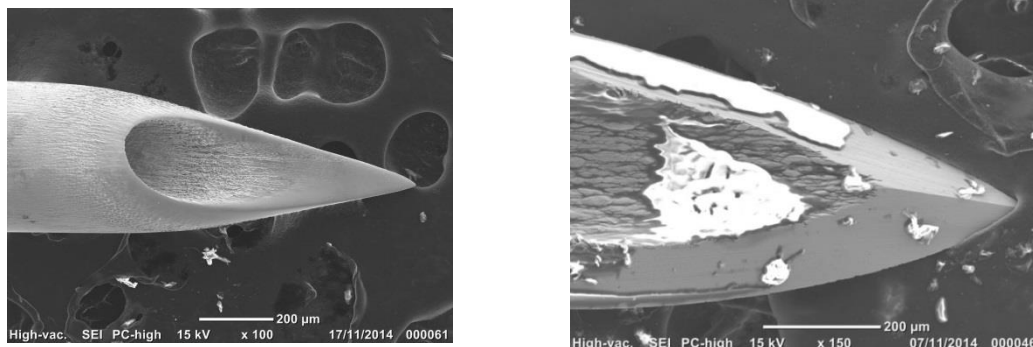


Figure 1-1: SEM image of micro ECM 3D sharpened needle (Left), SEM image of sterile medical needle (Right)

Although μ ECM has made a valuable progress in recent years, there is still need for further development and operation optimisation. This work has tried to investigate the current state of the μ ECM technology and offer an academic research to step forward towards further development of this process.

1.2 Justification, Aims and Objectives

There is an increasing demand for precise micro manufacturing for micro and nano products with application in MEMS, biomedical devices, automotive industry and electronics technology which it is expected to lead the research towards increasing utilisation of non-conventional micro manufacturing technologies widely.

μ ECM process can be used as one of the main alternatives in precise micro manufacturing due to its valuable advantages but its complex nature, expensive structure and operator dependency have been serious obstacles for advancing it at commercial level. The main motivation for this research is the importance and necessity of developing this process and the role it can play as a sustainable manufacturing process.

1.2.1 Justification

Production strategies are being continuously developed through the technology advancement, demands and utilisations. Demand for miniaturised products with improved quality, higher accuracy and precise dimensions is ever increasing; on the other hand, competitive market, raw materials and energy costs in addition to the environment concerns have pressurised manufacturer to find sustainable approaches towards their production and manufacturing systems.

μ ECM technology seems to be a key contributor in micro manufacturing industry by improving the material removal rate, dimension accuracy, low debris and minimum tool wear and defects. But this process is a complex multidisciplinary process in which various sciences and technologies are involved.

The complex nature of the process and uncertainty of the process due to complex electrochemical phenomenon has created limitation in wide application of the process at industrial level.

Despite worldwide attempts to investigate and demonstrate μ ECM process in full details, there is still knowledge gaps in different areas of the process, and it needs further organised and multidisciplinary research to be developed to the next level.

Examples of these gaps which highlighted in this research are as follows:

- Currently, there is a lack of information in setting the initial machining parameters; most of the research present a trial and error approach to find the initial values for machining parameters. Machining parameters including initial gap, feed rate, voltage features, current protection level, electrolyte features are among the parameters which need to be initialised at the start of the process and to be monitored during the process.
- There are hardly any records of detailed investigation to explore the electrochemical reaction which happens at electrode-electrolyte interface.
- Additionally, no records are available to demonstrate any progress towards sustainability assessment of this process although sustainability evaluation is one of the major requirements for any manufacturing processes.

μ ECM process is very dependent on operator experience and the lack of trained acknowledged operators in addition to the lack of a comprehensive database (combination of materials, electrolytes and machining parameters) have increased the time and the cost of its commercialisation.

1.2.2 Aims and objectives

The aim of this research is to develop further investigation towards μ ECM machining process with respect to the complexity of electro-chemical reaction which takes place at the electrode-electrolyte interface. Also, the research goal is to justify the initial high cost of the development of the μ ECM structure and process and to promote its value as a sustainable non-conventional micro manufacturing method.

The objectives of this research are as follow:

- To establish an analytical review on previous and current researches in order to identify the areas which need further investigation and can have an influential impact on the future of this process.
- To gain a deeper knowledge and understanding of the process by investigating the electrochemical reaction which takes place at the electrode-electrolyte

interface with focus on electrical features and behaviour of the equivalent RC circuit considering predominant parameters including voltage amplitude, electrolyte concentration and inter electrode gap (IEG).

- To develop a laboratory experimental work and mathematical analysis to find the best possible combination for predominant machining parameters in order to achieve higher material removal rate, better surface and lower overcut.
- To develop a laboratory experimental work and simulation analysis to explore the behaviour of the electrode-electrolyte interface and investigate the relation between pulse on time and faradic current.
- To introduce a set of comprehensive and functional indicators and measures to develop a sustainability assessment methodology to evaluate the process sustainability with respect to the defined dimensions of sustainability.
- To validate the theoretical and simulation findings through the machining experiment.

1.3 Methodology

In order to achieve the aims and objectives of this research following steps have been designed and implemented:

- A comprehensive review of the previous and recent works in the area of ECM and μ ECM was conducted and summarised. μ ECM is relatively young research area and there are areas of the process which are not yet explored completely; but ECM and μ ECM are based on similar fundamentals in terms of the core science of the process, hence to fill the lack of the knowledge and study gap at some special areas of the μ ECM process, ECM was reviewed as the background of the research.
- The μ ECM process was investigated in terms of the machining parameters, interrelation between parameters and the cause and effects of the parameters on the machining performance. As a result, available data in literature was gathered as a table (presented in chapter two) and predominant parameters were identified (including voltage level, electrolyte concentration and inter electrode gap).

- By identifying the critical parameters and important performance criteria, laboratory experiments were designed using iviumstat to investigate the behaviour of the electrochemical cell (tool electrode-electrolyte-workpiece interfaces). Based on the acquired information, a mathematical model was designed using Matlab to find the optimum values for the combination of the predominant machining parameters.
- The resulted optimum parameters were fed into the iviumstat impedance methodology in order to estimate a suggestive RC network for the electrode-electrolyte interface (electric double layer investigation as key factor to the machining performance).
- The suggested equivalent circuit was assessed using Matlab Simulink to evaluate pulse signal features to achieve higher level of the faradic current which is the fundamental part of the current signal to activate and complete the machining process.
- Finally, based on the theoretical, simulation and experimental knowledge which attained through this research and above activities, a sustainability assessment chart and relevant measures and indicators were introduced to create a reliable approach for sustainability evaluation of the process and to provide the opportunity to compare the sustainability of this process with similar machining processes when necessary.

1.4 Description of chapters

This section describes the structure of this thesis and the contents of different chapters. The thesis structure consists of research, laboratory trials, simulations and experiments.

Chapter 2- literature review: provides an analytical review of the history of electrochemical machining and its progress towards μ ECM. General foundation of the process and key areas of the process are discussed in detail with a glance on previous works in order to establish a framework to include all effective and predominant parameters that affect the μ ECM process performance and remark the problematic areas which need further investigation.

Chapter 3- Electrochemical investigation and mathematical analysis: this chapter presents the importance and necessity of deep understanding of the electrode-electrolyte interface to achieve successful μ ECM machining. It starts with introduction to the electrochemical cell features and highlights the critical role of the electric double layer in machining performance. Then a laboratory experimental work is presented using iviumstat to establish an experimental database for predominant machining parameters and their effects on machining performance using the rate of removed materials and extend of the overcut. Finally, by applying mathematical approach using Matlab curve fitting toolbox, a narrower range for the predominant parameters' values will be achieved.

Chapter 4- EDL equivalent RC circuit and simulation: this chapter presents a laboratory experimental approach using iviumstat impedance spectroscopy technique to find the EDL equivalent RC model. Then, the RC model is analysed using Matlab Simulink for further investigation and demonstration of the electrical features of the electrode-electrolyte interface and to find the relation between these features and minimum pulse on-time to increase the faradic current during the machining process. Also, a few examples of machining experiments using in-house built μ ECM machine is presented.

Chapter 5- Sustainable μ ECM process, indicators and assessment: this chapter demonstrates an innovative way to increase the awareness and confidence on using μ ECM process. Complexity of the μ ECM process together with uncertain machining performance have increased the initial cost of the investment for this technology; this chapter introduces a set of applicable indicators and measures to assess the sustainability of the process in order to promote and justify the high preliminary cost of the process and ease the progress of the μ ECM process to the industrial level. Additionally, the introduced assessment chart has been designed in a way to provide the opportunity to optimise the process.

Chapter 6- Conclusions and future works: this chapter is to summarise this research and its achievements alongside the recommendations for the future work.

CHAPTER 2

Literature Review

Chapter summary

μ ECM as an alternative machining process is gaining more attraction in micro and nano manufacturing industries. It has been the centre of the research and development activities at research institutes for a while, but it is still to gain a full recognition at industrial level.

This chapter will review the history of the electrochemical machining and its progress to the μ ECM. General fundamental of the process will be introduced, and different aspects of the process will be discussed in detail, previous published data will be briefly reviewed, examples of modelling and simulation works will be mentioned and the process sustainability assessment will be discussed. μ ECM is a complex process that involves a multidisciplinary approach towards its investigation and process analysis. There are various parameters effective to the performance of the machining process which need to be investigated individually and in relation with another. The aim of this chapter is to demonstrate an analytical review on previous researches and to highlight the knowledge gaps and the areas which need further investigation. The content of this chapter is organised in a way to create the required background for the chapters 3, 4 and 5 which demonstrate machining parameters assessment, mathematical analysis, simulation and process sustainability assessment.

2.1 Introduction

The word “machining” usually demonstrates a type of process, which removes materials from workpiece by means of mechanical energy. The foundation of traditional machining methods is based on contact between the tool and the workpiece and as a result of applied shear, the material is removed from the workpiece.

However, machining process is not limited to the conventional processes; there are different methods that are known as non-conventional machining (NCM) or non-

traditional machining in which there is no direct contact between the tool and the workpiece. In addition, there is no sign of shear as the main methodology of the process. Currently, non-traditional machining methods are used when traditional methods fail to deliver and are not applicable.

In general, the aim of the NCM is to offer efficient and cost-effective solutions to manufacture materials that are traditionally difficult to machine using state-of-the-art technologies including spark erosion and laser science. NCMs are usually used when traditional methods, technically and economically, fail. A few examples of application of NCMs are as follows:

- Machining of tough or very thin materials
- Machining of very complex shapes
- Where high surface finish and accuracy is required
- Where low cutting forces or clamping forces are required

One of the vital aims of this research is to demonstrate that NCM methods can be successfully engaged as a main option and not just as an alternative to the conventional methods.

ECM is one of the promising non-conventional machining methods for the future of manufacturing which has recently received more consideration in comparison with electro discharge machining (EDM) and electric discharge wire machining (EDWM). The following section is a brief introduction to a couple of NCM methods:

2.1.1 Electro Discharge Machining:

Electro-discharge machining is based on melting and vaporisation of materials on both electrodes. In the EDM two electrodes (the tool and the workpiece) are separated by a dielectric fluid. When the tool moves close enough to the workpiece and the voltage is sufficiently high, the dielectric fluid breaks down and electrical current conducts between them, which results in an electrical discharge or spark and it produces high temperature at a localised zone on the workpiece. The melting and vaporisation processes would affect the surface of both electrodes as melted materials suddenly erupt due to the implosion. The material removal would usually happen in form of the ball-shaped particles (Qin, 2015).

In EDM process, the main functionality depends on dielectric fluid; it isolates the electrodes, decreases the surface temperature and the remaining particles are removed by flushing dielectric.

Different control technologies have been applied for the EDM machining based on the application and its requirements. Most recent approaches and strategies are based on a fuzzy logic and adaptive control optimisation (Spieser and Ivanov, 2015).

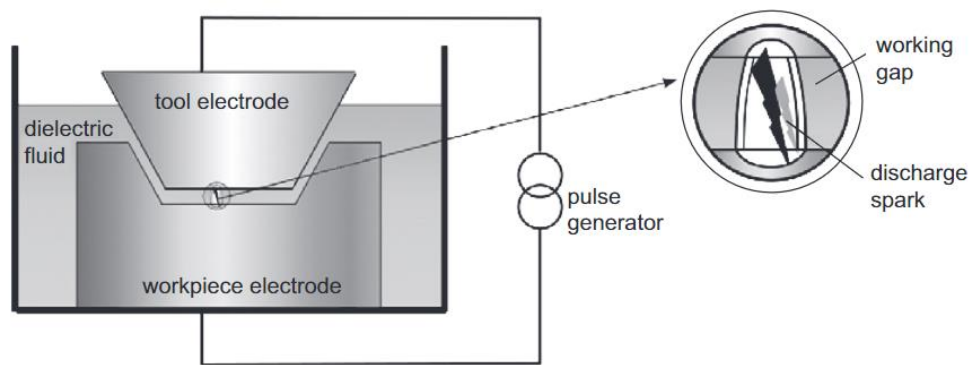


Figure 2-1: EDM process demonstration (Qin, 2015)

Figure 2-1 shows the EDM process diagram. EDM is a suitable method for micro manufacturing as it is a force-free process (extremely low machining force) since its material removal mechanism is thermal. EDM is a valuable machining technique and its main advantages are being almost force free mechanism, having high precise control and offering better surface finish and accuracy.

2.1.2 Chemical Machining (CM):

Chemical machining is a well-known non-traditional machining process in which the workpiece material is machined under controlled chemical dissolution through the contact with a strong acidic or alkaline chemical substance. The workpiece area which should not be machined is protected by special coating called maskants. This machining method has been broadly used to produce micro components for different industrial

applications such as microelectromechanical systems (MEMS) and semiconductor industries. Effective CM requires very close control of process parameters like composition of solution, temperature and mass transfer. Figure 2-2 shows the general CM process schematic; one of the challenges in CM technology is the environmental impact due to hazardous liquids.

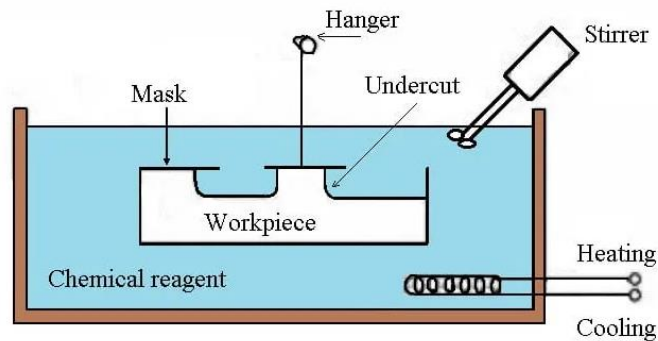


Figure 2-2: Chemical machining process demonstration (Cakir, 2007)

2.1.3 ECM:

ECM consists of oxidation-reduction or complex type reactions as CM does; however, the reaction in ECM is based on electrochemical features rather than chemical features. The Capability of machining different materials including high strength and hard to machine materials, simpler machining set up and no tool wear has made the ECM more interesting for manufacturing industries. Figure 2-3 shows a general schematic diagram for ECM.

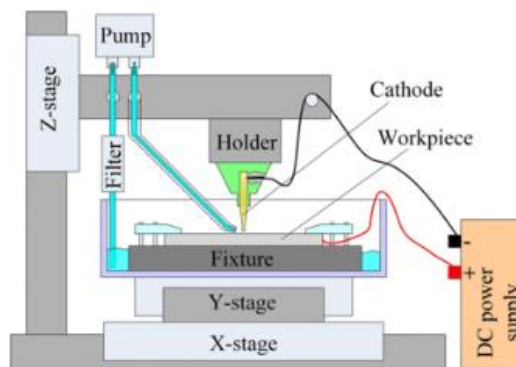


Figure 2-3: Schematic Diagram of ECM process (Bai, 2019)

However, there are a few disadvantages which should be taken into the account including: difficulty to create sharp corners and dependency on operator experience and knowledge.

In the last 20 years, manufacturing has faced significant changes and demand for better results in product life-cycle quality, energy consumption and environmental impact; in other words, manufacturing processes need to be sustainable.

This research focuses on μ ECM, however, as this is a young research field, the literature review starts with ECM and will progress to the μ ECM.

2.2 Introduction to ECM and μ ECM

The ECM method was invented in 1929 by Gusev (Ma, 2010) who developed anodic metal machining. However, electrochemical theory behind the machining principle was first presented by Faraday in the 19th century. He introduced the electrolysis law, which is the fundamental principle of dissolution and electrodeposition techniques. Another significant development was recorded in the 1950s in which Anocut Company of Chicago recognised anodic metal machining method as a suitable technique for commercial purposes. Finally, in the 1980s, a wider application for ECM was introduced.

Electrochemical processes include cathodic and anodic processes; cathodic processes are such as electrodeposition, electroforming and electroplating while anodic process includes electro-etching, μ ECM and electro polishing. Most of these methods are suitable for 2-dimensional structures but μ ECM is capable of machining 3-dimensional complex structures.

ECM is established on electrochemical dissolution of the workpiece (anode) using a desired shaped tool (cathode) based on Faraday laws of electrolysis which has been known as a controlled anodic dissolution at the atomic level. A continuous flow of electrolyte through the Inter Electrode Gap (IEG- the gap between two electrodes) is necessary to dissipate removed materials from the tool and prevent it from being deposited on the cathode. ECM creates a mirror image of the tool shape on the workpiece. ECM has been used in different manufacturing industries including cutting, deburring, drilling and shaping (Lee, 2002).

The main elements of ECM process are:

- Electrolyte, which is an electrically conductive solution and should be non-corrosive fluidic in relation to the electrodes with low viscosity and high heat resistivity and is preferred to be non-toxic
- Electrolyte creates the current passage between electrodes and removes insoluble products and produced heat due to the operation.
- The tool is a conductive metal (material) which should be rigid enough to bear the electrolyte flow pressure. In addition, it should be machined easily and efficiently to create the required shape on tool surface.
- The Workpiece is also a conductive metal which should be suitable for the application.
- The DC power supply plays an important role in the ECM accuracy and efficiency. DC power supply is used to generate a DC pulse wave as it increases the success of ECM significantly.
- A Control system to monitor and control the process in real-time.

The Advantages of ECM:

- The Capability of processing various materials
- Being free from burrs products
- Having no upper layer deformation, no thermal or physical strain in product (there is no contact between the tool and the workpiece)
- Having no (or minimum) tool wear and multiple use of the tool
- Being more efficient in creating complex geometries
- Having high dimensional accuracy and high surface quality
- Having high MRR (material removal rate)
- Being cost effective

Limitation:

- Environmental issue (possible harmful chemical products)
- Lack of capability to create sharp corners
- Requires research for different materials and products (it requires a wide range of database)

- The process' success depends on operator knowledge and experience. This is one of the major issues as setting the initial values for the machine setup are very often actioned based on time consuming trial and error method, therefore would be very much dependent on the operator knowledge and experience.

μ ECM follows the same approach as ECM; it is based on the same fundamental principles, but its structure is adapted for micro and nano scale products with the dimensions in the range of 5 to 500 μm . Table 2-1 compares the general setup and features between ECM and μ ECM (Li and Niu, 2008).

Machining Parameter /features	ECM	μ ECM
Voltage amplitude	10- 30V	<10V
Current density	20-200A/cm ²	75- 100 A/cm ²
Electrolyte flow rate	10-60 m/s	<3m/s
Electrolyte concentration	>20 g/l	<20 g/l
Inter electrode gap	100- 600 μm	5-50 μm
Machining rate	0.2-10 mm/min	5 $\mu\text{m}/\text{min}$
Side gap	>20 μm	<10 μm
Accuracy	0.1mm Ra	0.02-0.1mm Ra
Surface finish	Good, 0.1-1.5 μm	Excellent, 0.05-0.4 μm
Electrolyte temperature	24-65 °C	37-50 °C

Table 2-1 ECM & μ ECM parameters and features summary (Li and Niu, 2008)

μ ECM can be divided in two main categories including maskless and through mask approaches. Figure 2-4 shows this categorised classification. The main advantage of maskless approach is developing 3D micro-features. Developing 3D shapes are achievable by reducing the stray current effect, more effective gap control and using pulse power supply. The obvious feature is that the shape of the tool remains unchanged.

The newest approach is sinking and milling and has its own advantages over the layer by layer method; it has less machining time, smaller overcut, less risk for tool damage and less end deviation.

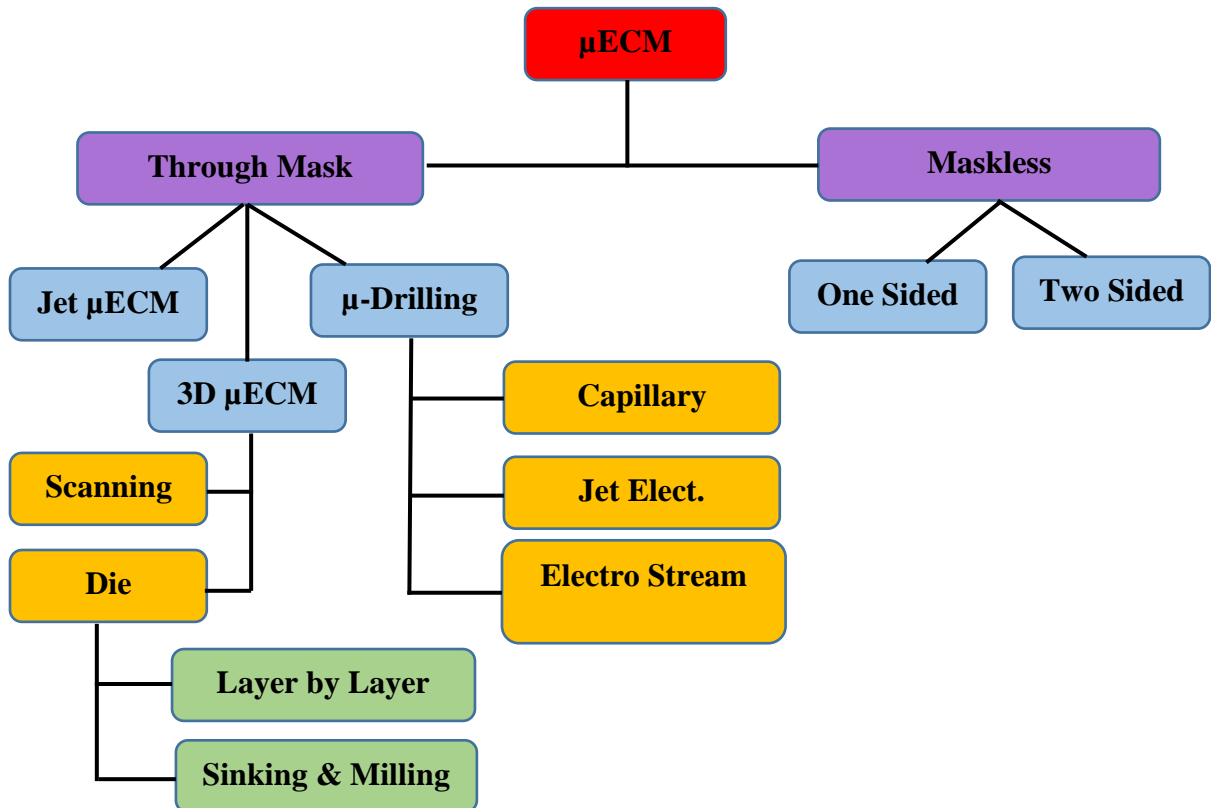


Figure 2-4: μ ECM sub methods (Bhattacharyya, 2015)

2.2.1 μ ECM process fundamental

μ ECM is a non-conventional machining process based on anodic dissolution of the workpiece in electrolysis process by applying a DC pulse voltage between the tool (cathode) and the workpiece (anode) electrodes in which material is removed from workpiece surface at the atomic levels (atom by atom). The aqua electrolyte flows through a very small gap between the tool electrode and the workpiece. Due to the presence of the electrolyte in IEG, the electric path between the supply voltage and the electrodes are closed and the current passage is formed between electrodes. The electric charges in the

current passage between the electrodes are transported by ions while electrons are responsible transporter outside this passage.

Due to the electrochemical reaction in the electrode-electrolyte interface, the metal removal takes place from anode (workpiece) and metal hydroxide and gas bubbles are generated in the small gap between the electrodes; this phenomenon follows Faraday's laws of electrolysis. The accumulation of removed materials in the gap area, can prevent further machining by blocking the current flow and creating sparks. Therefore, in order to continue the machining process, these by-products should be removed from the gap between electrodes by circulating a high velocity electrolyte through the IEG. Hence, as shown above, the IEG is playing a very critical role in μ ECM process success. The electrochemical reaction is the result of electrical and chemical changes caused by passage of the current and has been used in various technologies including μ ECM. The concept of the electrochemical reaction is very complicated and requires deep understanding of the chemical and physical properties of the electrodes and electrode-electrolyte interface. The movement of the electrons (in the electrode) and the movement of the ions (in the electrolyte) when conducting electrodes are placed in electrolyte create the passage of the current. Hence physical changes take place at the electrodes; a deep understanding of this phenomenon is the key for explanation of the μ ECM technology and the behaviour of the anodic dissolution in the machining process. The full investigation and discussion on anodic dissolution and its key effects on the μ ECM process will be demonstrated in chapter three. As mentioned, IEG plays a very important role in the μ ECM process success. The initial gap size increases as metal atoms are removed from the workpiece surface, which leads to an increase in the electrical resistance across the IEG and therefore reduces the current flow in the gap and consequently reduces the material removal rate. To maintain the same current flow and material removal rate, the size of the gap between the electrodes should be sustained at the same level during the machining process, which can happen by advancing the tool electrode towards the workpiece at the same rate as the material is dissolved. Due to the movement of the cathode towards the workpiece, gradually a shape is generated on the workpiece surface which is a duplication of the tool shape.

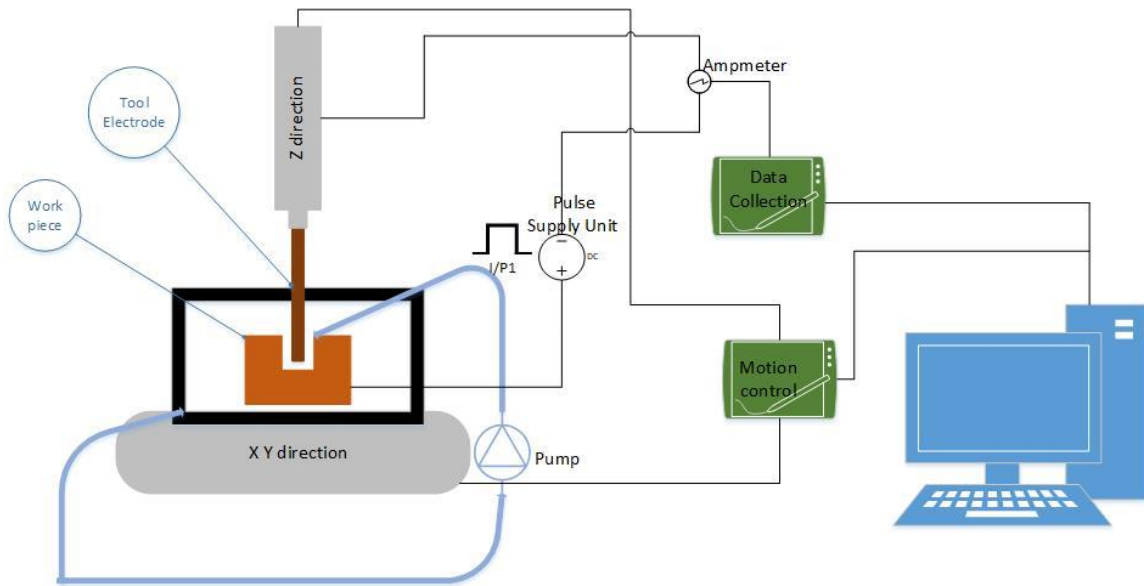


Figure 2-5: General μ ECM set up

Figure 2-5 presents a general set up for the μ ECM machine and its main blocks. The main blocks of the machine are the power supply unit, motion control unit, pump, and data collection and control unit.

Power supply unit provides DC pulses, motion control unit controls 3 dimensions movement, data collection unit collects data from different parts and stages of the machining in order to be used in control unit and finally the pump which provides fresh electrolyte for the process and flushes away the sludge and by-products.

The machining quality is very much dependent on localisation; localisation is the attempt to precisely remove the material from the workpiece surface. If the anodic reaction is limited to a few microns in the region between two electrodes, a high localised machining is achieved. Localisation is under the effect of various process parameters such as applied voltage, current density, electrolyte type and velocity, IEG and the tool feed rate. All these parameters can influence the machining features and final product quality, but the hardness of the material would not have any effect on μ ECM machining quality.

The material removal rate is a measure to investigate the success and sustainability of μ ECM machining and varies based on machining parameters. Any changes in the machining parameters can affect the MRR and generate new MR rates.

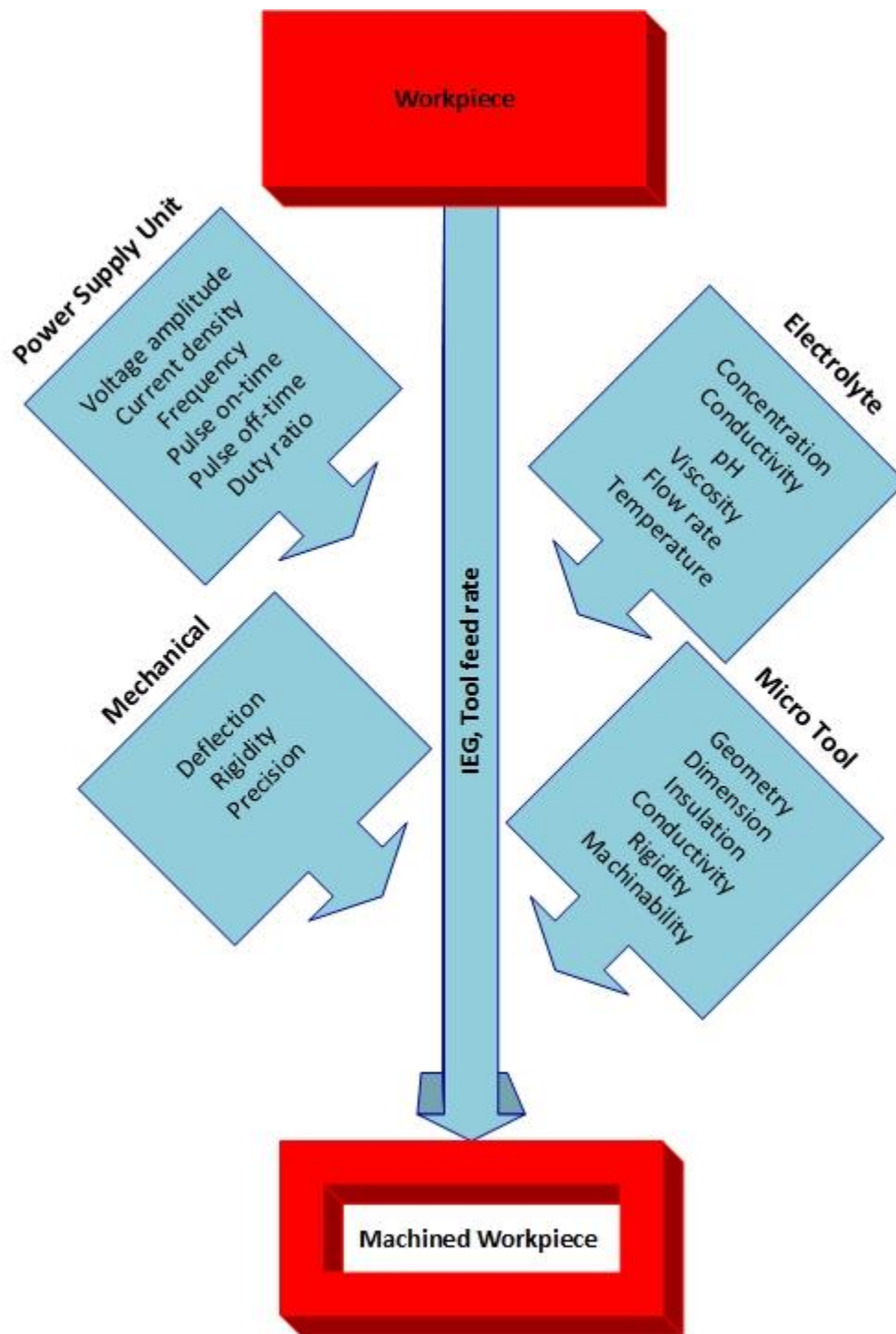


Figure 2-6: Some of effective factors in the μ ECM machining

Therefore, all effective parameters should be investigated independently as well as in relation to the other parameters.

In other words, μ ECM machining is a very complex process and a multidisciplinary phenomenon; it involves different sciences including chemistry, physics, electronics, fluidic dynamics, mechanics as well as interrelation between these sciences; so analysing this process requires a consideration of all forceful parameters and also the interrelation between them which would affect the machining process.

The chart in figure 2-6 has summarised some of these effective parameters in μ ECM operation; these parameters can affect the process both individually and in combination with other parameters. The investigation of the effects of these parameters is a challenge; most of the current researches had to consider at least a few constant parameters with no variances during the process.

In the remaining parts of this chapter, some of the research and published works will be investigated to present a general but comprehensive picture of the μ ECM process up to the current stage. Some of the works may have been mainly related to the ECM but the results are applicable in the μ ECM as well.

2.3 μ ECM process investigation

The fundamental mechanism in μ ECM is the removal of material based on electrolysis in which the material is removed from the workpiece surface in the form of metal ions; they may remain dissolved or may react with the electrolytic solution components, either way they will not be deposited on the cathode tool.

IEG plays a very important role in the workpiece material removal (machining) but as mentioned it is not the only factor. The understanding of the phenomena at IEG or at electrode-electrolyte interface is the key to a successful investigation of the μ ECM process. The complexity of this phenomenon and the lack of adequate understanding of the mass and energy transport processes of the multiphase electrolyte flow in IEG and complex electrochemical reactions on both electrodes make the investigation a very difficult task.

Placing an electrode in the electrolyte is usually leading to an equilibrium potential difference between the metal and the solution and therefore a specific interface regional between the electrode and the electrolyte is formed. At the interface of the solution and

the metal, a layer of ions is created (ions have equal and opposite charges to the cations in the solution). This interface can have a significant effect on electrochemical reaction due to its electrical properties.

The electrode with no charge transfer is known as ideal polarised electrode (IPE); in reality, there is no IPE for all range of potential, but the electrodes can behave as Ideal in some potential intervals.

When an electrode acts as IPE no charge would cross the interface but by applying a positive potential, potential difference will gradually increase due to the anodic metal ions transfer from metal into the solution and ions discharge from the solution which happens simultaneously; however, the generated current will rapidly deteriorate to zero if no active species exist at the surface. Consequently, ionic mobility generates an opposing charge layer on the solution surface. The behaviour of the interface can be analysed as a capacitor and it has been named as “Electrical Double Layer”. In fact, positive cations and negative electrons create the electrical double layer (EDL) that can be presented as a capacitor in an equivalent circuit. The EDL structure will be discussed in more details in chapter 3.

Knowing the above brief explanations and considering the chart in figure 2-6 can help to review the μ ECM process and investigate the effective parameters on the process through the literature review. The complexity of interrelation between effective parameters on machining accuracy and quality is undeniable; this dictates timely and costly research activities to carry on. In order to have a better explanation and introduction to the process effective parameters, introducing a few general descriptions and definition is necessary. In addition, the parameters will be categorised in two main groups: first group includes parameters which have primarily direct effects on other parameters and machining process performance; the second group are the parameters which have less known effects or indirect effects on other parameters. Group one parameters are known as predominant factors, such as pulse voltage, pulse on/off time and electrolyte concentration (Bhattacharyya and Munda, 2003; Kozak, 2004; Bhattacharyya, 2004). Mechanical attributes are examples of non-predominant (second group) factors.

In addition to the recognition and investigation of the effective process parameters, it is necessary to set up the features and characteristics to measure or evaluate the performance of the machining process. Material removal unit, machining speed,

machining accuracy and overcut (side gap) are examples of indicators, which can be used to evaluate the effect of the process parameters.

Although the concepts of these indicators are very clear, they may have been assessed in different ways in each work. To prevent any confusion, the details of how they have been used in this work are explained as follow:

Material removal unit: is the volume of the removed material per unit time (normalised).

Machining speed: is calculated by the ratio of travelled distance by micro tool during dissolution to the travelled time (pulse on-time)

Overcut (side gap): is calculated based on the average difference between the hole radius and the micro tool radius.

Taper: taper is described as the angle between the side gap and the tool at its face surface. The side gap at the tool entry level (workpiece surface) is larger than the side gap at the tool exit level (hole depth) due to the extra overcut which takes place at the entry level where the tool stays for a longer time and the current density is sharper. Taper is measured by the angle θ (figure 2-7) (Ghoshal and Bhattacharyya, 2013).

$$\tan \theta = \frac{\text{entry width } (w_1) - \text{exit width } (w_2)}{2 \cdot \text{hole depth } (h)} \quad (2-1)$$

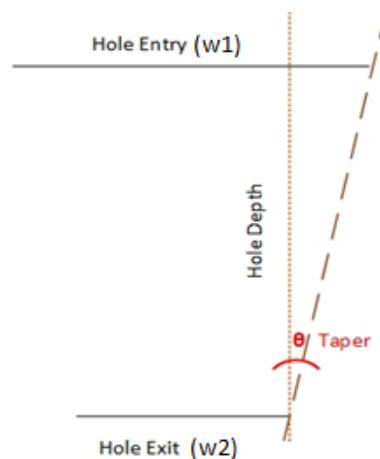


Figure 2-7 Taper schematic

Delocalisation: is described as material removal phenomenon beyond IEG area (desired machining zone). Delocalisation is the effect of spreading electrical field lines outside the machining zone which results in an undesired material removal action to take place.

The following subsections will focus on expanding the evaluation of the effective process parameters, interrelation between different machining parameters, brief review on the process modelling and simulation and finally a review on the process sustainability assessment. IEG as a critical condition in μ ECM operation is the first to be investigated through the literature review.

2.3.1 IEG

The investigation starts with the size of the gap between electrodes. IEG is the critical condition in μ ECM and should be maintained in a stable small size; it is important to keep the IEG as small as possible as it dictates the resolution of the machining. A smaller and stable IEG size will increase the shape accuracy and the surface finish quality.

IEG should be sustained between 5 and 50 μm ; in contrast with ECM, which the gap size could vary between 100 and 600 μm and more (Bhattacharyya, 2015). However, it is very difficult or impossible to measure the IEG directly.

It is a critical challenge to maintain and control the size of the gap between electrodes; in addition to the size of the gap, occurrence of other phenomena including electrochemical reactions at bulk electrolyte, generation of the gas bubbles at the tool electrode and the development of by-products influence the machining quality and accuracy. Any minor change in these factors or their causes can have enormous effects on the machining productivity. The direct and precise measurement of the IEG size has not been achieved yet, but researchers have worked on various investigations to monitor the effect of IEG size in the machining process and to demonstrate the appropriate control and optimisation methods to sustain a suitable gap between electrodes. This effort has resulted in a valuable information to identify any parameters that can affect the size of IEG during the machining process and their forms of effect.

A smaller IEG has been considered as an effective parameter in accuracy improvement, as it helps to have a better anodic dissolution. It accelerates the electrolyte-heating rate and will increase its temperature; the direct effect of the temperature rise is

the rise of the electrolyte conductivity (Skoczypiec, 2016). The final impact is the increased current density, which is supposed to improve localisation and machining process performance. This change is very dependent on the pulse features as an unrealistic pulse on time can neutralise all positive effects of a small gap size and even to worsen the machining outcomes.

Zhang et al (2008) experiment presented the effect of a decreased pulse voltage amplitude on IEG gap and a less efficient machining process.

IEG can be affected by different issues including but not limited to:

- Local deviation of the electrical conductivity in the IEG due to the formation of gas bubbles in the electrolyte.
- Difficulty in determining anodic over potential changes which affects the local anodic current efficiency.
- Nonhomogeneous distribution of the electric field in the IEG region
- The effect of occurrence of stray current lines

Maintaining a clean environment around IEG helps to reduce the effect of by-products and to focus the current flux towards workpiece (Reddy, 2013).

Gap size measurement: due to the transient and stochastic processes that occur in the gap, the need for online monitoring of the gap size is necessary. Researchers have followed different approaches in order to measure the gap size directly or indirectly, but further investigation is still needed. Bignon et al (1982) used the effect of eddy current technique to measure the gap size under specified frequencies, but this method could be problematic in μ ECM due to conductivity of electrolyte, micro tool size and composition of electrodes. Ultrasound is the other approach in measuring the gap size (Clifton, 2002). This method has gained popularity due to the development of ultrasonic technologies. Despite some achievement in IEG size measurement in the μ ECM process, there is still potential to improve the measurement.

In addition to the IEG size, distribution of the electric field in the gap is important to be investigated. As much as electric field distribution can be limited to the machining zone, the effect of the overcut can be eliminated, and the surface accuracy can improve.

2.3.2 Tool feed rate

Maintaining a small IEG is necessary to achieve accurate machining results in μ ECM. IEG is in close relation with the tool feed rate; the tool feed rate along the path of the tool electrode is defined as the speed of the tool electrode during the process. The micro tool feed rate should always be identical to the linear MRR to evade any short circuits or sparks during the machining. The aim of the μ ECM is to machine in the order of micrometres; hence, it requires the tool movement to be in micro orders and as low and precise as possible. If the tool feed rate is greater than the material removal rate, IEG decreases and after some time the tool will contact the workpiece, which creates micro sparks and will damage the delicate surface of the workpiece. On the other hand, if the feed rate is smaller than the material removal rate, then IEG increases and it would affect the machining accuracy. Therefore, it is important to maintain the tool feed rate in synchronisation with the material removal rate (known as equilibrium speed) to maintain the gap size. Nevertheless, as the IEG is continuously changing under the effect of different factors and material removal rate, the necessity of the development of a real-time monitoring system for the tool feed rate is confirmed. Therefore, one of the vital duties of the machine control unit is to monitor and control the movement of the tool and the workpiece position during the machining with very high resolution (0.09 μm /step was recorded (Zhang, 2011)).

An experimental investigation (Kozak, 2004) on the feed rate effect on the machining presented that the increased tool feed rate will reduce both side and longitude overcuts if the feed rate does not overtake the material removal rate. Also, a greater feed rate within the acceptable range generates sharper edges.

2.3.2.1 Material Removal Rate

The material removal rate is a measure to assess the general efficiency of the machining method; also, it is one of the indicators to evaluate the effect of the machining parameters, especially when it comes to the process optimisation. MRR in μ ECM depends on anodic reaction, current efficiency and mass transport effect as Chourasia et al (2014) mentioned in their work. In other words, and according to the Faraday's laws of

electrolysis, the volume of dissolved material is proportional to the machining current and the electrochemical equivalent of the material.

Zhang et al (2007) used the formula below to prove this dependency:

$$\mathbf{Removed\ materials\ (RM) = \omega i A t} \quad (2-2)$$

In which ω is the electrochemical equivalent, i is the machining current, A is the area and t is the real machining time.

Using Butler-Volmer equation as below

$$\mathbf{i = i_0 \exp\left(\frac{\beta n F}{R_g T_a} v\right)} \quad (2-3)$$

In which i_0 is the exchange current density, β is transfer coefficient, n is the number of electrons, F is the Faraday constant, R_g is the gas constant and T_a is the temperature.

By substituting the current in RM formula:

$$\mathbf{RM = \omega i_0 \exp\left(\frac{\beta n F}{R_g T_a} v\right) A t} \quad (2-4)$$

The concluded formula will present the amount of removed materials per unit time.

As the machining operation happens during the pulse on time, the time integration of this formula would assist to have volume of the removed materials per pulse period, (T is pulse period).

$$\mathbf{RM = \int_0^T \omega i A t dt = \omega A \int_0^T i_0 \exp\left(\frac{\beta n F}{R_g T_a} v\right) dt} \quad (2-5)$$

That shows that the major influential parameters (direct effect) on removed materials rate are over potential, pulse on time and EDL time constant (EDL capacitance, electrolyte resistance).

2.3.3 Power (pulse) supply unit

Designing a suitable pulse supply unit for μ ECM has been an important task since introducing this process. None of the commercially available pulse supply units have ever been qualified to fulfil the requirements of the μ ECM. Applied pulses are very crucial to the success of the process. The pulse amplitude should vary between 1 to 10 volts

(recommended: (Bhattacharyya and Munda, 2003)). Pulses should be capable of feeding currents up to 5 amperes and be able to generate high frequency pulses ranging from 1 KHz to 5MHz. The main weakness of on the shelf pulse supply units is the fact that they do not provide high DC currents in high frequency. Their current range covers up to 2 amperes, which is insufficient for μ ECM.

Voltage amplitude:

Voltage amplitude would influence other machining parameters including current density, IEG size and MRR. Voltage amplitude has an optimised level, same as any other machining parameters in μ ECM. Its rise can improve the machining rate and surface roughness but if it increases beyond the optimum level, it will increase the overcut. On the other hand, if it decreases to a very low level, it causes the formation of a passive layer which prevents the metal dissolution and the machining operation to take place.

If the pulse voltage amplitude increases, it can break down the gas bubbles which are leading to the generation of micro sparks. Micro-sparks influence the shape and surface accuracy of the products (Govindan, 2013).

Stray current:

The desired current flux density is expected to be in linear direction (Z-direction) along the electrode tool in IEG; its density should expand on the tool electrode surface to machine the workpiece surface only in the desired zone and it should almost be negligible in the outer area and in any other directions; but practically, it is not achievable, at least it has not been yet. In addition to the flow of the desired current between the tool electrode and the workpiece surface, there is a flow of current outside this machining zone known as stray current and the current due to the longitude effect of the tool; both of these currents create unwanted effects on machined surface. The longitude effect of the tool electrode can be eliminated by the side tool insulation, but stray current will remain.

Any changes in the voltage amplitude can change the current density; due to the voltage increase, localisation decreases, and stray current phenomenon increases remarkably. Because of the higher current density, the effect of the stray current increases and causes much lower localisation. This affects the accuracy of the machining by increasing the overcuts. This means that stray current removes materials from the outside machining zone, which creates a larger machined area and an inconsistent shape.

Therefore, overcut takes place and it increases more rapidly in higher voltage amplitude or longer pulse on time and shorter frequency.

Pulse time:

Duty cycle or duty ratio presents the ratio between pulse on time (T_{on}) and pulse period (pulse on time (T_{on}) + pulse off time (T_{off})).

$$\text{Duty Ratio} = \frac{T_{on}}{T_{on}+T_{off}} \quad (2-6)$$

If pulse on time increases, the average current density will increase and as a result MRR will increase. The rise of the MRR will continue up to a point at which the MRR does not increase any more as dissolution rate suddenly decreases. This reduction is due to an event which prevents any extra machining process to occur either as a result of a short pulse off-time which is not sufficient to remove all sludge and by-products from the gap, or due to formation of salty layer over machining zone or unbalance electrolyte resistance and conductivity leading to sparks and short circuits. Unbalance electrolyte conductivity resulted from longer pulse on time (pulse period) and subsequently is the result of increased generated Joule heat which cannot be removed efficiently. There is no evident of any exact optimum duty ratio because it changes based on other machining parameters. However, in some works it was suggested to maintain the duty ratio up to 35% (Mithu, 2014).

Researchers throughout the last two decades proved that short pulse voltages improve the μ ECM performance and machining outcomes (Reddy, 2013; Lee 2007; Rajurkar, 2006). Nevertheless, as it mentioned within other research works, it is very important to find the optimum pulse on time for the best machining performance (Kurita, 2006). Skoczypiec (2016) review paper, presented the successful application of ns pulse voltages in μ ECM at the lab level, however, the challenges are still preventing the application of μ ECM at industrial and commercial levels.

Short pulses will increase machining precision due to removing smaller amount of material per pulse while longer pulse on time will increase the gap due to the increase of removed materials if the tool feed rate could not follow the changes in the gap size and consequently, will decrease the machining precision.

In addition, researchers (Jo, 2009) experienced that increasing pulse on time beyond optimum level, will create a rough surface.

However, successful optimisation of pulse on time and pulse off time will improve MRR and product dimensional accuracy, respectively.

High frequency pulses would improve dimensional controllability, shaping accuracy and process stability; also, it will simplify the tool design procedure. (Zhang, 2011)

2.3.4 Electrolyte

Electrolyte, which is commonly a concentrated salt solution, completes the current path between tool electrode and workpiece; also, it facilitates the electrochemical reaction at IEG region. In addition to that, electrolyte is responsible to discharge any machining sludge, gas bubbles and the heat from IEG. There are various electrolytes solutions, which may be suitable for one or more electrode materials in the μ ECM. Electrolyte should be selected based on material features and machining requirements in order to facilitate the desired electrochemical reaction. Another important consideration in electrolyte selection is the electrolyte influence on the surface characteristics of the machined materials. The use of non-aqueous electrolyte or toxic electrolyte has been limited or eliminated due to their undesirable effect on environment. In general, electrolyte can be acidic, alkaline or neutral aqueous solutions. Acidic solutions are preferred as they do not create any insoluble by-products. There is another classification, which divides the electrolyte in two categories: passivating electrolyte and non-passivating electrolyte.

Passivating electrolytes such as NaNO_3 and NaClO_3 contain oxidising anions and provide better machining precision due to creation of oxide films and oxygen evolution in stray current region. Non-passivating electrolyte such as NaCl contains rather aggressive anions.

In case of machining passive electrodes and creation of passive oxide layer on the workpiece and exceeding its resistivity beyond the electrolyte resistance, process localisation will be eliminated. In order to overcome this issue, researchers (Sueptitz, 2013) suggested a few different solutions including:

- Using aggressive electrolyte
- Applying cathodic voltage pulse

- Using low conductivity electrolyte, which will increase electrolyte resistivity.

The characteristics of the electrolyte should be such that anions facilitate the dissolution of the workpiece without forming a film on its surface and the cations do not deposit on the tool. The most used anions are chlorides, sulphates, nitrates, and hydroxides.

Table 2-2 presents a few aqueous electrolytes, which have been used frequently for a range of metals. Electrolyte selection for μ ECM process requires good knowledge of electrode materials and electrolyte characteristics. Main electrolyte characteristics are as below:

Conductivity: electrolyte conductivity is recognised as one of the important parameters in the μ ECM (Lee, 2002). Conductivity is reciprocal of the electrolyte resistivity which can affect the flow of the current in IEG. Conductivity changes with temperature; reaction heat increases the electrolyte conductivity and subsequently decreases the electrolyte resistivity. Therefore, current density and stray current levels will increase which result in a poor quality of the final product surface due to occurrence of micro sparks and larger overcut.

PH: it stands for “power of hydrogen” and measures the total hydrogen ions concentration in aqua solution. Electrolyte pH should be chosen in a way to give good dissolution of the workpiece without attacking the tool electrode. Acidic electrolytes have been used more often as they do not generate insoluble reaction products.

Concentration:

By increasing the electrolyte concentration, the volume of ions causing machining operation in the desired machining area will increase. As a result, current density increases which simultaneously increases the stray current. The effect of stray current is unwanted removed material, which can increase the overcut. However, if the electrolyte concentration increases within an optimised level, MRR increases and machining speed improves. If the concentration rises beyond the optimum level, MRR takes over the tool feed rate; therefore, the flushing action does not comply with the accumulation of sludge, gases and metal hydroxide in the gap, which this boosts the sparks occurrences and causes shape inaccuracy.

Metal	Electrolyte	Features
Aluminium and its alloys	NaNO_3 (100-400 g dm ⁻³)	Excellent surface finishing
Cobalt and its alloys	NaClO_3 (100-600 g dm ⁻³)	Excellent dimensional control, excellent surface finishing
Molybdenum	NaOH (40-100 g dm ⁻³)	NaOH consumed and must be added continuously
Nickel and its alloys	NaNO_3 (100-400 g dm ⁻³)	good surface finishing
	NaClO_3 (100-600 g dm ⁻³)	good dimensional control, good surface finishing and low metal removal rate
Titanium and its alloys	NaCl (180 g dm ⁻³) + NaBr (60 g dm ⁻³) + NaF (2.5 g dm ⁻³)	good dimensional control, good surface finishing and good machining rate
	NaClO_3 (100-600 g dm ⁻³)	Bright surface finish, good machining rate above 24V
Tungsten	NaOH (40-100 g dm ⁻³)	NaOH consumed and must be added continuously
Steel and iron alloys	NaClO_3 (100-600 g dm ⁻³)	Excellent dimensional control, brilliant surface finish, high metal removal rate, fire hazards when dry
	NaClO_3 (100-400 g dm ⁻³)	Good dimensional control, lower fire hazard, good surface finish and good machining rate
	NaNO_3 (100-400 g dm ⁻³)	Good dimensional control, fire hazard when dry, low metal removal rates, rough surface finish

Table 2-2: Most used electrolyte for a range of metals

Inlet of electrolyte: in addition to all influential features and characteristics of the electrolyte on μ ECM-finished products, the position of the inlet of the electrolyte is critical as well and affects the anodic dissolution. The workpiece surface needs to be covered uniformly with electrolyte.

The position (distance and angle) of inlet of the electrolyte towards anode can improve the anodic dissolution if it distributes electrolyte uniformly on the workpiece surface or it can prevent the anodic dissolution if the distribution is heterogeneous. Although this is a very effective parameter, it has been mentioned and considered in a few publications (Kozak, 2004). Kim et al (2005) suggested that the height of electrolyte from workpiece surface should be maintained in a few micrometres to increase the current density.

Also, lower viscosity is preferred as it eases the flow of electrolyte in the narrow gap between two electrodes.

Sludge:

If the gap between electrodes is very small, the pulse off-time is not long enough and the electrolyte concentration is too high, reaction by-products may not be completely removed from the gap. The rise of contaminants in this area can create a deposition layer on the tool surface and therefore prevent uniform dissolution of the workpiece surface. Additionally, due to the electrolyte composition change (because of sludge) and temperature rise, electrolyte resistivity will increase. These changes in turn decrease the machining accuracy. Adding ionic species can improve the electrolyte environment by reducing the level of dissolved reaction by-products in the machining zone.

Also, generated gas bubbles increase at higher voltage and higher electrolyte concentration and it increases the chances of sparks and causes electrolyte flow interruption due to formation of cavitation (Bhattacharyya, 2005).

2.3.5 Micro tool

Micro tool design and manufacturing is a very critical task; the design of a micro tool is a time consuming and costly procedure which yet to fit in a systematic practice. Tool dimension, geometry, material, insulation and many other factors would deeply affect the success of the μ ECM machining operation. Also, depending on the machining method, micro tool features would vary and require different design and fabrication methodology.

Generally, micro tool electrode should be mechanically stiff and robust to withstand the vibration and electrolyte flow pressure, electrically conductive, corrosion resistant and thermally conductive. The most used materials are chosen between tungsten, platinum, titanium and super alloys; advantages of these materials are high melting point, low hydrogen over potential, chemically resistant and large anodic potential range (Bhattacharyya and Munda, 2003; Reddy, 2013). Other materials including nickel, copper and steel have had their applications too. (Mithu, 2012)

Tool insulation has been recognised as a very successful approach to minimise the stray current and overcut. By protecting the sidewall of the tool electrode, current only flows through the front face of the tool. Sidewall of the tools can be coated with chemically resistive materials such as silicon nitrate (Si_3N_4) or silicon carbide (SiC) by means of chemical vapour deposition while epoxy resin is known as unsuitable insulator (Bhattacharyya, 2004). Park et al (2006) used enamel as insulation coating in their research; the advantages of enamel are the short process time and creation of a very thin coating layer.

Dual pool tools are recommended as potential for increasing the machining accuracy. A dual tool electrode is an insulated negative charged tool, which is covered by positive charged insoluble metal bush. This cover will be helpful to reduce the overcut due to the stray current. (Bhattacharyya, 2004)

Tool vibration has been experienced as a method to improve the circulation of the electrolyte with the aim to reduce or eliminate the occurrence of micro sparks. Application of piezoelectric transducer is one of the successful examples (Munda and Bhattacharyya, 2008); also, they presented that the increase in tool vibration regardless any change in the duty ratio, can decrease the overcut.

Mithu (2012) evaluated the effect of the tool diameter and length on MRR and machining time. As observed, while tool diameter was increased, machining speed was increased and the ratio between entrance and exit of the drilled hole was decreased. As a result, the taper angle of the micro holes was reduced. Longer micro tools under the same machining parameters decreased the MRR and increased the machining time. In addition, it observed that the number of short circuits were increased by the length of the micro tool but overcut had inverse proportion with tool length. The complexity of tool electrode geometry is due to its direct effect on electrolyte resistance and EDL

capacitance. Any changes in electrolyte resistance and EDL capacitance would change the machining parameters specially pulse on time and amplitude.

Furthermore, their investigation (Mithu, 2014) presented that increased effective tool length (dipping length in the electrolyte) increases the machining time and subsequently decreases the machining rate.

Three main schemes of machining based on the tool profile and its movement have been reported; 1) still non-profile tool in combination with a mask placed on workpiece , 2) moving profiled tool electrode in one direction (usually z), 3) non-profiled tool electrode which follows a predesigned trajectory (numerically controlled path) along the workpiece surface. The third scheme has received more interest (Volgin, 2016) due to the advantageous simpler tool shape and tool fabrication, but the machine needs to have high resolution moving axis.

Liu et al (2017) suggested a novel retracted tip tool electrode design in which the tool tip is a few micrometres shorter than side insulators. Their design aimed on improving the machining accuracy by concentrating electrical field distribution in the IEG region. They also used a mathematical model and experiments to verify the effect of the main parameters on the machined micro-hole diameter using this novel tool. Although their findings were presented that this tool design can be a potential for industrial machining works, it is still early to see the results at industrial level.

One of the major progress in μ ECM is the successful machining of micro tools by reversing the power supply polarities. Micro tool manufacturing methodology has been expensive and challenging but by using μ ECM method, researchers successfully manufactured desired tools. μ ECM has been considered as a sustainable alternative process to manufacture micro tools (Mathew and Sundaram, 2012). This progress has been very useful towards cost and time saving. Examples of successful micro tool fabrication using μ ECM method are such as fabrication of tapered tungsten micro tool by Zhu et al (2006) and cylindrical tungsten microelectrode by (Fan, 2010)

2.3.6 Workpiece

In addition to the tool material features, workpiece material characteristics influence the machining performance, as well. Although, the μ ECM has been successfully examined on different materials and alloys, each group of materials or alloys would react

differently in terms of the final product. As an example, nickel-based, cobalt-based and stainless-steel alloys generate smoother machined surfaces while iron-based alloys present less smoothness in surface (Rajurkar, 2006).

μ ECM machining is based on anodic dissolution process that happens at atomic level. Therefore, workpiece with fine-grained structure is likely to create a better surface finish. Workpiece needs to be appropriately clamped and positioned in the machine chamber on a flat surface. It is always useful to have full material characteristics of the workpiece as it helps to predict its electrochemical reaction with the tool electrode and the electrolyte.

2.3.7 Mechanical features

The aim of μ ECM is to machine in a range of micrometres which requires high kinematic accuracy and rigidity. Resolution of axis movement is very crucial and needs extra precise control unit. Also, if the machining set up comprises a rotating or vibrating tool electrode, same consideration is applicable.

Rigidity and stiffness of the machining system is very crucial; the body of the μ ECM machine must be able to resist any vibration. Any vibration could end with tool electrode deformation and inaccurate machining. There is possibility that pump's motor and other motors used for the tool movement or workpiece movement create vibration. Therefore, it is important to minimise the effect of any unwanted vibration in the system; granite is a good choice to be used for the machine's stand as it can absorb generated vibration.

Workpiece holder or clamping device should be made of chemically and electrically resistive materials or insulators, but a conductive joint should be predicted to provide the connection between anode and pulse supply unit. Likewise, tool holder unit should be made of insulating or electrically and chemically resistive materials not to have corrosion. It is also important to minimise any undesired inductive features or resonance in the tool holder unit.

All electrical connectors and fixtures should be corrosion free to have longer working life and to avoid their frequent replacement.

Machining chamber or electrolyte bath needs to be made of chemically resistive and corrosion free materials.

Mechanical set up should be in the most optimum layout to minimise the length of the used cables between electrodes and the pulse supply unit. This will reduce the noise and inductive effects of the cables as well as power loss. Also, it needs to be considered that inductive noises can interfere with control signals if precautionary measures have not been taken.

Electrolyte inlet position and electrolyte flow rate should have flexibility; based on workpiece geometry it may require changing the angle and height of the electrolyte inlet to cover the workpiece surface uniformly. Also, tool electrode size may add limitation to the electrolyte flow rate in order to prevent the tool deformation.

2.3.8 Electric Double Layer (EDL)

By dipping an electrode in the electrolyte solution, a special interfacial region is formed between two surfaces, which its electrical features are very important and play significant role in the electrochemical reaction in this region. This region is known as electric double layer. Having two electrodes immersed in the electrolyte at μ ECM cell, two electrode- electrolyte interfaces are generated. The electrode-electrolyte interface (EDL) is the core of the electrochemical reaction and machining reaction. Therefore, the details of EDL structure in μ ECM will be discussed in detail in chapter 3 but as a brief introductory explanation, it should be mentioned that EDL behaviour could remarkably change the machining performance. EDL behaviour is unique for any metal-solution interface based on electrode material and electrolyte characteristics. Also, pulse features including pulse duty ratio, pulse on time and off time, voltage amplitude can affect its behaviour. In addition, machining zone which is equal to the tool surface area and IEG size affect the EDL behaviour.

2.4 Initial machining parameters setup

One of the challenges in μ ECM technology is the machining parameters setup due to complex interrelation between different parameters. Above review shows that there is an undeniable complex relation between machining parameters in the μ ECM process. Researchers have used different methodologies including mathematical models to obtain the best combination of the machining factors between a range of possible values for desired machining criteria.

Generally, among the machining criteria MRR, machining precision and overcut are the one which have been used frequently. The other important point is that the selection of the initial machining parameters (specially, predominant parameters) have been based on the theoretical evaluation or experimental results; it means that there is no specific guidelines in the selection of parameters range but using modelling results or experimental trial and error approach.

Munda et al (2007) aimed to improve performance of μ ECM machining through eliminating the micro-sparking and stray current effect. They established a comprehensive mathematical model for correlating machining parameters effective on micro sparks and material removal due to stray current using response surface methodology. They considerably managed to reduce micro spark and stray current affected zone under the achieved combination of machining parameters through their model validated by machining micro holes.

Following their research in 2007, Munda et al (2008) used similar mathematical model to investigate the correlation between predominant machining parameters and machining assessment criteria; Voltage, duty ratio, tool vibration, frequency and electrolyte concentration were considered as dominant parameters and MRR and overcut were investigated as machining criteria. Experimental activities were set up based on central composite half fraction second-order rotatable design and response surface methodology was used in order to investigate the result.

Asokan et al (2008), also developed a multi-objective optimisation model for ECM; they used a combination of four machining parameters and two machining assessment criteria and developed a multiple regression model and an artificial neural network method to find the optimised values for current, voltage, flow rate and the gap between electrodes. Their finding showed better results with neural network model in comparison with multiple regression model.

Saravanan et al (2012) used Taguchi L_{18} orthogonal array to find the effective machining parameters on MRR. They used stainless steel as workpiece and examined the effect of the electrolyte concentration, machining voltage and frequency, machining current and duty cycle on MRR; remaining factors maintained constant during the experiment. According their work, duty cycle found to be the most significant factor influencing MRR with 42% rate and frequency found to be least effective parameter.

Rao Et al (2013) applied similar approach on ECM considering voltage, current, electrolyte flow rate and gap size as effective dominant parameters and MRR, overcut and surface roughness as machining assessment criteria. The workpiece selected from high demanded aluminium metal matrix composites in aircraft industries. Their work was based on two level full factorial design of the experiments.

In addition to the mathematical optimisation works on ECM, researchers applied other algorithms such as particle swarm optimisation, cuckoo search, and artificial bee colony and ant colony optimisation. Goswami et al (2014) took a similar approach towards μ ECM parameters' optimisation using differential search algorithm (DSA) and compared the result with previous mathematical optimised model. As their finding showed, DSA resulted in more accurate or better optimisation and created the confidence that other algorithms rather than mathematical models are applicable for μ ECM as well.

Despite all above research and investigation to obtain the optimum values and levels for the machining parameters in μ ECM process, there is still need for further studies to obtain a comprehensive solution to this challenge. Most of the above works have been applied for a unique machining targets (either dominated by tool or workpiece materials or micro product shape) and none of the above can be used as a general guideline.

So, this is a real challenge in the μ ECM technology which has been so far faced rather being solved. The success of any optimisation methodology not only depends on the accuracy of the model, but it depends on the chosen machining parameters, the range of their variations and machining performance criteria, too. Hence, selection of appropriate parameters and their values is a critical task and its success heavily relies on the operator's experience due to possible numerous and diverse range. Therefore, a confident and reliable selection, needs strong understanding of the nature of the process and the correlation between different machining parameters.

2.4.1 Interrelation between predominant machining parameters

As concluded, the effective operation and precise μ ECM machining require the optimum parameters' setup and the best possible combination of the parameters. This can lead to the desired outcomes and fulfilment of the machining requirements.

	IEG	MRR	Overcut (side gap)	stray current	Localisation	Current	Electrolyte resistance	Improved Surface	machining precision
IEG		Increase Decrease				Decrease Increase	Increase Increase		Increase Increase Decrease
Electrolyte Concentration	Decrease Decrease	Increase Increase	Increase Increase	Increase Increase	Decrease Increase	increase increase			Increase Increase Decrease
Pulse Voltage Amp.	Decrease Decrease	Increase Increase	Increase Increase	Increase Increase	Decrease Increase	increase increase		Increase	
Pulse on-time (duty ratio)	Increase Increase	Increase Increase	Increase Increase		Decrease Increase	increase increase		Increase Increase	Increase Increase Decrease
Current		Increase Increase	Increase Increase		Decrease Increase				Increase Increase Decrease
Pulse period (frequency)		Decrease Increase	Increase Increase						
Feed rate	Decrease Increase	Decrease Increase	Decrease Increase						Increase Increase Decrease

1	Bhattacharyya & Munda, 2003
2	Skoczypiec, 2016
3	Reddy, 2013
4	Kozak, et al., 2004
5	Kurita, et al., 2006
6	Sarvanan, et al., 2012
7	zhang & Zhu, 2008
8	Zhang, et al., 2007
9	Lee, et al., 2007
10	Rajurkar, et al., 2006
11	Ghoshal & Bhattacharyya, 2013
12	Govindan, et al., 2013
13	Skoczypiec, 2016
14	Kozak, et al., 2004
15	Bhattacharyya, et al., 2005
16	Bhattacharyya, et al., 2004
17	Jo, et al., 2009
18	Kim, Jung, & Park, 2013
19	Rao & Padmanabhan, 2013
20	Mithu, et al., 2014
21	Munda & Bhattacharyya, 2008

Table 2-3: Interrelation between machining parameters and machining performance criteria (Left), Resources for the information (Right) (Full details- Appendix A)

In section 2.3, the influence of major machining parameters was discussed. Gathered information from previous researches were summarised in table 2-3. This table presents the qualitative interrelation between different parameters based on previous experimental or simulation works.

This table does not include any quantitative values or measures and it has only based on qualitative effect of the machining parameters on other parameters machining performances criteria. The reason is that each experiment or simulation has been taken place at different condition and with different initial values. Although the gathered information does not offer a quantitative measure for machining setup, it does provide a valuable pattern to know how machining parameters behave in combination with other parameters and to recognise the most effective parameters in terms of effectiveness on other parameters and machining criteria.

As table 2-3 shows, voltage amplitude, electrolyte concentration and pulse on time influence most of the other examined parameters and criteria. On the other hand, MRR, overcut and machining precision are responding to any changes applied to any of these studied machining parameters. Although the possibility of existence of other unknown or less known effective parameters in machining is not unlikely and further investigation may reveal new facts regarding the effective parameters and their correlation due to complex nature of μ ECM, the classified data up to this stage can provide an important image towards the optimisation of the machining parameters.

2.5 Modelling and simulation

The complexity of the μ ECM process has made its investigation very difficult and challenging; therefore, a combination of modelling, simulation and experimental investigation is necessary to ease the perception of the process and to suggest valid methods and options to optimise the operation.

Researchers have used different strategies and approaches towards modelling and simulation, and, in each work, a different part or science of the process has been investigated. As the nature of the μ ECM is very complex, it is very rare to find a comprehensive model to cover all details of the process. In the following section, some of the most relevant simulation and modelling works have been reviewed.

In general, and based on this brief review, undertaken simulation works can be categorised in two main divisions: the mathematical & numerical models and the multi-physics models.

2.5.1 Mathematical and numerical simulation

Rajurkar et al (1995) presented a mathematical model to establish the effective machining parameters for achieving the minimum gap size under the critical conditions due to electrolyte boiling. As the current has inverse proportion to the gap size, process joule heat increases when the inter electrode gap size decreases which will result in the electrolyte boiling and machining will be disrupted (Kozak, 1994). Based on this model, a shorter pulse on time would allow a smaller gap size without electrolyte boiling. Therefore, it is necessary to develop an online monitoring system to maintain the gap size within the acceptable interval.

Kozak (2004) introduced two numerical thermal models for the μ ECM process with and without heat transfer through the electrodes' surfaces to investigate minimum permitted gap size.

Purcar et al. (2004) developed a model for the simulation to investigate the changes of 3D electrode shape based on marker method using the ECM method. This work was one of the limited numbers of the works in three dimensions. They investigated the changes in electrode shape in the direction of the current density and validated their results using experimental work.

Kenney et al (2005) introduced a two-dimensional computational model which consists of two major components including a transient charging simulation and feature profile simulation. Transient charging simulation is to examine the over potential at the tool- workpiece surfaces and feature profile simulation which is based on converted over potential information to the dissolution current, used to calculate the etching rate. This has led to the estimation of etch resolution and degree of precision. The results suggested consistency between simulation and experimental outcomes in terms of transient current behaviour and generated dissolution current. The two-dimensional computational results allowed them to evaluate the etch resolution and degree of the precision in the desired etch pattern.

Marla et al (2018) introduced a detailed theoretical model for μ ECM and Nernst-Planck-Poisson equation which used as governing equation for μ ECM process. They investigated the distribution of high electric field and the current density in IEG area to predict MRR. In their model, one dimensional, time variant electric field was considered but the effect of the flow was neglected. In addition to the theoretical activity, experiments carried out for several attempts and average data have been used to compare the theoretical MRR and the practical values. They found $\pm 1 \mu\text{g/s}$ error. Based on their observation, high electric field, EDL formation and ineffective localisation could be the main reasons for discrepancy between the theoretical and experimental results; they found a good agreement between their simulation and experimental results.

Kozak (2008; 2009) introduced a mathematical model based on Butler-Volmer equation (for current) and Poisson equation (for electrical field in IEG) considering the unsteady transient phenomena in EDL using Matlab to analyse electrode potential, dissolution current and electrical charge during the machining. Simulation was used to predict the material removal rate for a set of given conditions and in house-built machine was used to compare the experimental results and simulation results. As their results show, the main factor affecting the localisation of the anodic dissolution in μ ECM is related to EDL capacitor charging and discharging behaviour. Also, the finding suggested that the pulse voltage, pulse on time and feed rate have significant effects on the process in comparison with other parameters.

A numerical/electronic simulation model has been discussed in Sueptitz et al (2013) research to investigate the machinability of passive stainless-steel workpiece in the μ ECM. Electrochemical properties of the cell measured and applied into the model and the results have been compared with the similar experiments. As result presents, it is possible to improve efficiency of the machining process for passive electrodes by polarising the electrode close to its trans-passive potential area. They suggested three different methods to solve the problem due to the creation of a passive layer on the electrode surface which include adding oxidising ions to the electrolyte, polarising workpiece (applying DC voltage to workpiece) and polarising both tool and workpiece electrodes (applying offset voltage to the electrodes).

Kamaraj et al (2013) introduced a mathematical model for the μ ECM to predict the diameter of a tungsten micro tool which was fabricated using an in house built μ EC

machine. They used mathematical model to investigate the changes in IEG while cathode was a flat plate and anode was a rotating electrode. In this study, the change of micro tool diameter was investigated in relation to the gap size and the machining time. As expected, the micro tool diameter decreased by time and smaller gap size. In addition, it was noticed that gas bubbles would affect machining in smaller gap sizes. The deviations in the tool diameter were found to be within 9% of the numerical model.

Hotoiu et al (2013) developed a software known as MuPhyS based on C++ and FEM to model the changes of anode shape and the effect of the temperature in pulsed electrochemical micro machining. Their calculations for potential and temperature were based on the local charge conservation and internal energy. In their model two steps/loops were considered. First, the potential and the temperature distribution were computed during the pulses. Secondly, the result of the first stage fed to the second loop and new temperature and anode position was computed and transferred back to the first stage. They confirmed that neglecting the EDL capacity would increase the quantified error. Furthermore, the temperature in the system is not critical but increasing the temperature for a few degrees would significantly influence the process.

Hotoiu, et al (2013) continued their work by another publication to evaluate the influence of DL capacitance, pulse parameters and IEG size on the dissolution current density and material removal depth (as a function of time). A time dependent numerical model was introduced to solve the potential distribution in the solution in combination with non-linear dependent boundary conditions. This model presented the transient potential response, current density distribution (capacitive current + faradic current) and finally, calculated the local material removal depth.

This investigation expanded to pursuit the influence of linear and non-linear polarisation, in addition to pulse details and its combination with DL on machining current density and the machine product at low time scale. They concluded that non-linear polarisation in combination with a small gap size and nanosecond pulses can increase the localisation.

One of the difficulties in numerical modelling in μ ECM is the extremely lengthy simulation due to different time scales of the machining process, including nano-scale pulses and a higher time scale for the electrode deformation.

Hotoiu et al (2013; 2014), used the time averaging approach and proposed a new approach named as pulse shortcut strategy to cut the calculation time further without losing any valuable data at nanosecond level.

Their innovative technique (pulse shortcut strategy) assumes that the first few voltage pulses are insignificant compared with the rest of the pulses by which a quasi-steady state can be reached. They proposed by using this method, they could avoid using the entire processing real time and reduce the runtime and computational time. This method is relying on introducing a new factor known as current density correction factor (CF), which transfers the steady-state faradic current distribution into a confined distribution without requiring expensive time-accurate simulation but relies on the electrolyte resistance, the interface polarisation and a double layer characteristics in the presence of the nanosecond pulses. They suggested a simulation mechanism based on the proposed strategy to find the final profile of the workpiece. Also, the behaviour of CF was compared with full time accurate pulse simulation with regard to the inter electrode gap, DL loading and polarisation effect on the electrode gap for both insulated and active tool electrodes and recognised that time accurate density distribution or confined current distribution (after applying CF) lead to the identical results and only depends on the pulse conditions.

Volgin et al (2016) developed a mathematical model based on Laplace equation of potential and the equation of workpiece surface to predict the effect of the current efficiency on μ ECM by moving the tool electrode. In this model, electrolyte features assumed to be constant with no change. The author claimed that based on this numerical model of workpiece surface with moving tool electrode, it is possible to predict the size and shape of the machined surface. They applied different shapes of the tool electrodes and different types of the motion to study the effect of the current density on the shape and size of the surfaces and microstructures.

Wang et al (2019) used a mathematical model to evaluate the influence of the oscillation of the workpiece on the machining efficiency. In this model, MRR and the pressure induced in the gap was investigated. The advantages of the vibrating workpiece summarised as a variation in the front gap without affecting the tool electrode, improving diffusion efficiency due to improved kinetic energy at EDL and subsequently increasing the current density due to increased ions exchange rate and finally increasing the mass

transport in the gap. Their experimental work presented that a larger oscillation amplitude and an appropriate frequency can improve the machining efficiency up to 150%.

2.5.2 COMSOL simulation

The main issue with the modelling and simulation of the μ ECM process based on the numerical models is the difficulty in assessing all effective parameters individually and in combination with other parameters and predicting the overall effect on the machining process quality and the final product conditions. Therefore, there is always a concern that the numerical simulation results considering one or a few parameters may not provide adequate and comprehensive knowledge to predict the machining process and the final product features. It seems that multi-physics simulation approach can address this concern in near future.

Multi-physics simulation has been used for ECM simulation by Hachert-Oschatzchen et al (2011; 2012) to simulate the ECM process and the electrochemical finishing for micro bores, respectively. COMSOL provides the opportunity to combine different physical phenomena together in one model as Klocke et al (2013) did to investigate the MRR for the manufacturing of aerospace components considering the fluid flow, the electric field and the heat transfer.

Kumar et al (2016) used multi-physics simulation with COMSOL to investigate the diameter of the overcut and the stray zone while machined a hole in a Titanium sheet. They used Taguchi orthogonal arrays to evaluate the effect of a few individual parameters (including electrolyte pH, voltage, sensitivity, feed rate, tool rotational speed and duty cycle) on overcut. Taguchi orthogonal array is a statistical approach that helps to overcome limitations associated with time consuming full factorial experimental design. Taguchi orthogonal array is a highly fractional orthogonal design that is based on a matrix. It allows the designer to consider a selected subset of combinations of multiple factors at multiple levels. Based on their findings pH and voltage were the most effective parameters in this research. After finding the optimum parameters, they applied COMSOL simulation alongside the experimental work with the same machining details. They compared the result of the machining for different tool tips with an insulated side and a bare side. Their simulation results were greatly in agreement with the experiential work and suggested to

use the side-insulated tool with a flat tip as cathode and the replacement of the trial and error experiments with multi-physics simulation.

Mi et al (2016) used COMSOL multi-physics to simulate the μ ECM process for complex shaped holes. The effect of current efficiency and the relation between the tool electrode conductive area and the machining depth were investigated in this research. The results suggested the importance of current efficiency in machining complex shapes. In addition, the tool conductive area ratio at a higher conductivity would not significantly affect the machining depth.

Although the multi-physics simulation approach has helped researchers to simulate the μ EC process in a multi-disciplinary environment and overcome some of the difficulties in the mathematical and numerical simulations, some challenges still remain; these challenges are including the exact way of calculating some of the initial parameters, applying any changes over these values and assigning the boundary conditions. Therefore, there is still a need to refer to the experimental works and measure the initial values and monitor their changes over the machining period. Consequently, the result of simulation would depend on experimental works and there is a need to create a loop between the simulation and experimental work to be able to verify the results. COMSOL has recently received more applications in research and industry and it is hoped to get benefit from its multidisciplinary environment towards the simulation and modelling of the complex processes such as μ ECM.

2.6 Sustainability assessment

Manufacturing industries are one of the biggest consumers of the natural resources and massive producers of by-products and wastes. They are at the centre of the global criticism regarding the concerns about sustainable performance. Hence, these industries are facing a major challenge to improve their performances in addition to improving their products. There are international organisations responsible for putting measures in place and providing robust indicators for assessing the performance and sustainability of the industries.

The United Nations has defined that the sustainable development is to meet present needs without compromising the ability of the future generations to meet their needs, which orders the organisations to advance their economic states without depriving

current and future global residents from healthy environment and social equity. (Harris, 2001)

U.S. Department of Commerce defines the sustainable manufacturing as the creation of the manufactured products which use processes that minimise the negative environmental impacts, conserve energy and natural resources, are safe for employees, communities and consumers and are economically sound (Mani, 2013)

Deficiency of measurement science and methodologies to compare the performance of manufacturing processes with respect to sustainability has resulted in inaccurate and uncertain comparisons. However different efforts have been made to suggest indicators and measurements for sustainability assessment of manufacturing processes. Also a few organisations made effort to introduce a comprehensive framework for sustainable manufacturing indicators. As an example, National Institute of Standards and Technology (NIST) addressed five dimensions of sustainability including environmental effects management, economic growth, social well-being, technological development and performance management. (Mani, 2013)

Currently, manufacturing industries are experiencing a lack of effective methodologies and measurement criteria with respect to the sustainability and this is worse when it comes to micro manufacturing, where there is still a huge knowledge gap in the selection and utilisation of the sustainable micro manufacturing methods and technologies. This is particularly so when it comes to non-traditional machining approaches due to their performance uncertainty. In many cases, due to the lack of knowledge, standards, manufacturing and production guidelines the selection of the appropriate technology and its competitiveness is affected, which will substantially influence the sustainability of the process.

2.6.1 μ ECM process sustainability assessment: current state

Different organisations around the world, such as OECD (Organisation for Economic Co-operation and Development), ASMC (American Small Manufacturing Coalition) put efforts into identifying and introducing sustainable manufacturing measurements criteria, indicators and qualitative and quantitative methods. The same applies to the machining processes as one of the most important branches of the manufacturing operations.

Regarding the current frameworks, various indicators and methods have been introduced and applied by engineers and researchers to evaluate the sustainability of the certain sectors. Simultaneously, industries and organisations are using different parameters and methods to evaluate their sustainability internally, which makes it impossible to have accurate comparable results between them. Therefore, the lack of united classification and references adaptable to all machining sectors (research and industry) is obvious and that felt most when it comes to micro and nano machining processes in spite of the increased demand for micro and nano scale products.

The micro machining process itself is very complicated and very much dependent on the operator experience; therefore, it is very hard to apply unique approach to a variety of materials. Hence, it is necessary to consider each material and its final products individually.

However, majority of the current research has been concentrated on the assessment of the traditional machining operations, including drilling, milling, turning and grinding (Kim, 2012), hence there have been very little non-tradition machining sustainability assessment. Although, the literature shows a rise in research focusing on micro manufacturing in recent years.

Hegab et al (2018) proposed and discussed a sustainability assessment algorithm for the machining processes based on machining quality characteristics and sustainable machining metrics results in order to find the optimum parameters. They used weighting factors for the measured process outputs, metrics and indicators, which made the algorithm flexible and applicable to any experimental case. Also, they (Hegab, 2018) conducted an experimental work to provide the optimised process parameters for machining Inconel 718 with multi-walled carbon nanotubes and Al₂O₃ nano-fluidics. They studied power consumption, environmental impact (CO₂) and personal health and operational safety as sustainability dimensions and they used average surface roughness and flank wear as investigated machining outputs. Peralta et al (2017) reviewed over 300 publications in the area of sustainable manufacturing engineering with the focus on machining and summarised published works in order to propose a unified framework including existing parameters and the new ones, aimed at achieving integral sustainability in machining. Priarone et al (2018) described an approach to integrate the environmental and economical assessment of the machining process. Their work and assessment are

based on considering one source (energy) and one type of environmental impact (CO₂ emission) and they suggested that the range of process parameters which allows maximum efficiency is influenced by the material machinability.

Above is a brief review on available practices in the literature which demonstrates that all these researches were aimed at traditional machining.

Gamage et al. (2015) extensive qualitative research in 2012 revealed that only 25 publications were concerned directly or indirectly about non-traditional machining operations sustainability and from those 70% date back to 2006 and afterwards. Figure 2-8 shows the distribution of these researches on different areas of the non-traditional machining methods. As it is clear, nearly half of the publications were investigating the EDM and only 10% of the publications were related to ECM.

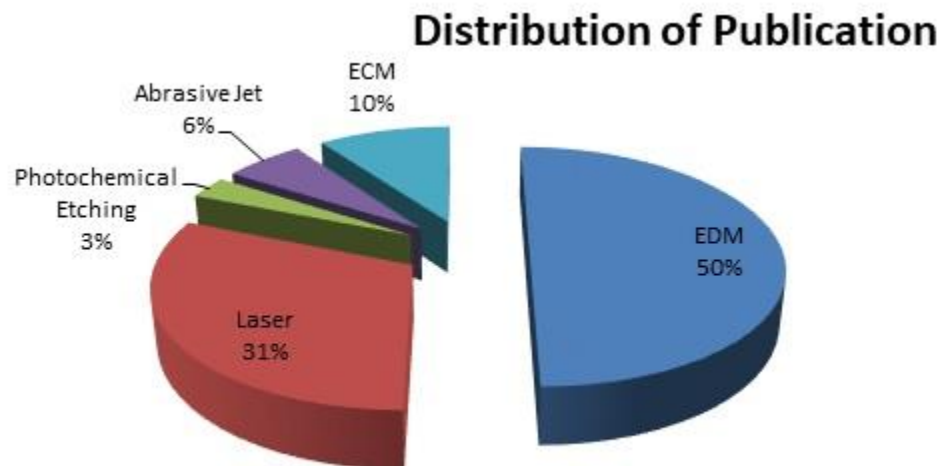


Figure 2-8: Distribution of 25 publications between different non-traditional machining methods

That reveals the wide gap between the sustainability assessment state of the art in non-traditional and traditional machining fields despite the importance of the contribution of manufacturing sector in the economy, which was estimated as € 7000 billion of turnover in 2012.

Krolczyk et al (2019) provided a comprehensive review in machining processes of hard-to-cut materials with the focus on the improvement of the process considering reduction of pollution generated by the coolants and emulsions. The targeted processes were dry cutting, MQL/MQCL, cryogenic cooling, high pressure coolant and the biodegradable vegetable oil. The approach was to minimise the total cost, cutting force, energy consumption and the temperature but to improve the surface quality, removed materials and tool life. Also, the influence on operators' health and impact on environmental areas were considered and finally the cutting parameters and cutting tool specifications were analysed and discussed.

The field of non-conventional micro machining including μ ECM needs strongly such a research and investigation.

The literature review has only presented a hand full of publications in the area of micro machining in general and a limited number of publications in the field of μ ECM sustainability assessment.

Kellans et al (2013) discussed the environmental impact of non-conventional processes. Tristo et al (2015) presented and analysed the online energy consumption in micro EDM and Modica et al (2011) discussed the sustainable micro manufacturing of micro components for micro EDM; and recent publication of the author (Mortazavi and Ivanov, 2017) presented a discussion related to μ ECM process sustainability . The author is not aware of any other specific publications that discuss the μ ECM sustainability assessment in any further details.

Knowing the above statistics and information and considering the μ ECM operation as a young and progressive technology, emphasises the need to introduce a reliable and scientific approach to assess the sustainability of the process to promote it as a valuable micro machining method.

2.7 Summary and conclusion

The successful employment of the ECM in aerospace, automobile and MEMS industries, has created a greater attention towards using ECM in micro-scale industries. The utilisation of the pulse voltages in macro scale ECM has provided a better control over the dimensional tolerances, gap recovery and discharge of removed materials. By

increasing the demand towards micro-scale components in high precision devices and applications, new activities were formed at academic research level to use and adopt the PECM technique to produce micro-scale components. The new, innovative process known as μ ECM was first published in the beginning of 2000 in Germany (Natsu, 2018); μ ECM follows the well-established foundation of the conventional ECM process but differs in terms of machining parameters' setup.

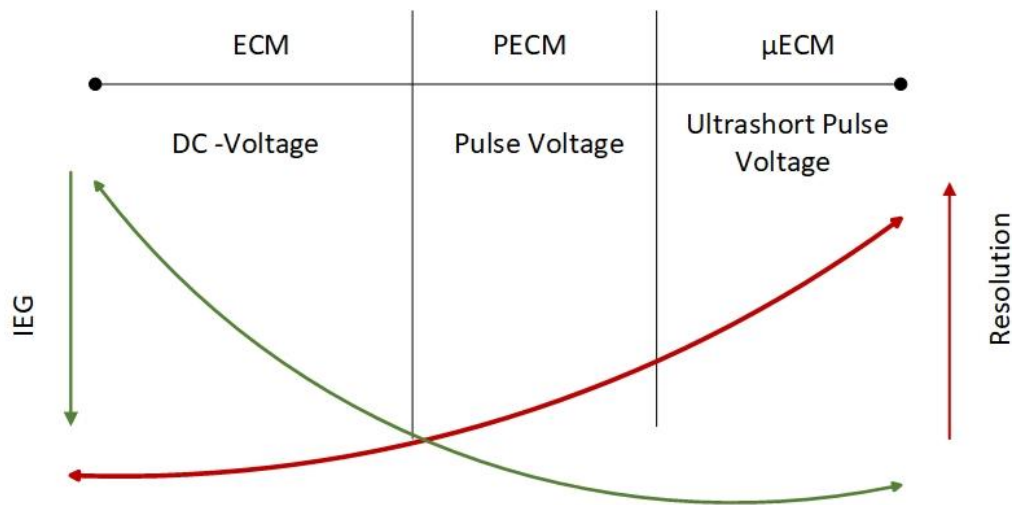


Figure 2-9: Comparison between ECM, PECM, μ ECM in terms of IEG and resolution

The main difference between conventional ECM and μ ECM is a smaller IEG, which makes the control of the process in μ ECM much harder but provides higher precision due to the narrow gap. Figure 2-9 shows the changes between ECM, PECM and μ ECM with focus on resolution and IEG size. IEG decreases from the ECM technology to the μ ECM and resolution has improved from ECM technology to the μ ECM.

Therefore, maintaining a smaller IEG during the process is the key to improve the final product quality.

In addition, the application of high frequency pulses (pulses with shorter period) increases the chances of noise and inductive effects. However, there are verified

solutions, which have been successfully applied and reduced the noise level and inductive effects of the cables in higher frequencies.

Due to a narrow gap between the electrodes and smaller tool dimension in the μ ECM, the electrolyte flow rate and the electrolyte injection direction in relation to the tool and workpiece position can influence the machining quality and performance. The tool vibration or bending under the influence of the electrolyte velocity should be prevented during the process; currently, there is not any guidelines available to address this issue or advise the setting. The danger of sparks and short circuits occurrence is enhanced due to the accumulation of machining by-products, gas bubbles, electrolyte boiling and anodic metal hydroxides in the narrow gap.

One of the most important consideration in this process is the machining parameters setup. The literature review presented in detail, that there is a complex multidimensional interrelation between parameters; the multi-disciplinary nature of the process requires a thorough investigation to identify and establish the interrelation between parameters. Based on research experiments during the last two decades, couple of parameters are considered as predominant parameters which include: voltage amplitude; duty ratio and pulse period; electrolyte type and concentration; they have stronger influence on other parameters as well as machining outcomes. It is suggested that smaller IEG, shorter pulse width and duty ratio, lower electrolyte concentration and tool electrode insulation can improve the machining accuracy. However, this is not a straightforward task as any changes in one parameter affects some or all other parameters; hence it is crucial to find the optimum levels for a combination of these parameters. This is recognised as one of the knowledge gaps in this field which needs further investigation. This issue will be addressed in chapter 3 by implementing a laboratory experimental work and mathematical analysis to find the optimum values for voltage, gap size and electrolyte concentration.

The complex nature of the electrochemical reaction at the electrode-electrolyte interface is still unknown and needs further investigation to be fully evaluated to demonstrate the phenomenon, which takes place at the interface. Currently, there is not any evidence of detailed approach to investigate the EDL structure. This is highlighted as the second knowledge gap in this research and will be addressed in chapter 4. EDL region behaves as a capacitor and in combination with electrolyte resistance and charge transfer

behaviour can be modelled as an RC network. The machining resolution depends on the structure of this region and is proportional to the time constant of the equivalent RC circuit. Therefore, a thorough investigation of EDL play an important role in process investigation and optimisation. In this research a laboratory experimental work was designed to estimate the RC equivalent network for the EDL and to present the relation between pulse on-time and EDL features by simulating the equivalent RC network.

Finally, due to the lack of activities in the area of sustainability assessment for non-conventional machining, no indicators or measures have been introduced to be used to assess the sustainability of the μ ECM process; as a result there is no justification available to reason the initial high cost of the process. This knowledge gap has been recognised and addressed by introducing a set of measures and indicators in chapter 5 to make it possible to evaluate the sustainability of the μ ECM process.

The industrialisation of μ ECM is still an incomplete task that needs further investigation, research and investment. The general μ ECM machining task requires:

- An understanding and evaluation of the machining parameters
- The choice of the tool materials and the electrolyte solutions
- The utilisation of the optimum parameters' combination
- The design of the tool electrode profile and the tool trajectory
- The monitoring and control of the process in real time
- The maintenance of the IEG size and MRR rate
- The achievement and maintenance of the high quality and accurate machined products

Each of the above tasks is a challenge; in addition, machining accuracy in μ ECM is related to the current density distribution over the machining zone. Therefore, it is indirectly related to the tool and workpiece geometry and the IEG size. Furthermore, achieving high localisation is another key task as the lower localisations means the spreading of material removal zone beyond the desired area and at a significant distance from IEG. As a result, dissolution can take place in a larger area than the desired machining area, therefore inaccuracy in the final work and low quality in surface roughness can be observed (Skoczypiec, 2016).

μ ECM technology has successfully demonstrated many applications especially where there is no other machining technology to create a high precise manufacturing for

hard and brittle materials without any mechanical forces or thermal effects. In principal, μ ECM can be applied to all electrochemically active materials, including semiconductors and superconductors (Zemann, 2012).

Current progress in μ ECM technology has presented valuable improvement in the process control and monitoring, shaping accuracy, simplifying the tool design and the process stability. This makes the μ ECM an outstanding alternative to produce accurate and complex 3-dimensional micro components. However, there is still a gap in application of μ ECM at research level and industrial level and the development and commercialisation of the μ ECM require further industrial investments.

CHAPTER 3

Electrochemical Investigation and Mathematical Analysis

Chapter summary

Following the discussion in chapter two and reviewing the current state of the research and development in the field of μ ECM machining and highlighting the current recognised knowledge gaps, this chapter will present the suggested methodologies and their implementations to provide further information and knowledge towards research aims and objectives.

Comprehensive and analytical review of the past and current academic and industrial activities brought to the attention that initial set up for the predominant machining parameters is still a challenge and needs further investigation. Also, EDL and its structure was recognised as one of the most important effective parameters in a successful machining process and thus an effective phenomenon in machining parameters' setup.

This chapter consists of several sections: first section is started with introductory concept of the electrochemical cells in general and μ ECM cell unit and a detailed review on EDL structure, charging and discharging currents, faradic and non-faradic processes. The second section includes the introduction to the electrochemical impedance spectroscopy and a brief review on standard electrochemical techniques (relevant to this research) followed by introducing an experimental approach to investigate the range of predominant machining parameters including voltage, IEG and electrolyte concentration.

Iviumstat will be used to run a series of experiments to investigate an efficient range for predominant parameters, then Matlab will be used to find the optimum values for the investigated initial predominant parameters. IviumStat is an equipped instrument suitable for electrochemical applications and Matlab is a programming environment for algorithm development, data analysis, visualisation, and numerical computation which has been used as the main and fundamental tools for research, development and prototyping in different research field. In this chapter, one of the Matlab toolboxes will

be used to apply the “response surface methodology” when analysing the obtained experimental data.

The outcome of this stage of experiments and Matlab analysis will be used to apply second stage of the experiments known as impedance spectroscopy in order to model the EDL equivalent RC circuit based on the experimental results. This stage will be introduced and discussed in chapter 4.

3.1 Introduction to electrochemical cell

Analytical chemistry is an approach towards solving chemical problems; and it emphasises on quantitative (and sometimes qualitative) techniques to analyse a sample and solve the problem. Electrochemical techniques are a category of analytical chemistry in which potential, current and charges are analytical signals to work on. Although there are only three fundamental signals in electrochemistry approach, there are too many methods to design and use to solve the problems. However, it is possible to create two main categories known as bulk techniques and interfacial techniques.

In bulk techniques, the property of the solution in electrochemical cell will be measured but in interfacial techniques, the interest is on the interface between electrode and solution and potential, current or charge will depend on species at this interface.

Although chemists may be interested in electrochemical techniques in order to measure the analyte’s concentration or to characterise an analyte’s chemical reactivity in general, the interest of this work is to discover the behaviour of EDL (electrode-solution interface) in μ ECM.

Before introducing the analytical techniques and their applications in this section, a few concepts should be briefly introduced.

Electrochemical cell: a typical electrochemical cell consists of two electrodes (two electronically conductors) and an electrolyte solution (ionic conductor). At each electrode, a half cell reaction (oxidation or reduction) takes place. The electrode at which the desired reaction (oxidation) happens is named as anode or working electrode (workpiece in terms of μ ECM). On the other hand, the electrode at which the other half reaction (reduction) happens, is named cathode or counter electrode (tool electrode in terms of μ ECM). In case of using any extra electrodes in the cell, the third electrode is known as reference electrode.

In addition to having two (simplest cell) or more electrodes, an electronic circuit is needed to control and measure the current and the potential of the cell.

Charge transport in the electrodes: takes place via the movement of electrons.

Charge transport in the electrolyte: occurs through motion of ions.

Potential:
$$E_{cell} = E_{cathode} - E_{anode} \quad (3-1)$$

Polarisation: polarisation is a deviance of the electrochemical process from equilibrium due to the passage of the current. In other words, a faradic reaction is accompanied by an equilibrium potential based on reaction free energy. By passing the faradic current, the equilibrium potential shifts to a new level; this shift is known as polarisation. Polarisation could occur at any of the anode or cathode electrodes.

Polarisation curve: The Polarisation curve is a plot to represent information about faradic reaction, using the current density (current) - potential relativity for a specified electrode-electrolyte combination. The polarisation curve will indicate the size of the modulation amplitude which can be used to retain the system in linear response area. At constant physical conditions there is only one value of the potential at that electrode may be at equilibrium; this potential is defined with Nernst's equation.

Ideally polarisable electrode (IPE): IPE is identified as an electrode at which no charge transfer would happen between electrode and the surrounding electrolyte over all potential range. However, in reality, there is no IPE for all range of potential but the electrodes can behave as ideal in some potential intervals and as soon as potential becomes sufficiently positive or negative, some sort of electrode process takes place (Figure 3-1).

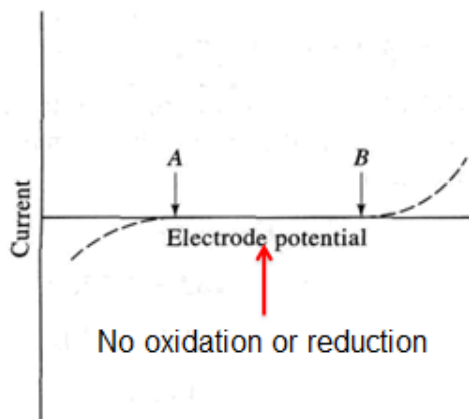


Figure 3-1: Current-Voltage curve for ideally polarised electrode, A and B present departure from ideal behaviour

The behaviour of electrode-electrolyte interface at such range looks like a plain capacitor. Therefore, an IPE can be represented using basic electronics components. As figure 3-2 shows, IPE interface with the solution can be modelled with a capacitor in series with resistor presenting electrolyte resistance. The features of this capacitor will be discussed in more details when the behaviour of electrode-electrolyte interface is reviewed.

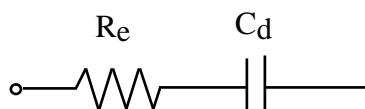


Figure 3-2: Electrolyte resistance and double layer capacitance model

Although a very basic RC combination has been used to demonstrate the electrode-electrolyte interface, there is a lot of complex sciences behind that which will be discussed in the following sections.

An Equivalent impedance for such a model is calculated as below:

$$Z = R_e + \frac{1}{j\omega C_d} \quad R_e: \text{resistance} \quad C_d: \text{capacitance} \quad \omega: \text{angular frequency} \quad (3-2)$$

An electrode which is not at ideally polarised state may be known as charge transfer electrode at which oxidation or reduction process can take place.

Equilibrium in electrochemical cell: equilibrium condition of the electrochemical system can be described as equality of the electrochemical potentials.

Over potential: By passing faradic current through the electrochemical system, potential shifts from equilibrium level. The shift generates an electrical potential difference between the polarised and the equilibrium (initial) electrode potential which is called over potential.

$$\text{over potential} = \eta = E - E_{equ} \quad (3-3)$$

Electrolyte conductivity: this is a property of electrolyte which indicates how well an electrolyte can conduct the electricity. Conductivity is proportional to the concentration, charge and mobility of ions. The conductivity determines the conductance of the electrolyte which is the inverse of resistance.

Electrolyte resistance: electrolyte resistance is generally an important factor in the impedance of the electrochemical cell. Electrolyte resistance depends on the electrode geometry (current passage area), the gap between the electrodes (current passage length), ionic concentration, type of ions and the temperature as temperature can affect electrolyte characteristics. The resistance of the electrolyte can be calculated using the formula:

$$R_e = \frac{1}{k} \frac{l}{A} \quad (3-4)$$

In which k (Siemens per meter) is the conductivity of the solution, l is the length of the resistor and A is the area (the gap size and the tool surface area in terms of μECM , respectively). The main challenge in resistance calculation is that the current distribution is not uniform and therefore it is difficult to determine the current flow path and the geometry of the electrolyte which carries that current. The greater the electrolyte resistance, the greater is the drop of voltage on electrolyte resistance.

Modes of mass transport: There are three fundamental modes of mass transport in a solution:

Diffusion: if the concentration of an ion or molecule at the electrode surface is different from its concentration at the bulk solution, diffusion will happen. Diffusion is under the influence of a chemical potential gradient. The area of the solution under the diffusion is called diffusion layer, the width of the diffusion layer increases with time.

Convection: if the solution is mechanically mixed and as a result reactance moves toward the electrode and products is removed from electrode, convection happens. Convection can be due to the density gradients or external factors such as stirring.

Migration: migration occurs when charged particles are attracted to or prevented from an electrode that carries surface charge. Migration is under the influence of the electrical potential gradient.

Faraday's first law: Faraday's law presents the relationship between the number of charges (quantity of the current) passing through the path and the chemical changes under the effect of the passage of the current. The mass of a substance reformed at an electrode during electrolysis is proportional (directly) to the quantity of the electricity (charges not electrical current) transferred at that electrode.

$$m \propto Q = m \propto I \cdot t \rightarrow m = ZIt \quad (3-5)$$

In this equation Z is a constant, known as "electro chemical equivalent" of the substance, I is the current and t presents the time. If one ampere of current is passed for one second: then $m = Z$

Therefore, electrochemical equivalent of a substance is defined as the weight (amount) of the substance deposited or liberated, when one coulomb of electric charge is passed through an electrolyte. Z in S.I unit is expressed in Kg / coulomb. Each element has its own electrochemical equivalent.

Faraday's second law: for a given quantity of electricity (electric charge), the mass of material reformed at an electrode is (directly) proportional to the material equivalent weight (molar mass divided by an integer which depends on the reaction undergone by the material). In other word, it states that the masses of different substances deposited or liberated, when the same quantity of current is passed through different electrolytes, connected in series are proportional to their chemical equivalent masses. Thus, Faraday's constant is defined as the quantity of the charges which deposits or liberates exactly one gram equivalent of a substance. ($1F=96500C$)

$$\text{Equivalent mass of an element} = \frac{\text{Atomic mass of an element}}{\text{Valency of the element}} \quad (3-6)$$

$$m = \frac{Mit}{nF} \quad (3-7)$$

In which

m is the mass of substance, M is the molecular weight of the substance, I is the current, t is the time period, n is the number of transferred electrons and F is the Faraday's constant.

Faradic process: well-known reduction and oxidation processes which follow the Faraday's law are known as faradic process; the common concept in faradic process is the electron transfer at the electrode-electrolyte interface. Experimentally, a steady-state current- voltage curve (known as polarisation curve) can be constructed during the faradic process at the electrode. In contrast with non-faradic process, the key requirement for the faradic process is that the electric charges are transferred away from electrode surface involving atoms, ions or molecules as reactants and by-products. Generated current known as faradic current is proportional to the rate of the electrode chemical reaction.

Non-faradic process: there are some changes at the electrode-electrolyte interface with no charge transfer; such process is named as non-faradic process. However, small transient external current can be generated by this process. At an ideal polarised electrode, only non-faradic process can take place. The state of a non-faradic process can be described as a charge-voltage curve. The key point in non-faradic or capacitive process is that the ionic charges stay in or at the electrode surface.

Faradic Impedance: If during the electrochemical reaction, electrons transference between electrode and solution species happens at some potential, the equivalent circuit model should include faradic impedance in parallel with the electrode capacitance. Faradic impedance consists of two components (real and imaginary parts), real part is known as the charge transfer resistance and the imaginary part is known as the mass transfer impedance (if the reaction is semi-infinite diffusion then the second part is called Warburg impedance). Faradaic impedance is inversely proportional to the active area.

Charge transfer resistance: The charge transfer resistance depends on the reaction kinetics which is the result of a single reaction at equilibrium. It is a function of the steady state potential. It needs to be considered that kinetics effects are recognisable at higher frequency. The charge transfer has a specific speed that can be changed by potential, type of reaction, temperature and concentration and reaction products. Figure 3-3 presents the schematic model for a cell including charge transfer.

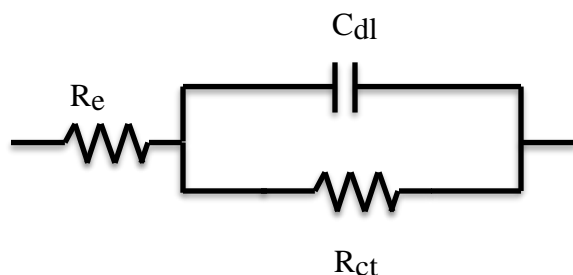


Figure 3-3: Schematic equivalent circuit

The general relation between the current and the concentration based on Faraday's law and the charge transfer is:

$$i = i_0 \left(\left(\frac{C_O}{C_O^*} \exp \left(\frac{anF\eta}{RT} \right) \right) - \left(\frac{C_R}{C_R^*} \exp \left(\frac{-(1-\alpha)nF\eta}{RT} \right) \right) \right) \quad (3-8)$$

in which i_0 is the exchange current density, α is the transfer coefficient, F is Faraday constant, R is universal gas constant, T is temperature, n is number of electrons, η is potential difference, C_O and C_R are local concentration in cathodic and anodic reactions.

If the concentration of the bulk is equal to the concentration of the electrode surface, then equation 3-8 is simplified to:

$$i = i_0 \left(\exp \left(\frac{\alpha n F \eta}{RT} \right) - \exp \left(\frac{-(1-\alpha) n F \eta}{RT} \right) \right) \quad (3-9)$$

This equation is known as Butler-Volmer equation and is applicable to the reaction when the charge transfer kinetics is the only factor in the reaction.

In practice and when over potential is very small and reaction is at equilibrium, the charge transfer resistance can be calculated by:

$$R_{ct} = \frac{RT}{nFi_0} \quad (3-10)$$

Mass transfer: mass transfer impedance (it has a real and an imaginary part with the same magnitude) has no dependency on kinetics and its effects will appear at low frequencies. To calculate the faradic impedance, the surface concentration needs to be known and the most straight forward option is when the bulk concentration has been known at the equilibrium potential (dc current equal to zero).

Warburg impedance: Warburg impedance is the result of a mass transfer in a semi-infinite diffusion. It is impossible to model it with a simple combination of passive electronic components as it contains equal real and imaginary values with opposite sign (imaginary part is negative); therefore, its phase angle is -45 degree. Figure 3-4 shows the Randles' equivalent model including Warburg impedance.

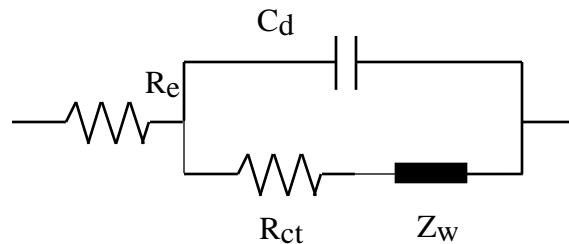


Figure 3-4: Schematic of Randles model

Following the above vital explanations and details, electrode-electrolyte interface will be discussed in the next section.

3.1.1 Electrode-electrolyte interface

Placing an electrode in the electrolyte is usually leading to an equilibrium potential difference between metal and solution and therefore a specific interface region between electrode and electrolyte is formed. This interface can have a significant effect on the electrochemical reaction due to its electrical properties. Among reactions which take place at this interface, faradic process is the most important one, likewise in μ ECM the behaviour of electrode-electrolyte interface and the faradic process in this area retains a particular information and a great importance.

3.1.1.1 Electric double layer

As mentioned, when electrode plays as IPE no charge would cross the interface but by applying a positive potential, gradually the potential difference increases and consequently the anodic metal ions transfer from metal into the solution and ions discharge from solution which happen simultaneously; however the migration of ions occur until the charge of electrode and electrolyte interface are equal and due current rapidly deteriorates to zero if no active species exist at the surface. The result of this movement (a non-faradic process) is a transient non-faradic current known as charging current. Consequently, ionic mobility creates an opposing charge layer on the solution surface. The behaviour of the interface can be analysed as a capacitor and it has been named as “Electrical Double Layer” capacitor. In fact, positive cations and negative anions create Electrical Double Layer (EDL) which can be presented as a capacitor in an equivalent circuit. This capacitor will obey the standard capacitor equation as below:

$$Q = C_{dl}E \quad (3-11)$$

In which

Q is the charge stored in EDL in coulombs, C_{dl} is EDL capacitance in Farad, E is the potential across the EDL capacitor in volt.

It is rational to say that by applying a potential across an IPE, a capacitive current will flow to charge the EDL capacitor and charges will be stored on metal plates (electrode-electrolyte interface) to satisfy the above formula. Although real capacitors show independent capacitance with respect to the potential across them, the EDL capacitance is a function of the potential.

The charging current is significant and should be considered as it will contribute to the total current measured in the cell; also, it may exceed faradic current in some cases when faradic current is very low.

Traditionally, three models have been introduced to describe the EDL structure (Gongadze, 2009)

1) Helmholtz model: this model is the simplest model to present the EDL structure which was introduced in 1879. This model presents the relation between stored charges on electrode-electrolyte surfaces. The two formed compact layers of stored charges are known as EDL. Electrode holds charge density due to excess or absence of electrons (at its surface) and the solution (at surface) will hold equal amount but opposite charged ions. Therefore, two layers of opposite charges are created at interface with a small distance. The outer boundary line is known as outer Helmholtz line (OHL) and the inner border is known as the inner Helmholtz layer (IHL) and the region between them is named the Helmholtz layer. The potential in the Helmholtz layer is described by the Poisson's equation voltage drop across the borders (EDL plates) and demonstrates a linear variation from electrode surface to the bulk solution. The EDL capacitance per unit area is given as equation 3-12 when EDL thickness is very small compared with the tool surface which is the case in μEC .

$$C_{Helmholtz} = \frac{\epsilon_0 \epsilon_r A}{L} \quad (3-12)$$

Where L is thickness of EDL, A is the area of stored charges (electrode surface area), $\epsilon_0 = 8.854 * 10^{-12} \text{ F/m}$ and ϵ_r is electrolyte relative permittivity.

The drawbacks of this model are the ignorance of the effect of voltage and electrolyte concentration on the EDL capacitance and the bulk solution away from OHL which has not been considered.

2) Gouy-Chapman model: suggested the idea of a diffuse layer and statistical mechanical approach to the model and is considering the thermal motion of ions. They suggested that ions are mobile, and they are driven under the impact of diffusion and electrostatic forces. In this model, the greatest concentration of excess charges accumulate next to the electrode and less concentration accumulates at greater distances. It means that by increasing the distance from the electrode surface, the concentration will

decrease. Therefore, instead of having fixed distance between plates (surfaces) the average distance would be replaced. If the electrode becomes more charged, diffuse layer becomes more compact and capacity becomes compact and capacitance rises (concentration effect). The scattering of ions is defined by the Boltzmann distribution formula as

$$n_i = n_i^0 \exp \frac{-z_i e \varphi}{KT} \quad (3-13)$$

Where n_i^0 is the concentration of ion i in the bulk, e is the unit charge, z_i is the charge on the ion i, k is Boltzmann constant and T is the absolute temperature.

Finally, the differential capacitance is obtained as follows

$$C_{Gouy-Chapman} = \frac{d\sigma_M}{d\varphi_0} = \left(\frac{2z^2 e^2 n_i^0 \epsilon_0 \epsilon_r}{KT} \right)^{1/2} \cosh \left(\frac{ze\varphi_0}{2KT} \right) \quad (3-14)$$

The drawback of this model is known as the overestimation of the ionic concentrations close to the charged surfaces. In case of a thin EDL, the capacitance can be approximated using equation 3-12.

3) Stern model: the stern model, also known as Gouy-Chapman-Stern model, suggested a more realistic model in 1924 based on the combination of previous models, adapting compact layer of Helmholtz layer near OHL in which ions are immobile and Gouy-Chapman diffuse layer extended into the bulk solutions in which ions are mobile. He presented linear variation of potential with the distance from the electrode surface up to the diffuse layer (OHP) and a quasi-exponential variation of potential at diffuse layer into the bulk layer. Basically, the mathematical concept of this model is to use both Helmholtz and Gouy-Chapman capacitance models in series. Therefore,

$$\frac{1}{C_{Stern}} = \frac{1}{C_{Helmholta}} + \frac{1}{C_{Gouy-Chapman}} \quad (3-15)$$

It has been suggested that the Helmholtz layer capacitance in stern model dominates the total capacitance if the electrolyte concentration and the surface potential are large enough (Wang and Pilon, 2011)

The Stern model is the most comprehensive model to be considered for the EDL structure. Figure 3-5 shows a schematic of EDL for the three mentioned models.

The larger the potential difference between the electrode potential and zero charge potential, the Debye-Hückel length is smaller; hence the thickness of the double layer in addition to the electrolyte characteristics depends on potential as well (Stojek, 2002)

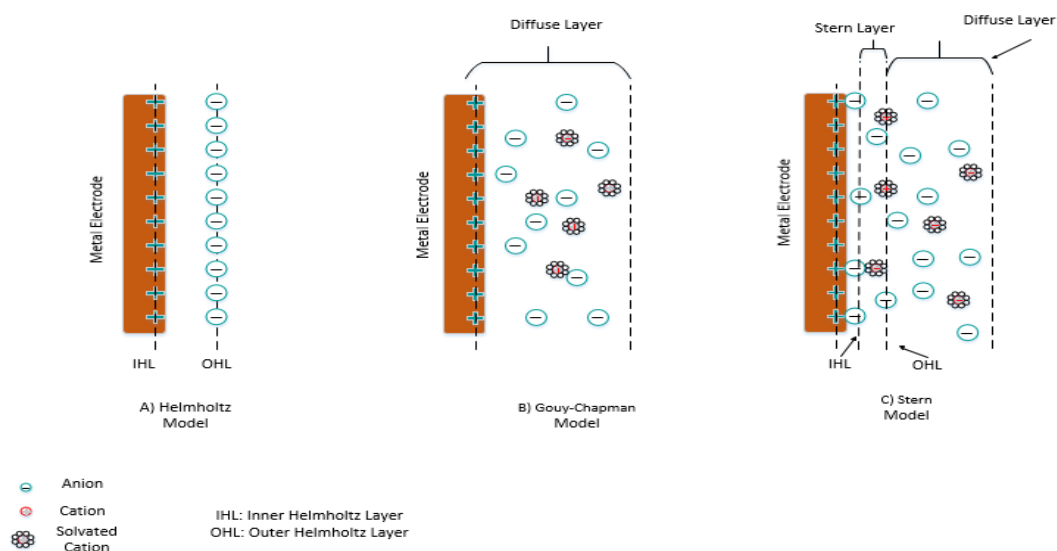


Figure 3-5: EDL schematic diagram A) Helmholtz B) Gouy-Chapman C) Stern model

3.1.1.2 Electric double layer equivalent model in μ ECM

Placing electrodes in the electrolyte and activation of electrolysis would lead to the formation of EDL in the process. By accepting the capacitive features of EDL in the μ ECM, researchers have offered two models for the EDL in μ ECM. In the model which figure 3-6 presents, EDL is modelled as a capacitor, and electrolyte resistance and the faradic reaction is modelled by impedance; the faradic impedance includes active charge transfer resistance and Warburg resistance. (The Active charge transfer resistance is to prevent

the backward reaction (discharging the ionised metal); the Warburg impedance demonstrates the lack of mass transfer between electrodes).

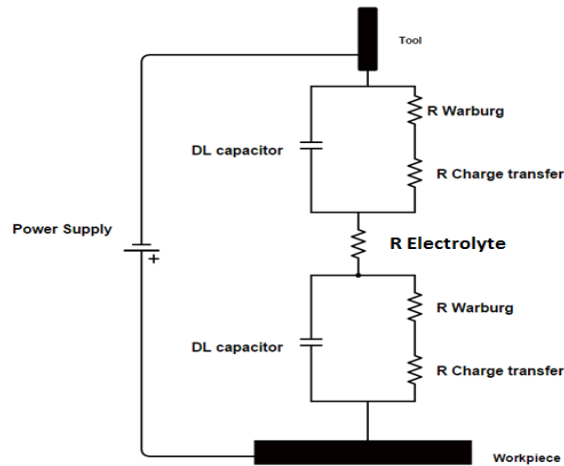


Figure 3-6: EDL equivalent electrical model in μ ECM (Bhattacharyya, 2015)

Finally, the electrolyte resistance is presented in series with parallel combination of EDL capacitance and impedance of the faradic reaction. This model has been extracted from Randles model (Bard and Faulkner, 2001).

Figure 3-7 presents the equivalent circuit for EDL when the effect of the current flow from the tool longitude surfaces has been considered. In this model, the electrolyte resistance (path of current) in IEG (short distance between tool surface and workpiece) is presented by R_{Short} and the electrolyte resistance of the long distance between tool and workpiece (path of current flow from the tool longitude surface to the workpiece) is presented by R_{Long} .

By using isolated electrode tools (isolating tool electrode longitude body), the first model is efficient and appropriate to be used and will be used as the reference model in the rest of this research.

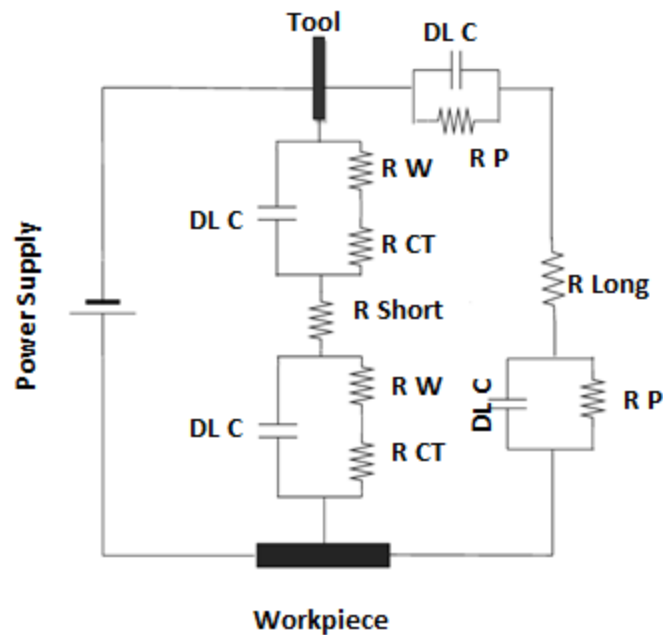


Figure 3-7: EDL equivalent electrical model in μ ECM presenting tool longitudinal surface (Bhattacharyya, 2015)

As discussed in previous sections, in the μ ECM fundamental mechanism is the removal of the material based on electrolysis in which the material is removed from the workpiece surface in form of metal ions; they may remain dissolved or they may react with the electrolytic solution components, either way they would be prevented from being deposited on the cathode tool.

It is important to notice that the electrochemical reaction would not be successful without applying an external voltage to create the current passages between electrodes. This external voltage is applied in the form of short pulses. Positive voltage is applied to the anode and the negative pole is connected to the cathode and the conductive medium (electrolyte) is the passage of the current between the two electrodes.

Electrode-electrolyte interface has a very crucial role in the μ ECM process. It is important to have an overall view of what is happening at this interface. There are two processes of interest which take place at this area.

One process - known as the faradic process- is based on Faraday's laws in which electrons transfer directly across the metal-solution interface. As the fundamental of this process is based on Faraday's law, it has been known as faradaic process.

The second one is known as non-faradaic process which presents the conditions in which no charge transfer occurs in the metal-solution interface for a range of voltage. In other words, electron will remain at the electrode surface and the EDL capacitance will increase.

For any application of electrode reaction, the faradaic process is the main point of interest. However, the non-faradaic process should be considered as it directly or indirectly affects the process.

The electrode-electrolyte interface presents two different behaviours based on the above process. Applying a pulse voltage to the process cell will increase the electrode potential from zero or equilibrium to the pulse value and will lead the charges to be stored at the electrode-electrolyte surface until the EDL capacitor is charged. This is a non-faradic process; the generated current during this period is named as the charging current. The generated current is a transient current which depends on different factors such as EDL structure, pulse voltage, electrolyte characteristics and solution temperature. When the EDL capacitor was charged and the reaction reached the equilibrium stage, the faradic reaction starts to take place. At this stage, anodic reaction takes place and the material will be removed from the workpiece. Therefore, the current which is flowing through the IEG at this stage is named faradic current and it is a steady state current. The current density depends on different factors including but not limited to the IEG size, pulse voltage, pulse on time, tool electrode material and section area, electrolyte and the solution temperature.

Although the full evaluation of these two processes and currents are necessary, there is another key process which needs deep investigation. The pulse off time and the EDL capacitor discharge need to be fully investigated as the removed materials should be flushed away from the narrow gap between the electrodes during the pulse off time.

Pulse on time non-faradic process:

Applying potential pulses to the μ ECM cell will activate a non-faradic process in the interfacial region between the electrode and the electrolyte surfaces. Initially, the surface voltage gradually increases and the capacitive current, which is not related to any of the reduction or oxidation processes flows in the cell and the EDL capacitor charges for a period of time; the charging time is less or equal to the pulse on time based on the

machining parameters, the electrode materials and the electrolyte. During this process, the material dissolution does not occur, instead, a transient current –known as non-faradic current- is generated and flows through the double layer capacitor. At this stage, the EDL capacitor charging current is decaying from its maximum level to nearly zero or it progresses to the negative range (opposite direction).

During this process charges would not transfer through the electrode-electrolyte interface, but the structure of the interface can change due to the movement of the electrolyte ions, reorientation of solvent dipoles and similar activities.

Considering the presented equivalent circuit in figure 3-6, at the start point of applying voltage to the cell, the faradic impedance is very high, and the branches of the faradic impedances act as open circuits. So, the time that EDL capacitor need to be charged at the pulse on time only depends on the EDL structure and the electrolyte resistor.

Pulse on time faradic process

When the EDL capacitor starts to charge, the faradic impedance behaves as an open circuit and gradually by increasing the potential at the electrode- electrolyte surface, the faradic impedance level changes from open circuit status and the faradic current flows through the interfacial region. It is very difficult to separate the faradic and non-faradic currents and evaluate their amplitude or period. The faradic process in μ ECM is the desired process in which anodic dissolution occurs and material is removed from the workpiece.

The interest is to find the optimum pulse on time in a way to have the maximum effective faraday current in the process.

Pulse off time (EDL capacitor discharge and sludge removal)

The next event which takes place at the electrode-electrolyte interface in μ ECM cell is the EDL capacitor discharge. This process is expected to start at the pulse voltage falling edge. In addition to this, sludge and by-products are flushed away from the gap between the electrodes. Although, electrolyte flow is a continuous process, its effective performance takes place during the pulse off-time.

Having completed a brief review on the EDL general specifications during a pulse voltage, the next step is to have a better understanding of the electrochemical techniques and their assistance in further investigation and analysis of the EDL's behaviour in μ ECM via possible simulation methods and laboratory work.

3.2 Electrochemical impedance spectroscopy (EIS)

Having the knowledge of the electrode-electrolyte interface structure and fundamental electrochemical concepts, it is possible to review and apply electrochemical techniques to demonstrate a practical equivalent model for EDL.

Electrochemical Impedance Spectroscopy (EIS) technique is one of the most valuable techniques in the electrochemical field and is a perturbative characterisation of the dynamics of the electrochemical process. EIS is a frequency domain technique which requires some knowledge in mathematics, Laplace and Fourier transforms. Although it may be a difficult approach, it provides a large amount of useful and analysable information.

One of the main advantages of EIS is its ability to extract properties of the individual components of investigated reaction or the cell. Its flexibility to provide time dependent and quantitative data is an advantage as well as the ability to distinguish between two or more electrochemical reactions. In contrast, the complexity of data analysis is considerable.

In addition, one of the main advantages of EIS is the fact that it is based on the linear time invariant system theory (LTI) and the validity of the data can be verified using integral transforms (Kramers-Kronig transforms) that are independent of the involved physical processes.

Chemical applications of EIS began with Nernst work followed by many other researchers including Warburg who developed the impedance of mass transfer (1880-1905). Later, during the 1930s, the structure of double layer was studied. The Arrival of potentiostat transformed the electrochemical process analysis and impedance measurements which were continued by the introduction of the electric analogue circuits for electrochemical reactions by Dolin, Ershler and Randles until the present time (Bard and Faulkner, 2001).

The Revolutionary shift in energy sectors, electrochemical sensors and rechargeable solid-state batteries has led the research interactively towards electrochemical engineering. As a result, the characteristics of solid-solid state and solid-liquid interfaces have increasingly attracted the interest of scientists. The Impedance spectroscopy as a relatively new method played an important role in investigating the dynamic and characteristics of the solid or liquid materials. The general approach is to apply an electrical provocation (known voltage or current) to the electrodes and observe the response which results in current or voltage due to a fundamental microscopic process that takes place throughout the system (Macdonald, 1987). This microscopic process includes the transport of electrons, the transfer of electrons at electrode-electrolyte interface and flow of the charged atoms via defects in the electrolyte.

The impedance spectroscopy (IS) can be categorised in two main groups: electrochemical IS (EIS) and everything else. EIS involves investigation and analysis of the material with strong predominant ionic conduction features such as solid and liquid electrolytes, conducting glasses and polymers (ionic conduct) and nonstoichiometric ionically bonded single crystals, where conduction can involve motion of ion vacancies and interstitials.

The second category of IS applies to dielectric materials including non-conductive solid or liquid whose electrical characteristics involve dipolar rotation, and materials with predominantly electronic conduction (Macdonal, 1992).

Regardless of this classification and in general, there are three different IS techniques to apply but the standard and common method is to measure the impedance in frequency domain by applying a single frequency voltage signal to the interface and measuring the phase shift and amplitude of the resulting current at that frequency.

Commercial instruments are using the same approach but measuring the impedance as a function of frequency and in a range of frequency about 1 mHZ to 1 MHz.

The importance of electrode-electrolyte interface behaviour in μ ECM has been the motive behind the application of IS to investigate and discover the details of the electrode-electrolyte interface and to provide input data for the simulation models for further in-depth process analysis.

The application of impedance spectroscopy to illustrate the electrochemical systems requires the interpretation of the produced data in the form of equivalent circuit

or process model which subsequently requires the selection of passive components which can faultlessly model the experimental results. Commonly used components and their relatedness and their behaviours in steady-state and transient conditions can be defined as below:

The fundamental laws of electrical circuits which will be used in the rest of this chapter are related to the main passive elements as below:

Resistor: Ohm's law relates the current passing through the resistor to the voltage. Current and voltage signals through a resistor are always in the same phase.

$$V = RI \quad (\text{V is voltage, R is resistor, I is current}) \quad (3-16)$$

Ohmic resistance $R\Omega$ known as potential drop between two electrodes in electrochemical systems is modelled by a resistor. The ohmic resistance depends on the electrolyte conductivity and the electrode geometry comparable with the electrical resistance which depends on the resistor dimensions and its resistivity. In general, a resistor describes the charge transfer activity between the electrode and the electrolyte.

Capacitor: DC current cannot flow through the capacitor, but the charge will be stored in it and it varies at each voltage. The current through the capacitor is leading 90 degree in phase with respect to the voltage.

$$V(\text{voltage}) = \frac{Q(\text{charge})}{C(\text{capacitance})} \quad (3-17)$$

$$Q(t) = \int_0^t i(t) dt \quad (i(t) \text{ is current}) \quad (3-18)$$

$$V(t) = \frac{1}{C} \int_0^t i(t) dt \quad (3-19)$$

The electric double layer at the electrode-electrolyte interface has been effectively modelled by a capacitor. The separation of the charges of the electrode from the charges of the solution ions at the interface creates capacitance characteristics and forms a double layer capacitance which is in size of angstroms.

Inductor: the familiar presentation of inductance is in the form of a coil in which current induces an electromotive force opposing any changes in the current. The current phase in the inductor is lagging the voltage by 90 degrees.

$$V(t) = L \frac{di(t)}{dt} \quad (\text{L is inductance}) \quad (3-20)$$

The Inductive behaviour of the electrochemical reaction can be the result of non-uniform current distribution, inductance of cell's cables or the adsorption-desorption process which occurs in the passive layer formation. In such cases, the impedance of the electrochemical system is modelled by an inductance.

3.2.1 EIS and μ ECM

The concept of the impedance spectroscopy dates back to the introduction of the impedance into the electrical engineering and Laplace transform of current and voltage and consequently transformation of Laplace domain to Fourier domain by Oliver Heaviside in the decade of 1880 (Macdonald, 2006). His work was soon expanded with the progress of the mathematics by other scientists. Warburg extended the concept of the impedance to electrochemical systems. Since then and during the last couple of decades IS has been developed rapidly despite its drawbacks including high cost and difficulty of measurement in low frequencies. Later in the 1940s electronic potentiostat was introduced and it was followed by the development of the frequency response analyser in the 1970s which both upsurge the use of the EIS in investigating diverse electrochemical processes ranging from electronic conduction in metal-solution states, polymers and electrochemical reaction mechanisms.

Macdonald (1987) published the first book on early experimental work and his work followed with other research publications including his research publication (1992) and many more. In recent years, EIS has been recognised as a powerful tool to investigate the electrochemical systems and to explore the properties and characteristics of material, solids and solutions in such systems. However, there are very limited published works on EIS approach specialised on μ ECM machining process in terms of electrochemical features of the process.

Samples of general works is included but not limited by Macdonal (2006) reviewed the history of EIS which presents the importance of the early 20th century works in defining the structure of EDL, Harrington et al (2011) discussed and reviewed difficulties of using equivalent circuits to analyse the EIS data and discussed the significance of charge transfer resistance and polarisation resistance, more recent development in local EIS was reviewed and discussed by Huang et al (2011) in micro dimension electrodes, Orazem et al (2007) argued that EIS is not a stand-alone technique and it needs to be accompanied

with experimental observation, model development and error analysis to validate the given interpretation of EIS data, and other publications which concentrate on general concept of EIS.

Another area of research using EIS tool concentrates on application of EIS to discover the electrode-electrolyte interface such as Pajkossy et al (2017) research on interfacial studies and Gongadze et al (2009) work on classical models for the interface.

The research areas using the usefulness of the EIS techniques are not limited to the above samples; it has been broadly used for investigation and discovery of the material and liquid features, electrochemical capacitors, fuel cells, lithium ion batteries, electrochemical sensors and also biological applications including surgical tools.

Relevant studies to μ ECM based on the application of EIS are handful in which EIS has been used to acquire tool-workpiece interfacial features and to apply the finding for further investigation through simulation or experimental work. Sueptiz et al (2013) worked on electrochemical micromachining of passive electrodes (stainless steel) to present that passive stainless steel can be treated as active electrode with high reaction over potential.

There are more publications in the area of ECM in which EIS has been used to investigate the machining process, tool-electrolyte interface or tool and workpiece characteristics. Weber et al (2013) used the result of EIS to establish a multi-physics simulation for pulse ECM of grey cast iron, also he used similar approach to model the steady state dissolution current in pulse ECM of cast iron (Weber, 2015), Rimer et al (2014) presented a case study on the effectiveness of EIS techniques in success of the electrochemical manufacturing and the importance of the EIS data interpretation to achieve better results in any research.

All above brief literature review presents the efficiency of the EIS in μ ECM process investigation and discovery; however, there is not much publication in this field. One reason could be the nature of μ ECM which is still a young field and subsequently expensive in terms of experimental work and process investigation.

In this work, it has been tried to use the benefits of the EIS methods to establish more accurate understanding of the phenomena which happen at EDL.

3.2.2 Experimental consideration

In any electrochemical system under impedance spectroscopy investigation, input is usually the potential and the output is current. The current will not flow if the electrochemical does not occur; and in order to have electrochemical reaction to start, a critical cell potential needs to be exceeded before current starts to flow. As a result, the relation between current and potential is completely nonlinear. Despite this nonlinearity, by working on a small portion of this relation, system can be considered as pseudo-linear.

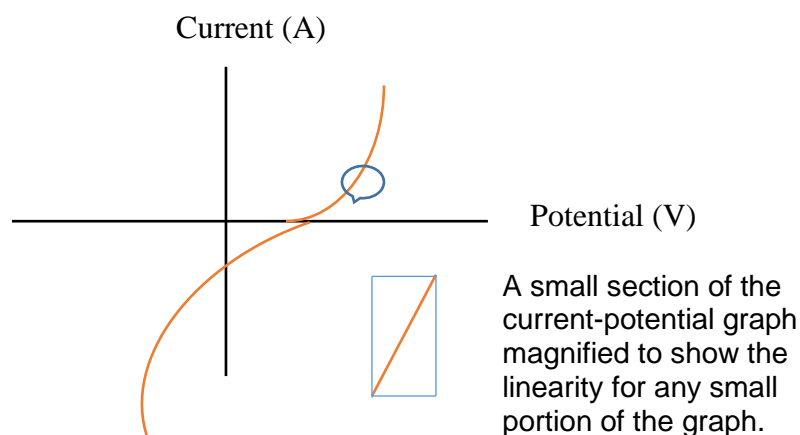


Figure 3-8: Pseudo-linearity for very small section of the curve

EIS is usually used in stationary conditions at a constant potential or current but there is always an interest to study systems which change with time or during potential cycling in cycle voltammetry and this will lead to dynamic electrochemical spectroscopy.

Compromise between low amplitude perturbation (to have linear spectrum) and high amplitude (to decrease the effect of noise) is another challenge. If a system shows a linear current-voltage curve, noise can be the priority but for a system with very nonlinear current-voltage curve, smaller amplitude is the priority.

EIS is the response of an electrochemical cell (system) to a perturbative voltage with small amplitude on top of the controlled DC voltage. In practice, the amplitude of the potential perturbation does not exceed 10 mV peak to peak as EIS performance is based on linearisation of non-linear electrochemical processes (pseudo-linear rules apply) and very small amplitude should be used to prevent the appearance of higher harmonics in response. It is also possible to apply current perturbative signals to measure the generated voltage in system, but this is not within the scope of this research rather can be used for Galvanostatic mode.

It is crucial to consider which features to be measured at transient or steady state phase. In practice, steady-state polarisation curves provide important information such as exchange current density, Tafel slopes and diffusion coefficient. But not all measurements can be processed by steady state and some of the parameters such as RC time constant should be measured through the transient state.

3.2.3 Design of Experiment

The experiment setup consists of hardware and software including Iviumstat (potentiostat device), software (Ivium software), SEM (scanning electron microscope), EDS (energy dispersive X-ray spectroscopy – known as EDX, as well), laboratory weighting device, temperature and conductivity meter.

In this work, IviumStat has been used as potentiostat in order to explore the electrochemical reaction which happens at EDL during μ ECM process. IviumStat is an equipped instrument suitable for electrochemical applications. The device specification can be reviewed at Appendix B; also, a few useful tips to consider when using iviumstat, has been mentioned in Appendix C.

IviumStat offers a complete package including all standard electrochemical techniques and integrated frequency response analyser for EIS measurement. (Anon., n.d.)

Diagrams in figure 3-9 and 3-10 demonstrate the experimental setup for the practical work and analysis and assessment steps, respectively.

The aim of the introduced experiments in this chapter is to investigate the most effective values for the predominant machining parameters including IEG size, voltage level and electrolyte concentration.

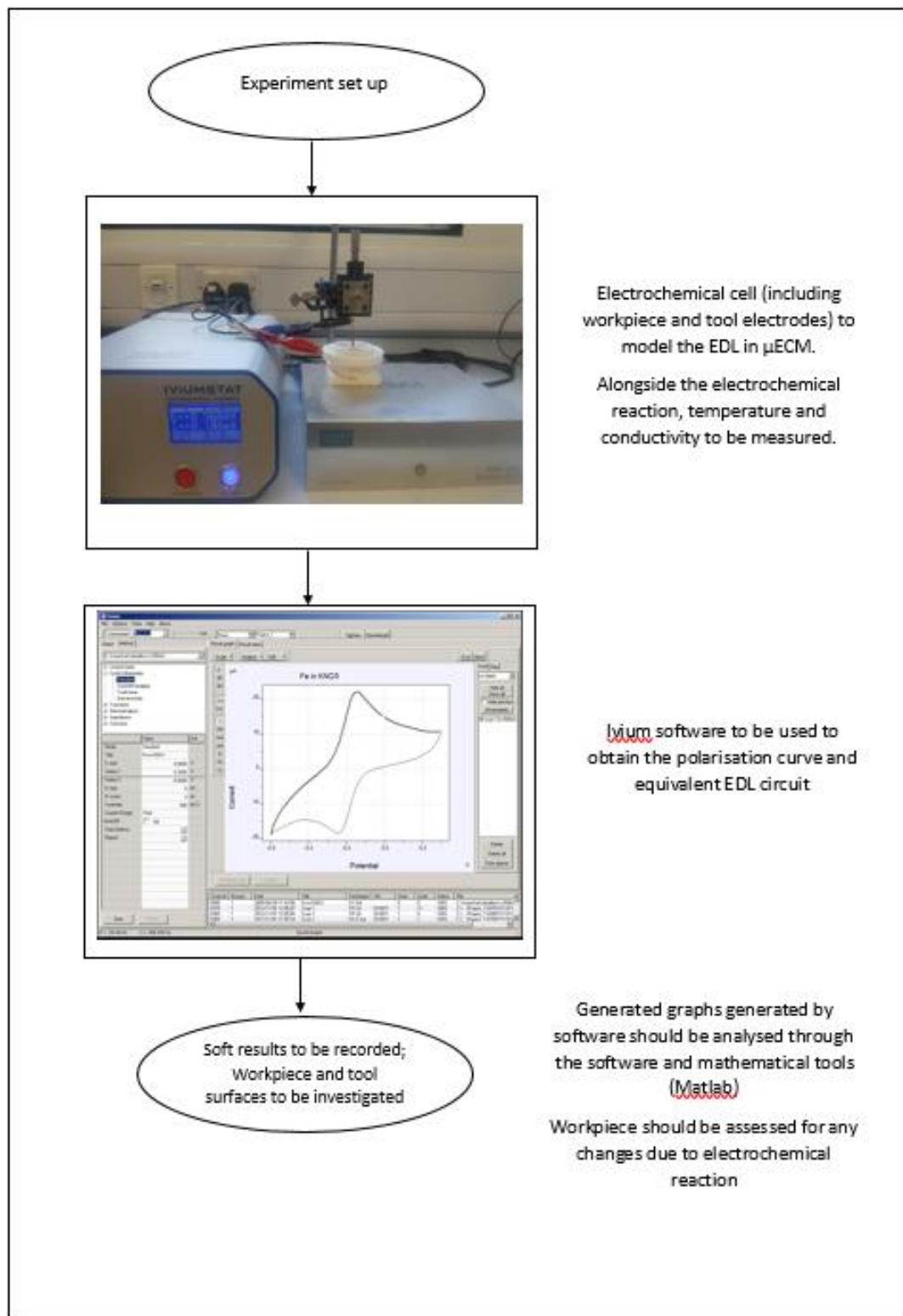


Figure 3-9: Experiment setup diagram

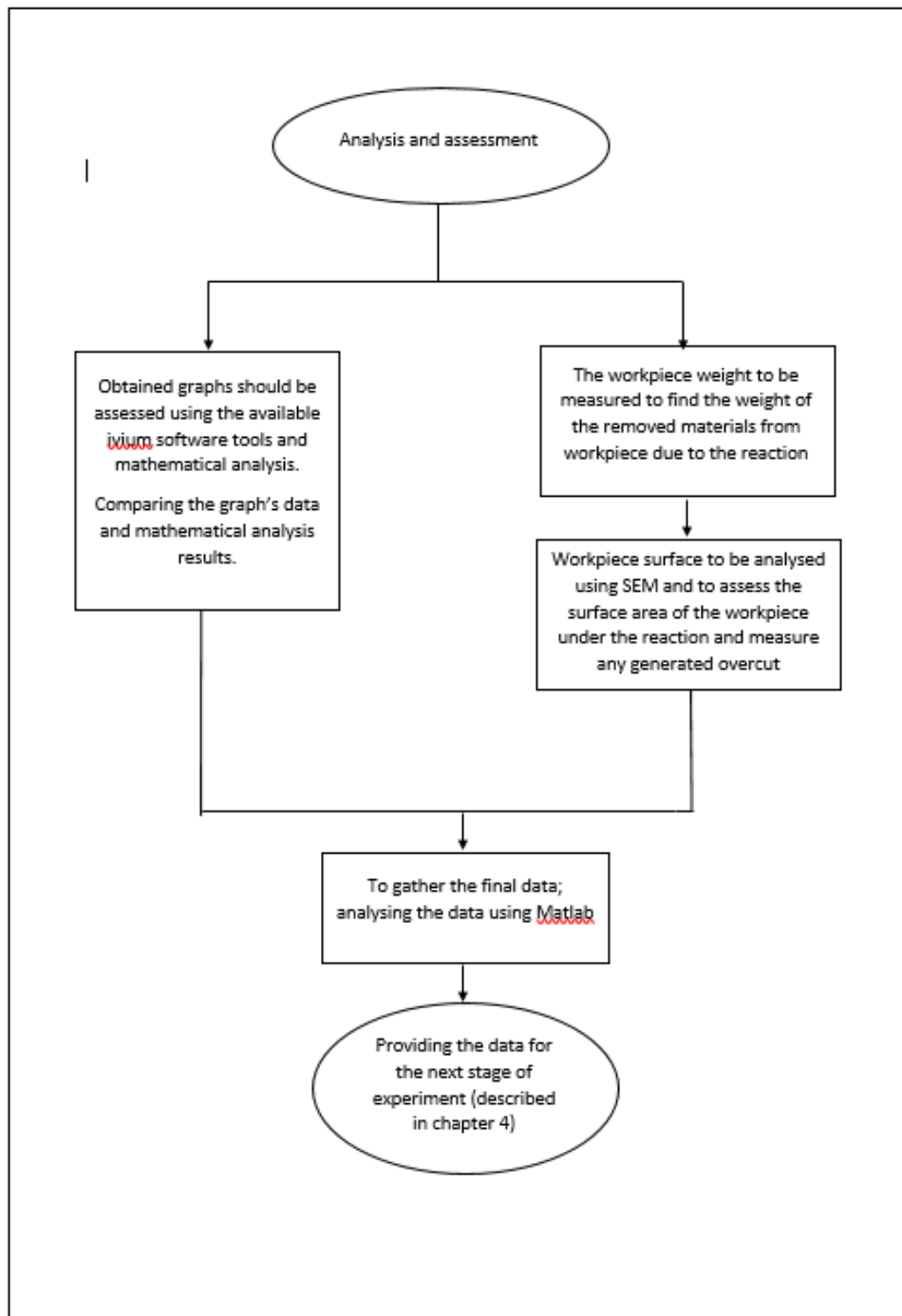


Figure 3-10: Analysis and assessment diagram

By obtaining the polarisation curves, the machinability of the workpiece for chosen parameters can be evaluated; by feeding the gathered data to the Matlab toolbox, the best range for the parameters can be achieved and finally those parameters can be used to estimate the electrode-electrolyte interface equivalent circuit. The devices, workpiece and tool electrode details as well as experimental details will be explained in the following sections.

IviumStat:

IviumStat includes the hardware and software. The hardware includes device, faraday cage, cell unit and standard cables and connections (figure 3-11).

There are 5 electrode cables, WE (working electrode), CE (counter electrode), GND (ground electrode), RE (reference electrode) and S (sense electrode).

Depends on the cell arrangement some or all these cables may be used. GND cable are not connect to any electrodes but it will be connected to a ground point or the faraday cage to reduce the noise.

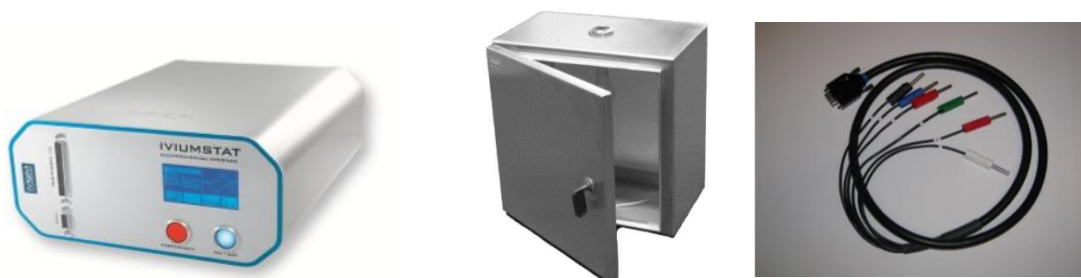


Figure 3-11: Iviumstat device, Faraday cage, standard cable

There are 3 different configurations available for the cell electrodes including 2-electrode, 3-electrode and 4-electrode setup. During this work, 2-electrode configuration has been adapted in 4-electrode cell arrangement in which WE and S cables are connected together and to the workpiece electrode and CE and RE cables are connected together and to the tool electrode.

The WE and CE cable leads are carrying the current and S and RE cable leads are measuring the potential across the target. In potentiostatic mode, the instrument force a current through CE and WE, and R-SE measures the voltage as close as possible to the target, therefore the potential difference is a fine accurate value. Figure 3-12 presents the cell unit which is connected to CE and WE electrodes.



Figure 3-12: Tool- workpiece cell

SEM & EDS:

Scanning electron microscope (SEM) is a type of electron microscope which uses the focused electron beam to produce high resolution images allowing sub-micron features to be seen. SEM provides information about the surface topography and composition.

Energy Dispersive X-ray Spectroscopy (EDS) is an analytical technique to provide the elemental analysis and chemical characterisation of a sample. Below are the main features of the SEM and EDS:

- Fast, high resolution imaging
- Analytical assessment of the elements present
- Spatial quantitative analysis of desired areas on a sample surface
- Examination of the grain structure
- Possible 2-Dimension, or 3-Dimension measurement



Figure 3-13: JCM-6000Plus Versatile Benchtop SEM

SEM has advantages in comparison with optical microscope in terms of maximum magnification, providing analytical features including assessment and characterisation of

the material structure, surface defects, stains and residues on metals, particulate and contaminant analysis on and within the materials.

In this work, JCM-6000Plus Versatile Benchtop SEM (JEOL) equipped with EDS has been used (figure 3-13). Considering its features, this device was the best available resources to fulfil the analytical and measurement requirements in this project.

Workpiece:

Workpiece electrode is selected from stainless steel – AISI 304 (Fe/Cr18/Ni10), from Goodfellow Limited. The workpiece which used in this experiment was a circular disc with 25 mm diameter and 3 mm thickness. Following pictures present the workpiece surface profile using SEM before and after polishing. Also, the profile details of the workpiece surface was analysed using SEM and EDX with an acceleration voltage of 15 kV. Figure 3-14 shows the profile and the highest elements of the workpiece surface and figure 3-15 shows the SEM captured workpiece surface topology.

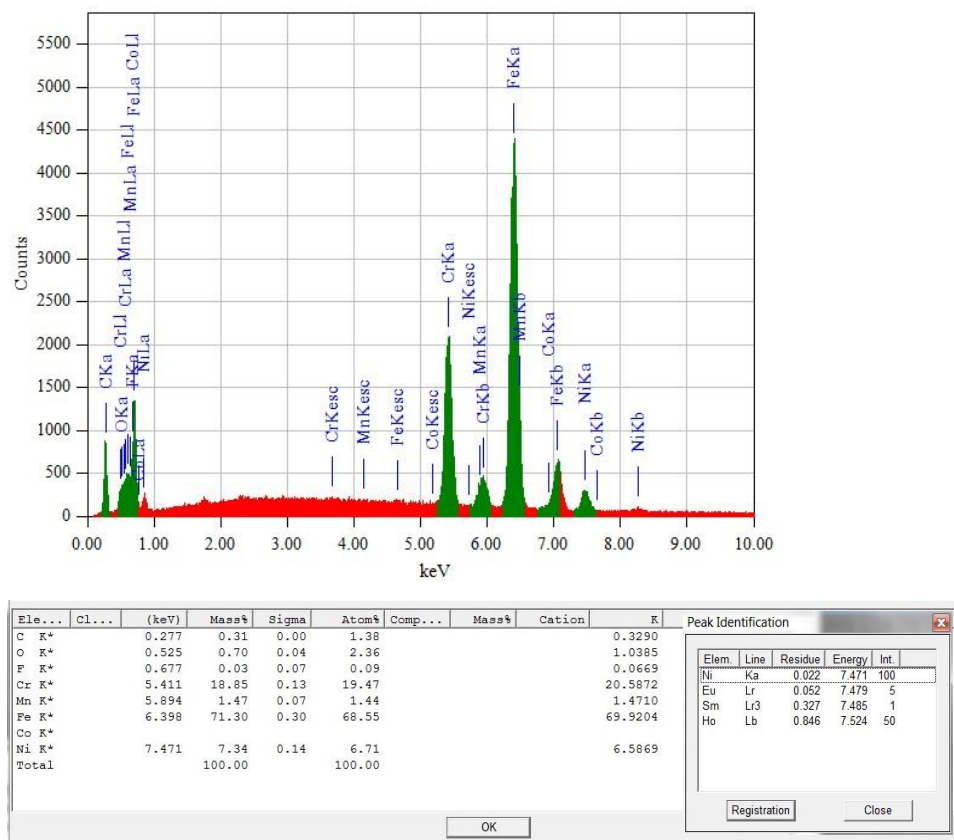


Figure 3-14: EDS spectrum of stainless steel – AISI 304 (Fe/Cr18/Ni10)

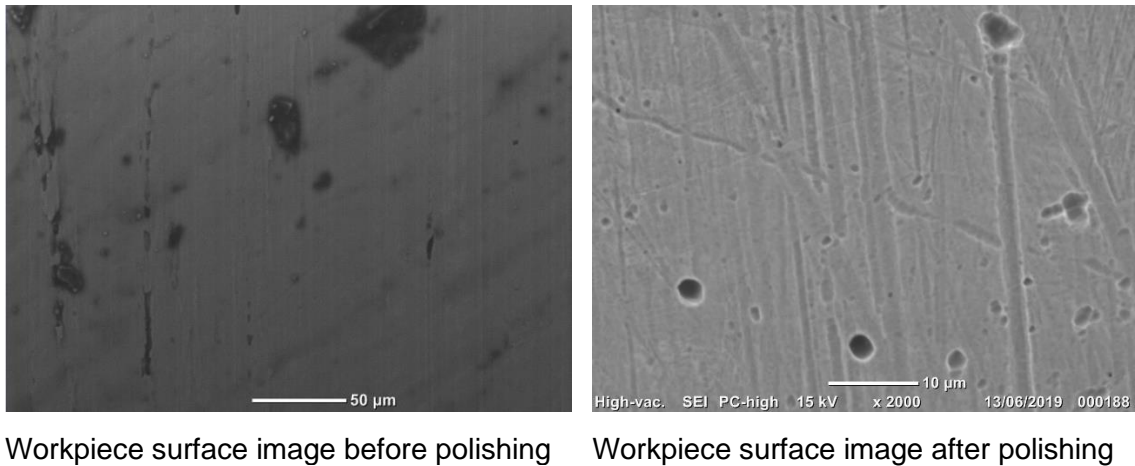


Figure 3-15: Workpiece surface image using SEM

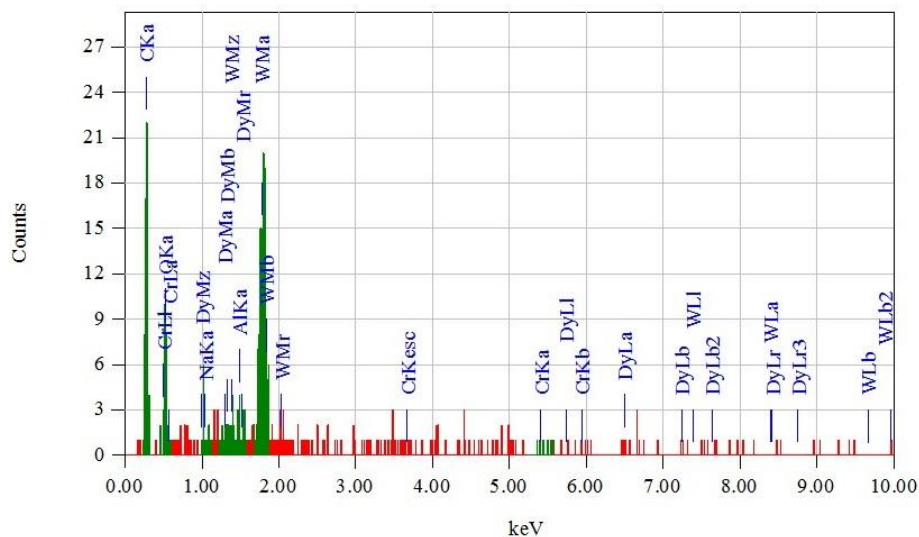
Tool electrode:

Tungsten (Goodfellow, 0.5 mm diameter, 99.95% purity) was used as the main electrode tool (counter electrode in terms of iviumstat). Images below present tool features and surface profile with SEM; although the expectation is that μ ECM process should have no or very limited tool wear, the tool surface profile will be examined during the experiments to evaluate the rate of tool wear if there is any.

As mentioned in the literature review, tool longitude isolation helps to minimise the effect of the stray current and improve the localisation by concentrating the electric field lines (flux) within the close area around the tool surface. Lacomit has been used as tool longitude isolator for this experiment.

Lacomit was easy to use; it generates a thin layer which is easy to be removed if necessary. (General physical and chemical features are available in Appendix D)

The peak elements of the tool material include W (Tungsten), Cr (Chrome), and C (Carbone). EDS spectrum of the tool electrode will be evaluated at different stages to highlight any changes due to the machining. In addition to tungsten tool electrode, nickel has been used as tool electrode as well in a few laboratory experiments. Figure 3-16 and figure 3-17 present EDS spectrum and surface image of tungsten tool electrode, respectively.



ZAF Method Standardless Quantitative Analysis

Fitting Coefficient : 0.6662

Element	(keV)	Mass%	Sigma	Atom%	Compound	Mass%	Cation	K
C K*	0.277	36.13	1.43	72.08				19.9764
O K*	0.525	13.46	1.70	20.16				11.0223
Na K*	1.041	0.42	0.26	0.44				0.6672
Al K*	1.486	0.55	0.39	0.48				0.9787
Cr K*	5.411	0.65	0.87	0.30				1.6180
Dy M*	1.293	10.61	3.52	1.56				13.8496
W M*	1.774	38.19	3.82	4.98				51.8879
Total		100.00		100.00				

Figure 3-16: EDS spectrum of tool electrode- Tungsten (9.95% purity)

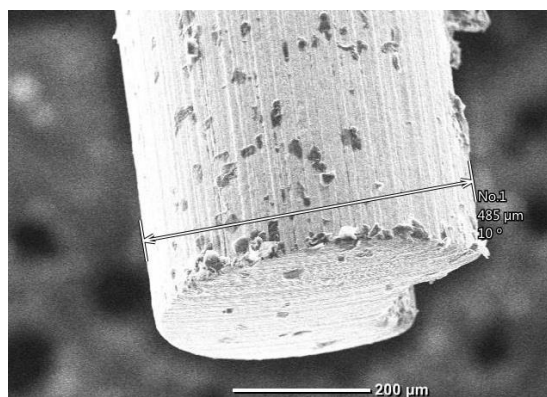


Figure 3-17: Tool surface image using SEM

Electrolytes:

NaNO_3 has been used as the electrolyte solution in this experiment. NaNO_3 is known as one of the most effective electrolytes in the μECM for its features through the literature review and previous experimental works.

3.3 Machinability evaluation for stainless steel 304

Although potentiostat device would automatically present the results of the experimental activities in form of graphs, tables and even recommended electric circuit equivalents, it is necessary to have profound knowledge and understanding of the output data to interpret the results for further investigation and deeper understanding of the reaction.

Experiments using iviumstat has two separate stages and each stage consists of multi experiments.

The first stage is a primary work and the aim is to evaluate machinability of the desired workpiece by studying the polarisation graphs for different combination of the parameters. In addition, the changes of temperature and conductivity of the solution is recorded. This practice includes 3 steps.

Step 1: is the transient investigation of the cell which helps to identify or set up the desired gap between workpiece electrode and tool electrode.

Step2: the second step is the application of linearSweep by which the polarisation curve of workpiece material is studied.

Step3: the collected data at this stage will be used by Matlab curve fitting toolbox to analyse the data mathematically and to provide the required input data for the next stage of the experiment which will be explained in chapter four.

As mentioned in previous chapters, setting the initial values for machining parameters is a challenge as parameters can behave differently in combination with each other. Initial values for machining parameters can be selected using the result of the former simulations and experimental works or they can be selected based on a trial and error approach.

Using iviumstat limits the freedom towards selection of parameters in comparison with experimental work on μECM machine. There are limits for the current and voltage which device is capable to provide, however it still provides a good range for the voltage

level suitable for the process. In this work, predominant parameters suitable for the investigation and compatible with the iviumstat features are voltage amplitude, electrolyte concentration and IEG size. For each of these parameters a suitable range was selected, and all experiments were repeated within those ranges. The selection of the range of predominant parameters values took place based on a trial and error approach; various experiments run and were observed and based on the gathered data, predominant parameters ranges were selected.

Table 3-1 presents the range of the variable parameters in this stage of the experiment. Five levels were selected for the applied voltage, three levels for the electrolyte concentration and four different gap sizes were selected.

Variable parameter	Levels				
Voltage (v)	5	6	7	8	9
Initial IEG size (μm)	25	25	30	40	
Electrolyte concentration (g/L) (mole/L)	25.5 (0.3)	42.5 (0.5)	85 (1.0)		

Table 3-1: Predominant parameters' range in iviumstat experiment

First stage of the experiment includes 60 ($5 \times 4 \times 3$) repeats; for a constant electrolyte concentration and for each level of voltage, four different gap sizes were evaluated and that repeated for five levels of voltage and three different electrolyte concentrations.

To set the desired gap, transient mode of the iviumstat has been used with the fixed parameters which is presented in figure 3-18 (left). Setting for the transient investigation includes recommendation by manufacturer (interval time, stability and filter type) and experiment requirements (minimum possible current range, time required to achieve desired gap between tools and voltage level). This practice helped establishing the desired gap, then standard option from linearsweep mode of the iviumstat was used to investigate the polarisation behaviour of the workpiece. The variable parameter in this mode is the end voltage level. Current level is selected as 1A which is the maximum current the cell may withdraw. 4-electrode cell arrangement and values for voltage step

and scan rate recommended by manufacturer. Figure 3-18 (right) illustrates the setup for the linearsweep mode.

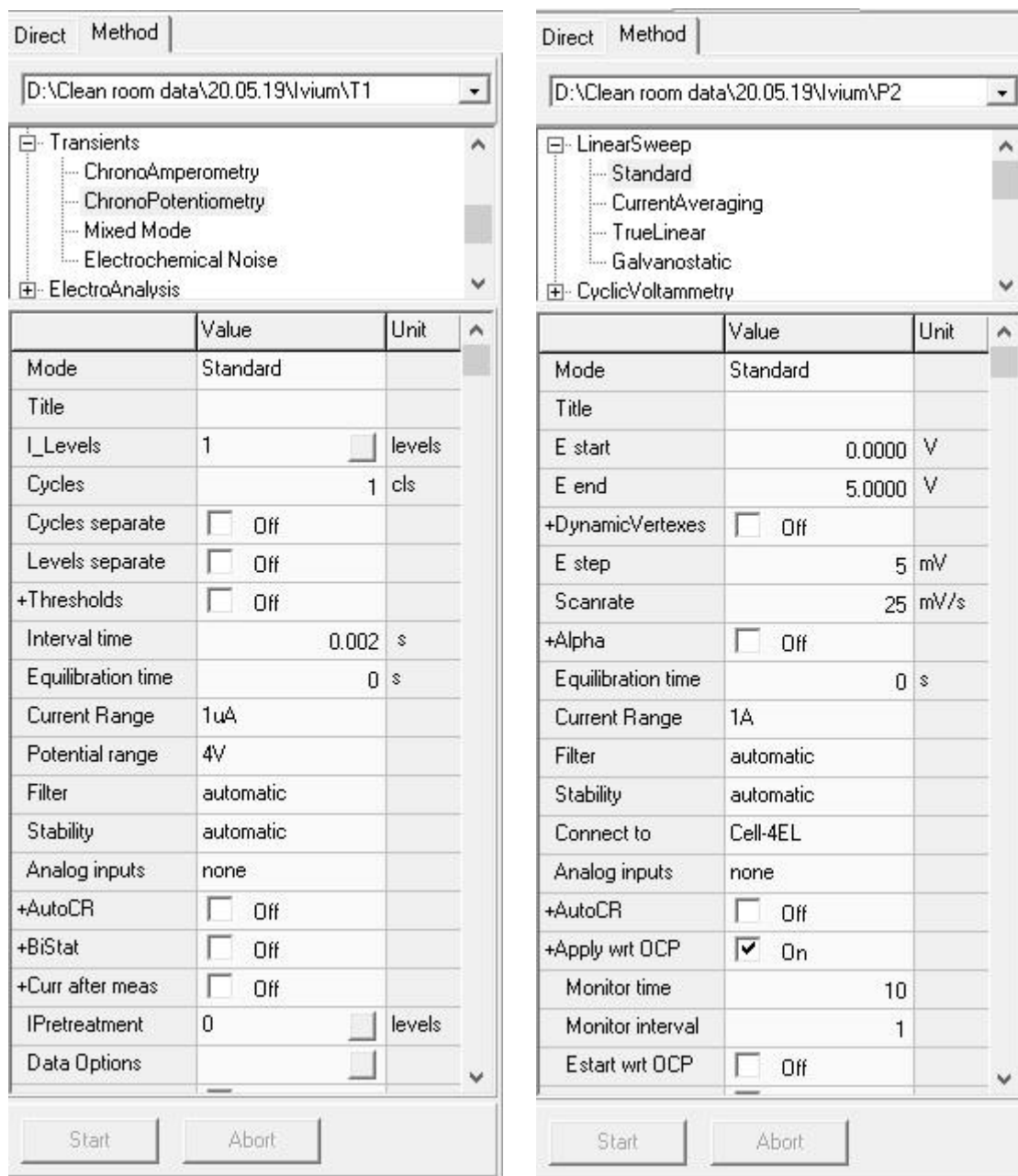


Figure 3-18 Transient mode (left) – Linearsweep mode (right)

This process was repeated for all different levels of the electrolyte concentration, gap sizes and voltage levels. In addition to the mentioned parameters, electrolyte temperature and conductivity were measured as well, also the final current was measured through the polarisation graph.

As part of the investigation and in order to evaluate the workpiece machinability, the machined surfaces were assessed by measuring the weight of the removed materials; also, the effect of the stray current was investigated through the overcut measurement. The machined area was examined using SEM in order to measure the effected surface dimensions. In addition to this, EDS has been used for selected results in order to investigate any changes on the specimen surface due to the machining effects.

It is necessary to be aware of the following points before continuing to the next section:

- The electrolyte was a static solution and there was no flow of the electrolyte.
- Tool electrode was placed at a constant distance from the workpiece (desired gap) and there was no tool feed rate.
 - Voltage applied as steps of voltage with 5mv steps and 25mv/s scan-rate.

3.3.1 NaNO₃ electrolyte (0.3 mole/L), variable voltage, variable gap size

Table 3-2 presents the parameters' details and measured values for 0.3 mole/L electrolyte concentration. Voltage changes from 5 volts up and including 9 volts with 1 volt step. Gap size changes between 20 and 40 μm . The time length for each reaction presented by period (unit is second) in the table 3-2.

Table 3-3 presents the acquired data through the calculations or iviumsoft analysis. In a way, table 3-2 shows machining parameters and the weight of the removed material from the workpiece, and table 3-3 shows the machining quality (overcut) and machining current. The gathered data includes maximum current, average overcut at hole entrance and equivalent resistor value for the transferred charges during the process. Current measured through iviumsoft data (graph) for the applied voltage, overcut was measured through the surface image which was taken and examined by SEM, equivalent resistor

value was calculated by finding the best fit for the polarisation curve. The equivalent resistor is known as “charge transfer resistor” or “faradic resistor” in EDL equivalent circuit.

Voltage	IEG	Period	Temp		Conductivity		Weight		
Final			Initial	Final	Initial	Final	Initial	Final	RM
(Volt)	(μm)	(sec)	($^{\circ}\text{C}$)	($^{\circ}\text{C}$)	(ms)	(ms)	(g)	(g)	(μg)
5	20	200	22	N.R	8.09	N.R	10.98602	10.98598	0.04
5	25	200	22.7	22.9	26.7	17	10.98598	10.98617	-0.19
5	30	200	22	23	12.2	0.983	10.98617	10.98612	0.05
5	40	200	22.2	22.5	28	0.006	10.98612	10.98612	0
6	20	240	21.9	22.9	0.004	1.88	10.98624	10.98607	0.17
6	25	240	21.9	23.1	26	20.5	10.98607	10.98593	0.14
6	30	240	21.8	23	25.8	20.8	10.98593	10.98579	0.14
6	40	240	21.9	23.2	22.6	10.88	10.98579	10.98579	0
7	20	280	24	26.2	17.33	8.39	10.98579	10.98559	0.2
7	25	280	24	23.7	19.69	15.86	10.98559	10.98552	0.07
7	30	280	22.8	24.3	25.6	18.7	10.98552	10.98543	0.09
7	40	280	22.8	24	18.29	11.6	10.98543	10.98521	0.22
8	20	320	22.2	25.4	18.96	8.28	10.98263	10.9822	0.43
8	25	320	22.3	24.6	25.4	21.2	10.9822	10.98185	0.35
8	30	320	22.4	25.3	21.3	6.96	10.98483	10.98453	0.3
8	40	320	22.4	25.1	24.5	17.63	10.98453	10.98427	0.26
9	20	360	22.4	26.6	26.9	27.5	10.98413	10.98389	0.24
9	25	360	22.1	26	26.5	17.55	10.98389	10.9834	0.49
9	30	360	22.3	26.1	27.2	20.9	10.9834	10.98304	0.36
9	40	360	22	26.1	26	22.8	10.98304	10.98263	0.41

*N.R: No data was recorded

Table 3-2: Experimental data for 0.3 mole/L NaNO₃

In order to measure the rate of removed materials from workpiece electrode, workpiece was weighted before and after the reaction using laboratory weighting device (Mettler AE200MC). Measurement has been repeated up to a maximum of five times to find the reproducible weight within 0.1mg. MR (material removed) shows the weight of the removed materials which was calculated from weighting results; MRR shows the material removal rate which was calculated by MR divided by the reaction period.

Voltage	IEG	Period	Current	Resistance	MR	Overcut
Final			Max	Charge Transfer	Rate	average
(Volt)	(μm)	(sec)	(mA)	(Ω)	($\mu\text{g/s}$)	(μm)
5	20	200	61.68	59.55	2.00000E-04	24.5
5	25	200	65.69	56.03	-9.50000E-04	19
5	30	200	76.82	52.06	2.50000E-04	41.5
5	40	200	65.08	49.71	0.00000E+00	0
6	20	240	112.2	27.66	7.08333E-04	171.5
6	25	240	141.4	21.56	5.83333E-04	120.5
6	30	240	123.6	24.29	5.83333E-04	139.5
6	40	240	112.7	26.87	0.00000E+00	104
7	20	280	151.6	31.45	7.14286E-04	122
7	25	280	168.9	29.53	2.50000E-04	127
7	30	280	155.9	31.07	3.21429E-04	181
7	40	280	151.4	32.56	7.85714E-04	152
8	20	320	191.5	29.7	1.34375E-03	168.5
8	25	320	206.8	27.66	1.09375E-03	147
8	30	320	202	27.71	9.37500E-04	164.5
8	40	320	205.4	28.12	8.12500E-04	191.5
9	20	360	247.7	26.32	6.66667E-04	275
9	25	360	231.5	28.46	1.36111E-03	260
9	30	360	237.5	28	1.00000E-03	247
9	40	360	253.4	25.93	1.13889E-03	219.5

Table 3-3: Measured and calculated values (0.3 mole/L)

Each group of the following images shows the relevant polarisation graph and the effect of the process on the workpiece for 0.3 mole/L electrolyte concentration, one voltage level and four different gap sizes.

The linearsweep experiment was repeated for gap sizes of 20, 25, 30 and 40 μm when the end voltage was set on 5Volt. The anodic reaction did not take place when the gap increased to the 40 μm and therefore, the workpiece surface did not present any changes. Also, as SEM images show, the average of the overcut is much less in comparison with the following experiments when the end voltage level increases. This was

expected as the time increases by the rise in the end voltage level while the gap does not change. So instead of any increase in the depth of the created hole, the sides of the machined zone were increased. This has been considered as overcut in comparison with the tool surface area. Overcut and the weight of the removed material from the zone, were used, later in this chapter to find the best combination for the machining parameters.

Figure 3-19 presents the collected results when 5 volts applied for the 20, 25 and 30 μm IEG gap.

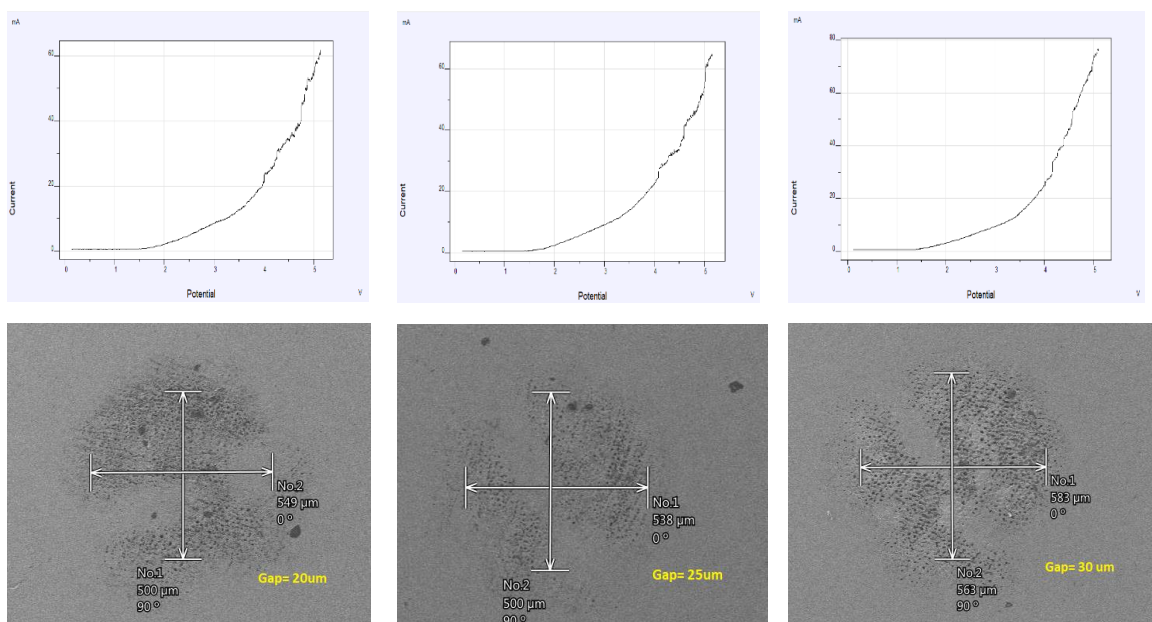


Figure 3-19: Polarisation graph & related SEM image (5V, 20, 25, 30 μm)

Figure 3-20 shows the voltage-current relation for 5 volts and 40 μm IEG gap when the anodic reaction did not take place. There are couple of changes between this graph and previous graphs in figure 3-19. Current rise had a smoother and linear trend when anodic reaction took place between 2 and 4 volts and a sharper jump after 4 volts. That jump was the point the anodic reaction speeded up. While in the fourth state, the current had a slower increase and showed a linear increase after 3 volts; although there are two rises after approximately 4.5 volts, but the environment was not suitable for the anodic reaction to happen.

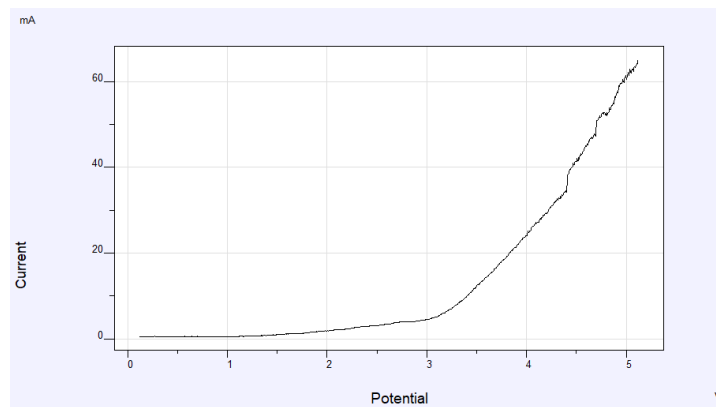


Figure 3-20: Polarisation graph for 0.3 mole/L NaNO₃, 5 volts and 40 µm gap

When 6 volts was selected as the end voltage level, gap 25 and 40 µm presented better machinability in combination with the voltage level. The surface showed better roughness, although the weight of the removed material for the 40 µm gap was negligible. Figure 3-21 and 3-22 demonstrate the polarisation curves and work piece surface for combination of 6Volts, 0.3 mole/L concentration and four different gap sizes.

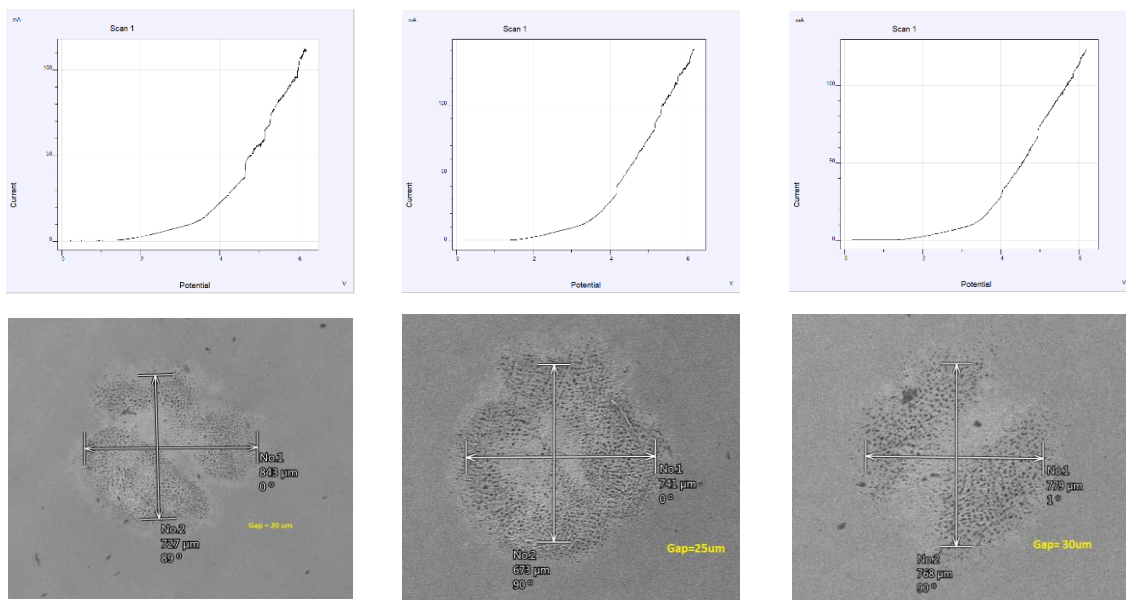


Figure 3-21: Polarisation graph & related SEM image (6 V, 20, 25, 30 µm)

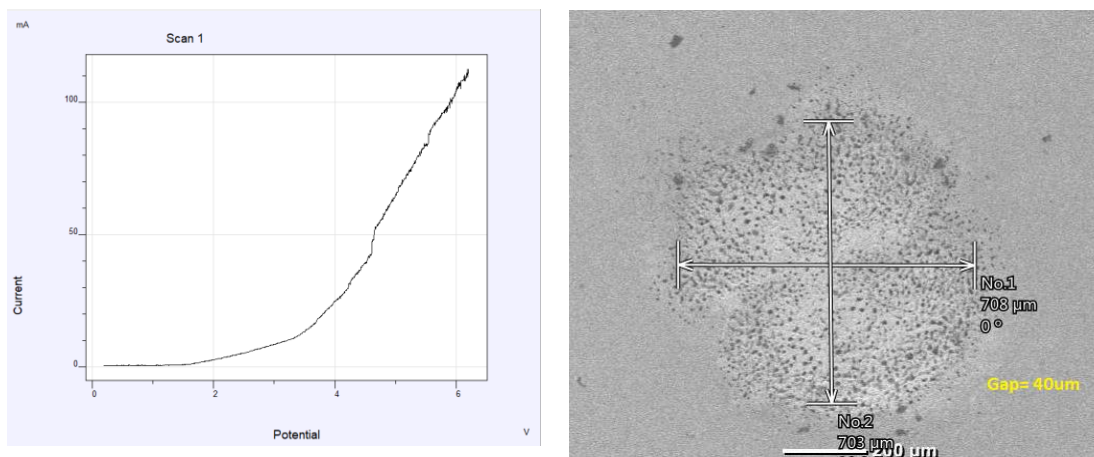


Figure 3-22: Polarisation graph & related SEM image (6 V, 40 μm)

The acquired results for 7 volts level present that the combination of 7 volts and 0.3 mole/L electrolyte concentration for all selected gap sizes, were among the weakest results. The removed materials for this voltage level was the minimum between all voltage levels while the overcut area was quite high for the volume of removed materials. (Figure 3-23, 3-24)

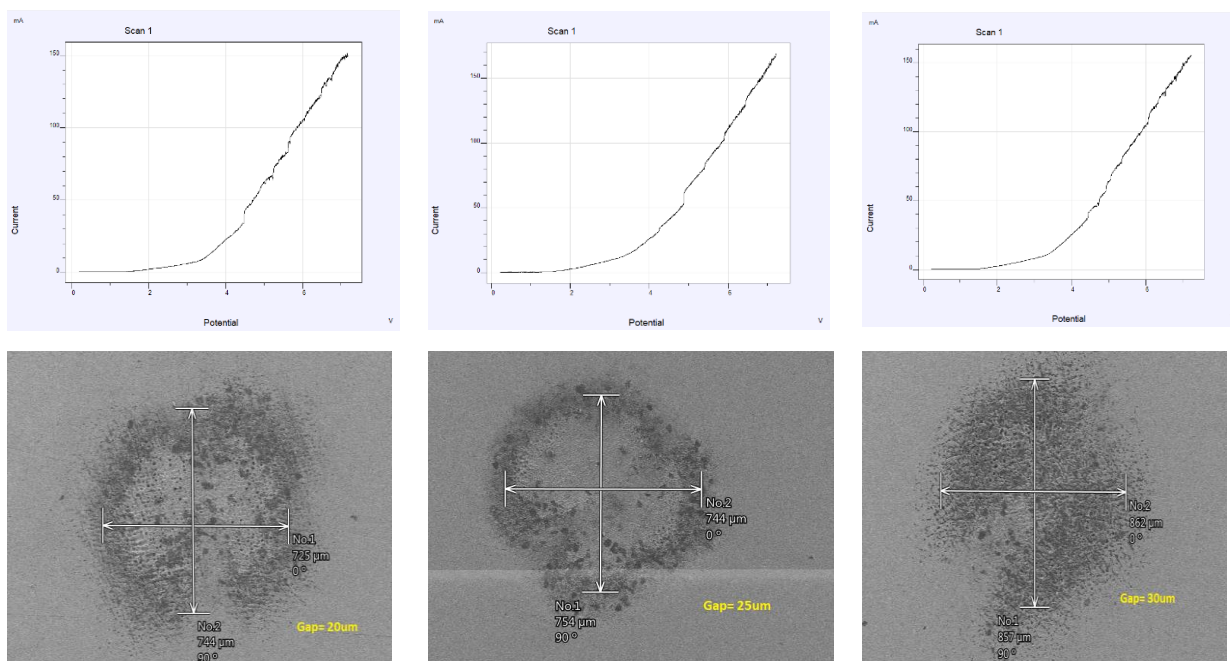


Figure 3-23: Polarisation graph & related SEM image (7 V, 20, 25, 30 μm)

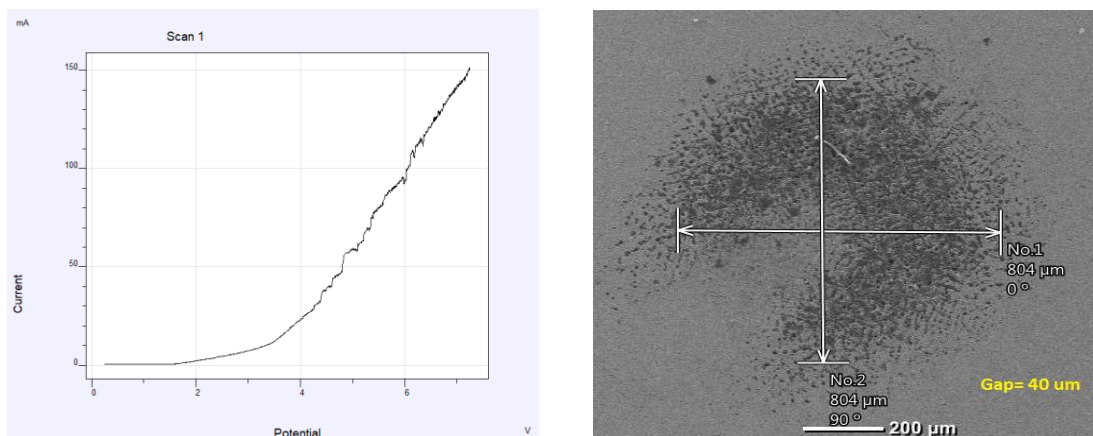


Figure 3-24: Polarisation graph & related SEM image (7 V, 40 μm)

Figure 3-25 and 3-26 show that the combination of 8 volts and 20 μm gap size was the only set experiencing short circuit, however the system managed to back to normal condition and the process continued normally for the whole period. Considering the SEM images and calculated removed material and overcut, confirm that the combination of 8 volts with 0.3 mole/L electrolyte concentration regardless the gap size has generated the best results.

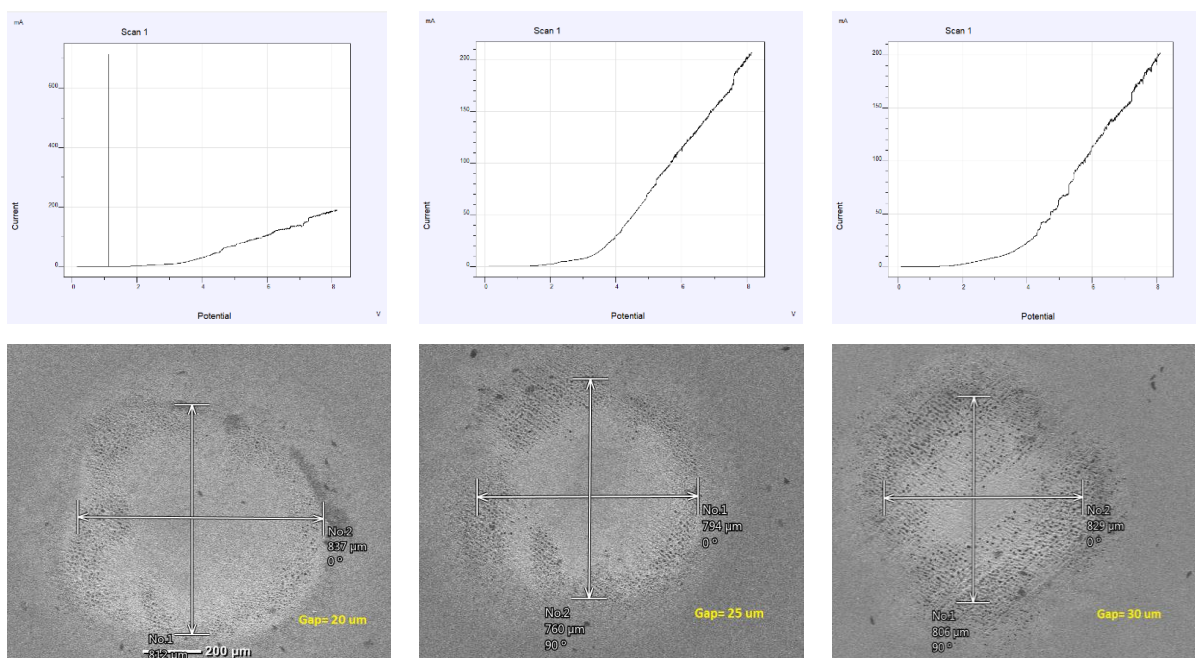


Figure 3-25: Polarisation graph & related SEM image (8V, 20, 25, 30 μm)

Although the overcut is higher than previous voltage levels, it is less than similar parameter for 9 volts level.

Despite the occurred short circuit at 20 μm gap in which current level reached to the highest value of 700 mA, there is no sign of any significant damage on the surface. Between four possible parameters' combination for 8 volts level, the 25 μm gap size, generated the optimum results.

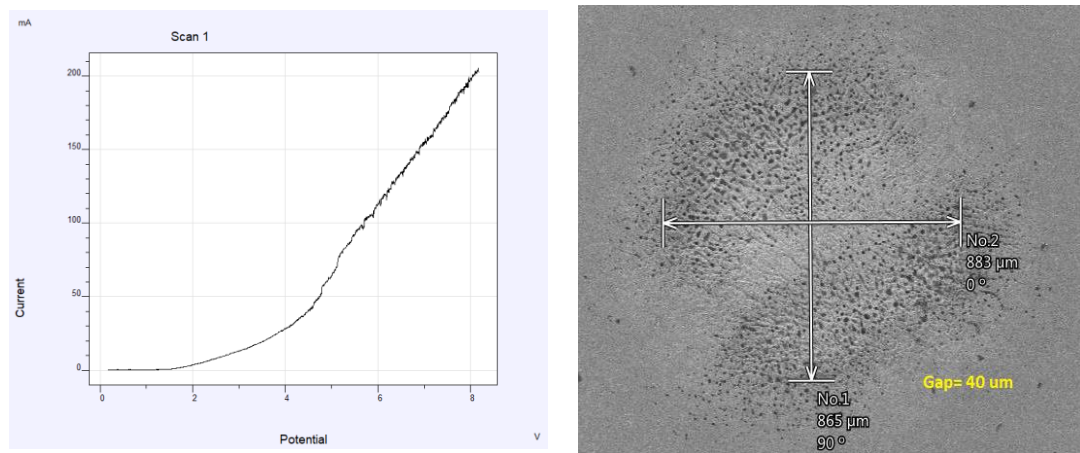


Figure 3-26: Polarisation graph & related SEM image (8 V, 40 μm)

It is expected that 9 volts generate the highest current level and perhaps create the maximum removal material levels. Polarisation curves and measured current levels, confirm this expectation; however, the material removal level considering the overcut on surface does not meet the expectations. Average overcut size for 9 volts was 250 μm which showed 49% increase from average overcut for 8 volts level while the average material removal only increases by 11% from 0.335 μg for 8 volts to the 0.375 μg for the 8 volts. In addition to this, the process for 9 volts took place 40 seconds longer. These observations prove that 9 volts level is not creating an optimised combination for the selected machining parameters.

Figure 3-27 & 3-28 present the graphs and SEM images for the 9 volts level and four different IEG sizes.

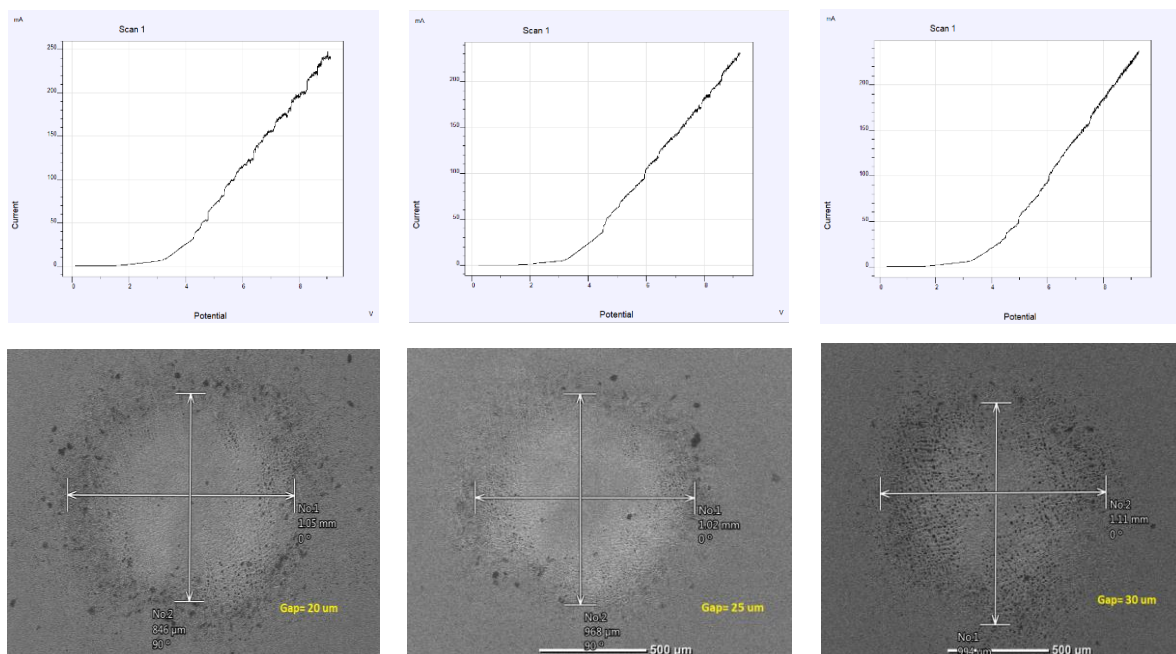


Figure 3-27: Polarisation graph & related SEM image (9V, 20, 25, 30 μm)

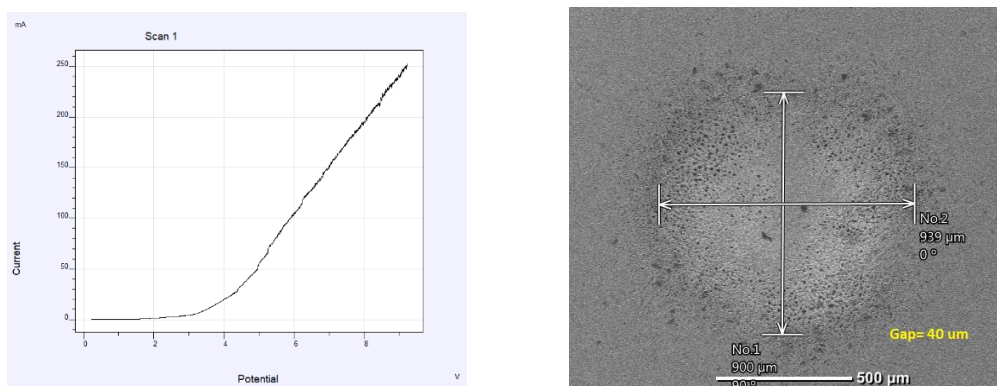


Figure 3-28: Polarisation graph & related SEM image (9 V, 40 μm)

In terms of charge transfer resistance, 6, 8 and 9 volts presented similar resistance values; 5-volt level had the maximum resistance value for charge transfer equivalent resistor by great difference and 7 volts presented the second-high value for the charge transfer resistivity.

Charge transfer resistor is the parallel element with EDL capacitor in equivalent circuit for μ ECM electrode-electrolyte interface (figure 3-6). Its effect in μ ECM process will be discussed in detail in chapter four.

MRR shows the rate of the removed materials from workpiece surface but it does not necessary shows the performance of the process. Material can be removed from the target surface (under the tool surface area) or from surrounding area outside the target zone. The latter is the removed material under the effect of the eddy current and is considered as overcut.

Therefore, MRR and overcut should be compared jointly when the performance of the process is under the evaluation.

Figure 3-29 shows the MRR during the experiments using 0.3 mole/L electrolyte concentration. As the chart shows, 5 volts has not been an optimum voltage level for this process, 6 and 7 volts present similar level for MRR and 8 and 9 volts show a jump in MRR level.

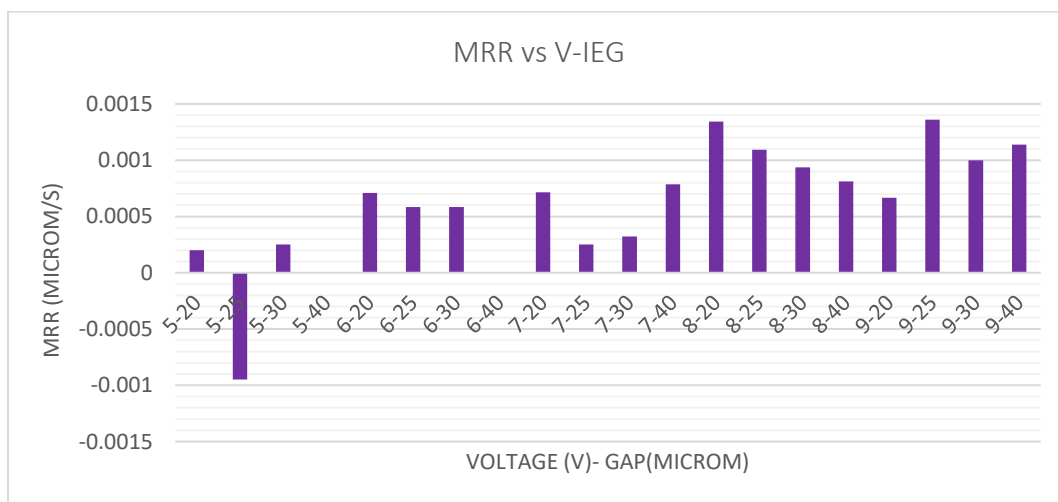


Figure 3-29: MRR (0.3 mole/L NaNO₃)

Considering the chart in figure 3-30 which shows the average overcut at each experiment, it is noticeable that increased voltage level has increased the average overcut. But between 6, 7 and 8 volts, average overcut showed less increase. General

speaking smaller gap size can generate higher overcut level as the current density increases sharply. This is visible for all but 5 volts.

Comparing both graphs in figure 3-29 and 3-30 (simultaneously) leads to the conclusion that the best results for MRR (maximum) and overcut (minimum) achieved for the voltage level equal to 8 volts. For this level, the effect of the eddy current has been less in terms of removing materials outside the reaction zone.

The range of overcut for 7 and 9 volts are very high in comparison with 8 volts and it makes the MRR level unreasonable for these two voltage levels.

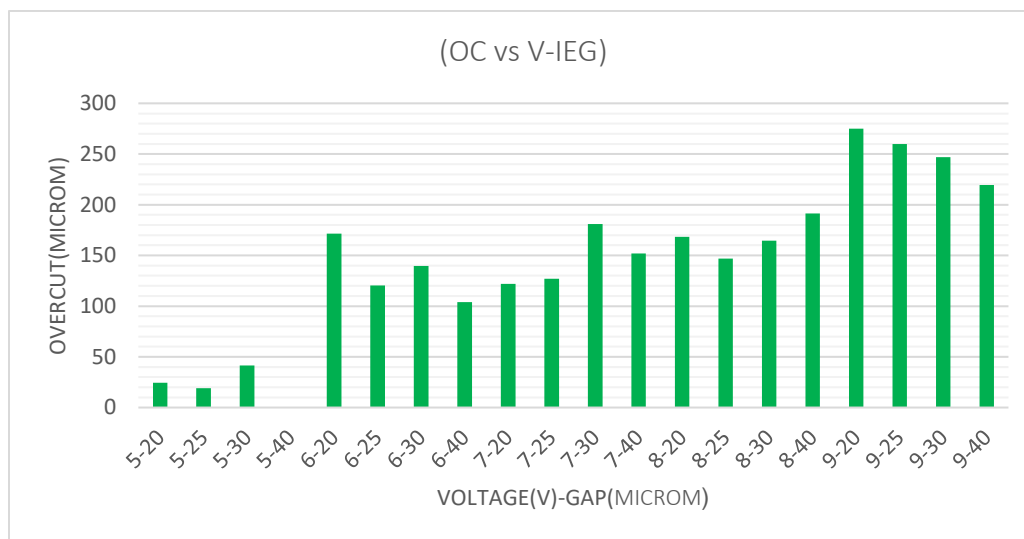


Figure 3-30: Overcut (0.3 mole/L NaNO₃)

3.3.2 NaNO₃ electrolyte (0.5 mole/L), variable voltage, variable gap size

Similar experiments were repeated for the 0.5 mole/L NaNO₃ electrolyte concentration. Table 3-4 presents the parameters' details and measured values. Voltage varies from 5 volts up and including 9 volts with 1-volt step. Gap size changes between 20 and 40 μm for each voltage level. The changes in electrolyte temperature and conductivity have been monitored as well.

Voltage	IEG	Period	Temp		Conductivity		Weight		
Final			Initial	Final	Initial	Final	Initial	Final	RM
(Volt)	(μm)	(sec)	($^{\circ}\text{C}$)	($^{\circ}\text{C}$)	(ms)	(ms)	(g)	(g)	(μg)
5	20	200	22.3	22.3	N.R	N.R	N.R	10.97241	N.R
5	25	200	23.3	23.6	41.5	37.4	10.97241	10.97232	0.09
5	30	200	22.9	23.2	41.9	40.2	10.97232	10.97244	-0.12
5	40	200	22.6	22.7	42.2	36.9	10.97244	10.97244	0
6	20	240	22.6	23	42.3	24.6	10.97244	10.97233	0.11
6	25	240	22.7	23.2	42.5	24.8	10.97233	10.97215	0.18
6	30	240	22.9	23	39	34.3	10.97215	10.97204	0.11
6	40	240	23.2	23.4	42.2	32.4	10.97204	10.97198	0.06
7	20	280	22.5	24.1	41.6	40.7	10.97198	10.97185	0.13
7	25	280	22.5	24.1	41.9	24.9	10.97185	10.97138	0.47
7	30	280	22.7	24.2	32.3	12	10.97138	10.97123	0.15
7	40	280	22.5	24.6	42.4	26.2	10.97123	10.97102	0.21
8	20	320	22.6	26.1	41.2	18.45	10.97102	10.97044	0.58
8	25	320	22.9	26	36.5	13.92	10.97044	10.96981	0.63
8	30	320	22.4	25.5	37.7	14.03	10.96981	10.96942	0.39
8	40	320	22.5	25.6	27.3	18.83	10.96942	10.96926	0.16
9	20	360	22.3	26.4	41.4	37	10.91361	10.91313	0.48
9	25	360	22.2	27.9	40.3	35.1	10.91313	10.91235	0.78
9	30	360	21.7	28.9	13.5	7.52	10.91235	10.91159	0.76
9	40	360	22.5	29	42	27.9	10.91159	10.91091	0.68

Table 3-4: Experimental data for 0.5 mole/L NaNO₃

Data for initial weight and conductivity was not recorded for 5 volts and 20 μm , so the MR data was not calculated.

Table 3-5 presents the acquired data through the calculations or iviumsoft analysis. The gathered data includes maximum current, average overcut at hole entrance and equivalent resistor value for the transferred charges during the process. Current was measured through the iviumsoft data (graph) for the applied voltage, equivalent resistor value was calculated by finding the best fit for the polarisation curve and the overcut was measured on the studied images through SEM.

Voltage	IEG	Period	Current	Resistance	MR	Overcut
Final			Max	Charge Transfer	Rate	average
(Volt)	(μm)	(sec)	(mA)	(Ω)	($\mu\text{g/s}$)	(μm)
5	20	200	71.57	31.56	0.00000E+00	45.5
5	25	200	62.14	35.72	4.50000E-04	28.5
5	30	200	55.34	45.38	-6.00000E-04	29.5
5	40	200	55.96	46.62	0.00000E+00	0
6	20	240	121.3	26.33	4.58333E-04	118.5
6	25	240	125.6	25.71	7.50000E-04	104.5
6	30	240	119.6	27.29	4.58333E-04	149
6	40	240	112.5	32.04	2.50000E-04	163.5
7	20	280	161.8	24.42	4.64286E-04	142.5
7	25	280	168.1	22.75	1.67857E-03	157.5
7	30	280	169.4	24.23	5.35714E-04	154
7	40	280	195.2	20.02	7.50000E-04	244
8	20	320	248.6	20.45	1.81250E-03	260
8	25	320	248.2	19.68	1.37500E-03	227
8	30	320	257.4	19.43	1.21875E-03	365
8	40	320	232.1	21.77	5.00000E-04	360
9	20	360	272	22.65	1.33333E-03	500
9	25	360	367.7	16.12	2.16667E-03	515
9	30	360	386.6	15.46	2.11111E-03	505
9	40	360	399.4	15.13	1.88889E-03	505

Table 3-5: Measured and calculated values (0.5 mole/L)

Similar to the experience for the 5 volts and 0.3 mole/L electrolyte concentration, when 5 volts was applied for the gap size of the 40 μm , the anodic reaction did not take place and therefore, no changes was observed on the workpiece surface. Although the current level was increased up to 55.96 mA, it was not enough to activate the electrode-electrolyte interface reaction. Charge transfer resistor reached the highest level for the 5 volts at this gap size and no anodic reaction took place. The machined surface roughness was the best when gap size was 25 μm although the overcut was at its maximum for 5 volts at this gap size.

Figure 3-31 presents the polarisation graphs and SEM images for the reaction results when 5 volts was applied to the cell. The graph in figure 3-32 shows that the current

was not as smooth as it was in previous experiments (smaller gap sizes) and it showed a sudden jump at 4.5 volts, but the condition of the reaction was not suitable to activate the anodic reaction.

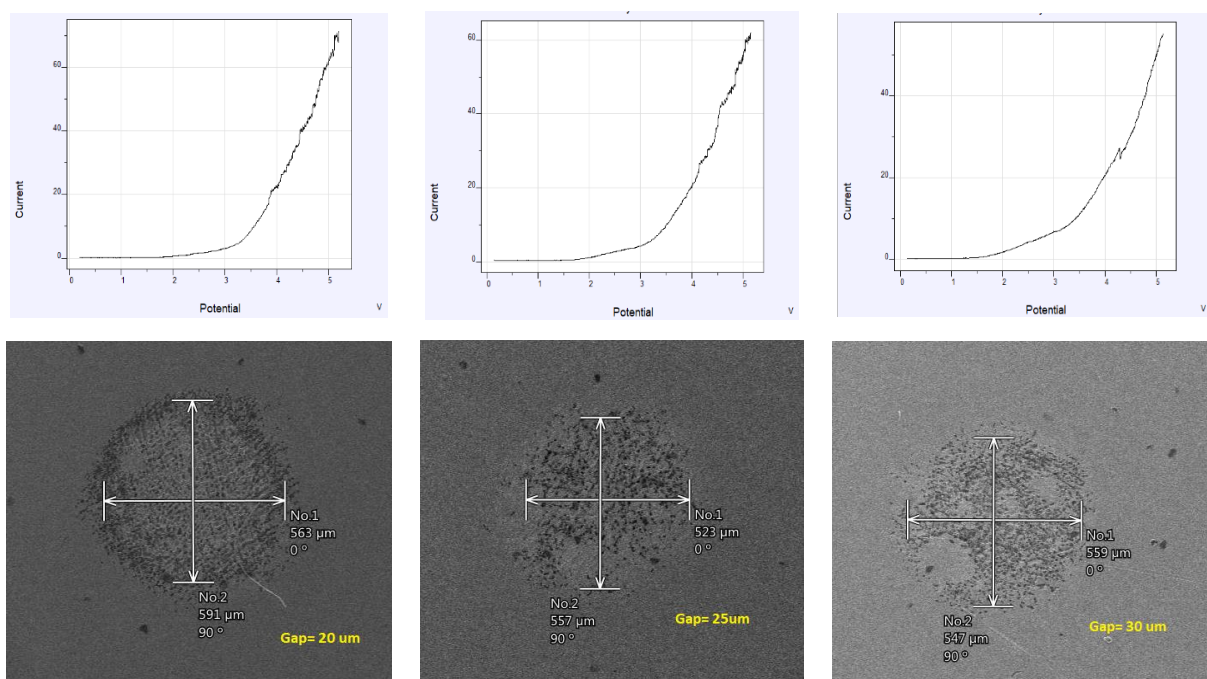


Figure 3-31: Polarisation graph & related SEM image (5V, 20, 25 & 30 μm)

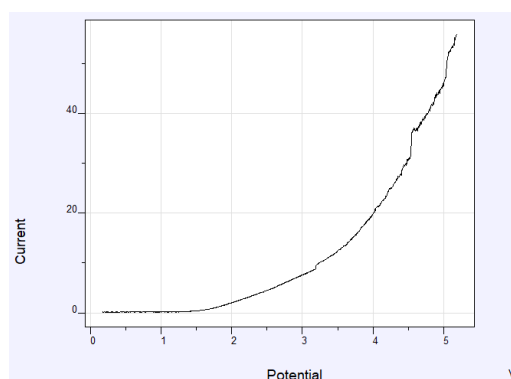


Figure 3-32: Polarisation graph (5V, 40 μm)

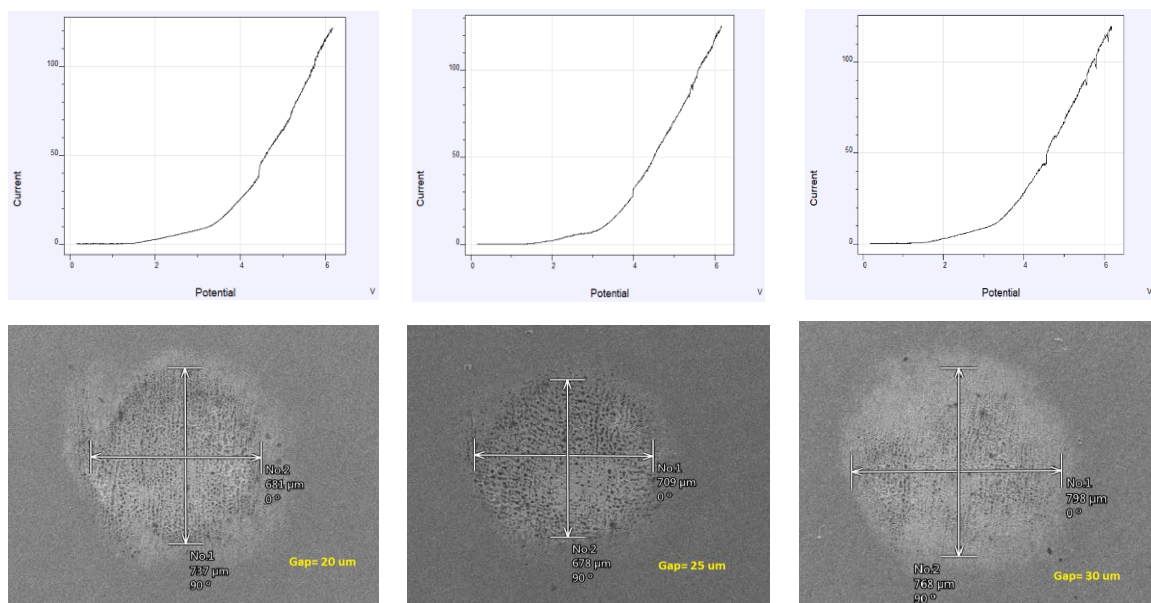


Figure 3-33: Polarisation graph & related SEM image (6V, 20, 25, 30 μm)

Surface roughness and quality of the machined surface with 6 volts (end voltage) seemed to be among the best results for the 0.5 mole/L electrolyte concentration experiments. With 6 volts voltage, the best results achieved for the gap size of 25 μm , while 20 and 30 μm showed similar behaviour and 40 μm gap size had the lowest MRR while it presented the highest overcut and stray currents effect. (Figure 3-33 & 3-34)

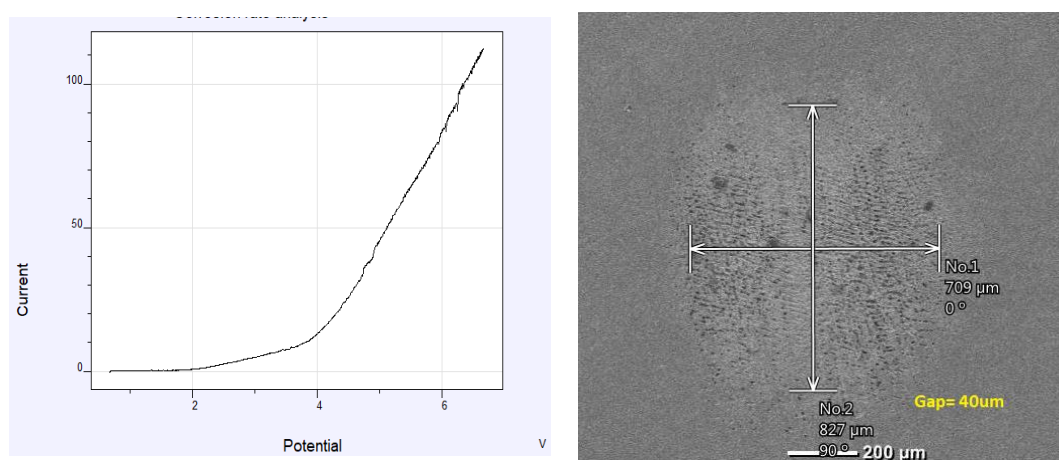


Figure 3-34: Polarisation graph & related SEM image (6V, 40 μm)

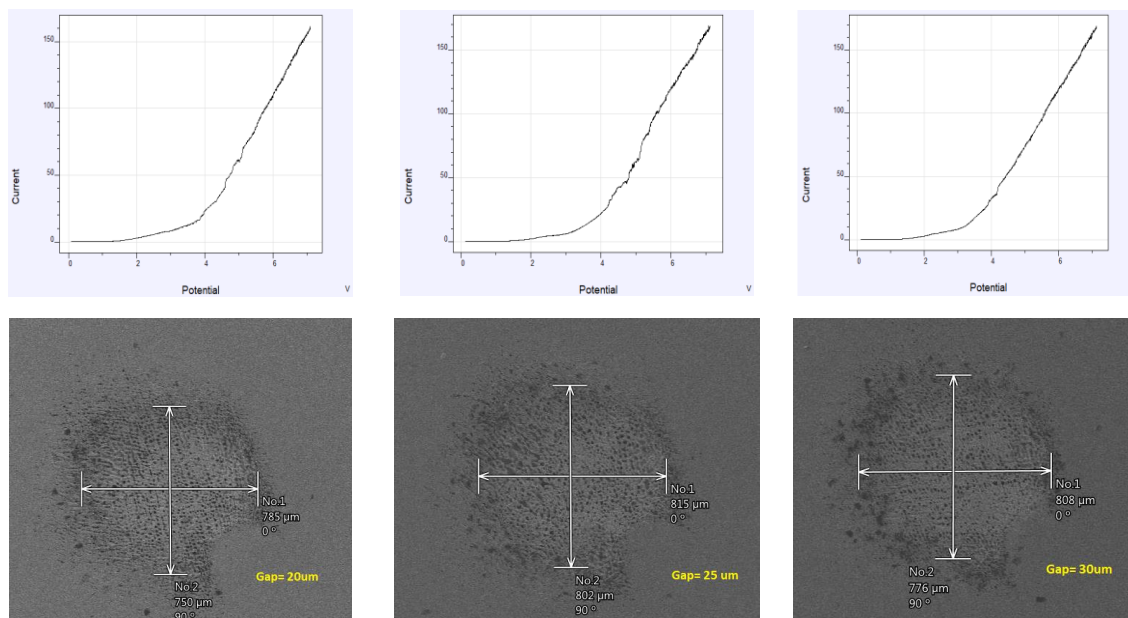


Figure 3-35: Polarisation graph & related SEM image (7V, 20, 25, 30 μm)

As figure 3-35 & 3-36 present, 7 volts voltage level in combination with 0.5 mole/L electrolyte concentration generated acceptable results in comparison with the combination of 7 volts and 0.3 electrolyte concentration. For 0.5 mole/L concentration, 7 volts voltage and 6 volts voltage produced similar results in terms of figures and measures. Best MRR rate was achieved for the 25 μm gap size between electrodes.

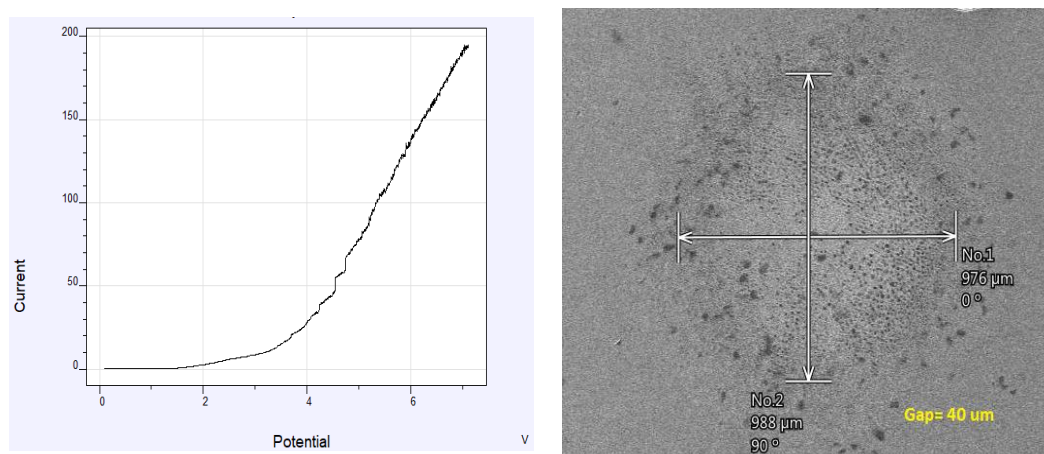


Figure 3-36: Polarisation graph & related SEM image (7V, 40 μm)

Although the MRR rate was relatively better for the 40 μm gap size in combination with 7 volts, the overcut was suddenly increased by nearly 50% and made the 40 μm gap size an unrealistic option.

Like the 0.3 mole/L electrolyte concentration, the combination of 8 volts and 0.5 mole/L concentration produced quite acceptable end results. The best MRR was observed for the 20 μm gap, while the 25 μm generated lower MRR and lower overcut. The effect of the stray currents was increased sharply for the gap sizes at 30 and 40 μm and resulted in unproportioned removed material considering the overcut rate. (Figure 3-37)

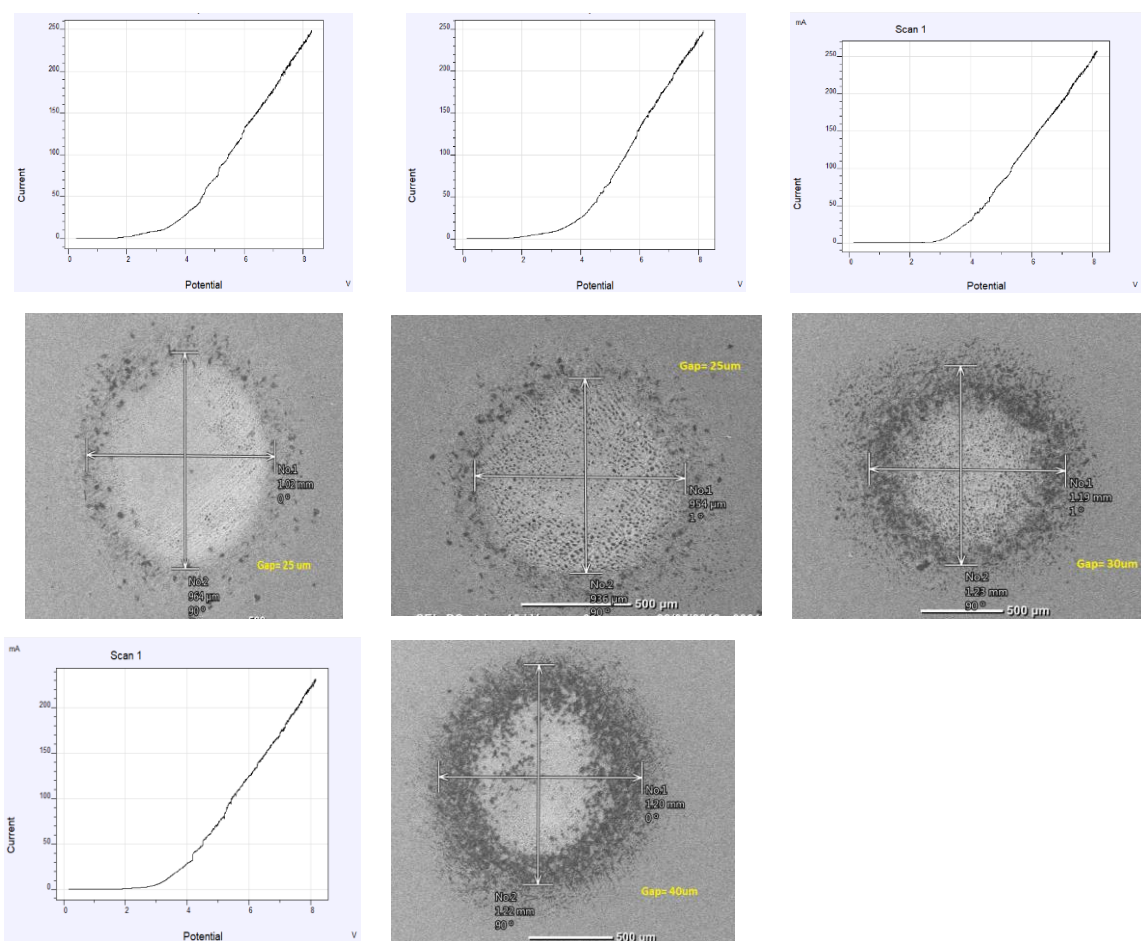


Figure 3-37: Polarisation graph & related SEM image (8volts)

Finally, 9 volts relatively generated acceptable material removal rate but the overcut went up to 200% increase from 8 volts; therefore, the combination of 9 volts and 0.5 mole/L electrolyte concentration is out of the question with regards to the stray current effect.(Figure 3-38)

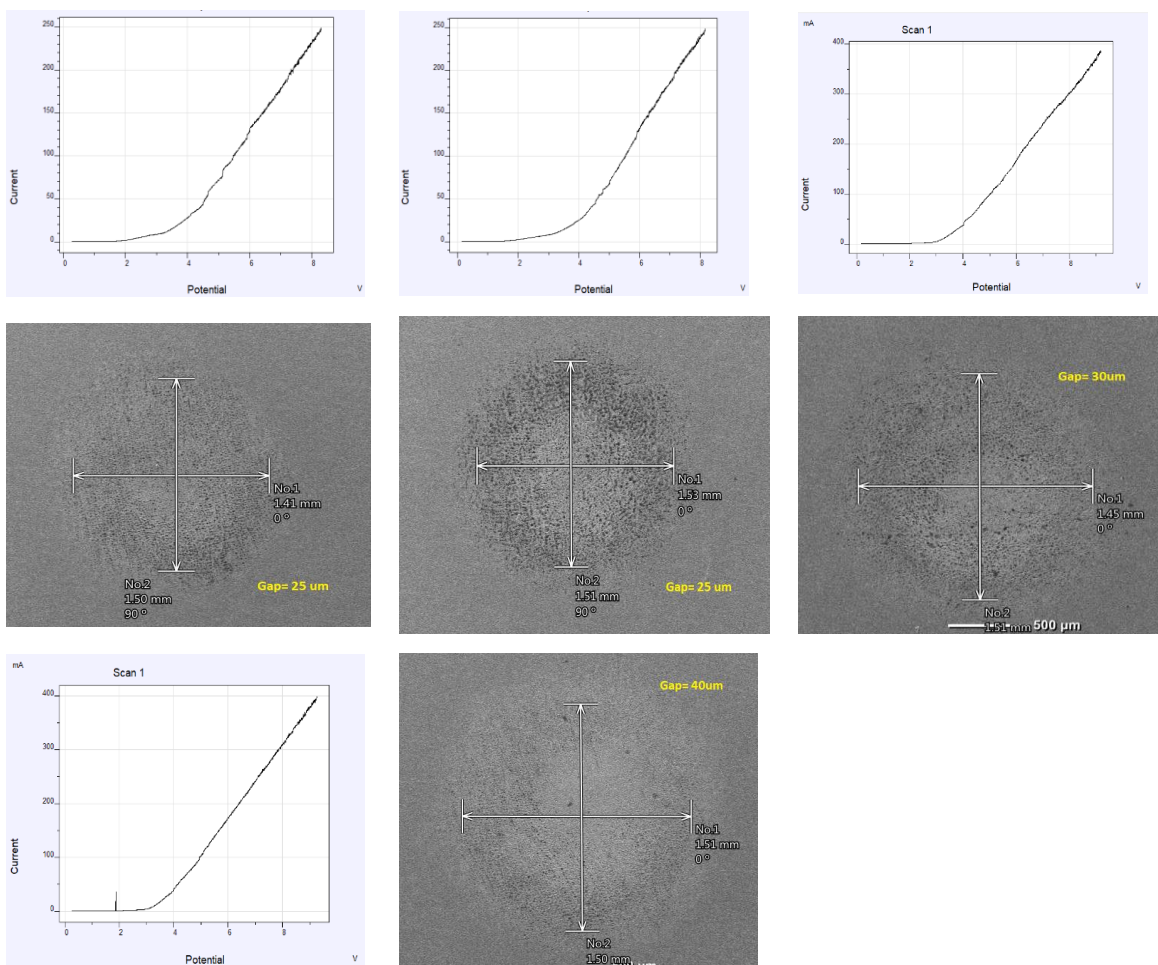


Figure 3-38: Polarisation graph & related SEM images (9 volts)

In general, charge transfer resistance showed smooth change from 5 volts to 9 volts and decreased from nearly 46 Ω at 40 μm gap and 5 volts to the lowest value equal to 15 Ω at 9 volts and 40 μm gap size. But the change trend for the voltage levels was different. For 5- and 6-volts, charge transfer resistance value has increased with the rise in the gap size, but from 7 volts to 9 volts, charge transfer resistance gradually showed

lower values at higher voltage levels. That explains the different behaviour for 7 volts voltage between 0.3 and 0.5 mole/L electrolyte concentration.

Following the experiments for the 0.5 mole/L electrolyte concentration, figure 3-39 and 3-40 illustrate the calculated MRR and the overcut for these experiments.

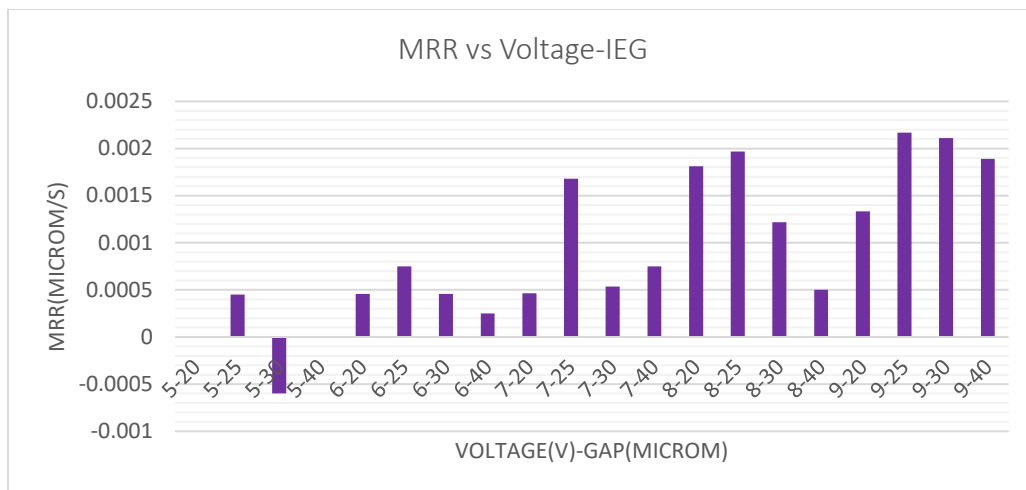


Figure 3-39: MRR (0.5 mole/L NaNO₃ electrolyte)

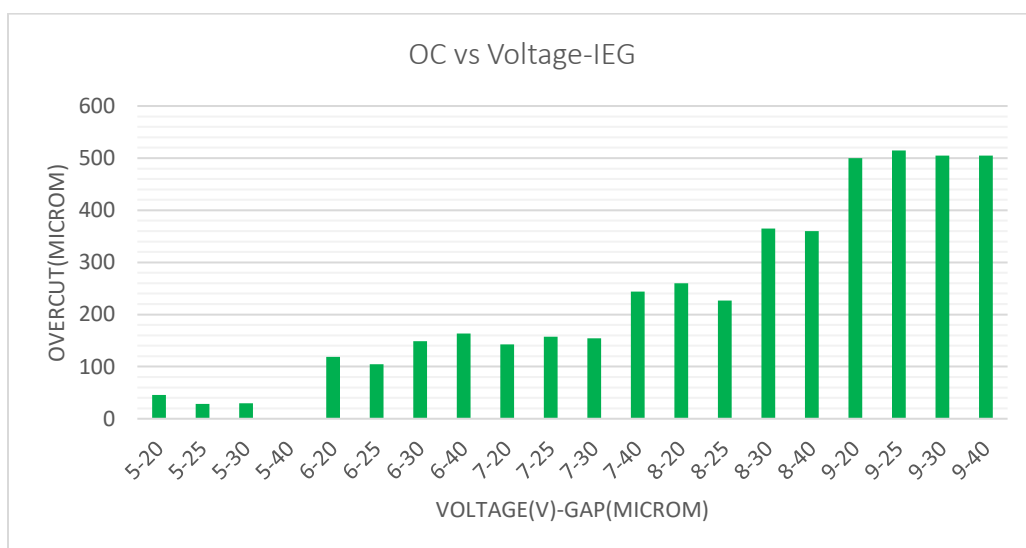


Figure 3-40: Overcut (0.5 mole/L NaNO₃ electrolyte)

The MRR chart shows very small material removal rate for 6 volts level and a considerable jump for the voltages greater than that. However, the efficiency of the voltage levels in terms of MRR should be concluded by comparing the OC results.

Average overcut shows gradual rise when voltage has been increased (figure 3-40). The difference between overcut at 6 volts and 7 volts is not significant, although MRR was noticeably different between these two voltage levels. Also, OC has increased sharply from 8 volts to the 9 volts; this shows that 9 volts is not optimum level for 0.5 mole/L concentration either. Considering OC and MRR simultaneously, would bring the 7voltes-25 μm and 8 volts-25 μm as the best sets for 0.5 mole/L concentration.

3.3.3 NaNO₃ electrolyte (1.0 mole/L), variable voltage, variable gap size

Voltage Final (Volt)	IEG (μm)	Period (sec)	Temp		Conductivity		Weight		
			Initial ($^{\circ}\text{C}$)	Final ($^{\circ}\text{C}$)	Initial (ms)	Final (ms)	Initial (g)	Final (g)	RM (μg)
5	20	200	21.6	22.3	79.3	35.3	10.8983	10.89826	
5	25	200	20.9	22.1	75.3	41.9	10.89826	10.8982	0.06
5	30	200	20.9	22	79	55.7	10.8982	10.89813	0.07
5	40	200	21.6	22.5	76.7	62.1	10.89813	10.89807	0.06
6	20	240	21.6	22.8	82	66.6	10.8977	10.89767	0.03
6	25	240	21.3	22.7	78.9	44	10.89767	10.89753	0.14
6	30	240	21.5	22.6	82.4	82.4	10.89753	10.89734	0.19
6	40	240	21.5	22.6	81.7	65.5	10.89734	10.89716	0.18
7	20	280	21.5	23.1	82.1	73.3	10.89716	10.89685	
7	25	280	21.5	23.6	72.2	41.8	10.89685	10.8964	0.45
7	30	280	21.4	24.2	63.1	31.1	10.8964	10.89583	0.57
7	40	280	21.6	24.1	69.3	34.4	10.89583	10.89544	0.39
8	20	320	21.7	26	79	51.6	10.89544	10.89455	0.89
8	25	320	20.4	25.8	73.8	61	10.89455	10.89367	0.88
8	30	320	21.3	25.3	79.4	69.9	10.89367	10.89282	0.85
8	40	320	21.3	25.2	80.5	78	10.89282	10.8917	1.12
9	20	360	21.2	26.9	66.1	54	10.8917	10.89059	1.11
9	25	360	21.4	27.5	80.9	69.3	10.89059	10.88919	1.4
9	30	360	21.3	27.9	64.9	40.9	10.88919	10.88822	0.97
9	40	360	21.3	28.3	55.6	25.2	10.88822	10.88708	1.14

Table 3-6: Experimental data for 1.0 mole/L NaNO₃

Final set of experiments for this stage was based on 1.0 mole/L NaNO₃ electrolyte concentration and same voltage range and gap sizes. Table 3-6 summarises the applied parameters and measured values. Also, table 3-7 presents the acquired data through the calculations or iviumsoft analysis for this group of experiments.

Voltage Final (Volt)	IEG (μm)	Period (sec)	Current Max (mA)	Resistance Charge Transfer (Ω)	MR Rate ($\mu\text{g/s}$)	Overcut Average (μm)
5	20	200	59.51	33.78	0.00000E+00	35.5
5	25	200	107.3	18.93	3.00000E-04	105
5	30	200	101.2	20.69	3.50000E-04	129
5	40	200	117	17.47	3.00000E-04	185.5
6	20	240	146.5	20.21	1.25000E-04	220
6	25	240	150.1	19.72	5.83333E-04	280
6	30	240	165	17.92	7.91667E-04	290
6	40	240	146.5	21.38	7.50000E-04	335
7	20	280	199.8	20.2	1.10714E-03	380
7	25	280	208.5	19.66	1.60714E-03	475
7	30	280	255.1	16.12	2.03571E-03	450
7	40	280	227.8	17.9	1.39286E-03	470
8	20	320	308.6	15.73	2.78125E-03	535
8	25	320	305.6	16.73	2.75000E-03	445
8	30	320	287.3	17.71	2.65625E-03	670
8	40	320	315.2	16.19	3.50000E-03	1140
9	20	360	378.9	16.18	3.08333E-03	625
9	25	360	401.9	14.65	3.88889E-03	770
9	30	360	402.8	14.99	2.69444E-03	635
9	40	360	361.9	16.51	3.16667E-03	705

Table 3-7: Measured and calculated values (1.0 mole/L)

1 mole/L electrolyte concentration was strong enough to activate the anodic reaction when 5 volts applied at the 40 μm gap size. The maximum current level was very high in comparison with 0.3 and 0.5 mole/L concentration and that explains the sharp increase in overcut. Although the MRR was not so great for lower voltage levels including 5 volts, the overcut rate was relatively high, and the surface roughness was declined

considerably. Figure 3-41 shows the results for the combination of 5 volts and all four different gap sizes.

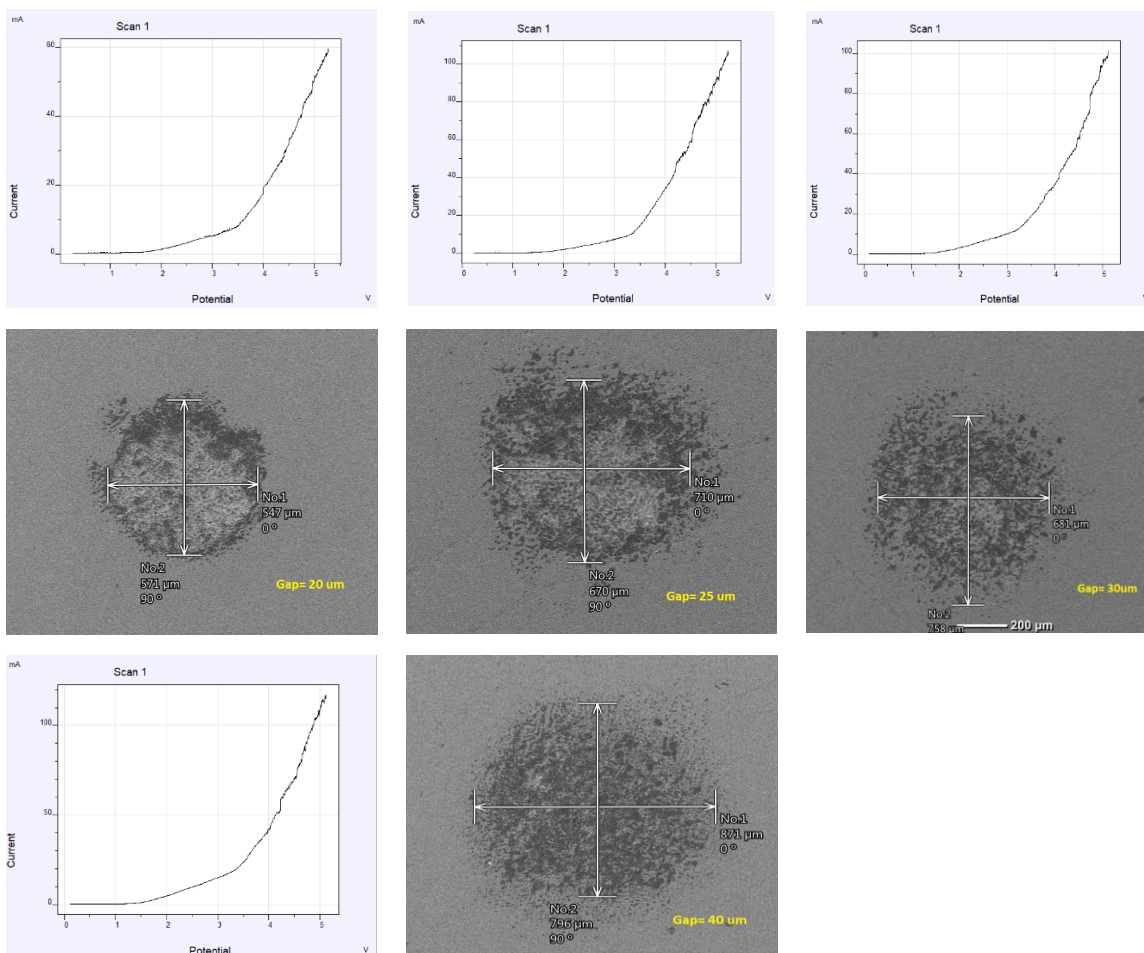


Figure 3-41: Polarisation graph & related SEM image (5 volts)

For the combination of 6 volts and 1 mole/L electrolyte concentration (figure 3-42), MRR result was in the same range as 0.3 and 0.5 mole/L concentration but the overcut was as twice as the range for lower electrolyte concentrations. Although 6 volts level was in good combination with lower concentration levels, it seems that it is not a good match for high concentration electrolyte as the effect of the stray currents takes over. Also, the surface finish for 6 volts showed two separate region, one inner side which was the result of the main reaction and outer side which was the result of stray currents. Except for the

20 μm , the difference between the inner side and the outer side was very obvious for 6 volts and 40 μm gap size.

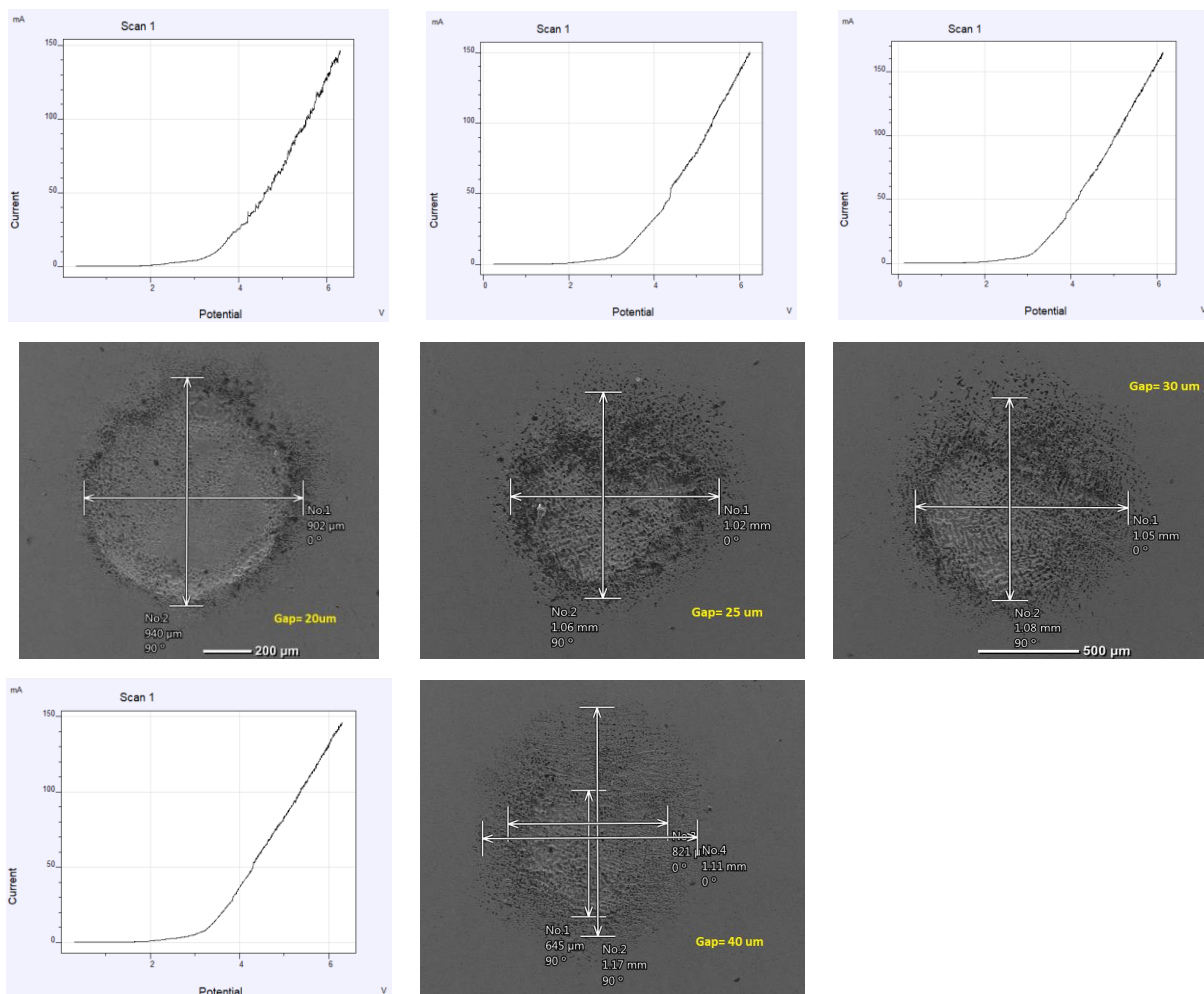


Figure 3-42: Polarisation graph & related SEM image (6 volts)

The surface roughness and quantitative results noticeably improved for 7 volts level (figure 3-43) in comparison with smaller voltages and same electrolyte concentration or in comparison with the same voltage level and lower electrolyte concentration levels. MRR and overcut were approximately similar for all gap sizes when the end voltage level was 7 volts and among them, 30 μm gap was associated with a better result. SEM images and iviumstat graphs can be observed in figure 3-43.

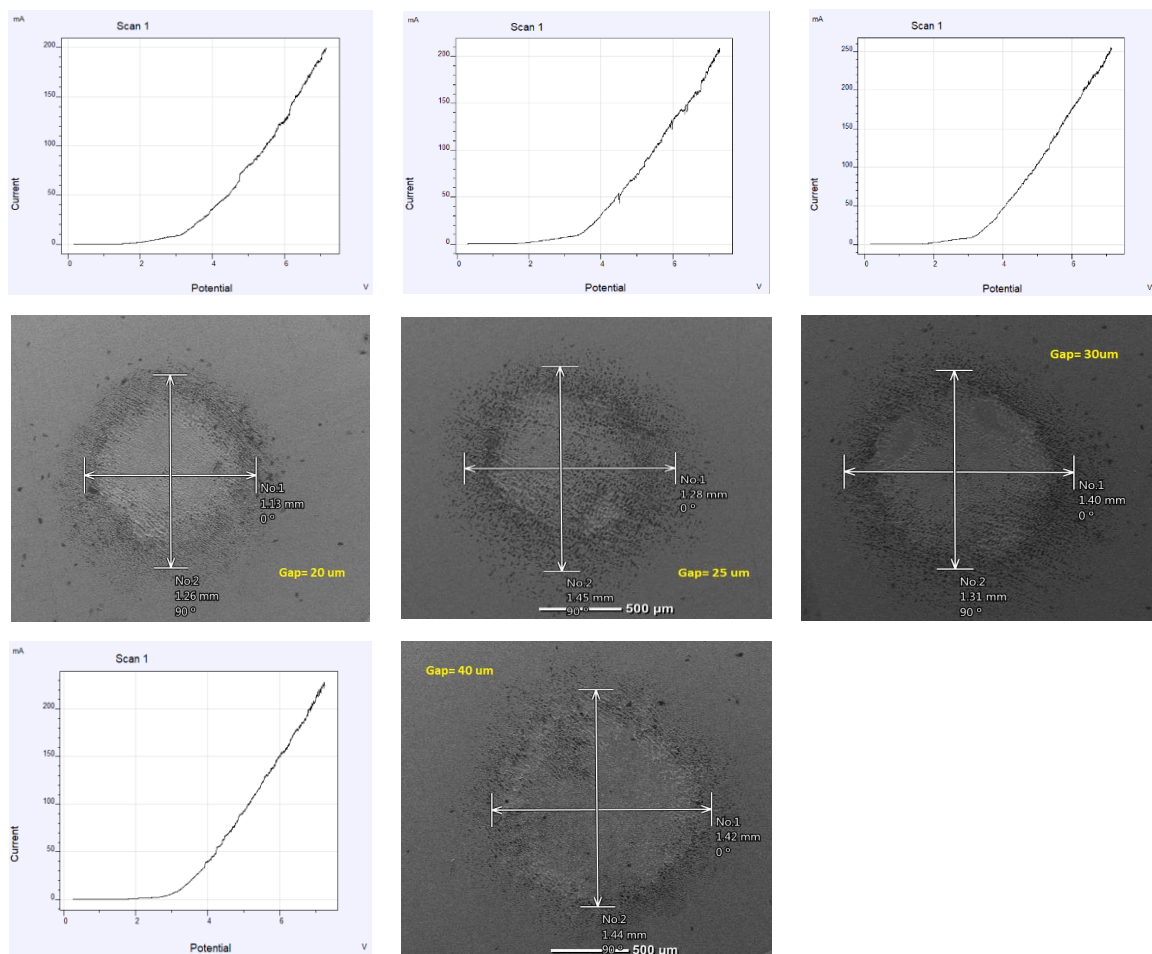


Figure 3-43: Polarisation graph & related SEM image (7 volts)

The combination of 8 volts voltage and 1 mole/L concentration generated the best results with the exception for the 40 μm gap size (figure 3-44); for that gap size the result was remarkably different from all other experiments although the maximum current and charge transfer resistance were within expected range. Increasing the voltage to 9 volts (figure 3-45) and 1 mole/L concentration, generated the highest removed material level but the material removal rate was remained within the same range as 8 volts level. The reason is that 9 volts was applied for a longer period in comparison with 8 volts. Also, average overcut for 9 volts and all gap sizes except for 30 μm was nearly increased by 30% in comparison with 8 volts' overcut levels.

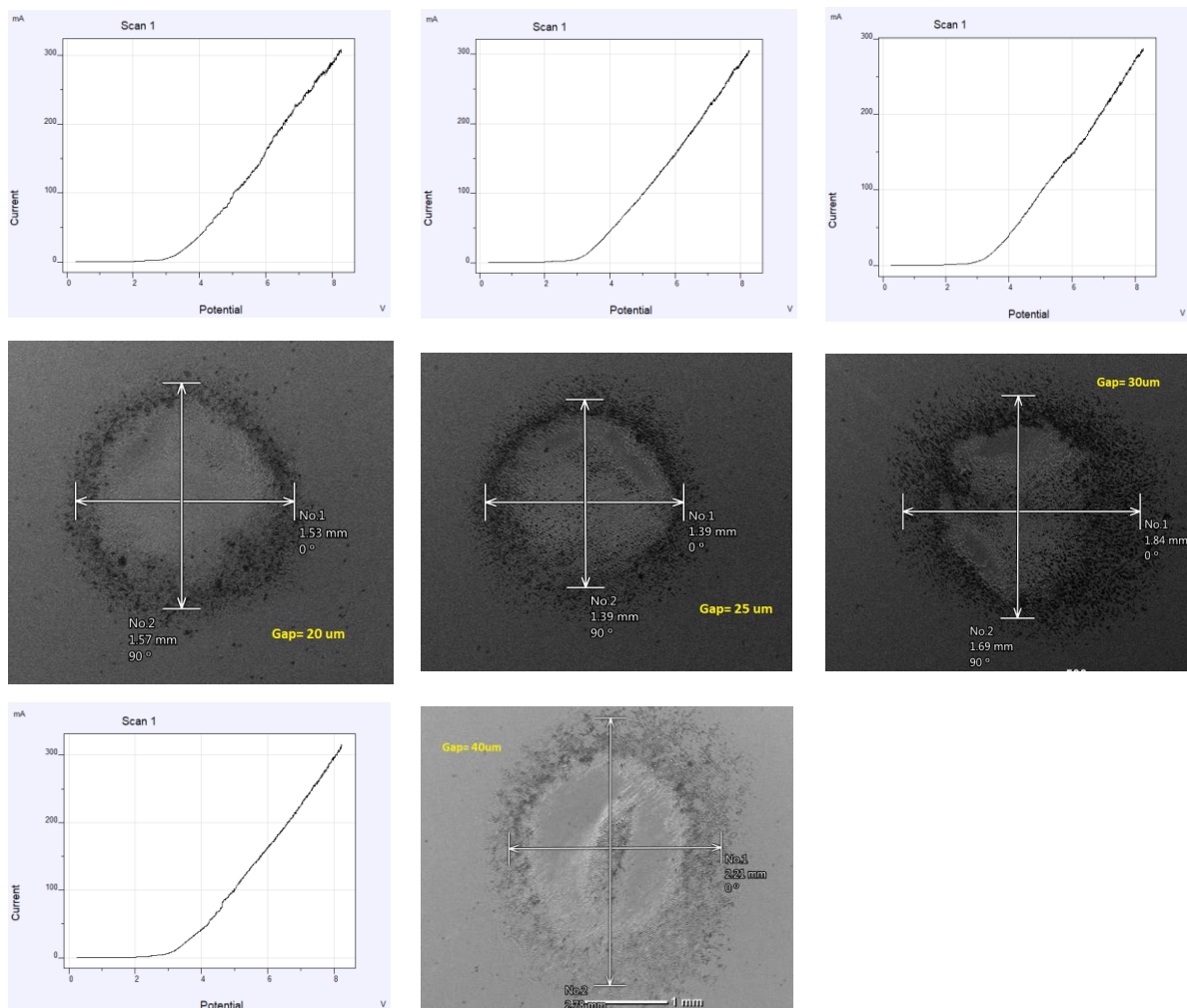


Figure 3-44: Polarisation graph & related SEM image (8 volts)

General speaking, higher voltage levels associated with 1 mole/L concentration, produced better results in comparison with the same voltage levels and lower electrolyte concentration and smaller gap sizes. For example, 9 volts and 1 mole/L electrolyte concentration, produced better performance for 30 μm gap size while 7 volts produced more efficient results for 25 μm gap. Figure 3-45 shows the results for the 9 volts and all different gap sizes.

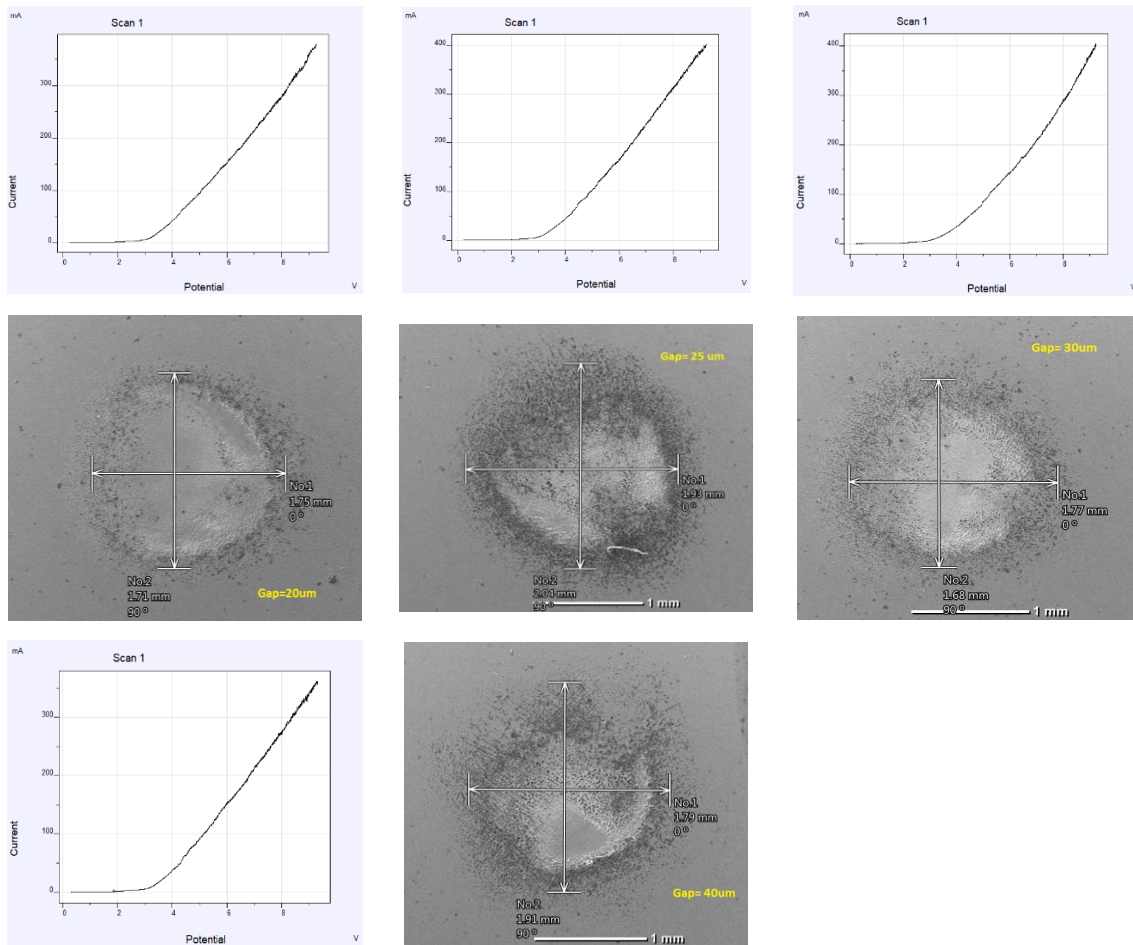


Figure 3-45: Polarisation graph & related SEM image (9 volts)

In terms of the charge transfer resistance, it is impossible to find the same rise or decay pattern for all voltage levels, but all voltage levels presented their maximum MRR rates at lowest charge transfer resistance values. This is in agreement with the ohms law as lower resistance provides higher current density and in case of μ ECM machining, higher MRR.

Figure 3-46 and 3-47 are visualising the comparison for MRR and overcut between different voltage-gap levels. The general trend for both criteria is linear increase from lower voltage to the higher voltage levels. Also, current levels showed growing trend and charge transfer resistance presented decreasing slope. However, the 8 volts level generated better results considering MRR and overcut quantities simultaneously.

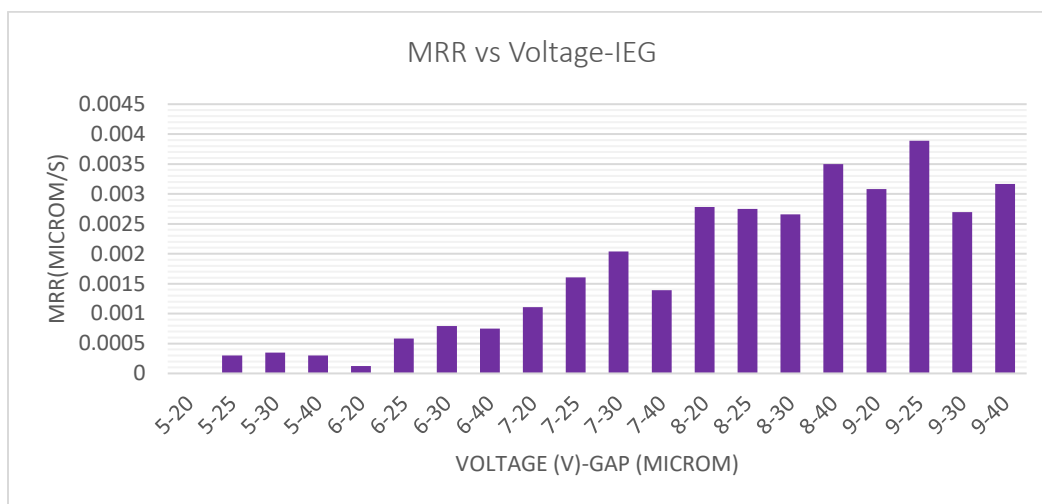


Figure 3-46: MRR (1.0 mole/L NaNO₃ electrolyte)

Figure 3-46 shows better MRR levels for voltages greater than 6 volts but simultaneous check with overcut results in figure 3-47 shows that overcut was more ideal for midrange voltages. Ignoring the exceptional case for 8 volt and 40 μm gap, leads to the conclusion that combination of 8 volts and 25 μm gap has generated the best results for 1 mole/L electrolyte concentration.

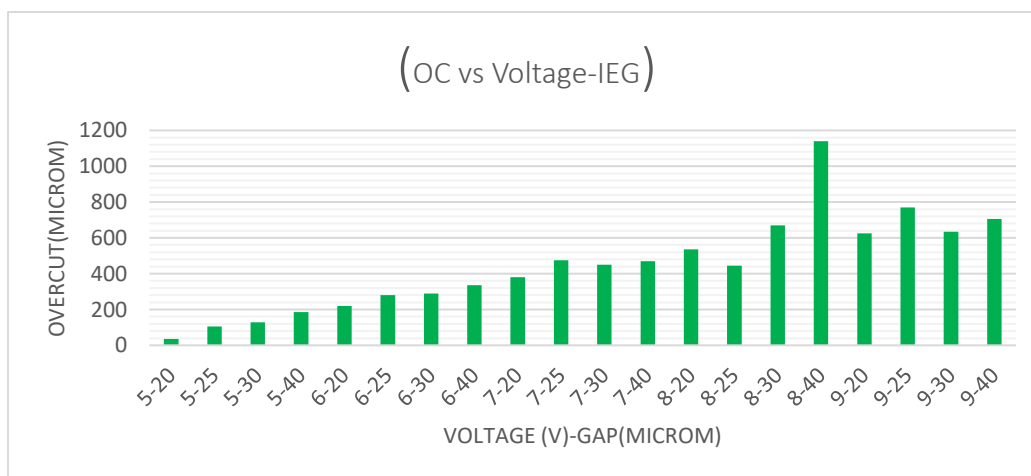


Figure 3-47: Overcut (1.0 mole/L NaNO₃ electrolyte)

This stage of experiments provided a database to include the initial parameters values and reaction outcomes. Recalling the aim of this experiment which was to help to achieve the best optimum initial values for the predominant parameters, will lead to the next stage which is analytical assessment of the above experiments using Matlab curve fitting toolbox. The details and analysis results are presented in next section. The results of mathematical assessment of the combination of the parameters agree with the collected data and relevant comparisons in the above section.

3.4 Response surface methodology using MATLAB toolbox

As mentioned in chapter two, finding the optimum initial values for machining parameters has been an unsolved challenge; the literature review showed different approaches towards optimisation of the machining parameters including mathematical model, simulation and try and error approach. One of the available mathematical approaches is based on experimental results which can provide the optimum values for a few parameters based on machining performances. This method, known as response surface methodology, is applied on experimental data to reach the optimised values.

The experiments in section 3.3 include 60 times repeat for a combination of values for voltage, electrolyte concentration and IEG size. (parameters and their values mentioned in table 3-1)

The aim of this practice is to find optimum parameters values based on achieved results which are MRR and average overcut.

Matlab is providing the curve fitting toolbox with various options. In this work, the best curve fits have been found for every two predominant parameters and one machining criterion as follow:

- Input: voltage & gap, performance criterion: MRR
- Input: voltage & electrolyte concentration, performance criterion: MRR
- Input: gap & electrolyte concentration, performance criterion: MRR
- Input: voltage & gap, performance criterion: Overcut
- Input: voltage & electrolyte concentration, performance criterion: Overcut
- Input: gap & electrolyte concentration, performance criterion: Overcut

The input data for the Matlab curve fitting toolbox are presented in table 3-8.

Voltage Final (Volt)	IEG (µm)	Electrolyte concentration (mole)	Overcut (µm)	MR Rate (µg/s)	Voltage Final (Volt)	IEG (µm)	Electrolyte concentration (mole)	Overcut (µm)	MR Rate (µg/s)	Voltage Final (Volt)	IEG (µm)	Electrolyte concentration (mole)	Overcut (µm)	MR Rate (µg/s)
X	Y	W	V	Z	X	Y	W	V	Z	X	Y	W	V	Z
5	20	0.3	24.5	0.0002	5	20	0.5	45.5	0	5	20	1	35.5	0
5	25	0.3	19	-0.00095	5	25	0.5	28.5	0.00045	5	25	1	105	0.0003
5	30	0.3	41.5	0.00025	5	30	0.5	29.5	-0.0006	5	30	1	129	0.00035
5	40	0.3	0	0	5	40	0.5	0	0	5	40	1	185.5	0.0003
6	20	0.3	171.5	0.000708333	6	20	0.5	118.5	0.00045833	6	20	1	220	0.000125
6	25	0.3	120.5	0.000583333	6	25	0.5	104.5	0.00075	6	25	1	280	0.000583
6	30	0.3	139.5	0.000583333	6	30	0.5	149	0.00045833	6	30	1	290	0.000792
6	40	0.3	104	0	6	40	0.5	163.5	0.00025	6	40	1	335	0.00075
7	20	0.3	122	0.000714286	7	20	0.5	142.5	0.00046429	7	20	1	380	0.001107
7	25	0.3	127	0.00025	7	25	0.5	157.5	0.00167857	7	25	1	475	0.001607
7	30	0.3	181	0.000321429	7	30	0.5	154	0.00053571	7	30	1	450	0.002036
7	40	0.3	152	0.000785714	7	40	0.5	244	0.00075	7	40	1	470	0.001393
8	20	0.3	168.5	0.00134375	8	20	0.5	260	0.0018125	8	20	1	535	0.002781
8	25	0.3	147	0.00109375	8	25	0.5	227	0.00196875	8	25	1	445	0.00275
8	30	0.3	164.5	0.0009375	8	30	0.5	365	0.00121875	8	30	1	670	0.002656
8	40	0.3	191.5	0.0008125	8	40	0.5	360	0.0005	8	40	1	1140	0.0035
9	20	0.3	275	0.000666667	9	20	0.5	500	0.00133333	9	20	1	625	0.003083
9	25	0.3	260	0.001361111	9	25	0.5	515	0.00216667	9	25	1	770	0.003889
9	30	0.3	247	0.001	9	30	0.5	505	0.00211111	9	30	1	635	0.002694
9	40	0.3	219.5	0.001138889	9	40	0.5	505	0.00188889	9	40	1	705	0.003167

Table 3-8: Input data for Matlab curve fitting toolbox

Different curve fitting approaches including polynomial second order, polynomial second order with centre & scale option, and nearest neighbour interpolant methods were tested and obtained graphs and results were presented in the following sections.

The second order polynomial response surface mathematical model evaluates the influence of selected parameters on the numerous outcome criteria. The general form of the function is as equation 3-22 where Z_k presents the corresponding response for the input parameters x_{ik} and β_0 , β_{ii} and β_{ij} are the second order regression coefficients. The second and third terms in this equation feature the linear and higher order effects respectively and fourth term attributes the interactive effects of the parameters.

$$Z_k = \beta_0 + \sum_{i=1}^n \beta_i x_{ik} + \sum_{i=1}^n \beta_{ii} x_{ik}^2 + \sum_{i < j} \beta_{ij} x_{ik} x_{jk} \quad (3-21)$$

Interpolation is a process of estimating values that lie between a discrete set of known data point. This method helps to estimate the values of a function for intermediate value of the parameter. The simplest interpolation method is to find the nearest neighbour values for the variable and assign the same value. For multivariable function, the piecewise constant interpolation is being used while linear interpolation is used for single variable function.

In Matlab curve fitting toolbox and intended work in this section, the general 2nd order polynomial model follows the equation 3-23 and for two parameters only:

$$f(x, y) = P_{00} + P_{10}x + P_{01}y + P_{20}x^2 + P_{11}xy + P_{02}y^2 \quad (3-22)$$

In this equation and the rest of the equations in this section, x and y are input variables and f is the function of these variables.

3.4.1 Voltage & gap parameters, MRR & overcut (OC) criteria

All three mentioned methods for curve fitting applied for the combination of voltage and gap size and the outcome as MRR & overcut.

The mathematical relationship for MRR and overcut criteria based on voltage and gap size are listed in the following equations respectively when data were normalised:

$$f(x, y) = \text{MRR} = 0.001148 + 0.0007717x - 5.069e - 06y - 2.787e - 05x^2 + 1.525e - 05xy - 6.713e - 05y^2 \quad (3-23)$$

$$f(x, y) = \text{OC} = 271.1 + 151.1x + 28.27y - 2.052x^2 + 9.306xy + 3.086y^2 \quad (3-24)$$

Table 3-9 illustrates the details of the fits and figure 3-48 & 3-49 present the curves for the above fitting. X and Y in table 3-9 are voltage level and gap size respectively and Z and V are MRR and OC values, respectively.

Fit Name	Data	Fit Type	SSE	R-square	DEF	Adj R-sq	RSME	#Coeff
2 nd order MRR	z vs x, y	Poly22	2.8005e-05	0.5585	54	0.5176	7.2014e-4	6
2 nd order MRR-Nor.	z vs x, y	Poly22	2.8005e-05	0.5585	54	0.5176	7.2014e-4	6
Interpolant MRR	z vs x, y	Nearstinterp	2.5846e-05	0.5925	0	-	-	60
2 nd order OC	v vs x, y	Poly22	1.59126+06	0.4688	54	0.4196	171.6577	6
2 nd order OC-Nor.	v vs x, y	Poly22	1.59126+06	0.4688	54	0.4196	171.6577	6
Interpolant OC	v vs x, y	Nearestinterp	1.4751e+06	0.5075	0	-	-	60

Table 3-9: Table of fits - Voltage & gap parameters, MRR & overcut (OC) criteria

As the figure 3-48 interpolant shows, the higher the voltage is and for medium level gap size, the MRR is higher. The benefit of the interpolant curve fitting is that it makes it easier to compare the combination of that gap size and voltage for the MRR but there is

no general pattern how the combination of the voltage level and gap sizes is working but for all voltage levels with the exception of 5 volts, the higher MRR occurs for the gap sizes between 22 and 38 μm . A close look at polynomial fits is showing the same pattern in which the higher MRR can happen for the gap up to 27 μm , also it shows that for higher voltage levels, bigger gap sizes can align with the higher MRR.

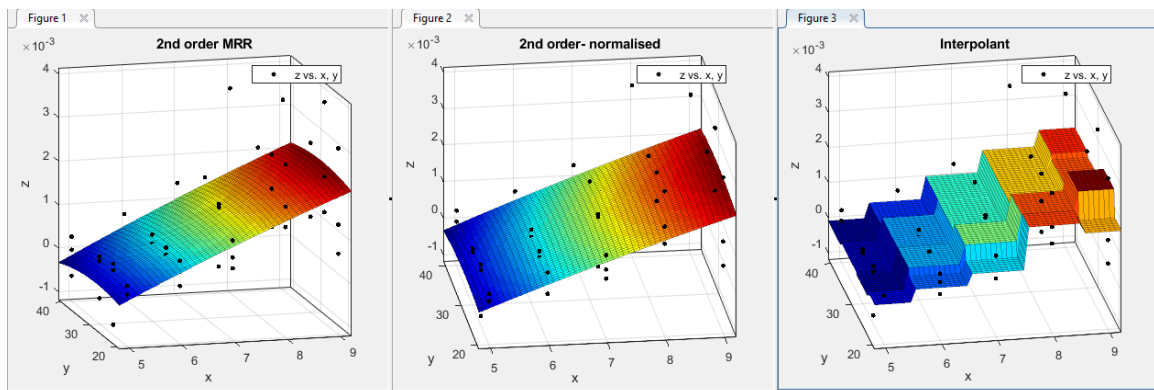


Figure 3-48: Curve fit for Voltage & Gap parameters and MRR

According to the figure 3-49 and based on all three different fits, for all voltage levels, by increasing the gap size, the overcut, has increased. While the expectation is that the bigger overcut should lead to the greater material removal level and subsequently higher material removal rate, but the curve fits do not approve this idea. The curves present the larger overcut at greater gap sizes while the better MRR occurred at medium towards lower gap sizes.

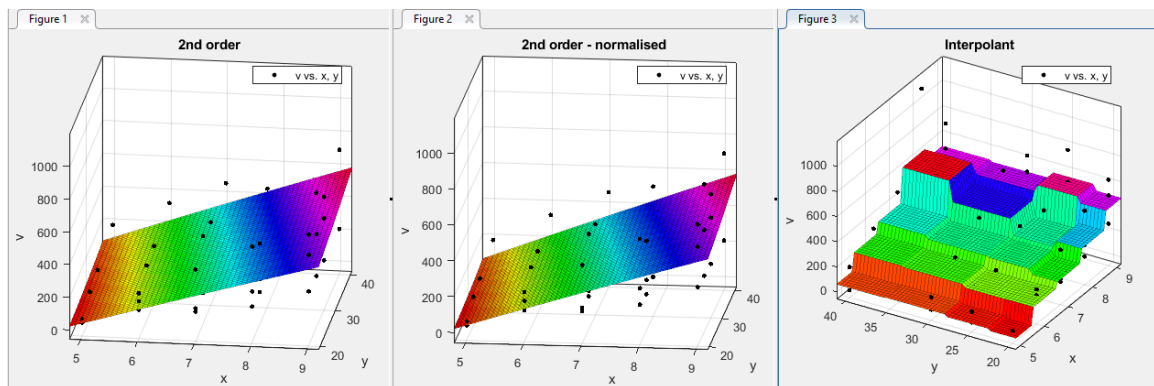


Figure 3-49: Curve fit for Voltage & Gap parameters and OC

Therefore, by comparing two sets of the graphs in figure 3-48 and 3-49, it is possible to conclude that the undesired effects of stray currents are clearly evident at greater gap sizes and hence, the optimum voltage-gap combination can be observed around medium to small gap sizes.

3.4.2 Voltage & electrolyte concentration parameters, MRR & OC criteria

All three mentioned methods for curve fitting were applied for the combination of voltage and gap size and MRR & overcut were considered as performance criteria same as previous section.

The mathematical relationship for MRR and overcut criteria based on voltage and electrolyte concentration are listed in the following equations respectively when data were normalised:

$$f(x,y) = MRR = 0.001104 + 0.0007717x + 0.0004883y - 2.787e-05x^2 + 0.0003069xy - 2.289e-05y^2 \quad (3-25)$$

$$f(x,y) = OC = 273.4 + 151.1x + 127.1y - 2.052x^2 + 58.92xy + 0.7523y^2 \quad (3-26)$$

In this practice, X and Y are voltage and electrolyte concentration values and Z and V are MRR and OC levels, respectively.

Table 3-10 illustrates the details of the fits and figure 3-50 and 3-51 present the curves for the above fitting.

Fit Name	Data	Fit Type	SSE	R-square	DEF	Adj R-sq	RSME	#Coeff
2 nd order MRR	z vs x, w	Poly22	9.3246e-06	0.8530	54	0.8394	4.1555e-4	6
2 nd order MRR-Nor.	z vs x, w	Poly22	9.3246e-06	0.8530	54	0.8394	4.1555e-4	6
Interpolant MRR	z vs x, w	Nearstinterp	7.4078e-06	0.8832	0	-	-	60
2 nd order OC	v vs x, w	Poly22	4.8881e+05	0.8368	54	0.8217	95.1426	6
2 nd order OC- Nor.	v vs x, w	Poly22	4.8881e+05	0.8368	54	0.8217	95.1426	6
Interpolant OC	v vs x, w	Nearestinterp	3.5745e+05	0.8807	0	-	-	60

Table 3-10: Table of fits - Voltage & electrolyte concentration parameters, MRR & OC criteria

As figure 3-50 shows, the combination of voltage and electrolyte concentration generates a wider non-linear relation with MRR. According to the graphs with polynomial fits, up to 7 volts, the change of the electrolyte concentration does not create much difference in MRR but for the 7 volts and higher, the change in electrolyte concentration has significant effect on MRR; the graphs illustrate that for the higher voltage, a lower electrolyte concentration can generate same performance for a lower voltage with higher electrolyte concentration. Therefore, if the machining needs lower voltage level as initial setup, it is recommended to use the electrolyte with higher level concentration. Assessment of the interpolant graph presents that for each voltage level, the MRR increases with the rise of the electrolyte concentration but the rise for higher voltage levels (>7.5 volts) is remarkable in comparison with the lower levels.

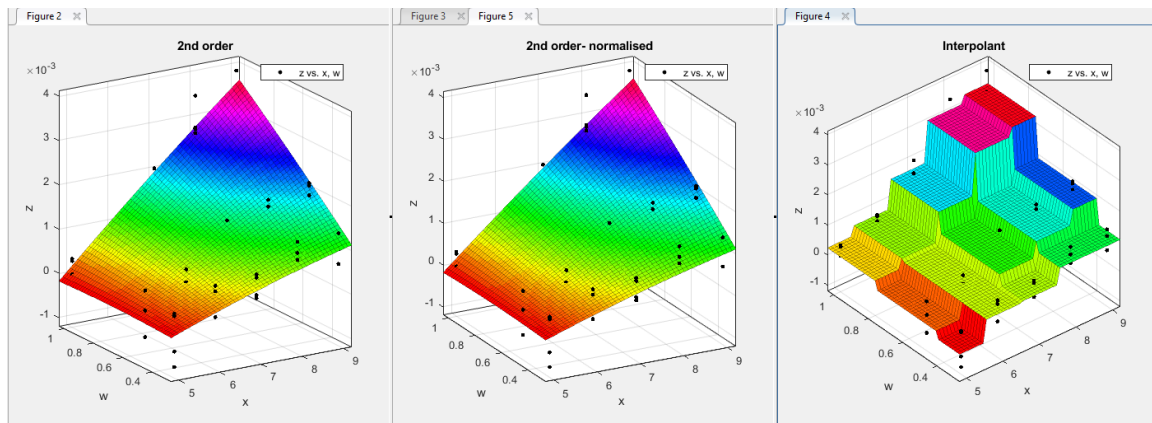


Figure 3-50: Curve fit for Voltage & electrolyte concentration parameters and MRR

Figure 3-51 presents the curve fits for overcut for the combination of the voltage and electrolyte concentration. Like MRR criterion, for the voltages up to 7 volts, the electrolyte concentration level, does not apply significant changes on overcut rate and the size of the overcut remains within a small interval. But by increasing the voltage level, greater electrolyte concentration generates greater overcut.

Also, the interpolant curve fit presents a general pattern for each voltage level in which increasing electrolyte concentration will create larger overcut and clearly it is not desirable to have such a big overcut. Also, this graph shows that for each voltage level, the concentration greater than 0.8 mole/L, increases the overcut level sharply. The

maximum overcut happened for voltages above 8 volts and concentration near 1 mole/L with a significant difference. Therefore, it is recommended to use lower electrolyte concentration level to reach less overcut ratio.

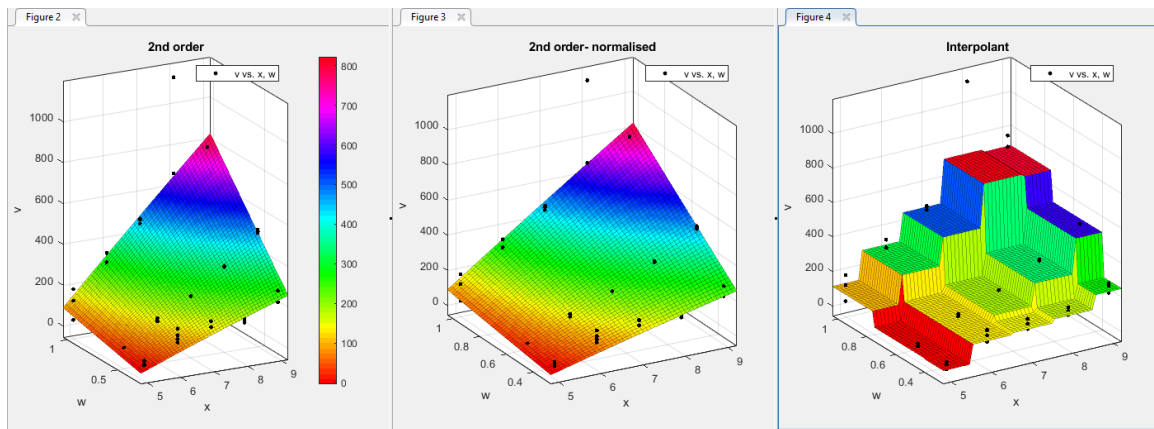


Figure 3-51: Curve fit for Voltage & electrolyte concentration parameters and OC

Finding the optimum combination of voltage and electrolyte concentration parameters for both performance criteria simultaneously is a challenge; but the comparison between the above graphs, suggests that the mid-range voltages for medium level electrolyte concentration may bring the optimum overcut and maximum MRR. Therefore, the voltage range between 6.5 and 7.5 volts and medium range of electrolyte concentration around 0.4 and 0.7 mole/L can be selected for the further investigation.

3.4.3 Gap size & electrolyte concentration parameters, MRR & OC criteria

All three mentioned methods for curve fitting were applied for the combination of voltage and gap size and the MRR & overcut outcomes.

The mathematical relationship for MRR and overcut criteria based on the gap size and electrolyte concentration are listed in the following equations respectively when data were normalised:

$$f(x, y) = MRR = 0.001143 - 5.069e - 06 x + 0.0004883 y - 6.713e - 05 x^2 + 9.678e - 05 xy - 2.289e - 05 y^2 \quad (3-27)$$

$$f(x, y) = OC = 268.4 + 28.27x + 127.1y + 3.086x^2 + 34.29xy + 0.7523y^2 \quad (3-28)$$

Table 3-11 illustrates the details of the fits and figure 3-52 and 3-53 present the curves for the above fitting. In this table X and Y are gap size and electrolyte concentration while Z and V are MRR and OC levels, respectively.

Fit Name	Data	Fit Type	SSE	R-square	DEF	Adj R-sq	RSME	#Coeff
2 nd order MRR	z vs y, w	Poly22	4.9175e-05	0.2247	54	0.1529	9.5428e-4	6
2 nd order MRR-Nor.	z vs y, w	Poly22	4.9175e-05	0.2247	54	0.1529	9.5428e-4	6
Interpolant MRR	z vs y, w	Nearstinterp	4.7458e-05	0.2517	0	-	-	60
2 nd order OC	v vs y, w	Poly22	1.9171e+06	0.3600	54	0.3007	188.4199	6
2 nd order OC-Nor.	v vs y, w	Poly22	1.9171e+06	0.3600	54	0.3007	188.4199	6
Interpolant OC	v vs y, w	Nearestinterp	1.9113e+06	0.3619	0	-	-	60

Table 3-11: Table of fits - gap & electrolyte concentration parameters, MRR & OC criteria

As figure 3-52 polynomial fits show, the higher level of electrolyte concentration matches the smaller or greater gap sizes which is either less than 25 μm or greater than 35 μm for any specific MRR. The behaviour of the process for the MRR criterion with regard to the electrolyte concentration is dividable to four separate regions; concentration up to 0.5, between 0.5 and 0.6 mole/L, between 0.6 and 0.9 and concentration greater than 0.9 mole/L and each region shows same trend with respect to the gap size.

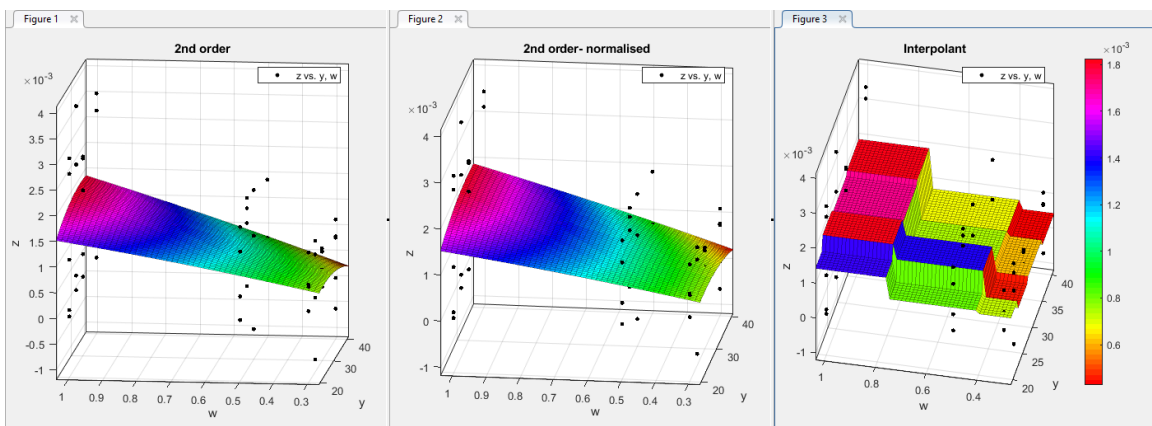


Figure 3-52: Curve fit for gap & electrolyte concentration parameters and MRR

Similarly, the interpolant graph shows a general trend between gap size neighbourhoods in which by increasing the electrolyte concentration the MRR is increased with for each gap size region. In addition to this, MRR significantly increases for all gap sizes when the electrolyte concentration is greater than 0.7 mole/L. But the greatest change is observed for the gap sizes between 22 and 28 μm for the concentration between 0.4 and 0.7 mole/L.

Assessing the curve fits for the overcut criterion leads to the conclusion that for lower electrolyte concentration up to 0.45 mole/L, the range of overcut does not change significantly with the rise or fall of the gap size. For the electrolyte concentration greater than 0.45 mole/L, the overcut increases when the gap size increases; the maximum overcut observed for the highest electrolyte concentration level and 40 μm gap with a great difference. Interpolant curve creates a clear visual map for the change of the overcut size with the change of the electrolyte concentration and the gap size between electrodes; however, it presents the maximum overcut for the highest concentration and gap size neighbourhood as polynomial fits do. Interpolant fit generates four visible areas for OC including the lowest OC for electrolyte concentration up to 0.4 mole/L and any gap sizes, second level OC for electrolyte concentration between 0.4 and 0.75 mole/L and gap sizes up to 28 μm , third level of OC for the gap sizes greater than 28 μm and medium electrolyte concentration between 0.4 and 0.75 mole/L and finally second highest OC level for the electrolyte concentration above 0.75 mole/L and gap sizes between 25 μm and 35 μm .

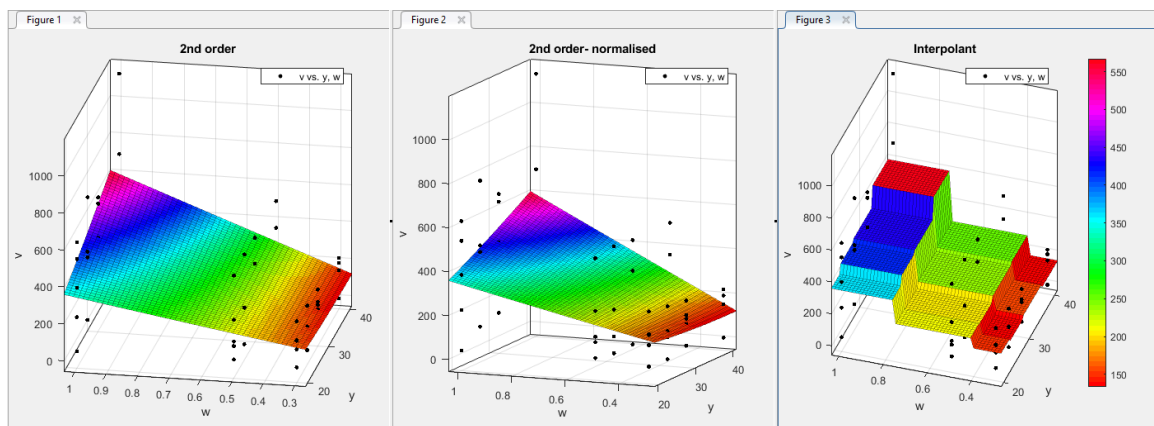


Figure 3-53: Curve fit for gap & electrolyte concentration parameters and OC

Combining both performance criteria and resulted graphs can lead to find the optimum combination of the gap size and electrolyte concentration for the maximum MRR with the lowest OC. According to the curve fits for OC, the range of the electrolyte concentration lies between 0.4 and 0.75 mole/L while the gap size remain between 20 μm and 28 μm ; while curve fits for MRR minimise the optimum levels to the range of 0.4 and 0.7 mole/L and the 22 μm and 28 μm for electrolyte concentration and gap sizes respectively.

Table 3-12 summarises the above discussion and shows the optimum levels for the combination of all three selected machining parameters and machining performances. The optimum levels have been used in chapter four as input data for the impedance investigation using iviumstat in order to obtain the equivalent circuit for the electrode-electrolyte interface.

Parameters combination	Gap sizes (μm)	Electrolyte concentration (mole/L)	Optimum range
Voltage-Gap	22-27	6.5-8.5	Gap: 22-27 (μm)
Voltage- Electrolyte concentration	6.5- 7.5	0.4-0.7	Voltage: 6.5-7.5 (V)
Gap- Electrolyte concentration	22- 28	0.4- 0.7	Concentration: 0.4- 0.7 mole/L

Table 3-12: Optimum values for voltage, electrolyte concentration and IEG size

3.5 Tungsten tool electrode assessment

During different stages of this experiment, the tool surface (front face) was examined using SEM and EDS to monitor any changes and possible effects of the machining process on the tool surface in form of tear and wear.

The SEM image and EDS spectrum analysis of the tool surface were presented in figure 3-54 and 3-55. Following figures present the spectrum analysis of the tool surface after the first experiments which was linearsweep method.



Figure 3-54: Used Tungsten tool surface SEM image

After a group of experiments, a dark layer covered the tool surface and its longitude sides. Spectrum analysis has been used to investigate whether any reactions have been occurred between tool surface and electrolyte or sludge. Comparing the peak elements between EDS spectrum before and after experiments demonstrate a few additional peak elements after experiments including Fe, N and Na; presumably, Na & N elements from electrolyte can react with tool electrode materials or a layer of new reactants can be deposited on the tool surface. This layer did not stop the polarisation experiment nor changed the current level or current rise but if the thickness of the layer increases, it is expected that the dissolution to be stopped due to decreased current flow.

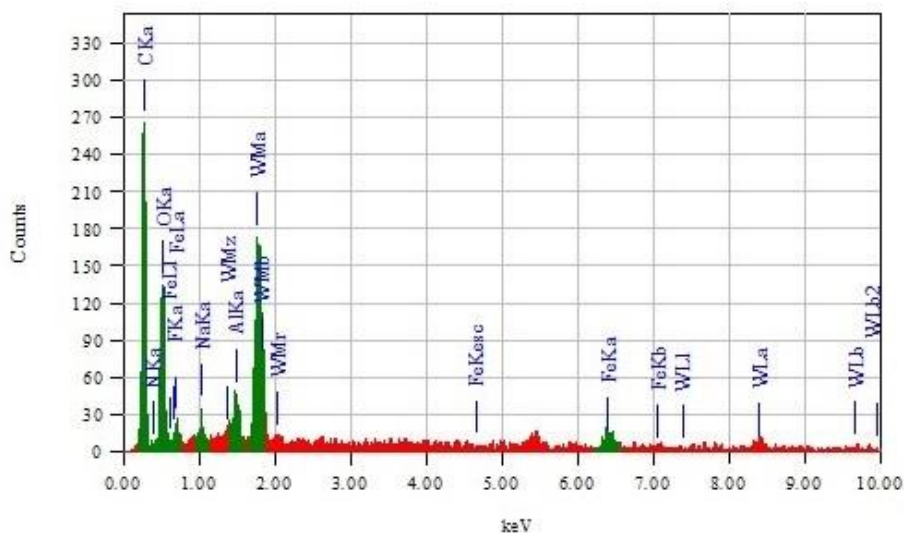


Figure 3-55: Used Tungsten EDS spectrum

Although the rate of the tear and wear in μ ECM tool electrode is negligible, electrode materials and electrolyte selection can change it; therefore, the electrolyte selection is as important as any other machining parameters. Currently, the success of finding matching electrolyte and workpiece & tool electrodes can be achieved through the trial and error approach or by access to any previous research or experiment results.

It has been suggested that adding acidic solution to NaNO_3 electrolyte can improve the tool electrode surface condition by preventing the creation and deposition of the black layer on tool surface, but it can deteriorate the edge profile of the machined zone. Guodong et al (2016) added H_2SO_4 , and composite Na_3Cit and NaGlu to NaNO_3 and compared the effect of the new solution on deposited dark layer on the tool surface and machined edge profile quality. Their experiments showed that H_2SO_4 can prevent the deposition of the dark layer, but it generates a poor edge profile, but Na_3Cit and NaGlu generates a good edge profile in addition to eliminating the black layer deposition on the tool surface.

3.6 Conclusion

This chapter has provided further details and information with respect to the highlighted areas as knowledge gaps which were identified in chapter two. An introduction to the electrochemical cells features, electrochemical analytical techniques and further details about EDL structure and electrode-electrolyte interface were provided. Also, the proposed methodology and laboratory experimental results were demonstrated.

Currently, the initial values for the predominant machining parameters are being set based on trial and error approach or operator experience. As a result, machining process is expensive and time consuming and dependent on operator knowledge and experience.

In this chapter, a laboratory experimental method using iviumstat has been designed and implemented in order to investigate and obtain the best possible ranges for the initial values of the predominant machining parameters based on the machining performance criteria including MRR and OC.

Predominant parameters which were investigated in this research are voltage level, electrolyte concentrations and IEG size. The result of the iviumstat experiments

were mathematically analysed using Matlab toolbox to provide a narrower range for the initial predominant parameters' values.

Iviumstat is a very useful tool to investigate electrochemical features of different applications and it has been positively responsive in the case of μ ECM. The comparison between anodic solution outcomes (MRR and OC) for different experiments carried out by iviumstat led to the similar results as mathematical analysis using Matlab. Therefore, iviumstat and designed experiments (Linearsweep) confirmed to be an acceptable approach towards setting the initial values for the μ ECM machining setup. This method is a time and cost-effective approach in comparison with the trial and error approach; it is also much easier to train the operator to use iviumstat rather using a developed μ ECM machine to try and attain initial parameter's values for a machining purpose.

Also, Matlab is a user-friendly environment which can speed up the data analysing and prototyping. Its application alongside the iviumstat has provided reliable data and information. It is important to mention that mathematical approach is a strong method in modelling and assessment of the complex processes including μ ECM process but due to the complex and multidisciplinary nature of the μ ECM process and its uncertainty, mathematical approach is not enough and should be accompanied with some sort of experimental works. That is why, in this research the mathematical analysis took place based on the obtained results through the laboratory experiments.

As a result of the designed experiments and mathematical analysis, a narrow range for predominant parameters achieved including 0.4-0.7 mole/L electrolyte concentrations, 6.5 to 7.5 volts and an inter electrode gap of 24 to 27 μ m.

Gathered data in graphs (figures 3-29, 3-30, 3-39,3-40,3-46, 3-47) demonstrate the complexity of the interrelation between machining parameters and machining criterial. MRR and OC show significant changes when one or a few machining parameters have changed. Identification of the interrelation between machining parameters and machining performances needs further development. It is necessary to apply further investigation in order to find any changing point between machining parameters' interrelation. Prioritising the investigation in order to find this changing point will significantly help to stablish an effective range for the machining parameters with regard to other parameters.

CHAPTER 4

EDL Equivalent RC Circuit and Simulation

Chapter summary

Following the chapter 3 which demonstrated the experimental approach towards the first highlighted challenge in μ ECM process, this chapter is devoted to present the proposed approach towards tackling the second highlighted challenge in μ ECM process. First challenge was to find the initial values for the predominant parameters including voltage, IEG and electrolyte concentration and the second challenge is to model the equivalent RC circuit for the EDL. Chapter 3 presented the application of iviumstat in order to investigate the anodic reaction for the desired range of the predominant parameters and application of surface roughness methodology to reach the optimum values for these parameters.

This chapter will present the application of iviumstat as impedance spectroscopy tool to find the equivalent RC values for the EDL structure using optimum values; additionally, this chapter will present the application of Matlab Simulink as a tool to analyse the acquired RC equivalent circuit electrically and to propose an approach to find the minimum required pulse on time for the anodic dissolution based on the EDL structure. Although there are a few examples in literature review in which pulse features have been analysed, the main difference between suggested approach in this research and those examples is the way RC equivalent values have been estimated. In this research RC values were estimated based on the experimental results using iviumstat but in other available published works RC values were estimated using simulation results or no clear methodologies were mentioned to show how RC values have been estimated.

This chapter presents the iviumstat impedance methodology and experimental results based on the achieved optimum values in chapter 3, then it demonstrates Matlab Simulink analysis for the obtained equivalent RC circuit and finally a few examples of the machined holes using in house built μ ECM machine will be presented.

4.1 Equivalent circuit for μ ECM electrode-electrolyte interface

As mentioned earlier, the equivalent circuit for μ ECM electrode-electrolyte interface is modelled with an RC network. Experiment results from section 3.3 and mathematical assessment in section 3.4 from chapter 3 will be used for this stage to find the values for equivalent circuit based on the optimal machining parameters which are summarised in the table 4.1.

Optimum range:	Gap: 22-27 (μm)	Voltage: 6.5-7.5 (V)	Concentration: 0.4- 0.7 mole/L
-----------------------	--	--------------------------------	--

Table 4-1: Optimum values for voltage, electrolyte concentration and IEG size

The results of the linearsweep experiments using iviumstat and the results of curve fitting from Matlab toolbox were led to a smaller range for the machining parameters with the best machining performances; at this stage, the aim is to find the electrochemical impedance of the cell and to find the possible values for RC equivalent circuit's components. Impedance method on iviumstat is providing the opportunity to find an equivalent circuit for the process under the investigation. Electrochemical impedance is usually measured by applying a small sinusoidal excitation to the cell and measuring the current flowing through the cell.

The applied AC signal has the form of

$$\text{voltage: } E_t = E_0 \sin \omega t \quad (4-1)$$

and the response signal is a same frequency ($\omega = 2\pi f$) current signal with a shifted phase (φ) based on the electrochemical cell's equivalent circuit (figure 4-1):

$$\text{current: } I_t = I_0 \sin(\omega t + \varphi) \quad (4-2)$$

therefore, the impedance of the system is equal to:

$$\text{Impedance: } Z = \frac{E_t}{I_t} = \frac{E_0 \sin \omega t}{I_0 \sin(\omega t + \varphi)} = Z_0 \frac{\sin \omega t}{\sin(\omega t + \varphi)} \quad (4-3)$$

Impedance can be expressed in terms of absolute value and a phase angle for logarithmic frequencies (Bode plot) or in terms of real and imaginary numbers (Nyquist plot).

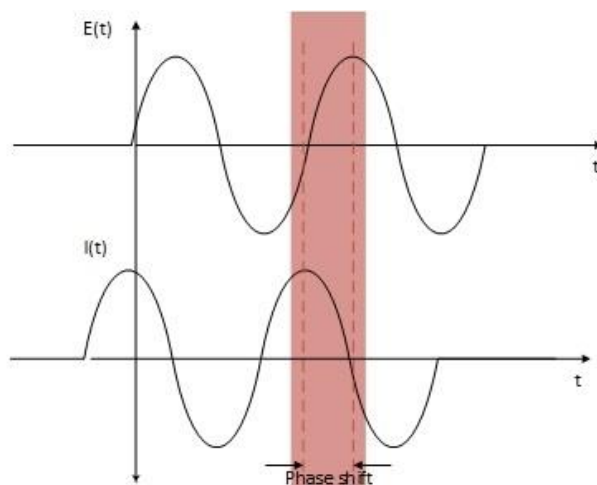


Figure 4-1: Voltage and current signals' phase shift

4.1.1 Equivalent circuit electrode-electrolyte interface – Tungsten tool electrode

In this practice a 0.01-volt amplitude AC signal over a range of frequencies from 10 KHz up to 1 MHz has been applied for a constant voltage of 6.5, 7 and 7.5 volts. By starting the process on the iviumstat, a logarithmic spread of the frequencies is calculated. There are different options available to choose for the results' presentation including absolute value of impedance and phase graphs, admittance, resistive and capacitive graphs.

According to the literature review, applying micro and nano seconds' pulses has improved the μ ECM machining process, equally the higher frequency improves the process, too. Hence the selected range for the frequency for this experiment is between 10 KHz and 1 MHz for 0.5 mole/L concentration and between 10 KHz and 5 MHz for 0.6 mole/L concentration. Each test last for nearly 40 seconds which consists of 20 seconds monitoring time in order to reach the steady-state and around 20 seconds for the actual process to take place. Figure 4-2 shows the setup for the Impedance method on iviumstat (left) and the selected frequencies (right) for this experiment.

The figure shows two windows from the ivium software. The left window is the 'Direct Method' dialog for 'Impedance' mode. The right window is the 'Edit frequencies' dialog.

Direct Method - Impedance Settings:

Parameter	Value	Unit
Title		
E start	6.5000	V
Equilibration time	0	s
Frequencies	21	
Current Range	1A	
+Noise Reduction	<input type="checkbox"/> Off	
Filter	automatic	
Stability	automatic	
Connect to	Cell-4EL	
+AutoCR	<input type="checkbox"/> Off	
+DualCR	<input type="checkbox"/> Off	
+Apply wrt OCP	<input checked="" type="checkbox"/> On	
Monitor time	20	
Monitor interval	1	
Estart wrt OCP	<input type="checkbox"/> Off	
Vtx/End wrt OCP	<input type="checkbox"/> Off	
Estandby wrt OCP	<input type="checkbox"/> Off	
Record real E	<input type="checkbox"/> Off	
Accept if dE/dt <	0.00	mV/s

Edit frequencies Dialog:

Single sine | Multi sine | Dual sine

Frequencies each decade: 10 (Apply)

Frequency scan: Manual override

Start: 1000000 Hz
End: 10000 Hz
Amplitude: 0.01 V

freq	freq / Hz	amp / mV
freq[1]	1000000	10.0
freq[2]	794328	10.00
freq[3]	630957	10.00
freq[4]	501187	10.00
freq[5]	398107	10.00
freq[6]	316228	10.00
freq[7]	251189	10.00
freq[8]	199526	10.00
freq[9]	158489	10.00
freq[10]	125893	10.00
freq[11]	100000	10.00
freq[12]	79433	10.00
freq[13]	63096	10.00
freq[14]	50119	10.00
freq[15]	39811	10.00
freq[16]	31623	10.00
freq[17]	25119	10.00
freq[18]	19953	10.00

Figure 4-2: Impedance mode on ivium stat (left) & selection of frequencies (right)

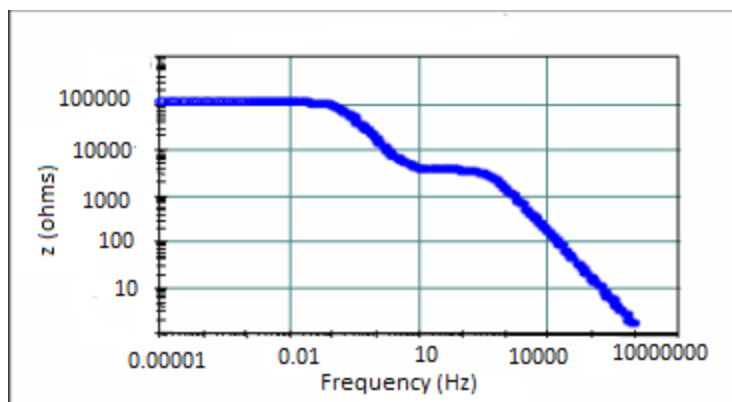
Although the experiments will be solely used to find the equivalent circuit for the electrode-electrolyte interface but the conductivity and the weight of removed materials were measured for all tests, as well. Also, the affected surfaces have been analysed using SEM and EDS.

EIS is a very powerful tool to investigate the electrochemical process features, but it is a very complicated tool when it comes to data analysis and interpretation of the results. Iviumstat suggests an equivalent circuit for any impedance response but it is usually the simplest possible option. Therefore, it is very important to have a comprehensive analysis before accepting the equivalent circuit results. There are a few steps available to help to find the most realistic answer for each impedance response. First, it is recommended to use the Kramers-Kronig (K-K) analysis to evaluate the data. K-K analysis is performed by fitting a general model to data, if the spectral data do not comply with the K-K relation, the data has poor quality and it would not be suitable to fit an equivalent circuit.

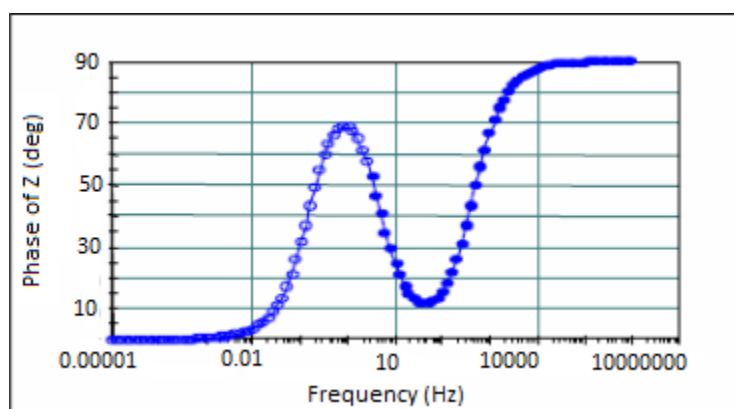
Second step is to analyse the frequency response (Bode or Nyquist graphs). The general form of the Bode graph for a system with one time constant is very simple and easy to recognise; therefore, the Bode plot for a simplified Randles cell is very simple, too. The impedance graph presents two separate flat lines which represent electrolyte resistance and polarisation resistance and the phase graph shows one minimum or maximum stationary point.

But the general form of the Bode plot with two time constants is a bit more complicated as figure 4-3 demonstrates. One of the available options on iviumstat impedance response is the Bode graph, which has been widely used in this research.

In order to analyse the Impedance data from iviumstat, it is necessary to check if data is reliable and trustworthy; K-K transform is a tool to do so. The next step is to know if the resulted Bode plot would fit a system with one time constant or two time constant. Finally, an equivalent circuit can be considered for the Bode plot under the investigation and whether the considered equivalent circuit is suitable or not.



a)



b)

Figure 4-3: Bode plot for a two time constant cell, a) Impedance vs Frequency, b) Phase angle vs Frequency

Following images present the steps taken to analyse the data from Impedance method in order to find the equivalent circuit components for electrode-electrolyte interface. This procedure has been repeated for 24 experiments but only the details for one of the experiments from 0.5 mole/L electrolyte concentration group and one from 0.6 mole/L electrolyte concentration group are presented here.

Table 4-2 shows the applied voltages and electrolyte concentration for a range of the gaps during Impedance experiments on iviumstat. The gap has been set up on 22, 24, 25 and 26 μm . Also, the equivalent circuit components for 0.5 mole/L electrolyte concentration are summarised in this table.

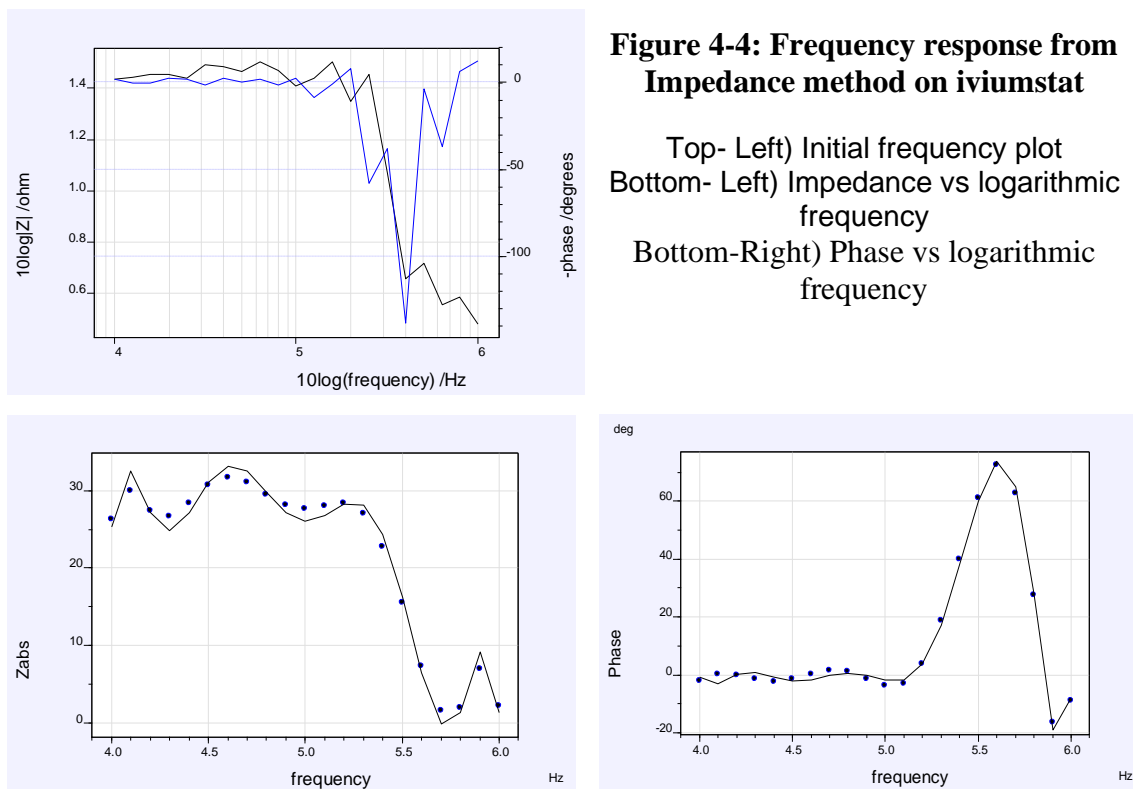
Concentration (mole)	Voltage (Volt)	Gap (μm)	R1 Ohm	C1 F	R2 Ohm	R3 Ohm	C3 F
0.5	6.5	22	1.50E+01	6.38E-08	1.51E+01	3.01E+10	9.89E+00
0.5	6.5	24	1.31E+01	8.57E-08	1.20E+01	3.01E+08	1.286
0.5	6.5	25	1.44E+01	6.43E-08	1.24E+01	1.68E-02	1.00E-13
0.5	6.5	26	1.36E+01	7.00E-08	1.14E+01	1.00E+11	1.381
0.5	7	22	1.07E+01	1.80E-07	1.71E+01	1.42E+09	2.87E-01
0.5	7	24	1.21E+01	1.93E-07	1.21E+01	4.50E+10	0.01384
0.5	7	25	1.27E+01	8.03E-08	1.33E+01	2.48E+09	9.88E-01
0.5	7	26	1.08E+01	7.01E-08	1.46E+01	8.81E+10	0.2147
0.5	7.5	22	9.07E+00	1.01E-07	1.62E+01	5.98E+11	6.68E-02
0.5	7.5	24	1.38E+01	8.41E-08	1.30E+01	4.16E+11	7.773
0.5	7.5	25	1.16E+01	7.24E-08	1.36E+01	2.04E+12	1.76E-02
0.5	7.5	26	1.45E+01	5.86E-08	1.28E+01	1.44E+12	0.01186
Average values			1.26E+01	9.36E-08	1.36E+01	3.97E+11	1.83E+00

Table 4-2: Equivalent circuit components values (0.5 mole/L)

The impedance experiment's results for the 0.5 mole/L electrolyte concentration, 7 volts voltage and 25 μm gap size are presented in figure 4-4. The frequency response was investigated for the interval between 10 KHz and 1 MHz.

Figure 4-4 illustrate the initial graph in the form of Bode plot which then was smoothed using the curve fitting options in iviumstat.

As figure 4-4 demonstrates the system shows significant changes at higher frequencies. Capacitive impedance decreases by the rise of the frequency; knowing that the total impedance of the equivalent circuit is the result of the parallel R and C, the total impedance of the system decreases as well. Also, for lower frequencies the cell presents a resistive behaviour, hence there is no phase change between current and voltage signals but at the higher frequencies when the cell capacitive behaviour is dominant, there is a phase shift between current and voltage signals.



Although curve fitting has eliminated some useful data from the frequency response, reviewing the initial frequency response presents that the first significant change (cut-off frequency) happens at 251 KHz and the second one happens at 500 KHz. Figure 4-5 and 4-6 show these two frequencies. Between these two frequencies, the capacitive behaviour of the cell is predominant.

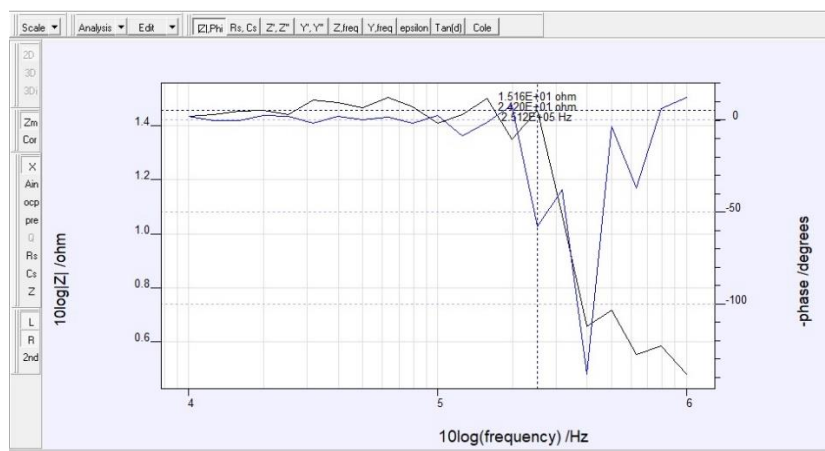


Figure 4-5: Impedance results- frequency response at 251 KHz



Figure 4-6: Impedance results- frequency response at 500 KHz

After general assessment, the Bode plots have been tested using K-K transform (figure 4-7) and finally the desired equivalent circuit was calculated for the curve. The equivalent circuit was calculated based on the Randles network (figure 4-8)

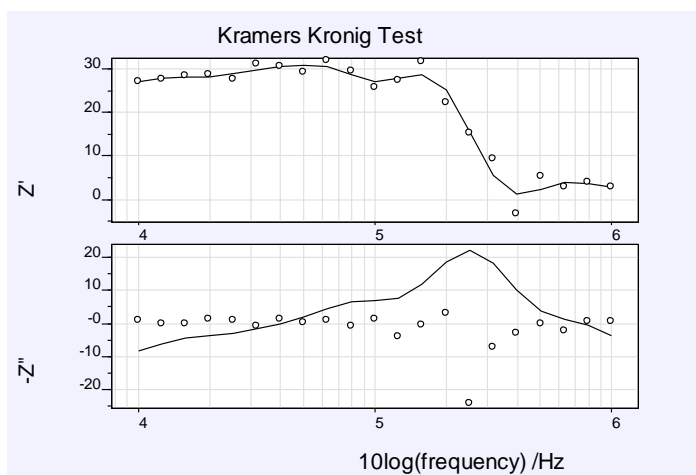


Figure 4-7: Impedance results: Kramers Kronig test

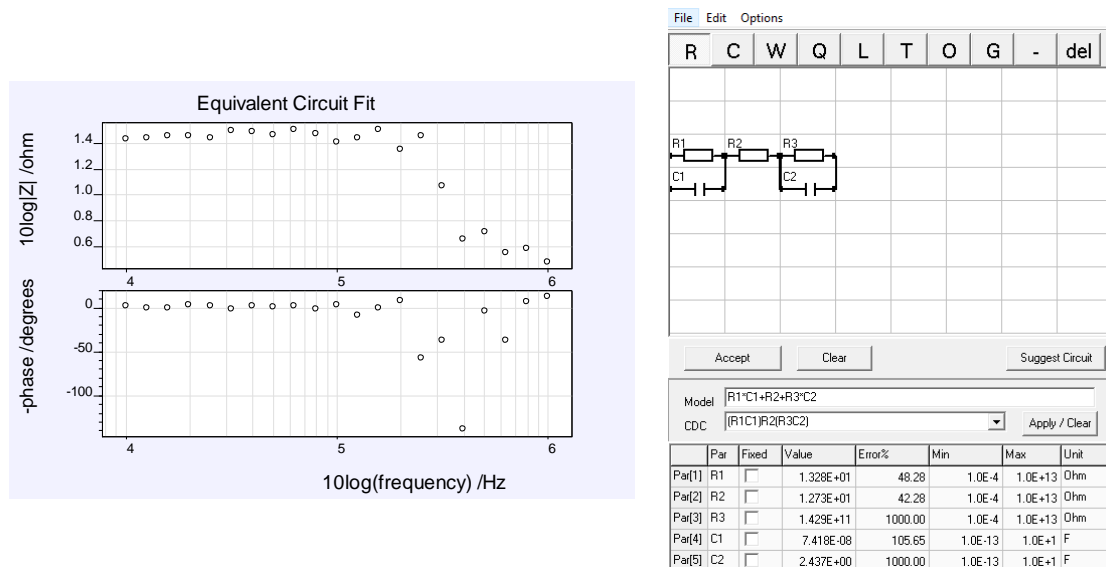


Figure 4-8: Impedance result: Equivalent circuit fit and components values

As iviumstat works in a way to have one electrode as the working electrode (workpiece) and the other as counter electrode (tool electrode), it is logical to consider that the R1 and C1 are demonstrating the interface between working electrode and electrolyte, R2 is representing electrolyte resistance and R3 and C2 are demonstrating the tool electrode- electrolyte interface.

The pair of R1, C1 is representing charge transfer resistance and EDL capacitance at workpiece end while the pair of R3, C2 representing tool electrode end.

Using the stated formulas in chapter3, it is expected to have the following values for the RC components when 7 volts voltage applied at 0.5 mole/L electrolyte concentration and 25 μm gap was maintained.

Electrolyte concentration calculation: Conductivity of the solution has been changed during the experiment, so for the calculations, the average conductivity has been used.

$$R = \frac{1}{k} \frac{L}{A} = \frac{1}{10.98} \frac{25 \times 10^{-6}}{(25 \times 10^{-5})^2 \pi} = 11.59 \text{ ohm} \quad \text{vs software calculation} = 13.6 \text{ ohm}$$

EDL capacitance calculation does not follow the capacitor calculation formula as EDL capacitance is changing by voltage and charge transferred on its surfaces between

the solution and metal. But the instance capacitance can be calculated using the formula considering the dielectric layer distance is in Angstrom range. Also, relative permittivity of NaNO₃ depends on the temperature and concentration and its other features.

$$C/\varepsilon = \varepsilon_0 \frac{A}{L} = 8.85 * 10^{-12} \frac{\pi(25 * 10^{-5})^2}{x * 10^{-10}} = \frac{0.174 * 10^{-6}}{10} = 0.174 * 10^{-5}$$

If the dielectric layer width considered in the range of 10 and 20 angstroms, and relative permittivity to be taken around 79, the capacitance value fell in the calculated range. Although these nominal values are used in similar studies but cannot be taken for sure as any insignificant change in the experimental environment, can affect the results significantly.

Same procedure has been applied for the impedance experiment at 0.6 mole/L electrolyte concentration. All applied voltages and IEG gaps values for the 0.6 mole/L electrolyte concentration together with the equivalent RC values for these experiments are presented in the table 4-3.

Concentration (mole)	Voltage (Volt)	Gap (μm)	R1 Ohm	C1 F	R2 Ohm	R3 Ohm	C3 F
0.6	6.5	22	2.22E+01	2.05E-08	8.23E+00	2.77E-01	1.07E-05
0.6	6.5	24	2.11E+01	4.26E-08	9.00E+00	3.00E+03	0.2953
0.6	6.5	25	1.99E+01	4.45E-08	4.71E+00	3.20E+00	1.00E-13
0.6	6.5	26	1.88E+01	3.78E-08	7.54E+00	1.41E+07	2.156
0.6	7	22	1.83E+01	3.33E-07	7.07E+00	8.07E+05	7.921
0.6	7	24	2.26E+01	3.37E-08	6.78E+00	3.49E+07	3.121
0.6	7	25	1.89E+01	1.25E-08	7.57E+00	1.72E+10	5.38E-01
0.6	7	26	2.03E+01	3.44E-08	8.56E+00	7.15E+09	1.367
0.6	7.5	22	1.89E+01	3.60E-08	7.35E+00	2.01E+12	5.06E-01
0.6	7.5	24	2.31E+01	2.16E-08	6.08E+00	2.87E+12	8.597
0.6	7.5	25	1.93E+01	3.99E-08	4.38E+00	2.16E+00	1.00E-13
0.6	7.5	26	1.86E+01	3.29E-08	7.08E+00	1.96E+07	7.47E+01
Average values			2.02E+01	3.25E-08	7.03E+00	4.08E+11	2.10E+00

Table 4-3: Equivalent circuit components values (0.6 mole/L)

Below, presents the detailed analysis for one of the experiments at 0.6 mole/L electrolyte concentration.

The graphs and calculations for the 7.5 volts and 26 μm gap with 0.6 mole/L electrolyte concentration are presented as follow. For the experiments at 0.6 mole/L, the frequency interval was extended to 5 MHz, therefore the frequency response was calculated at 28 different frequencies on iviumstat.

Figure 4-9 illustrates the general Bode plot of the frequency response and smoothed Impedance and phase angle plots vs logarithmic frequency between 10 KHz and 5 MHz using curve fitting option available on the iviumstat software

As expected, at lower frequencies, the cell shows resistive behaviour and subsequently, there is no phase change between current and voltage signals. As the frequency increases the impedance absolute value decreases and simultaneously cell presents a phase change. At frequencies greater than 100 KHz, the cell presents capacitive behaviour and phase angle moves to the negative area in which voltage signal lags the current signal and impedance decreases to the lowest level.

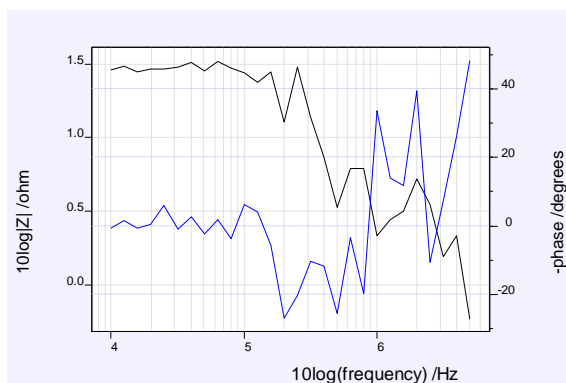


Figure 4-9: Frequency response from Impedance method on iviumstat (0.6 mole/L)

Top- Left) Initial frequency plot
Bottom- Left) Impedance vs logarithmic frequency
Bottom-Right) Phase vs logarithmic frequency

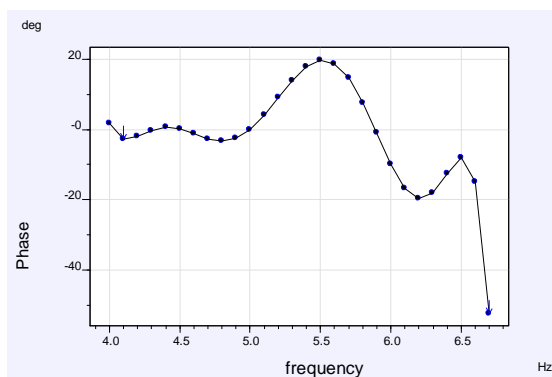
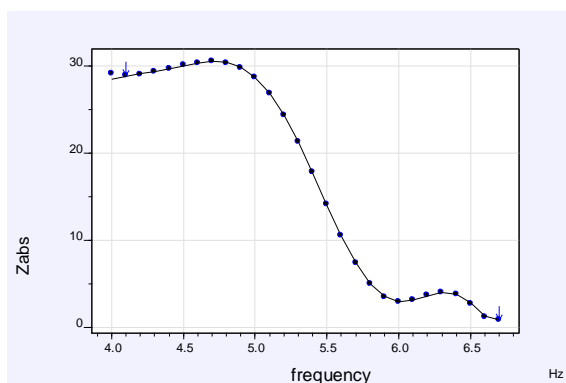


Figure 4-10 and 4-11 show the cut-off frequency at 99.1 KHz and 998.2 KHz, respectively.

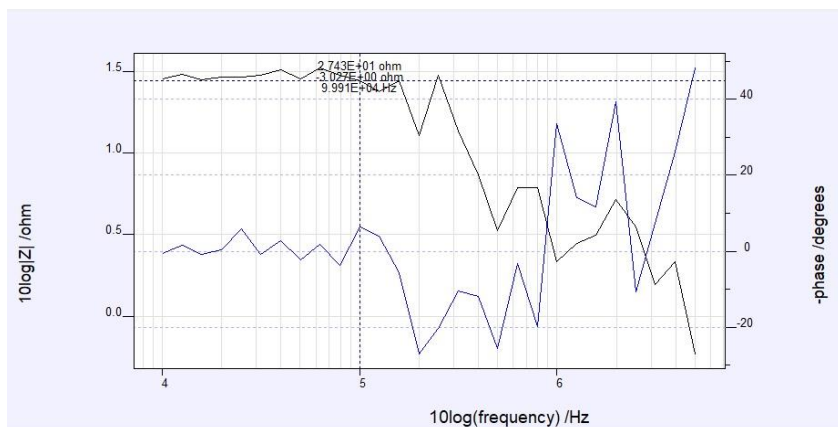


Figure 4-10: Impedance results- frequency response at 99.1 KHz

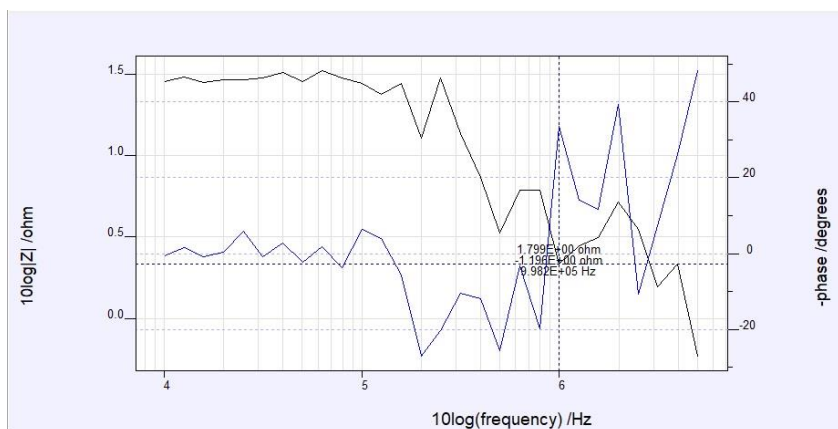


Figure 4-11: Impedance results- frequency response 998.2 KHz

After general assessment, the Bode plots have been tested using K-K transform by software and finally the desired equivalent circuit was calculated for the curve.

The equivalent circuit was calculated based on the Randles network (Figure 4-12 and 4-13).

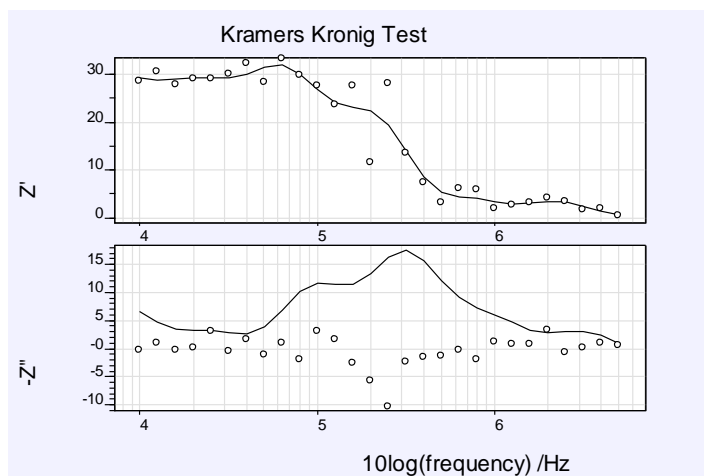


Figure 4-12: Kramers Kronig test (0.6 mole/L, 7.5 volts, 26 μm)

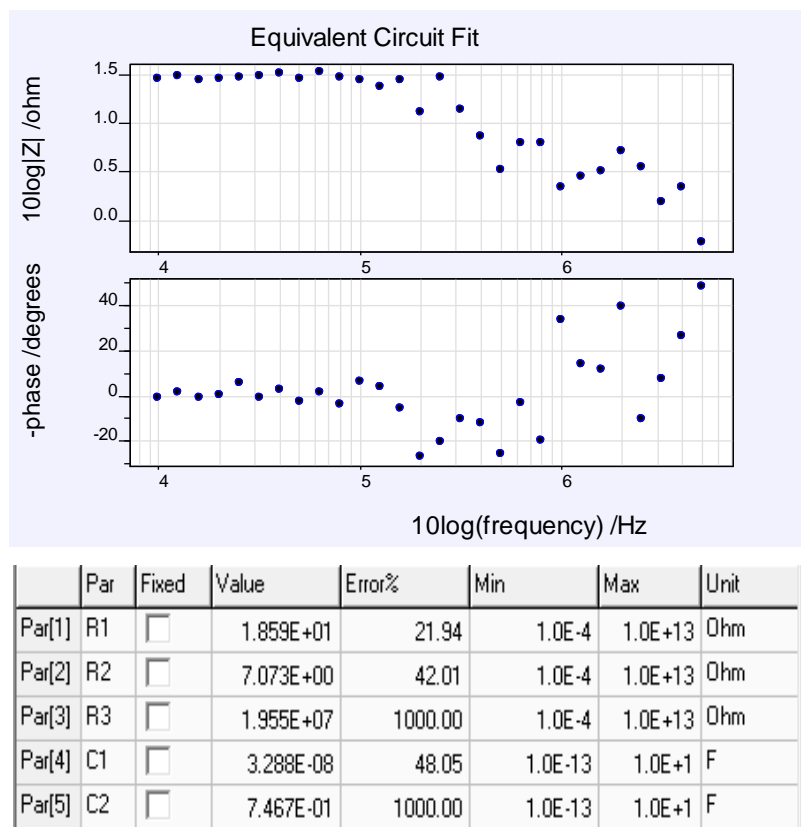


Figure 4-13: Impedance result: Equivalent circuit fit and components values

R1 and C1 are charge transfer resistor and EDL capacitor at workpiece-electrolyte side, respectively.

$$C/\varepsilon = \varepsilon_0 \frac{A}{L} = 8.85 * 10^{-12} \frac{\pi(25 * 10^{-5})^2}{x * 10^{-10}} = \frac{0.174 * 10^{-6}}{x}$$

If the dielectric layer width (x) considered to be in the range of 20 and 40 angstroms', and relative permittivity to be taken around 75, the capacitance value fell in the calculated range.

Although these nominal values have been used in similar studies, cannot be taken into the account for sure as any insignificant changes in the experimental environment, can affect the results significantly. Therefore, only the experimental values have been taken into the account for any calculations or analytical purposes.

Electrolyte resistance, which is presented by R2, can be calculated as below:

$$R = \frac{1 L}{k A} = \frac{1}{23} \frac{26 * 10^{-6}}{(25 * 10^{-5})^2 \pi} = 5.75 \text{ ohm} \text{ vs software suggested } 7.08 \text{ ohm}$$

All 12 experiments which took place for 0.6 mole/L electrolyte concentration, presented similar electrolyte resistance, an average value of 7.03 ohm.

Electrolyte resistance depends on the effective geometry of the machining area in which current flows and solution conductivity. During the impedance investigation, the geometry of the machining zone and the gap between electrodes were kept similar and only electrolyte concentration changed from 0.5 mole/L to the 0.6 mole/L. Although this change seems very little but its effect on the electrolyte resistance was very significant in which the average resistance changed from 13.6 ohm at 0.5 mole/L electrolyte concentration to 7.03 ohm for 0.6 mole/L. This proves that electrolyte concentration has a very strong influence on the electrolyte resistance and consequently on machining outcomes.

Conductivity depends on temperature, ionic concentration, mobility and valence of ions. Ideally, conductivity should proportionally increase by solution concentration, but this ideal behaviour is never the case. Conductivity increases by concentration up to a maximum value and then starts to decline as the concentration rises.

Finally, table 4-4 demonstrates the weight and conductivity measurements for all experiments. Although each experiment took only forty seconds, the changes in conductivity and the volume of removed materials are considerable. The gathered data in

this table will be used in chapter 4, section 4-3 to evaluate the combination of the parameters and their interrelation.

Concentration (mole)	Voltage (Volt)	Gap (μm)	Conductivity (S)		Weight (g)		
			Start	End	Initial	End	MR
0.5	6.5	22	43.6	34.6	10.91060	10.91058	
0.5	6.5	24	43.1	42.9	10.91058	10.91055	3E-05
0.5	6.5	25	42.8	28.4	10.91055	10.91051	4E-05
0.5	6.5	26	42.3	34.9	10.91051	10.91049	2E-05
0.5	7	22	N.R	N.R	10.91049	10.91045	4E-05
0.5	7	24	27.1	31.2	10.91045	10.91035	0.0001
0.5	7	25	16.92	5.04	10.91035	10.91028	7E-05
0.5	7	26	28.4	7.81	10.91028	10.91023	5E-05
0.5	7.5	22	22.7	5.4	10.91023	10.91009	0.00014
0.5	7.5	24	41.4	29.6	10.90994	10.90988	6E-05
0.5	7.5	25	24.8	7.17	10.91008	10.91002	6E-05
0.5	7.5	26	14.47	1.16	10.91002	10.90994	8E-05
0.6	6.5	22	51.7	36	10.90984	10.90982	2E-05
0.6	6.5	24	51	32.8	10.90982	10.90979	3E-05
0.6	6.5	25	51.1	47	10.90979	10.90975	4E-05
0.6	6.5	26	52.1	45.7	10.90975	10.90971	4E-05
0.6	7	22	51.7	36	10.90971	10.90961	1E-04
0.6	7	24	45	22.6	10.90961	10.90958	3E-05
0.6	7	25	52.1	39.6	10.90958	10.90948	1E-04
0.6	7	26	51.5	32.3	10.90948	10.90942	6E-05
0.6	7.5	22	48.7	28.2	10.90942	10.90927	0.00015
0.6	7.5	24	47.9	22.8	10.90927	10.90918	9E-05
0.6	7.5	25	51.8	37	10.90918	10.90915	3E-05
0.6	7.5	26	48.2	25.4	10.90915	10.90898	0.00017

Table 4-4: Conductivity and removed material measurement during impedance experiment

In addition to the above analysis, the workpiece surface features have been investigated using SEM and EDS in order to generate further details and assessment for the reaction outcomes.

4.1.2 Equivalent circuit electrode-electrolyte interface – Nickel tool electrode

In addition to tungsten, the impedance test was repeated using nickel as tool electrode stainless steel as workpiece. nickel wire with 1.00 mm diameter and 99.98% purity from Goodfellow was selected.

The equivalent circuit for the pair of stainless steel and nickel was evaluated while frequency response assessed between 10 KHz and 5 MHz, at 6.5, 7 and 7.5 volts for the 22, 24, 25 and 26 μm gap sizes. Table 4-5 presents the suggested RC values for 0.5 mole/L and table 4-6 presents the RC values for 0.6 mole/L electrolyte concentration.

Voltage	Gap	R1	C1	R2	R3	C3	Weight
(Volt)	(μm)	Ohm	F	Ohm	Ohm	F	MR(g/s)
6.5	22	4.044E+00	4.211E-08	6.517E+00	8.416E+08	2.043E-01	0.000150
6.5	24	5.365E+00	5.321E-08	1.448E+00	2.517E+00	1.000E-13	0.000170
6.5	25	6.020E+00	4.932E-08	3.444E+00	5.277E+09	1.895E+00	0.000050
6.5	26	4.663E+00	7.971E-08	3.495E+00	9.031E+06	1.457E+00	0.000040
7	22	4.223E+00	7.665E-08	3.810E+00	1.071E+09	7.009E+00	0.000490
7	24	4.504E+00	1.691E-07	3.911E+00	3.644E+08	1.356E+00	0.000460
7	25	3.925E+00	1.060E-07	3.910E+00	2.848E+10	1.875E+00	0.000400
7	26	4.189E+00	1.779E-07	4.155E+00	4.756E+09	2.682E+00	0.000120
7.5	22	5.440E+00	5.929E-08	3.289E+00	6.100E+00	3.803E+00	0.000160
7.5	24	5.143E+00	1.056E-07	2.547E+00	6.474E+02	6.334E+00	0.000450
7.5	25	4.699E+00	9.808E-08	3.292E+00	1.677E-04	2.739E-03	0.000330
7.5	26	5.237E+00	4.485E-08	2.814E+00	7.773E-01	1.723E-01	0.000270
Average		4.79E+00	8.85E-08	3.55E+00	3.40E+09	2.23E+00	

Table 4-5 Equivalent circuit values (Nickel tool electrode, 0.5 mole/L electrolyte concentration)

Electrolyte resistance (R2) has decreased remarkably in comparison with the electrolyte resistance when tungsten electrode was used as tool electrode. The difference between two electrodes' dimensions has hugely affected the electrolyte resistance by which equivalent resistance with nickel electrode tool decreased nearly by a third.

Figure 4-14 presents the anodic reaction spot on the workpiece surface and the average size of the spot.

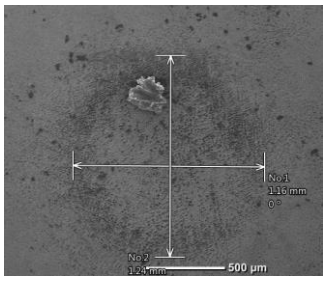
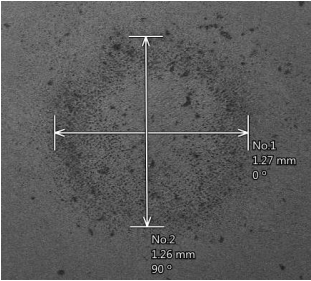
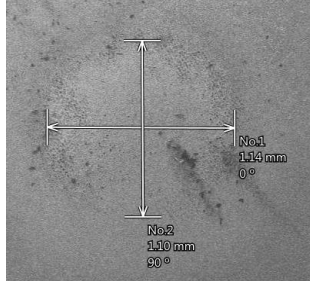
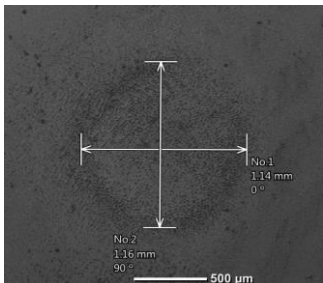
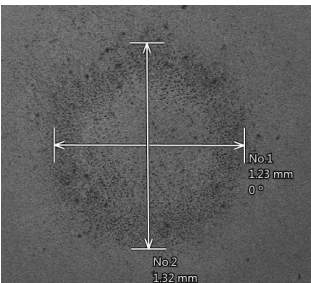
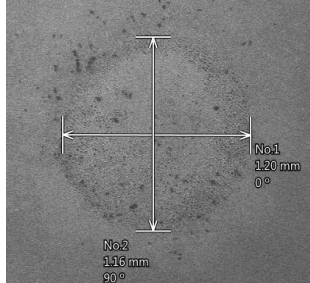
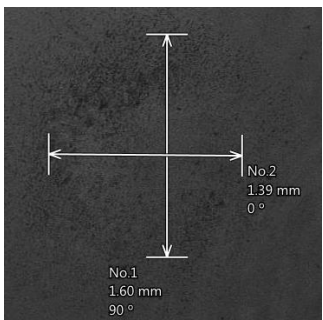
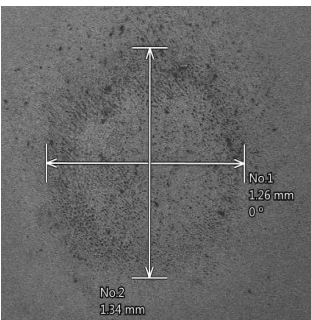
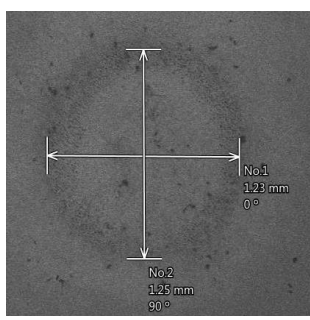
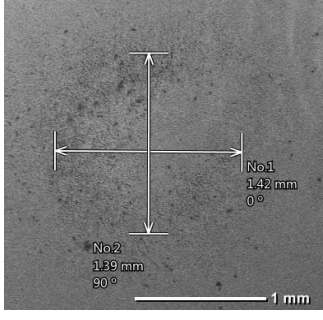
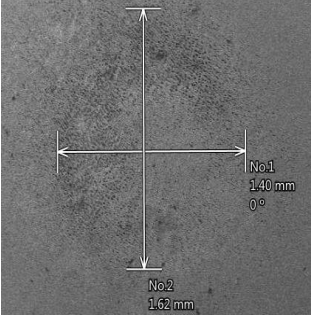
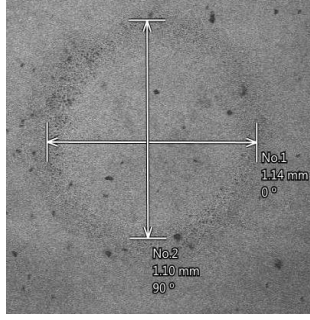
Gap/Voltage	6.5 (V)	7(V)	7.5 (V)
22 (μm)			
24 (μm)			
25 (μm)			
26 (μm)			

Figure 4-14: Impedance experiment marks on workpiece (Nickel tool electrode, 0.5 mole/L electrolyte concentration)

Combination of the three factors including workpiece surface quality, overcut size and level of removed materials presented the best results for the 7.5 volts.

Table 4-6 and figure 4-15 demonstrate the equivalent circuit components' values for nickel tool electrode and 0.6 mole/L electrolyte concentration and the SEM images of the workpiece, respectively.

Voltage	Gap	R1	C1	R2	R3	C3	Weight(g)
(Volt)	(μm)	Ohm	F	Ohm	Ohm	F	MR
6.5	22	4.942E+00	6.722E-08	3.354E+00	2.168E+09	2.904E+00	0.00021
6.5	24	4.038E+00	1.037E-07	3.665E+00	1.871E+03	1.668E+00	0.00019
6.5	25	3.759E+00	9.548E-08	3.745E+00	2.297E+12	5.760E-01	0.0002
6.5	26	4.689E+00	1.040E-07	3.762E+00	1.120E+05	3.247E+00	0.00035
7	22	5.362E+00	7.419E-09	3.320E+00	3.410E+04	3.104E-01	0.00025
7	24	3.015E+00	2.072E-07	3.012E+00	1.125E+00	4.372E-08	0.00031
7	25	4.495E+00	3.939E-08	3.003E+00	2.272E+10	3.465E+00	0.00037
7	26	4.629E+00	1.239E-07	3.740E+00	5.852E+09	7.301E+00	0.00022
7.5	22	4.454E+00	9.482E-08	2.943E+00	1.911E+11	1.598E-01	0.00024
7.5	24	5.131E+00	7.295E-08	2.653E+00	2.562E+09	1.085E+00	0.00049
7.5	25	3.460E+00	4.062E-08	2.837E+00	9.849E-01	1.306E-06	0.00045
7.5	26	4.490E+00	8.372E-08	2.940E+00	1.755E+05	1.653E+00	0.00039
Average		4.37E+00	8.67E-08	3.25E+00	2.10E+11	1.86E+00	

Table 4-6: Equivalent circuit values (Nickel tool electrode, 0.6 mole/L electrolyte concentration)

In contrast with RC equivalent circuit for tungsten tool electrode, there is not much change between electrolyte resistance in case of nickel tool electrode at 0.5 mole/L and 0.6 mole/L electrolyte concentration. Although the experiments for both cases run at the same environmental conditions including ambient temperature, the different behaviour of these cases about the electrolyte resistance presents the importance of the tool electrode dimension and the effective interface area. Nickel tool electrode diameter and surface area was as twice and four times as tungsten diameter and tool surface area, respectively; considering similar environmental condition and electrolyte conductivity, electrolyte resistance for the tungsten tool electrode should be four times greater than electrolyte resistance for the nickel tool electrode.

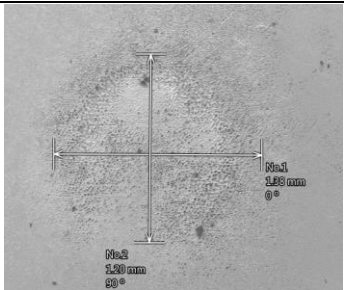
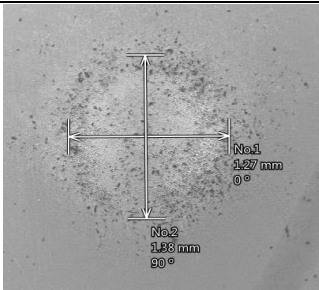
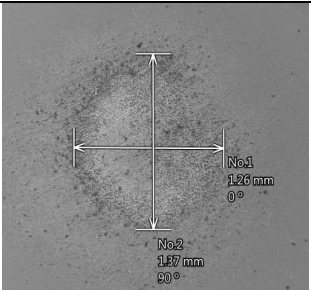
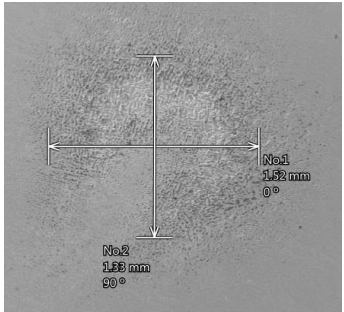
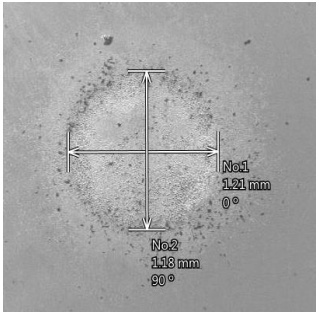
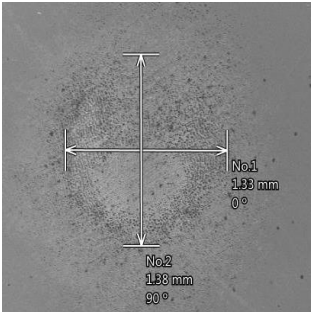
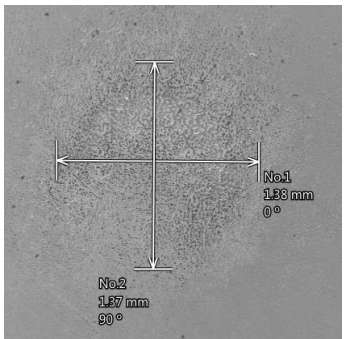
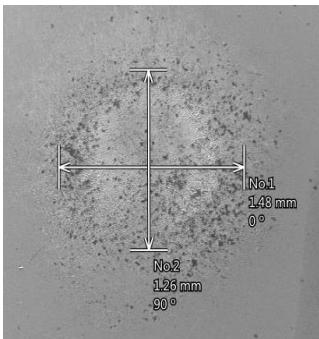
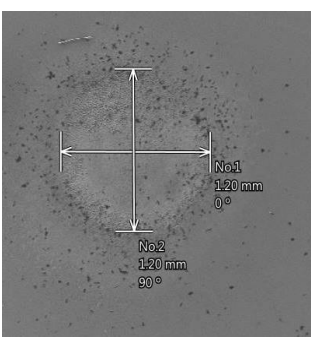
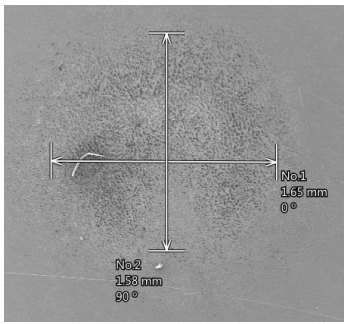
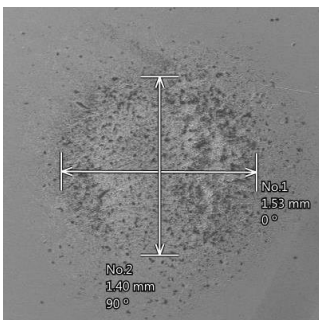
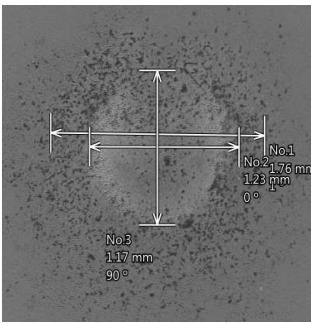
Gap Voltage	6.5 (V)	7(V)	7.5 (V)
22 (μm)			
24 (μm)			
25 (μm)			
26 (μm)			

Figure 4-15: Impedance experiment marks on workpiece (Nickel tool electrode, 0.6 mole/L electrolyte concentration)

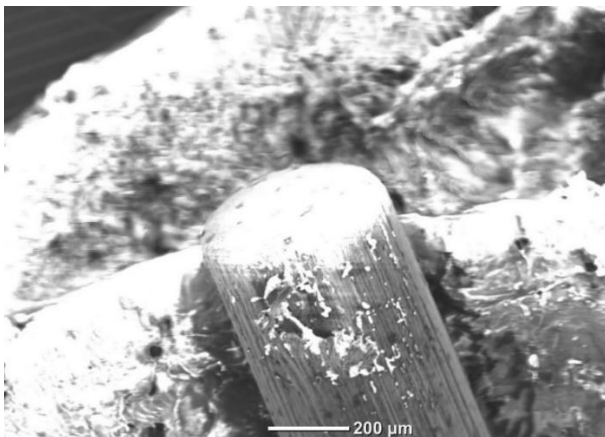
This expectation is valid at 0.5 mole/L electrolyte concentration, but it is not valid at 0.6 mole/L electrolyte concentration. This comparison shows that the effect of the conductivity can override the effect of the tool dimensions for thicker tool electrodes.

4.2 Impedance experiment tool assessment

Tungsten and nickel tool electrodes were assessed after impedance experiments to have a visual picture of any changes may happen on the tool surface during this experiment.

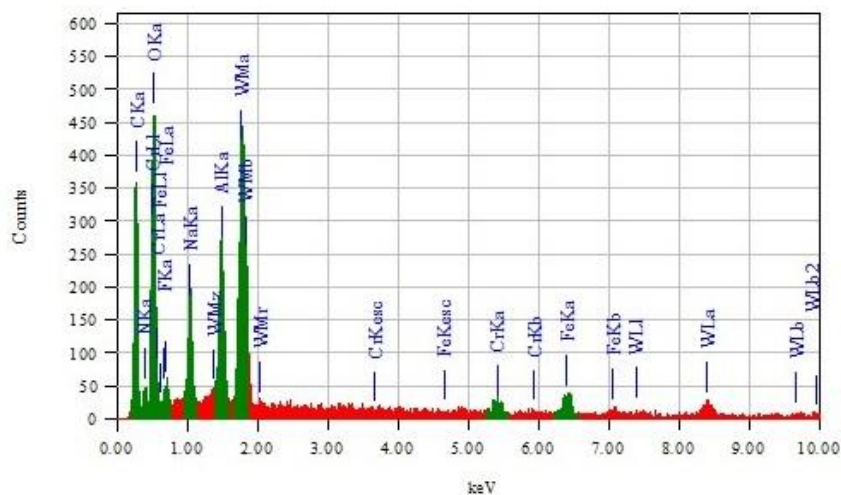
4.2.1 Tungsten tool electrode assessment (impedance experiment)

Figure 4-16 and 4-17 illustrate the tool surface SEM and EDS spectrum after impedance experiments. There was a total of 24 experiments and each experiment only took 20 seconds effectively. Although, similar black layer covered the tool surface, the thickness and the darkness were not as much as previous experiments. The length of the reaction is certainly an effective parameter in creation of the thickness of this layer.



**Figure 4-16:
Tungsten tool
surface SEM
image at the end
of the impedance
experiment**

The EDS spectrum presents similarities with the previous assessment (section 3-5, figure 3-55) in terms of the peak elements but mass% are slightly different between two assessments with the maximum deviation for the Na and W.



ZAF Method Standardless Quantitative Analysis
Fitting Coefficient : 0.0908

Element	(keV)	Mass%	Sigma	Atom%	Compound	Mass%	Cation	K
C	0.277	0.80	0.01	1.49				0.9858
N	0.392	13.61	0.47	21.73				32.4866
O	0.525	44.61	0.68	62.34				33.9431
F								
Na	1.041	5.71	0.19	5.55				3.7299
Al	1.486	4.72	0.13	3.91				4.4930
Cr	5.411	1.23	0.10	0.53				1.3259
Fe	6.398	3.15	0.17	1.26				3.4372
W	1.774	26.17	0.58	3.18				19.5984

Figure 4-17: Tungsten tool surface EDS spectrum at the end of the impedance experiment

4.2.2 Nickel tool electrode assessment (impedance experiment)

Nickel tool electrode was only used for the impedance experiments using iviumstat. Figure 4-18 and 4-19, present the nickel tool electrode profile and its EDS analysis before it was used for the experiments. As figure 4-19 shows, the peak elements of the EDS spectrum are C, O, Ni and F.

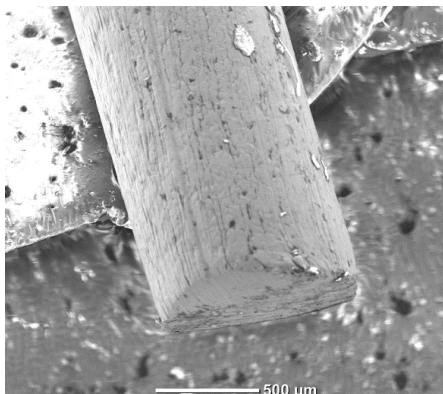


Figure 4-18- SEM image Nickel tool electrode before impedance experiments

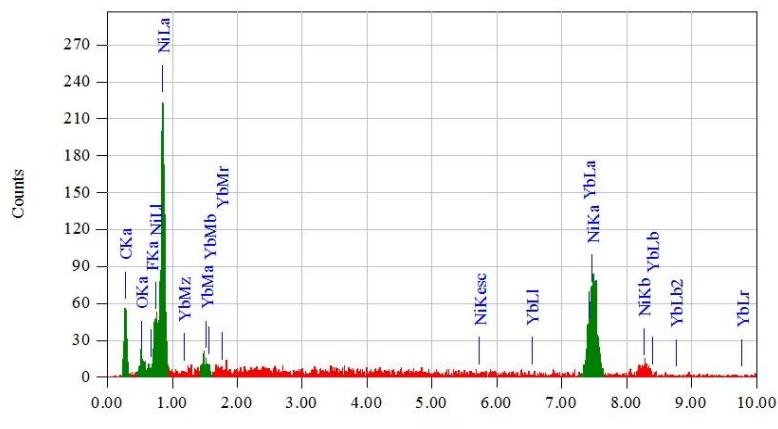


Figure 4-19: EDS spectrum- Nickel tool electrode before impedance experiments

The tool electrode profile was examined using EDS in case there is any changes in its peak elements. The result is presented in figure 4-20. As figure 4-20 shows, a dark layer has fully covered the tool surface. This layer in comparison with similar situation using tungsten tool electrode is undoubtedly significant. However, the creation of this layer on the tool surface did not create any significant changes on impedance experiments but the main reason is that each experiment took only 20 seconds. The EDS spectrum in figure 4-21 shows the C, F, Ni, N and Al as peak elements after the experiments. The main difference between two spectrums is Al, and increased level of C.

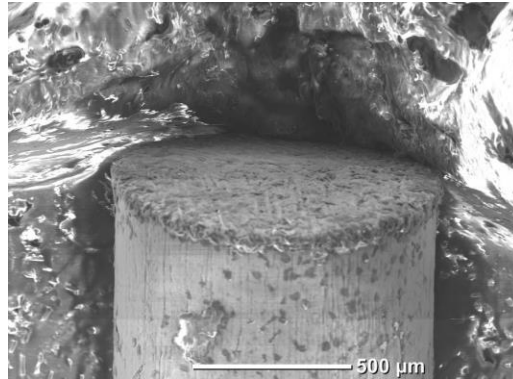


Figure 4-20: SEM image - Nickel tool electrode after impedance experiments

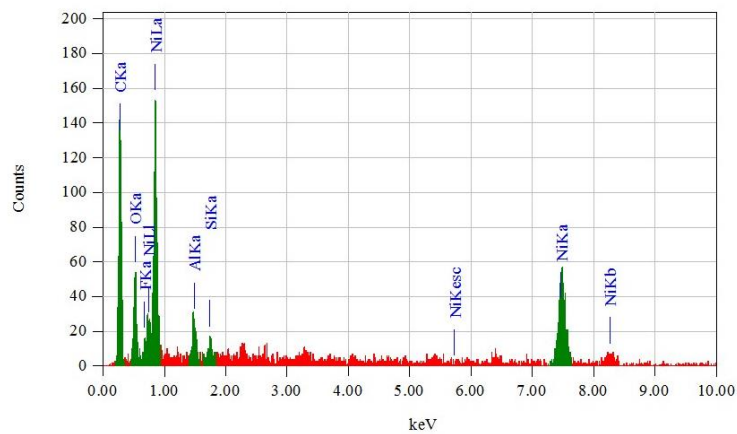


Figure 4-21: EDS spectrum- Nickel tool electrode after impedance experiments

4.3 Matlab Simulation

AS mentioned, the electrode- electrolyte interface in μ ECM can be electronically modelled as Randles model (figure 3-6). Following the previous experiments using iviumstat in order to understand and evaluate the electrochemical features of the electrode-electrolyte interface, this section will emphasis on electrical features of the applied voltage signals to the cell.

It has been an interest to find a way to present the relation between EDL capacitor and any effective parameters including potential, IEG size, frequency and electrolyte features. Hotoiu et al (2014) work in which they introduced their novel approach to simulate nanosecond pulses in μ ECM process to reduce the computational effort and run time, Weber et al (2013) run their simulation model on COMSOL considering material-electrolyte interface to predict current evolution. They used EIS (Electrochemical Impedance Spectroscopy) to have impedance details at interface, which are constant values. Kozak et al (2008) mathematical simulation presented a good example of change of potential, current density and charge density with IEG. Sueptitz et al (2013), used the RC model for electrode-electrolyte interface simulation for passive electrodes. They used EIS to determine the capacitance of EDL and showed the dependency of capacitance to potential and frequency for both electrodes. In most of these works, the main concentration was on machining system and performance rather than the electrical features of the system with regards to the equivalent RC network while in the current study, the main focus is on electrical features of the electrode- electrolyte interface using Randle model.

A simulation model has been created using Simscape, Matlab 2018a to investigate the voltage- current response of the model for the applied pulse voltage signals in order to investigate and analyse pulse width, pulse amplitude and duty cycle and pulse relation with the electrochemical features of the cell. The model is based on Randles and it is a simple RC network, initial values for capacitors and resistors are extracted from EIS results in previous section, therefore the simulation results can be applied to the same cell unit which was under the investigation with iviumstat.

The aim of this work is to investigate behaviour of interface in terms of electrical condition and establish a foundation to predict some of the machining parameters including pulse amplitude, pulse duty and period.

4.3.1 μ ECM electrode-electrolyte interface model (0.5 mole/L electrolyte concentration) - Tungsten tool electrode

The components in the model include electrolyte resistor (R_{EL}), charge transfer resistor which is known as faradic resistor (R_{CT}) and EDL capacitor (C_{DL}); there is a parallel set of C_{DL} and R_{CT} for anode and one set for cathode(differentiated in the

model with letter A for anode and letter C for cathode). Warburg impedance is very small at high frequencies and can be neglected (Bhattacharyya, 2015); hence It has not been modelled in this simulation.

Table 4-7 shows the parameters' values for the equivalent RC network. The values for EDL capacitor and faradic resistance were obtained through EIS data analysis, and electrolyte resistance was calculated through the equation. Considering the removed material and overcut from the impedance results, the most successful combination of the parameters found when the electrolyte concentration was 0.5 mole/L, volt was 7 volts and gap size was 24 μm .

Parameter	Symbol in model	Equation	Value
Electrolyte resistance	R_EL	$R = \frac{L}{k A}$	12.1 Ω
Charge transfer resistance	R_CTA (Anode)	$R_{ct} = \frac{RT}{nFi_o}$	12.1 Ω
EDL capacitance	C_DLA (Anode)	$C_{dl} = \frac{\epsilon_0 \epsilon_r A}{L}$	1.93e-07 F
Charge transfer resistance	R_CTC (Cathode)	$R_{ct} = \frac{RT}{nFi_o}$	4.5e+10 Ω
EDL capacitance	C_DLC (Cathode)	$C_{dl} = \frac{\epsilon_0 \epsilon_r A}{L}$	0.01384 F

Table 4-7: Equivalent circuit's components' value for Matlab model

Figure 4-22 shows the designed model with Matlab Simulink for the μECM equivalent RC network.

In this model, in Matlab Simulink, the equivalent RC network for EDL was designed based on Randles model. EDL capacitor and faradic resistor are in parallel for tool electrode-electrolyte interface; this pair is in series with the electrolyte resistor and finally another pair of EDL capacitor and faradic resistor is used to model the workpiece-electrolyte interface in series with electrolyte resistor.

In order to have better understanding of the RC circuit, it is important to analysis the circuit in terms of electrical features which includes equivalent impedance values at low and high frequencies and capacitive time constant.

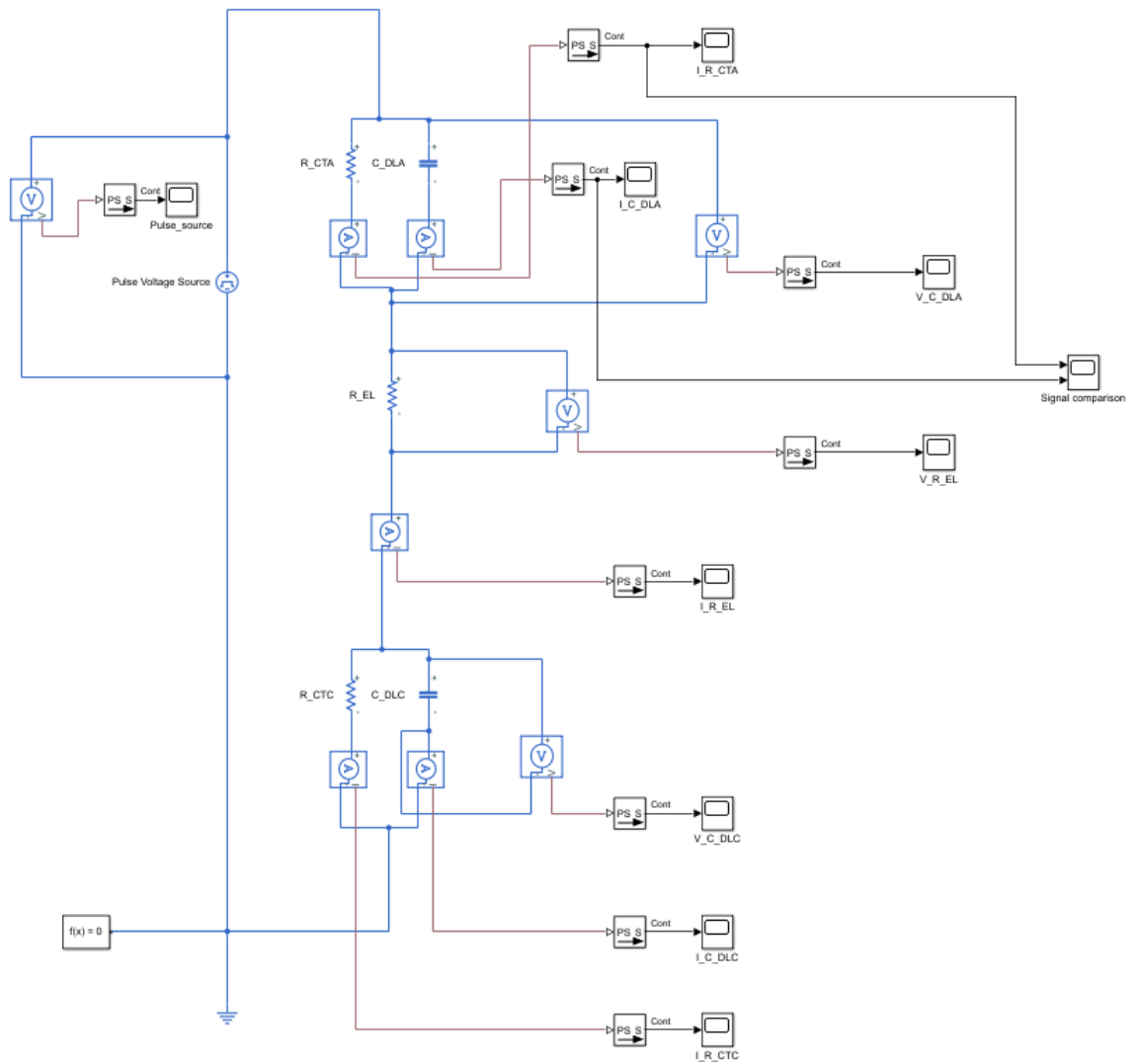


Figure 4-22: Matlab constant RC model

The equivalent impedance for the circuit is calculated using the formula below:

- Parallel RC equivalent Impedance:

$$Z = \frac{RX_c}{R+X_c} = \frac{R \frac{1}{\omega C}}{R + \frac{1}{\omega C}} = \frac{\frac{R}{2\pi f C}}{R + \frac{1}{2\pi f C}} \quad (4-4)$$

Hence, the equivalent impedance of the Randle circuit is calculated as below:

$$\text{Equivalent Impedance} = Z = R_1 \parallel C_1 + R_2 + R_3 \parallel C_2 \quad (4-5)$$

$$Z = 12.1 \parallel \frac{1}{j2\pi f 1.93 * 10^{-7}} + 12.1 + 4.5 * 10^{+10} \parallel \frac{1}{2\pi f 0.01384}$$

$$Z = \frac{\frac{0.997811 * 10^7}{jf}}{12.1 * jf + 0.082463 * 10^7} + 12.1 + \frac{\frac{51.748356 * 10^{+10}}{jf}}{4.5 * 10^{10} jf + 11.499635}$$

$$Z = \frac{0.997811 * 10^7}{j12.1 * f + 0.082463 * 10^7} + 12.1 + \frac{51.748356 * 10^{+10}}{j4.5 * 10^{10} f + 11.499635}$$

$$= \begin{cases} f \rightarrow 0 \Rightarrow |Z| = 12.1 + 12.1 + 4.5 * 10^{10} = 4.5 * 10^{10} \\ \quad \quad \quad \angle Z \cong 0^\circ \\ f \rightarrow \infty \Rightarrow |Z| = 0 + 12.1 + 0 = 12.1 \\ \quad \quad \quad \angle Z \cong 0^\circ \end{cases}$$

As this calculation proves, applying DC voltage to μECM is not a good option as the electrode-electrolyte interface demonstrate high resistance; on the other hand, at very high frequencies, electrode-electrolyte interface demonstrates a low resistance which equals to the electrolyte resistance. For this specific cell, increasing the pulse voltage signal frequency from 1 MHz to higher frequencies does not apply any significant changes to the equivalent circuit's impedance. But applying pulse voltage signals within the range of 100 KHz and 1 KHz will increase the equivalent circuit's resistance from 30% up to 100% respectively; the lower the frequency is, the higher the absolute value of the resistance will be, but the phase shift is acting inversely means that it changes from -35 degree to nearly 0 degree for 1 KHz frequency. Therefore, it is necessary to find an optimum frequency for the pulse voltage signal from electrical structure of the electrode-electrolyte equivalent circuit in order to have the most suitable interface behaviour required for the μECM . For this cell arrangement, the frequency needs to be greater than 10s of KHz and lower than MHz's.

- **Time constant (τ):**

Any RC network is known with a time constant feature which shows the time needed for the capacitor to charge to the 63.2% of the maximum possible voltage; by applying voltage across the capacitor, capacitor voltage exponentially increases until it reaches the maximum possible value. Table 4-8 shows the time which is needed for the capacitor voltage to reach different levels.

Time constant	% Maximum Voltage	Time constant	% Maximum Voltage
1τ	63.2%	4τ	98.2%
2τ	86.5%	5τ	99.3%
3τ	95%	6τ	Maximum possible

Table 4-8 Time constant and capacitor charging percentage

To find out the time domain behaviour of the equivalent RC network in figure 3-65, time constant needs to be calculated.

As polarisation curves in section 3-4 show, charge transfer resistance is very high at the start of the reaction and it goes to infinity; therefore the parallel RC sets for both anode and cathode changes to a simple capacitor and subsequently the equivalent RC circuit converts to a serial C-R-C circuit. This new circuit time constant is very simple to calculate:

$$\tau = RC_{equ.} = R_2(C_1 \text{ in series with } C_2) \quad (4-6)$$

$$\tau = R_2 \left(\frac{C_1 * C_2}{C_1 + C_2} \right)$$

$$\tau = 12.1 * \left(\frac{1.93 * 10^{-7} * 0.01384}{1.93e * 10^{-7} + 0.01384} \right) = 2.335 * 10^{-6} = 2.335 \mu sec$$

The time constant shows that capacitor needs 2.335 μs to charge up to 63% of its final voltage and it needs 14.01 μs to reach its maximum possible voltage.

The presented model in figure 4-16 has been simulated by applying a pulse voltage with different pulse on-time and pulse width values to evaluate the μ ECM cell behaviour and to compare the voltage and current signals. A pulse voltage source is applying pulses with 7 volts amplitude and 30% duty cycle to the network. The pulse on-time will change from τ to 6τ . The expectation is that voltage across EDL capacitor reaches the maximum possible value when pulse on time is 6 times greater than time constant.

The table 4-9 summarises the input values for pulse signal and also measured voltages across EDL capacitor and currents through it and charge transfer resistor.

Pulse on-time (μs)	Pulse width (μs)	Max C-DL Voltage (V)	Max C-DL Current (A)	Max R-CT Current (A)
$\tau = 2.335$	7.78	3.032	5.738e-01	2.506e-01
$2\tau = 4.67$	15.57	3.437	5.784e-01	2.841e-01
$3\tau = 7.01$	23.37	3.492	5.784e-01	2.886e-01
$4\tau = 9.34$	31.13	3.499	5.784e-01	2.892e-01
$5\tau = 11.68$	38.93	3.5	5.784e-01	2.892e-01
$6\tau = 14.01$	46.7	3.5	5.784e-01	2.892e-01

Table 4-9: Applied pulse time, measured currents and voltages details

Voltage signal across EDL capacitor was increased by increasing the pulse on time and followed the calculations as it was expected. But the changes of the maximum voltage for any pulse time greater than 4τ was insignificant, hence the pulse on time for the pulse voltages can be selected equal to 4τ and it is not necessary to exceed that. However, other consideration may change this conclusion.

Figure 4-23 presents the voltage signal across EDL capacitor at workpiece-electrolyte interface.

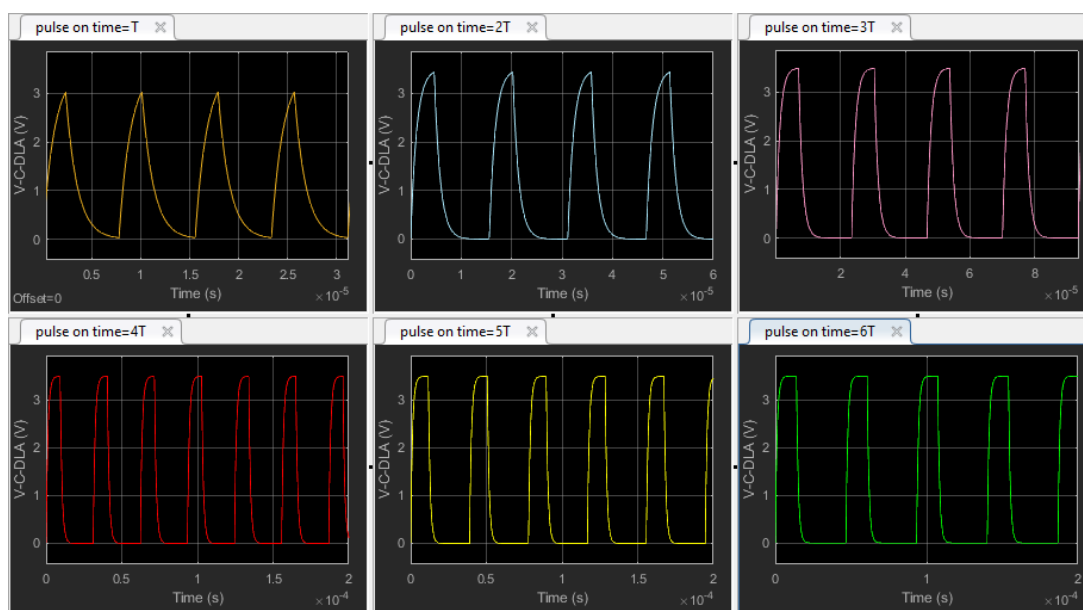


Figure 4-23: Voltage signal across EDL capacitor (anode side)

Figure 4-24 presents the current signals flowing through EDL capacitor and charge transfer resistor. As mentioned earlier in this chapter, charge transfer current known as faradic current is the current which helps the electrochemical reaction and consequently machining to take place. As the pulse on time increases, the faradic current amplitude is increasing but it does not change significantly for the pulse on time between 4τ and 6τ .

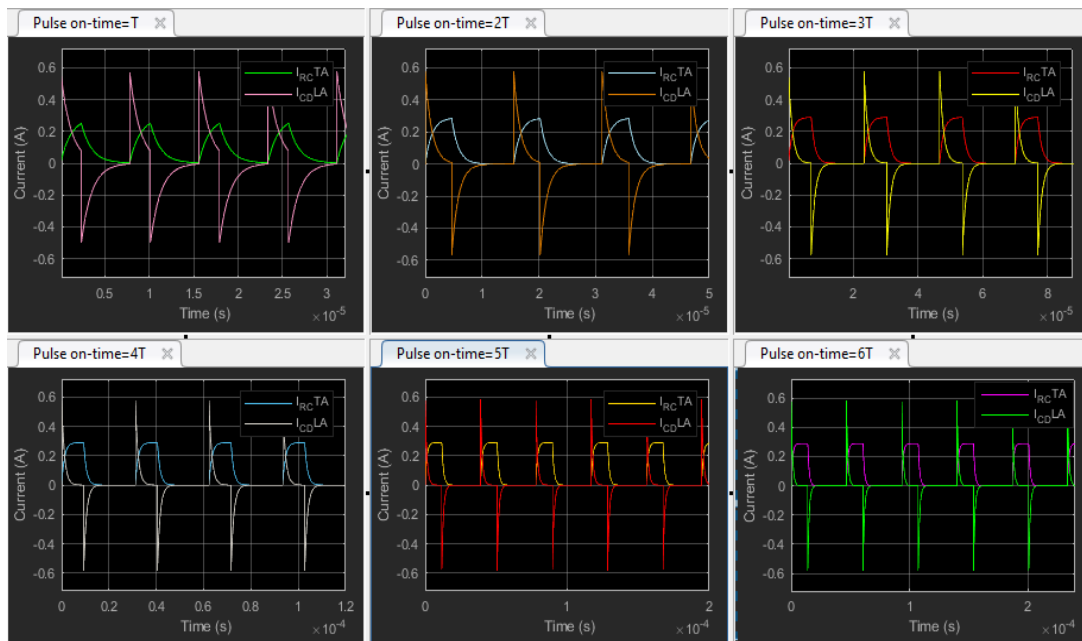


Figure 4-24: Current signals through charge transfer resistor and EDL capacitor

In addition to the current amplitude, there is another factor very important for machining and that is the length of the period faradic current can stay at its maximum level. This has been measured through the Matlab graphs. As table 4-10 shows, the time period at which maximum faradic current happens changes from 4.28% to 62.81% with respect to the pulse on time. This is crucial information, although the faradic current amplitude does not change remarkably for the pulse on time greater than 4τ but it does considerably change with respect to the time period it stays at maximum level. Therefore, the results suggest that optimum pulse on time should be selected to provide higher level and longer period of faradic currents.

Pulse on-time (μs)	Δt (current at max. level)	% of pulse on time
$\tau = 2.335$	0.1	4.28%
$2\tau = 4.67$	0.573	12.27%
$3\tau = 7.01$	1.871	26.69%
$4\tau = 9.34$	3.986	42.68%
$5\tau = 11.68$	6.294	53.89%
$6\tau = 14.01$	8.799	62.81%

Table 4-10: Max faradic current period as % pulse on time

The final assessment is related to the current flowing through the electrolyte resistor (figure 4-25); the current signals follow the same pattern as capacitive and faradic currents.

It is a sum of the both signals; signal which shows a sharp peak is capacitor charging current and it quickly declines to a lower level which will stay at that level for a longer time. The period of this flat level is approximately equal to the flat level of the faradic current and slightly longer than that. Figure 4-26 compares the flat level of the faradic level at charge transfer resistor and electrolyte resistor and it shows they are approximately equal.

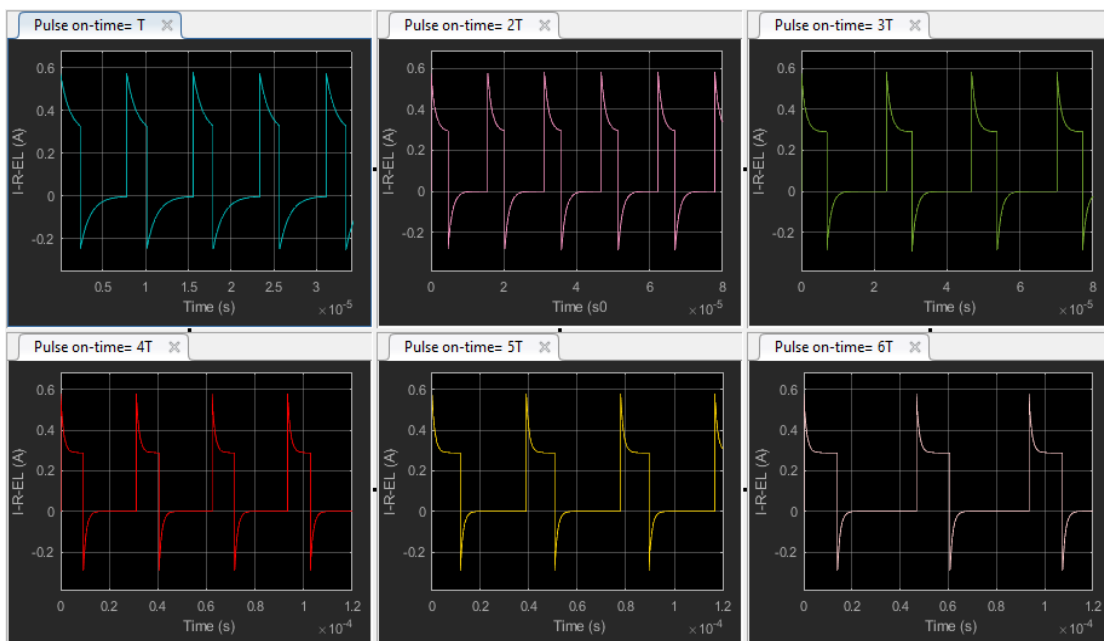


Figure 4-25: Current signals through electrolyte resistor

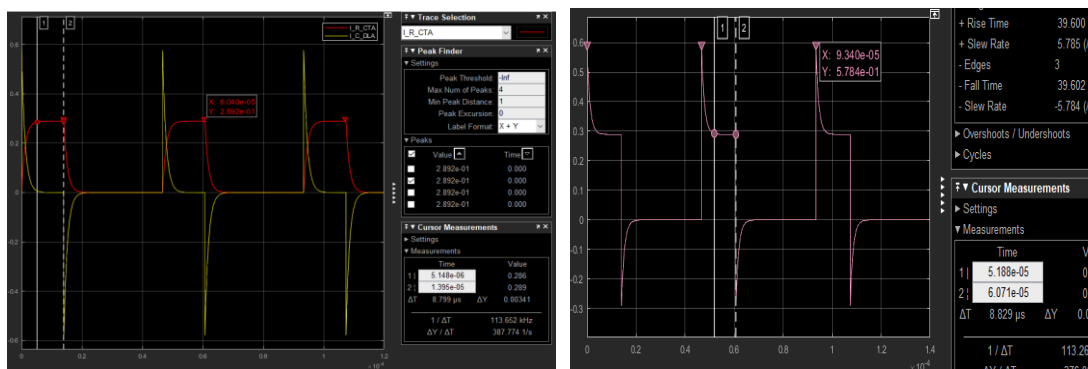


Figure 4-26: Current signal: charge transfer (Left), electrolyte (Right)

A similar simulation was repeated for the same pulse on time but with 50% and 75% pulse duty cycle. EDL capacitor voltage and current signals followed same pattern as they did for the 30% pulse duty cycle with slight decrease in maximum voltage and current values. Charge transfer resistor current signal also followed the same pattern as it did for the 30% pulse duty cycle, and it reached nearly same maximum level. Also, the faradic current flat period presented similar approach as it did for the 30% duty cycle.

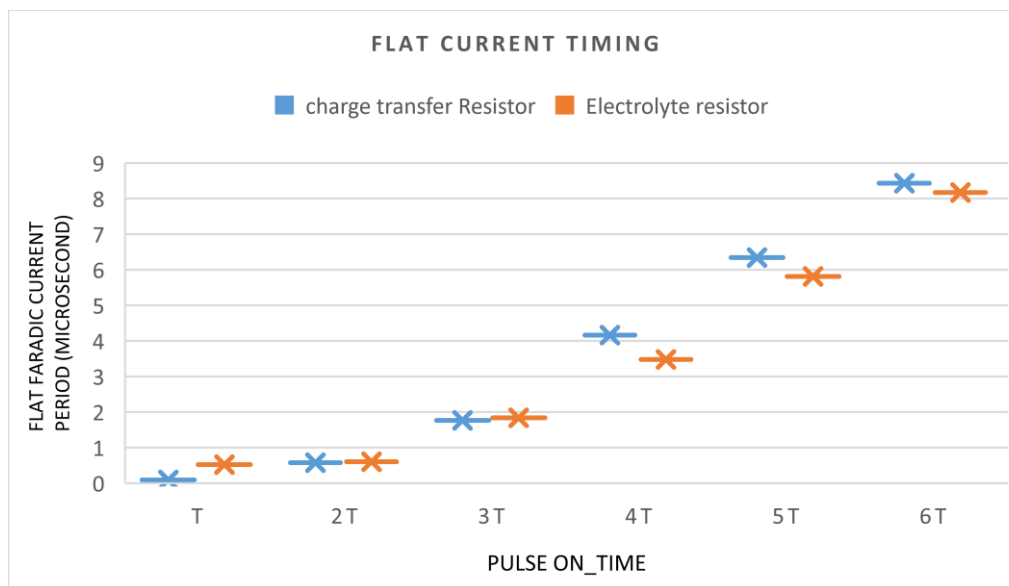


Figure 4-27: Flat faradic current timing (duty cycle = 50%)

But there was slight difference between the electrolyte current flat periods when duty cycle was 30% and when it increased to 50% and 75%.

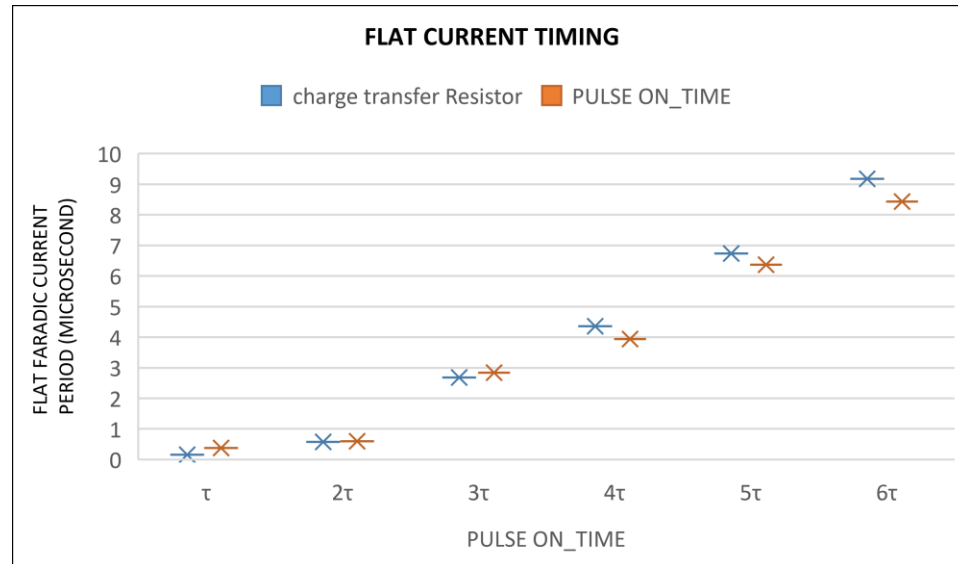


Figure 4-28: Flat faradic current timing (duty cycle = 75%)

For the former one, electrolyte resistor current showed longer flat level in comparison with the charge transfer current flat period for all pulse on times but the latter, presented longer flat level period for the electrolyte current for the pulse on time up to and including 3τ and it showed decreased period for the pulse on time equal and greater than 4τ . This is very important and critical issue as machining is very much dependent on the faradic current and the greater and longer it can be applied to the machining zone, the greater results can be achieved. Figure 4-27 and 4-28 present comparative data for 50% and 75% duty cycle. Full simulation results are available at Appendix F

4.3.2 μ ECM electrode-electrolyte interface model (0.6 mole/L electrolyte concentration) - Tungsten tool electrode

Same as the section 4.3.1, it was aimed to process similar simulation for the best parameters' combination based on the EIS results when electrolyte concentration was 0.6 mole/L. The combination of 7.5 volts and 26 μ m gap size created the best combination for the removed material rate and overcut.

Table 4-11 shows the parameters' values extracted from EIS experiment.

Parameter	Symbol in model	Equation	Value
Electrolyte resistance	R_EL	$R = \frac{L}{kA}$	18.6 Ω
Charge transfer resistance	R_CTA (Anode)	$R_{ct} = \frac{RT}{nFi_o}$	7.08 Ω
EDL capacitance	C_DLA (Anode)	$C_{dl} = \frac{\epsilon_0 \epsilon_r A}{L}$	3.29e-07 F
Charge transfer resistance	R_CTC (Cathode)	$R_{ct} = \frac{RT}{nFi_o}$	1.96e+07 Ω
EDL capacitance	C_DLC (Cathode)	$C_{dl} = \frac{\epsilon_0 \epsilon_r A}{L}$	0.747 F

Table 4-11: Equivalent circuit's components' values (0.6 mole/L)

Similar simulation using Matlab model practiced with the new data from table 4-11. Parallel RC equivalent impedance is:

$$\text{Equivalent Impedance} = Z = R_1 \parallel C_1 + R_2 + R_3 \parallel C_2$$

$$Z = \frac{0.8997817 * 10^7}{j18.6 * f + 0.0483754 * 10^7} + 7.08 + \frac{0.417595 * 10^{+7}}{j1.96 * 10^7 f + 0.213059}$$

$$= \begin{cases} f \rightarrow 0 & \Rightarrow |Z| = 18.6 + 7.08 + 1.96 * 10^7 = 1.96 * 10^7 \\ & \angle Z \cong 0^\circ \\ f \rightarrow \infty & \Rightarrow |Z| = 0 + 7.08 + 0 = 7.08 \\ & \angle Z \cong 0^\circ \end{cases}$$

As it was expected, the total network impedance is equal to R3 (high resistance) at low frequencies and equal to electrolyte resistance at high frequencies. For this specific cell, increasing the pulse voltage signal frequency from 1 MHz to higher frequencies does not apply any significant changes to the equivalent circuit's impedance. But applying pulse voltage signals within the range of 100 KHz and 1 KHz will increase the equivalent circuit's resistance absolute value from 16% to 260 % respectively which is much higher in comparison with the similar situation for the 0.5 mole electrolyte concentration, and the

phase angle changes between 28 degree and 1.6 degree (negative phase) for the frequencies between 100 KHz and 1 KHz.

- **Time constant:**

The starting time constant for the equivalent circuit based on above component is calculated as below:

$$\tau = R_2 \left(\frac{C_1 * C_2}{C_1 + C_2} \right)$$

$$= 7.08 * \left(\frac{3.29 * 10^{-7} * 0.747}{3.29 * 10^{-7} + 0.747} \right) = 2.329 * 10^{-6} = 2.329 \mu sec$$

Interestingly, despite the significant changes in the value of RC components, the time constant is in a very close approximate with the first model time constant.

Current and voltage signals followed similar pattern as they did at first simulation model. Table 4-12 presents the maximum voltage across EDL capacitance and the currents flowing through this capacitor and charge transfer resistor.

Pulse on-time (μs)	Pulse width (μs)	Max C-DL Voltage (V)	Max C-DL Current (A)	Max R-CT Current (A)
$\tau = 2.329$	7.76	4.09	1.027	2.210e-01
$2\tau = 4.658$	15.53	5.067	1.058	2.738
$3\tau = 6.987$	23.29	5.321	1.059	2.875
$4\tau = 9.316$	31.05	5.384	1.059	2.909
$5\tau = 11.645$	38.82	5.4	1.059	2.918
$6\tau = 13.974$	46.58	5.404	1.059	2.920

Table 4-12: Applied pulse time, measured currents and voltages

Pulse voltage signal amplitude was set at 7.5 volts, hence the maximum EDL capacitor voltage increased to 5.404 volt in comparison with the first model which was only 3.5 volt; the main reason is the significant decrease in electrolyte resistor value in second model which subsequently decreased the potential drop across the resistor and increased the voltage across the capacitor. However, this did not increase the faradic

current flowing through the charge transfer resistor as it is very much dependent on characteristics of the workpiece.

Also, the maximum period of the faradic current flat rate at charge transfer resistor and electrolyte resistor was measured; similar to the first simulation, the current flat rate period for electrolyte resistor was slightly less than that for the charge transfer resistor. Also, the current flat rate period was compared with the pulse on time. The result shows that the current flat rate percentage of pulse on time jumps at pulse time equal to 3τ and after 4τ the percentage increases with smaller steps. The capacitor's voltage reaches the 95% of its maximum at 3τ and 98% at 4τ . However, the maximum voltage percentage is achievable at 6τ but pulse voltage amplitude did not have any significant effect on the current flat rate period and its percentage of the pulse on time. Table 4-13 shows the results.

Pulse on-time (μs)	Δt (R-CT current at max. level	Δt % of pulse on time	Δt (R-EL current at max.)	Max R-EL Current (A)
$\tau = 2.329$	0.092	3.96%	0.048	1.036
$2\tau = 4.658$	0.429	9.21%	0.250	1.058
$3\tau = 6.987$	2.771	39.66%	1.803	1.059
$4\tau = 9.316$	4.824	51.78%	3.424	1.059
$5\tau = 11.645$	6.198	53.22%	5.416	1.059
$6\tau = 13.974$	8.958	64.10%	7.774	1.059

Table 4-13: Max faradic current period as pulse on time%- Tungsten tool electrode

4.3.3 μECM electrode-electrolyte interface model (0.5 & 0.6 mole/L electrolyte concentration) - Nickel tool electrode

Similar simulation was processed for the RC equivalent circuit for electrode-electrolyte interface using nickel tool electrode. Table 4-14 presents the equivalent RC components' values for 7.5 volts, 0.5 mole/L concentration and 25 μm gap between electrodes.

Parameter	Symbol in model	Equation	Value
Electrolyte resistance	R_EL	$R = \frac{L}{kA}$	3.290 Ω
Charge transfer resistance	R_CTA (Anode)	$R_{ct} = \frac{RT}{nFi_0}$	4.699 Ω
EDL capacitance	C_DLA (Anode)	$C_{dl} = \frac{\epsilon_0 \epsilon_r A}{L}$	9.808e-08 F
Charge transfer resistance	R_CTC (Cathode)	$R_{ct} = \frac{RT}{nFi_0}$	1.677e-04 Ω
EDL capacitance	C_DLC (Cathode)	$C_{dl} = \frac{\epsilon_0 \epsilon_r A}{L}$	2.739e-03 F

Table 4-14: Equivalent RC component's values for impedance test (7.5 V, 0.5 mole/L, 25 μm gap)

Total impedance of the equivalent circuits is calculated using equation 4-4 and time constant is calculated using equation 4-6.

$$\text{Equivalent Impedance} = Z = R_1 \parallel C_1 + R_2 + R_3 \parallel C_2$$

$$Z = \frac{0.076251 * 10^8}{j4.699 * f + 0.016227 * 10^8} + 3.29 + \frac{0.097445 * 10^{+3}}{j1.677 * f + 0.58107}$$

$$= \begin{cases} f \rightarrow 0 \Rightarrow |Z| = 4.699 + 3.29 + 167 = 174.989 \\ \quad \angle Z \cong 0^\circ \\ f \rightarrow \infty \Rightarrow |Z| = 0 + 3.29 + 0 = 3.29 \\ \quad \angle Z \cong 0^\circ \end{cases}$$

Calculating the total impedance and the phase of the impedance for frequencies between 10 KHz and 1 MHz, leads to the change of the phase angle from 1.4 degree to the 82 degrees and the absolute value of impedance from 7.99 ohm to 2 ohms. Impedance frequency response agrees with the above calculations, which are presented in figure 4-29 and 4-30.

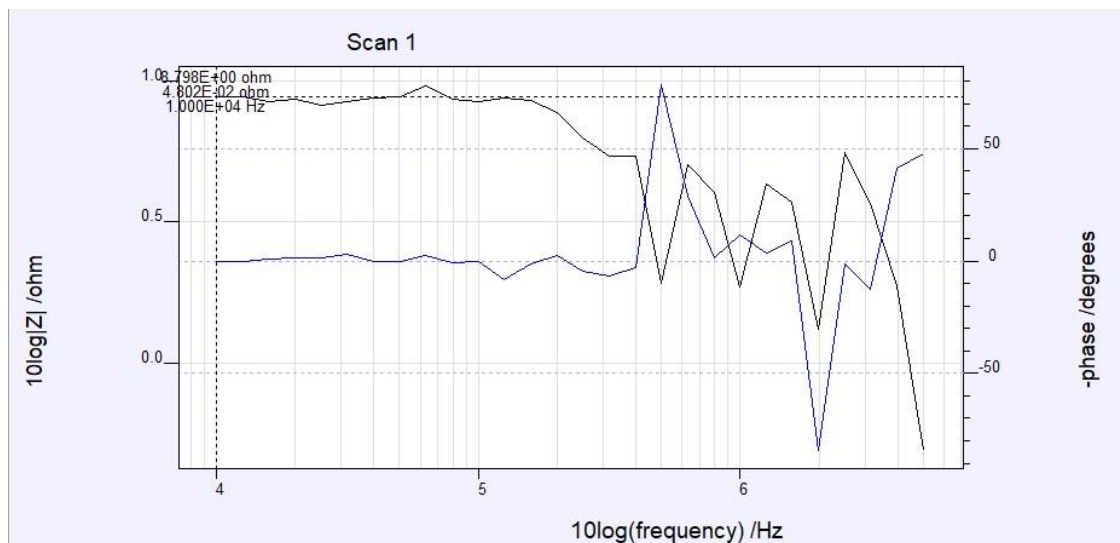


Figure 4-29: Frequency response for equivalent circuit (7.5 V, 0.5 mole/L, 25 μ m gap)- from 1KHz

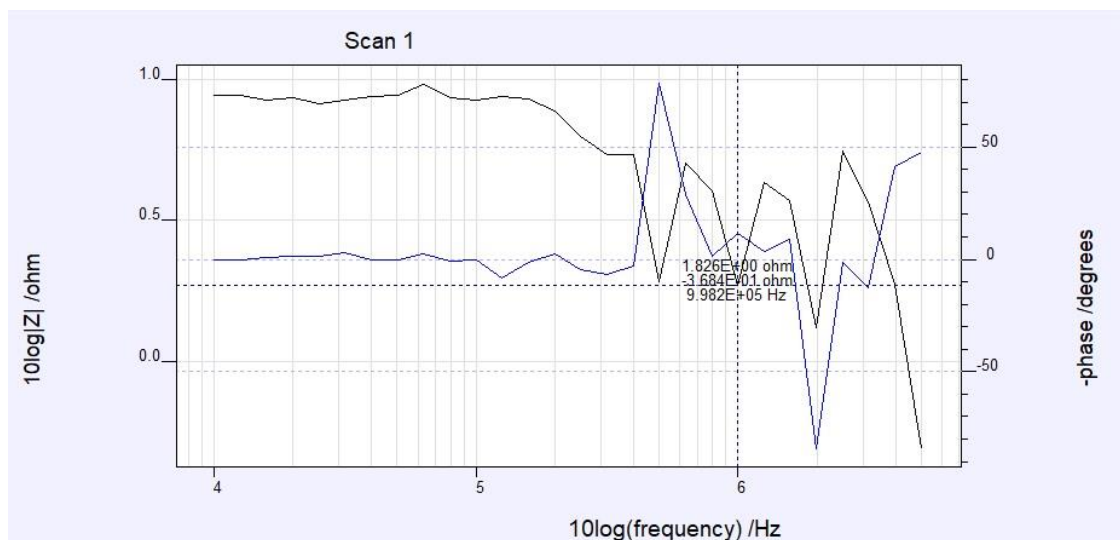


Figure 4-30: Frequency response for equivalent RC circuit (7.5 V, 0.5 mole/L, 25 μ m gap)- up to 1MHz

Like the previous cases, time constant can be calculated using equation 4-6, as charge transfer resistance is indefinite at the start of applying pulses.

$$\tau = R_2 \left(\frac{C_1 * C_2}{C_1 + C_2} \right)$$

$$= 3.290 * \left(\frac{9.808 * 10^{-8} * 2.739 * 10^{-3}}{9.808 * 10^{-8} + 2.739 * 10^{-3}} \right) = 32 * 10^{-8} = 0.32 \mu sec$$

The time constant for nickel tool electrode is about a tenth of the time constant for the case of tungsten tool electrode. Electrolyte resistance itself is 6 times less than that for the tungsten electrode equivalent circuit.

Matlab simulation took place for the RC equivalent values given at table 4-14. All current and voltage graphs were studied and the numerical data for the ratio between faradic current period and pulse on time are summarised in table 4-15. The pulse duty was selected at 30% rate.

Pulse on-time (μs)	Pulse period (μs)	Δt (R-CT current at max. level)	Δt % of pulse on time	Δt (R-EL current at max.)	Max R-EL Current (A)
$\tau = 0.32$	1.07	0.124	38.75%	0.114	2.257
$2\tau = 0.64$	2.13	0.353	55.16%	0.288	2.277
$3\tau = 0.96$	3.2	0.654	68.13%	0.564	2.278
$4\tau = 1.28$	4.27	1.079	84%	0.860	2.278
$5\tau = 1.6$	5.33	1.362	85.13%	1.110	2.278
$6\tau = 1.92$	6.4	1.653	86.1%	1.414	2.278

Table 4-15: Max faradic current period as pulse on time%- Nickel tool electrode

The ratio of the maximum faradic current level to the pulse on time are greater than similar ratio for the tungsten tool electrode when time constant was around 2.3 μs . One of the major differences between these two cases is the electrolyte resistance and it seems that it has great effect on the EDL structure. In other words, the tool electrode dimension can remarkably affect the EDL structure and RC behaviour of the equivalent electrode-electrolyte interface model. Figure 4-31 shows the current signals which flow through charge transfer resistor, EDL capacitor and electrolyte resistor.

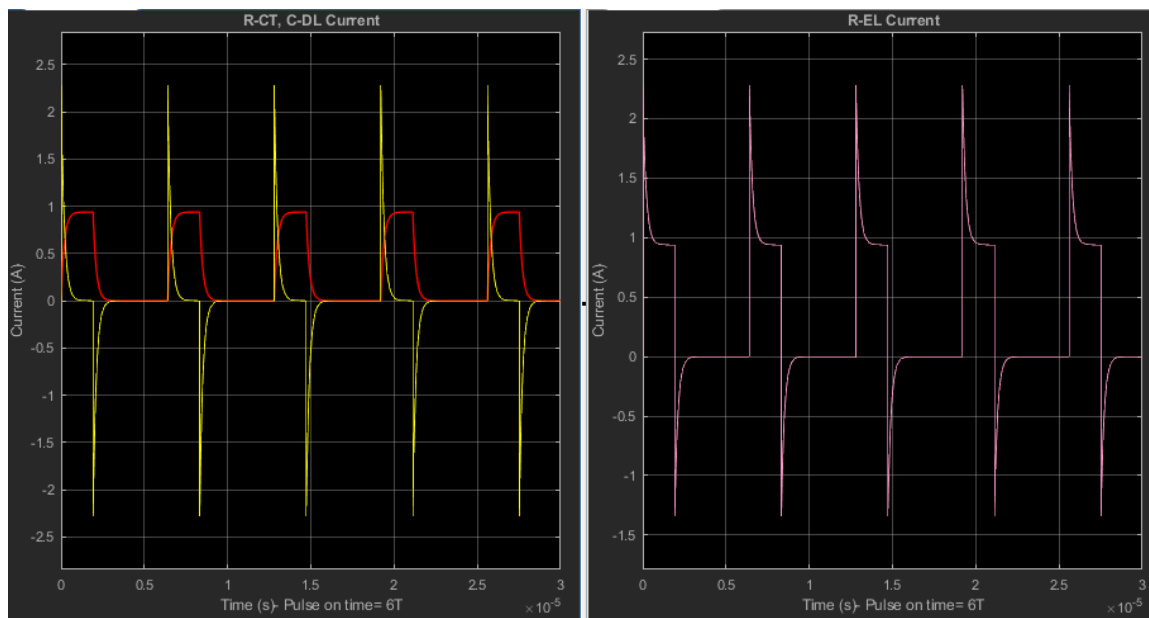


Figure 4-31: Current signals for pulse on time= 1.92 μ s (Red: R-CT current, Yellow: C-DL current & pink: R-EL current signals)

4.4 Performance assessment based on impedance results (Tungsten tool electrode) and initial parameters

In this section, calculated MRR and OC values from Impedance experiments will be used to assess the reaction performance based on the initial values for voltage, gap size and electrolyte concentration.

The first graph in figure 4-32 presents the changes of MR and OC for different voltage levels and gap sizes for 0.5 mole/L electrolyte concentration. In this graph and all other graphs in this section, horizontal axis shows voltage-gap values. First number for each category on horizontal axis is voltage value and second number on horizontal axis is the size of the gap; voltage levels are 6.5, 7 and 7.5 volts and gap sizes are 22, 24, 25 and 26 μ m.

Figure 4-32 observations can be summarised as follow:

OC increases by the rise of the voltage. But OC levels and gap sizes do not follow a simple change trend; 22 μ m gap size has produced nearly the highest OC for each voltage level.

MR increases as voltage increases and at 26 μm gap, it has its minimum level. Considering MR and OC simultaneously, shows that the process has better MR rate at 7 volts and mid-range gap sizes.

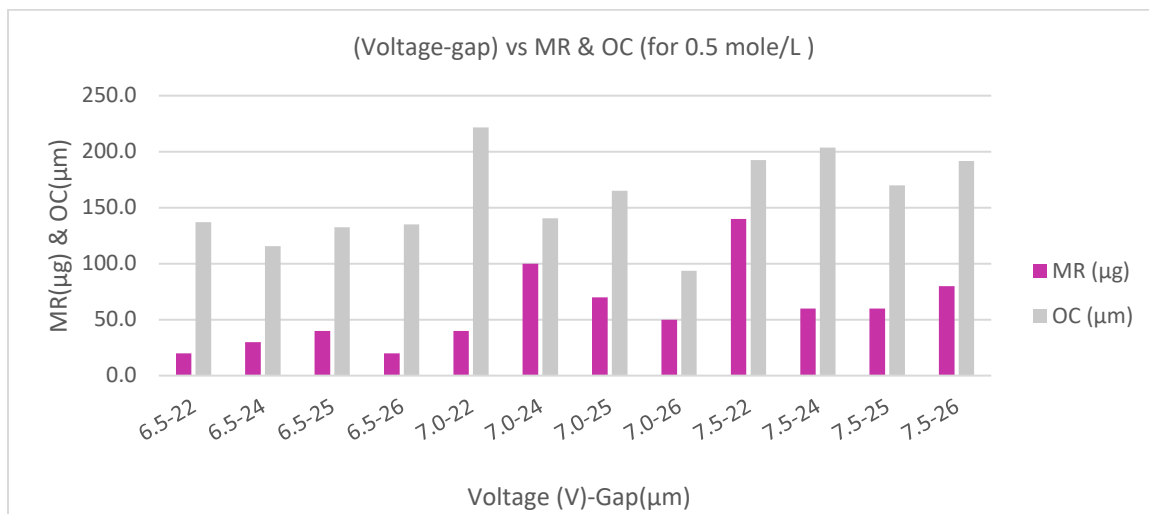


Figure 4-32: Voltage – MR & OC graph for 0.5 mole/L electrolyte concentration & Tungsten tool electrode

Similarly, figure 4-33 shows the changes of MR and OC for different voltage and gap sizes when electrolyte concentration was 0.6 mole/L.

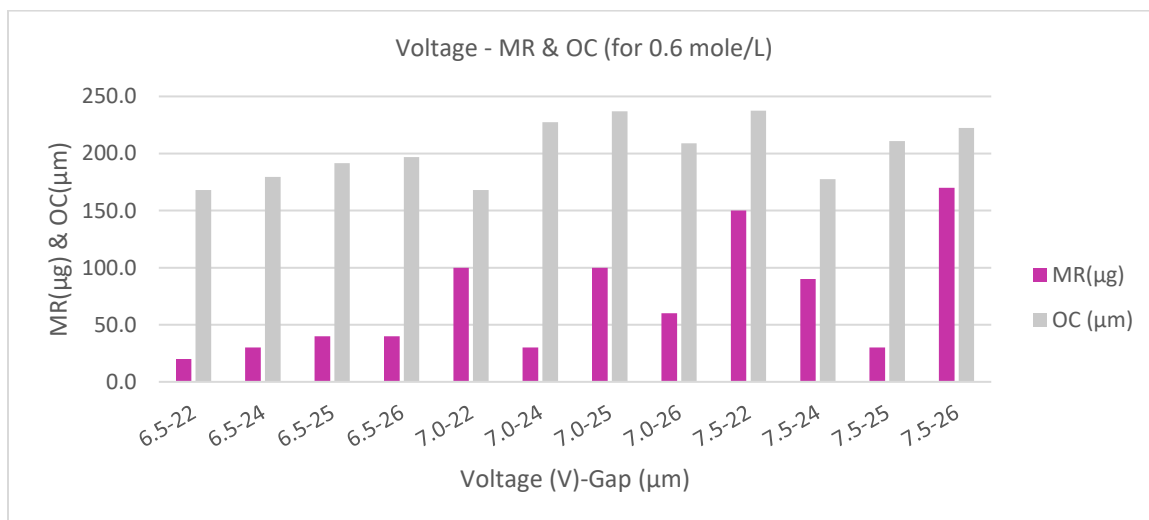


Figure 4-33: Voltage- MR & OC graph for 0.6 mole/L electrolyte concentration & Tungsten tool electrode

Figure 4-33 observations can be summarised as follow:

OC increases by the rise of the voltage. But for each 7 and 7.5 voltage levels and a greater gap size OC decreases. MR increases with voltage level and it has better rate for 7- and 7.5-volts level when considering the OC levels as well.

To compare the MR and OC levels with change in the electrolyte concentration, figure 4-32 and 4-33 should be considered simultaneously. Higher electrolyte concentration increases the both MR and OC levels but the rise in OC is more significant. Machining performance improves if OC decreases, therefore higher electrolyte concentrations would be recommended for the machining process. Based on the above discussion and comparison, the best combination for initial parameters include 7 volts, 24 μm gap and 0.5 mole/L electrolyte concentration and 6 volts, 22 μm gap and 0.6 mole/L electrolyte concentration.

Impedance experiments carried out with nickel tool electrode as well (section 4.1.2). The initial values together with obtained MR and OC data through the impedance experiment have been demonstrated in figure 4-34 and figure 4-35.

Nickel tool electrode had larger face forward surface in comparison with the tungsten tool electrode. As a result, the reaction zone (machining zone) was larger. Therefore, the graphs for nickel tool electrode present higher level for MR rate in comparison with the results obtained through the impedance experiment for the tungsten electrode. Also, the OC levels for nickel tool electrode are remarkably smaller than the OC levels for tungsten tool electrode.

This confirms that the tool electrode geometry is as important as tool electrode material. Tool electrode geometry can have effects on the stray current distribution on the workpiece surface, subsequently, it can affect the OC levels.

Figure 4-34 presents the changes of MR and OC for different voltage levels and gap sizes for 0.5 mole/L electrolyte concentration.

Figure 4-34 observations can be summarised as follow:

At low voltage and bigger gap size, MR rate is not desirable and OC level increases. At higher voltages, MR improves significantly while the increase in OC levels is limited. But the best OC levels happen at 7.5 volts while the best MR rate happens at 7 volts. The best voltage- gap combinations for the best MR and OC levels is 7 volts and 22 μm gap.

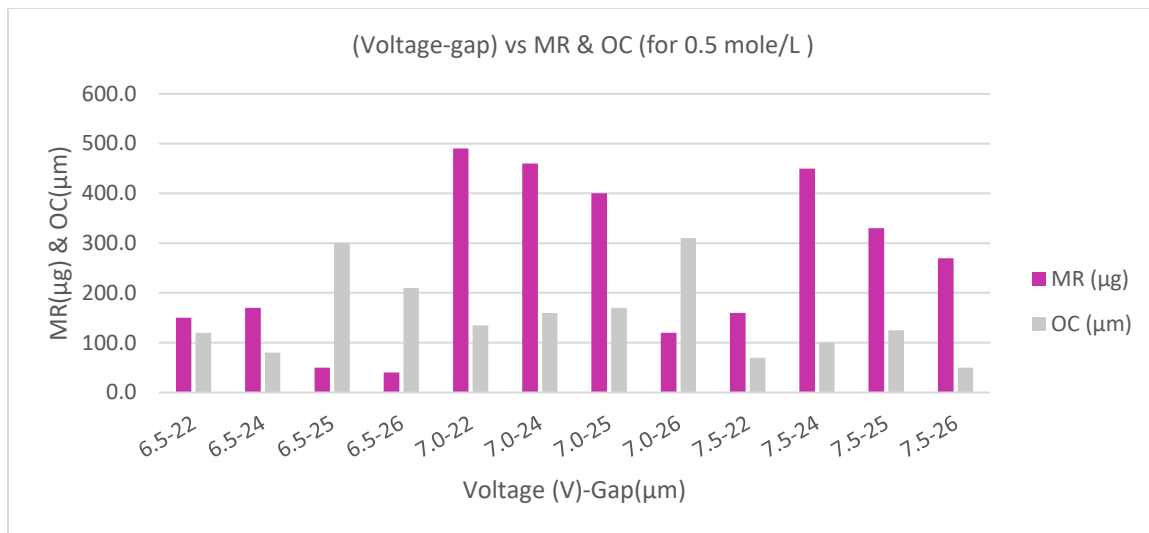


Figure 4-34: Voltage – MR & OC graph for 0.5 mole/L electrolyte concentration & Nickel tool electrode

Figure 4-35 observations can be summarised as follow:

MR level increases by the rise of voltage but the effect of the gap sizes on MR is not linear. OC has higher rate at lower voltages, and it shows a decline as the voltage increases. The best combination for the voltage and gap size is the set of the 7.5 volts and 25 µm gap to achieve the highest MR and the lowest OC levels.

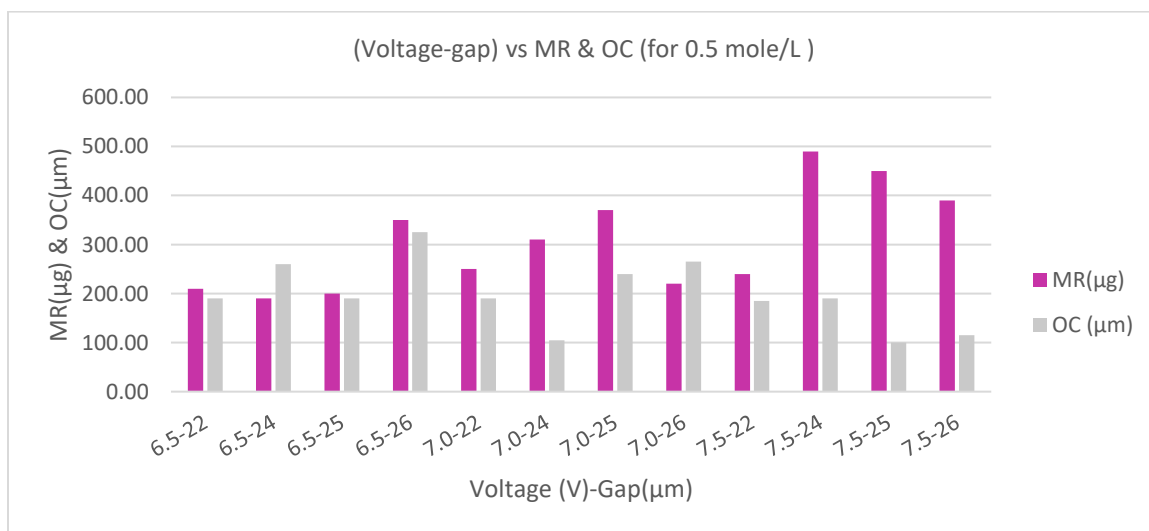


Figure 4-35: Voltage – MR & OC graph for 0.6 mole/L electrolyte concentration & Nickel tool electrode

To consider the effect of the electrolyte concentrations for the impedance experiment results using the nickel tool electrode, both figures (4-34 and 4-35) should be considered simultaneously.

OC increases by the rise of the electrolyte concentrations, but this do not increase the MR rate. Also, MR at some higher voltage levels increases with the rise of the electrolyte concentration. In general, MR and OC have less changes over the voltage and gap sizes when electrolyte concentration increases.

Based on literature, increasing electrolyte concentration, should increase the MRR and overcurrent; above graphs are in agreement with this claim. The next claim is that by increasing voltage, both MR and overcurrent should increase. This claim is valid at constant gap sizes and if the gap changes with the voltage, then the pattern is changing. The gap size effects the rate of the removed materials and overcut significantly. This is due to the electric filled between electrodes and subsequently the current distribution.

Therefore, this summary leads to the need for a careful consideration to set up initial parameter's values and their combination to establish better machining performances and higher accuracy rates. The introduced mathematical approach has generated an acceptable narrow range for the initial parameters' values based on the electrodes' materials and geometries. But a successful application of the obtained results needs to apply this method to various electrode materials and geometries to establish a comprehensive database for the combination of the materials, initial parameters and machining conditions.

4.5 μ ECM machine

This section presents a few experimental cases based on achieved mathematical and simulation results for the initial machining parameter's set up.

4.5.1 In house- built μ ECM machine

All experimental works carried out using in house designed and built μ ECM machine. Figure 4-36 shows the 3D view of the assembled machine and figure 4-37 shows the developed machine. Both pictures belong to the previous research by Spieser (2015). However, the power supply unit for the machine was upgraded to a new version during the current research.

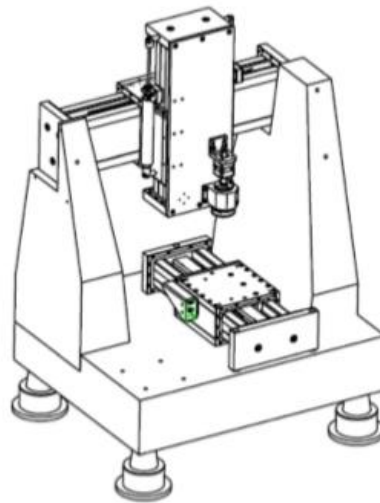


Figure 4-36: 3D view of the assembled machine (more details- Appendix G)

The mentioned experiments in this section mainly took place in order to verify the results of the iviumstat and simulations. One of the main challenges during the experimental work was the repeatability of the process.

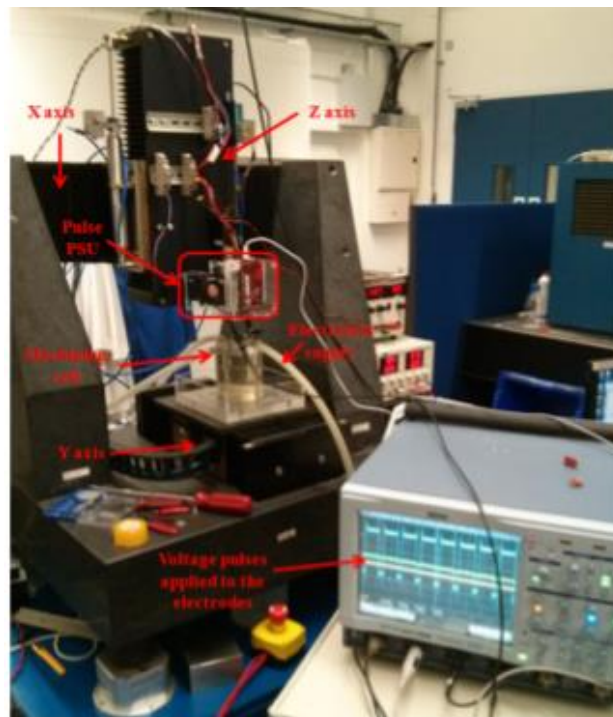


Figure 4-37: Developed μ ECM machine with initial power supply unit

To achieve similar results for the similar condition, more than one attempts had to take place. Although, the environmental condition for all the attempts were kept similar but It was impossible to control the flow rate of the electrolyte and its inlet position. As a result, the direction and rate of the electrolyte flow was inconsistent during the practice which made it harder to repeat the experiments and achieve similar results. As it was mentioned in chapter two as well, electrolyte inlet is very effective on the performance quality; it does affect the current density and also the electrode-electrolyte interface and subsequently the structure of the electrode-electrolyte changes significantly with even minor changes in electrolyte inlet position.

The second effective factor was random noises; although the power supply was designed considering the importance of the elimination of all possible noises, but there was still the effect of high frequency noises on the performance.

Finally, the number of occurred over current faults which was retracting the tool electrode from the surface had enormous effect on the repeatability of the results. The following sections demonstrate samples of the experimental works using stainless steel as workpiece and tungsten and nickel as tool electrodes.

4.5.2 Micro-hole machining using Tungsten tool electrode

Machining process was tested on two stainless steel pieces with two different thicknesses, one with 1.01 mm and the second piece with 3.1 mm thickness as workpiece using a tungsten tool electrode. The environment and physical conditions were kept as close as possible to the condition in which iviumstat experiments took place. Pulse voltage level, electrolyte concentration and pulse on time selected based on the result from chapter 3.

Figures 4-38 presents the machined hole using tungsten tool electrode (0.5 mm diameter) on the workpiece with 1.01 mm thickness.

During the above attempt, overcurrent protection (OCP) was set up on 3 A and the process took place with no interrupt. During the process, no overcurrent happened, and the by-products were flushed away from the gap between the tools efficiently. Same experiment was repeated but the OCP level set on 1 A. Although the same tool electrode and machining setup were used in this experiment, the produced hole was much bigger than the tool electrode surface area. The process was interrupted with occurrence of the

OCP fault several times and subsequently tool was retracted from the gap area. The hole was finally machined throughout the workpiece, but it took about 10 minutes for the process to finish.

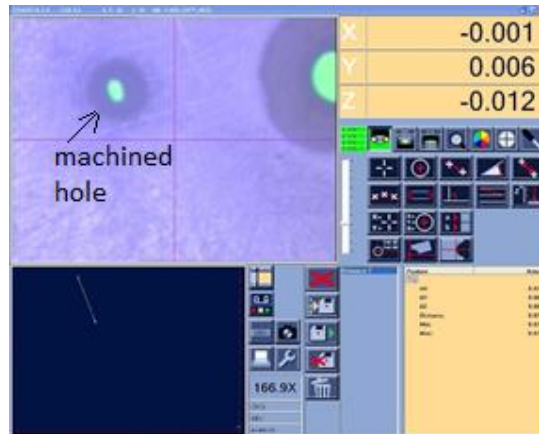


Figure 4-38: Micro hole on stainless steel (1.01 mm thickness), Tungsten tool electrode, OCP=1A

The next experiment took place on the workpiece with the 3.1 mm thickness under the same machining conditions; As figure 4-39 demonstrates, it was impossible to have the hole throughout the workpiece, although the OCP level was set on 3A. At the depth of 1.5 mm, an OCP fault occurred was not eliminated. Therefore, the process stopped, and machining did not continue.

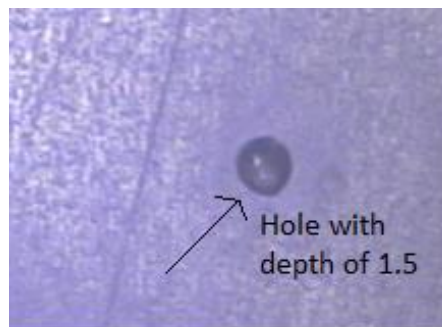


Figure 4-39: Micro hole on stainless steel (3.1 mm thickness), Tungsten tool electrode, OCP= 3A

In this experiment, the main challenge was to flush the by-products away after the depth of 1.1mm; between 1.1 mm and 1.5 mm depth, by-products were still flushed away

by help of the OCP fault occurrence in which the tool electrode was retracted from the machining area and an extra gap was created between electrodes. This gap and the time required for the tool to move back to its previous position helped to remove the remaining by-products from the gap between electrodes. However, after the depth of 1.5mm, a permanent OCP fault happened and the process was stopped.

4.5.3 Micro-hole machining using Nickel tool electrode

Machining process was tested on stainless steel workpiece using nickel tool electrode. Machining process was successful with the workpiece with 1.01 mm thickness and 3A OCP level. Figure 4-40 presents the machined hole throughout the workpiece using nickel tool electrode.

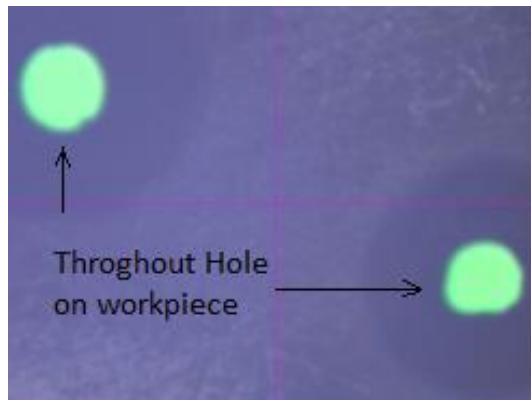


Figure 4-40: Micro hole on stainless steel (1.01 mm thickness), Nickel tool electrode, OCP= 3A

Machining a hole on the workpiece with 1.01 mm thickness was very straightforward action using nickel tool electrode with both 3A and 1A OCP levels. However, the best result achieved with the workpiece with 3.1 mm thickness was a hole with 1.7 mm depth. Similar to the tungsten tool electrode experiments, the main issue was to clear the sludge from gap which was creating continuous OCP fault after a depth of 1.5mm and eventually after the depth of 1.7mm, a permanent OCP fault happened. Figure

4- 41 presents the hole with depth of 1.7 mm which was unfinished and could not be machined throughout the workpiece.

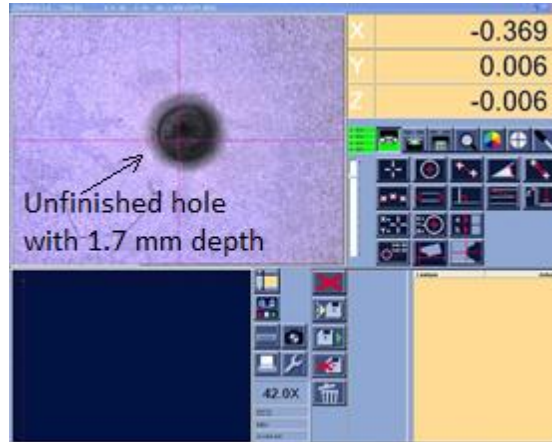


Figure 4-41: Micro hole on stainless steel (3.1 mm thickness), Nickel tool electrode, OCP= 3A

The above experiments provided acceptable results for the application of initial machining setup, but they pointed additional challenges which need to be investigated and to be addressed.

Initial parameters set up including voltage level, electrolyte concentration and pulse on-time were effective to run the process and achieve the above results but there are other parameters including electrolyte inlet position, removal of sludge and geometry of electrodes which need further investigation.

4.6 Conclusion

The work presented in this chapter was based on the achieved narrow range for the predominant initial values through the experimental work and mathematical analysis which were presented in chapter 3.

This chapter presented the proposed laboratory experimental work and its implementation using iviumstat impedance mode to investigate and find the equivalent RC circuits for the EDL structure.

EDL behaviour is one of the key elements in a successful μ ECM machining performance but current knowledge and the state of the research do not reflect sufficient effort to emphasis on the exploring EDL features and behaviour in μ ECM process; therefore the lack of this effort was identified as one of the knowledge gaps in this research.

There are examples of EDL structure investigation through the available published works but most of them analysed the EDL structure based on process simulation results or mathematical calculations.

In this research, EDL behaviour was investigated considering its equivalent RC network. The RC components values evaluated by implementing experimental work using iviumstat impedance mode and investigating the anodic reaction which took place at IEG and electrode-electrolyte interface.

Then, obtained RC equivalent circuit was simulated using Matlab Simulink to investigate electrical features of the EDL structure. As a result, voltage signal, current signal, faradic and charging currents were assessed considering the effect of the pulse on-time and duty cycle.

Finally, anodic reaction performance was evaluated using MRR and OC criteria and generated graphs were used to compare the performances within the applied ranges of predominant parameters' values. Considering the above proposed approach, it is necessary to highlight the following observation and finding:

Impedance spectroscopy is a valuable technique that can be used to discover more details about machining process with emphasis on anodic reaction which happen at IEG and is the core activity of the process.

This technique is time and cost effective in comparison with trial and error approach. It is possible to demonstrate the reaction under same condition as real machining process if equipment's features and specifications permits.

Current research and work confirm the complexity of the interrelation between predominant parameters and their effects on MRR and OC as machining criteria. There was no sign of any linear changes between these criteria and machining parameters within the scope of this research; that emphasises on the complex nature of the process and the need for further investigation to explore the core science of the process including EDL behaviour.

At this stage and with the current state of the μ ECM technology, this would not happen unless a very effective and comprehensive database can be created; this requires cooperation between researchers and developers to establish a general framework and follow similar rules and approach to build a valid and reliable database to save the time by preventing repetitive experiences.

In addition to the above general results and conclusions, it was noticed that tool electrode diameter could override the trend between conductivity and resistivity ratio and subsequently affect the current density. In case of nickel tool electrode, current density declined despite the voltage and concentration rise. As a result, OC did not increase with the voltage rise for the tool with greater face surface.

Pulse on time need to be equal or greater than EDL capacitor time constant to achieve maximum faraday current. But Duty cycle should less effect on faraday current.

By increasing the electrolyte concentration, pulse signal should be generated within higher frequency range; as at lower frequencies equivalent circuit total impedance increases sharply, therefore, current amplitude and current density will decrease.

On the other hand, increasing the electrolyte concentration will increase the conductivity of the solution and consequently electrolyte resistance decreases, and current is expected to increase. This example demonstrates the need for further investigation in order to find any changing point between machining parameters' interrelation.

It is very important to find the turning points for the interrelation between all identified predominant parameters in μ ECM process. This will help to find a limited domain for each parameter and to maximise the chances of optimising the machining parameters.

Consuming nickel tool electrode demonstrated that tool dimension can override the effect of the concentration and subsequently the effect of the conductivity. This confirms the importance of the tool electrode features for a successful μ ECM machining. Tool preparation is a costly and challenging process; materials, dimension and shape selection as well as the preparation and manufacturing need huge effort to address these challenges and make the operation an optimised process.

Experiments carried out using in house-built machine led to the following observation and conclusions:

Applying initial machining parameters based on the finding from proposed approaches in chapter 3 and 4 led to an acceptable machining performance but it highlighted a few more challenges which need to be carefully investigated and addressed.

Electrolyte inlet position, angle and flow speed are very crucial and can play a very important role in the success of the machining performance. During the experiments it was noticed that electrolyte flow direction and speed can increase the occurrence of the over current faults.

Pulse off-time set up is as important as pulse on-time set up and it is more critical when machining a deeper hole; clearing the IEG from sludge is more difficult when the depth of the hole is increasing and inefficient disposal of the sludge can prevent the machining process.

OCP level setup is also crucial; a higher OCP level may not recognise a short circuit and let the machining to continue. In this case, the overcut will increase significantly, and finished work quality will be very poor.

Designing a slow and accurate tool forward movement when an activated OCP was cleared is very crucial as it can affect the overcut and taper angle in negative way.

CHAPTER 5

Sustainable μ ECM process, indicators and assessment

Chapter summary

There is an increasing demand for precise micro-manufacturing for MEMS, biomedical applications, automotive industry and IT applications which is expected to lead the research widely towards increasing utilisation of the μ ECM technology.

As it was highlighted in this work and previous researches, μ ECM method can be used as one of the main alternatives in micro and nano manufacturing industries, especially when working with hard materials to machine. The result of the recent activities has proved that μ ECM has valuable potential to be used in different applications while its full capacity has not been explored yet due to its complex nature, expensive initial setup and knowledge based (operator or database) operation. Therefore, further research needs to utilise this method effectively at the industry level and also it is necessary to establish required fundamentals in order to assess and evaluate its advancement and sustainability individually and in comparison with the other methods to justify its initial high cost.

Current research and published works do not demonstrate any methodology and assessment criteria to be used to evaluate the sustainability of the μ ECM technology considering the dimensions of the sustainability in spite of the current focus on sustainable process, production and products.

The complex nature of the process has made this assessment a difficult task and hard to be generalised. In addition to the lack of valid measures and indicators to evaluate the sustainability of the process, the need to evaluate the process for different combination of electrode materials and electrolyte solutions, has made it very hard to provide a comparable quantitative and qualitative results when sustainability of the process is assessed.

In this chapter, it has been tried to introduce several indicators and measures considering the five dimensions of the sustainability to assess the process sustainability. Also, the suggested indicators and their assessment approach, provides the opportunity to compare the results and be able to generalise them when necessary. These indicators have been selected based on the existing knowledge and the experiences gained through

this research and similar activities. Also, the suggested approach, provides the opportunity for the user to optimise the process based on the sustainability assessment.

It is evident that μ ECM can be considered as an environmental friendly process, economically profitable and sustainable in terms of energy consumption; its valuable advantages in process features, productivity and quality have been proved by maximising the metal removal rate, minimising shape errors and improving the energy consumption. By optimising the initial machining parameters, these advantages can be achieved, and process can reach its highest sustainability and performance.

5.1 Introduction

As it was highlighted in chapter 2, there is not enough evident published works in the area of sustainability assessment of the μ ECM process, despite the importance of the sustainability of any manufacturing process. In this research it has been aimed to recognise and introduce the relevant measures and indicators which can be used to establish a methodology to assess the sustainability of the μ ECM process based on dimensions of the sustainability.

Any sustainability assessment has to consider three different levels, including system, process and product (figure 5-1), with each level having its own criteria and indicators that can be assessed individually (Jayal, 2010).

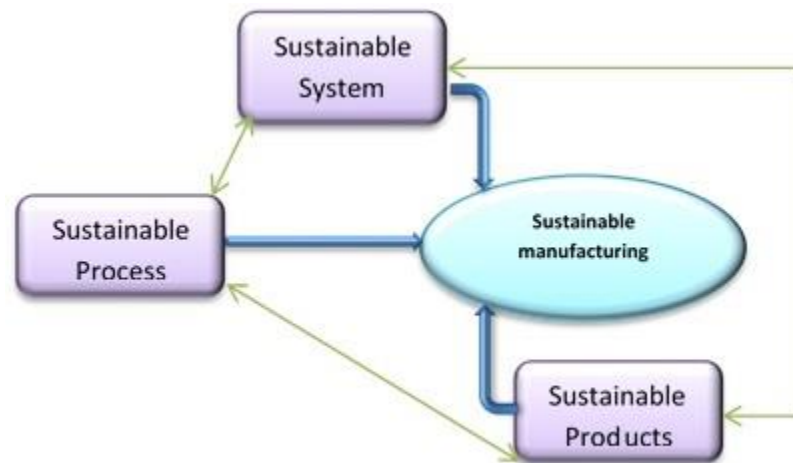


Figure 5-1: Sustainable manufacturing: System, process and production

It is believed that lifecycle assessment is the main tool for the environmental assessment of the products and it has been developed to cover the analysis and assessment of the environmental impact of any product through its whole lifecycle including resources, production and disposal (De Grave, 2010).

There is another view which looks at complete product development sequence while considering the technologies involved in the production:

- The final product: is the artefact that is the closest to the requirement of the end-user.
- Intermediate parts: these are parts that are not included in the final product, but they use a high portion of the production resources.
- The production system: it is considered as the manufacturing process chain, but it includes all necessary material production, recycling and disposal chain.

This view is especially relevant in the case of micro-product fabrication in which intermediate parts can take up to 98% of the product components (De Grave, 2010).

Machining processes are important contributors to GDP in the developed countries. Also, due to the demand for shorter production life cycle and more optimised manufacturing systems, it is expected that their contribution to the economic development will increase.

5.2 Dimensions of the sustainability

The common perspective in all available definitions and documents is the development of sustainable manufacturing by protection of the natural resources and raw materials, maintaining environmental conditions suitable for human beings' lives and fulfilment of economic, customers and employees' demands. Accordingly, manufacturing industries, including machining industries, are expected to align their activities with the three main aspects of the sustainability, namely, economy, environment and society (Heilala, 2015;Peralta, 2017).

These three aspects can be extended to include cost management, energy consumption, waste management, environmental impact and finally, health and safety. The most deployed model or framework observed in the industries is presented in figure

5-2 which forms the foundation for the introduced indicators and measures for μ ECM sustainability assessments in this chapter.

The general approach towards sustainability of the machining operations is to analyse the process regarding the following features:

- Environmental friendliness
- Cost effectiveness
- Reduced energy consumption
- Reduced material waste
- Improved personnel Health and operational safety

In addition to the individual effect of these elements on sustainability of the process, the interrelation between these factors needs to be included for a full picture of the sustainability assessment. This makes it harder to define the assessment criteria as these elements are correlated in a complex way. The sustainability measures should be assessed qualitatively, quantitatively or both.



Figure 5-2: Elements of machining process sustainability

Before continuing this chapter and introducing the relevant indicators for μ ECM sustainability assessment, it is important to highlight three fundamental grounds related to

the sustainability assessment of the non-traditional machining in general and μ ECM in particular.

1. Non-traditional machining methods are known as alternative machining methods and yet to be recognised as the main method (except for special cases) in comparison with the traditional machining methods. In addition to this, the choice between different applicable non-traditional methods on a production line is mainly based on operator experience or a trial and error approach. Both these conditions would add extra complexity to the sustainability assessment of a machining operation as operator experience can influence the methodology and the performance significantly. This means that the sustainability of any selected method should be compared with other machining methods, to determine whether more than one approach is applicable and acceptable.
2. As it was briefly mentioned, the 5 dimensions of the sustainability assessment are in a complex inter-relation which needs to be considered for any process. Hence, these criteria can present direct or indirect, qualitative or quantitative impact on each other and that needs to be considered in detail in order to obtain an accurate comprehensive result.
3. The performance of the dimensional sustainability of the process should be analysed quantitatively and qualitatively using relevant indicators. Different organisations have introduced a list of indicators. The indicators' developers have used different methodologies in establishing these frameworks. However, generally, the main purpose of these frameworks is for external reporting to the stakeholders, rather than being used for decision making and optimisation of the operations. Hence, it is vital to acknowledge that the aim of sustainability assessment should be not only to present more interesting reports to the stakeholders, but also to help to improve and optimise the operation.

The rest of this chapter will focus on discussion about dimensions of sustainability and introducing possible indicators and signs for μ ECM sustainability assessment.

5.3 Sustainability indicators

Essence of success and strength of the sustainability framework is very much dependent on the selection of the indicators and metrics and their setup for the assessment of the performance. Feng et al (2009) suggested some characteristic for indicators including being measurable, relevant, meaningful, reliable, accessible and flexible. Regardless that, there are two approaches towards definition and introduction of the indicators and metrics: bottom-up or top-down approach. In top-down approach, five dimensions of sustainability will be listed as leaders or headers and all possible indicators will be introduced as sub-categories while in bottom-up approach all possible indicators and metrics are introduced and then, they will be assigned to the relevant dimension of sustainability. Either way, the trick is that there will be indicators which would fit in two or more areas and that needs to be investigated carefully to reach the best possible results.

Indicators and metrics for sustainability assessment of any desired operation can be originated and adapted from existing frameworks (GRI, UN, OECD,...) or can be developed based on a deep knowledge and understanding of the operation and in alliance with a standard or regulation.

The Global Reporting Initiative (GRI) provided guidelines for measurement and sustainability reporting and introduced 91 sustainability indicators (GRI (G4) 2013) (Rahdari and Rostamy, 2015) , whilst the OECD has proposed 18 indicators for sustainable manufacturing (OECD 2011) and Eurostat has suggested just 15 sustainable indicators. (Heilala, 2015)

Whilst different organisations and researchers have proposed a variety of indicators, measures and tools, the adapted or developed indicators should have the following features and specifications:

Measurable: selected indicators should be measurable qualitatively or quantitatively from various perspectives such as economic benefits, environmental impact and so on and the measurement should be repeatable.

Relevant: indicator should be relevant to the machining operation under the investigation and should provide useful information.

Meaningful: an indicator should be meaningful and easy to understand by experts and non-experts.

Reliable: indicators should provide reliable and useful information or measurements.

Available data access: indicators should be based on the available and accessible data; they should be collected based on real information, existing sources or inexpensive methods.

Flexible: indicators should be flexible in terms of the investigation and assessment also in archiving and future referencing. They should be adaptable for general performance reporting, engineering decision making, stakeholders and investors.

Most of the indicators are normalised and instead of presenting the total measured parameters, the measured values are calibrated in relative terms as a ratio of performance or an important concept. This will provide real insight into the concept and performance and make it possible to have simple comparison with any similar operations.

In practice, sustainability indicators provide a framework that will be used to assess and evaluate the performance of the operation whether it is a sustainable practice or not and if it is following the global regulations and agreements. Furthermore, the generated measures, numbers and reports can be used in combinations with available benchmarks and target metrics to investigate possible options in order to redesign the process and optimise the operation. In addition, reports can be used as guidelines for current and future market opportunities in terms of investment and expansion activities. Therefore, sustainability assessment is not just a methodology to assess and investigate the performance of the operation rather it is about providing reliable data for design, engineering and financial decision making at the production and management levels. Ultimately, the impact and quality of the measurements, analysis and results determine the success of the decision, design and actions.

Thus, it is very important to define a meaningful list of indicators with realistic metrics that can achieve all mentioned aims as they determine how successful and achievable a process would be.

This practice is vital for all machining operations, especially non-traditional micro machining methods, including μ ECM, which are quite nascent and with the help of a feasible sustainability assessment, a smoother and economic development can be achieved.

Whilst the common belief would suggest that micro scale machining implies improved sustainability by reducing raw material usage, less energy consumption and less environmental impact, this may be challenged. Recent researches show that some factors can prevent achieving the expectation in sustainable micro-machining (De Grave and Oslen, 2006). Therefore, it is necessary to establish similar framework for micro machining sustainability as macro industries.

In the next parts, various indicators will be introduced for the five presented dimensions of the sustainability assessment. These indicators have been adapted from previously presented frameworks or they have been introduced based on practical experiences gained using μ ECM process in laboratory environment.

The indicators and metrics should be developed in a way to include the machining process in whole with its inputs, intermediate parts and outputs, figure 5-3 presents these three stages. Intermediate parts can include up to 98% of the process and it mainly considered as the waste. FIMECC (Heilala, 2015) introduced a generic model for factory/machine level which has been adapted in this work for μ ECM process. This model is the base for the following sections.

In this research the top-down approach has been selected in order to identify and introduce relevant indicators for a sustainable μ ECM process.

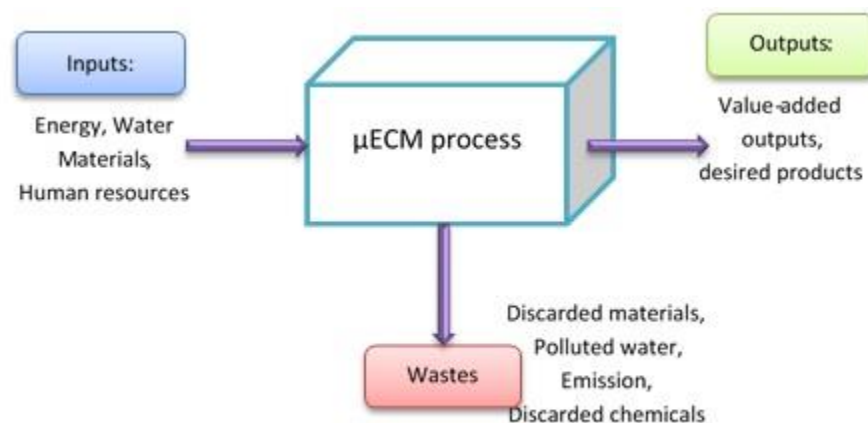


Figure 5-3: Basic model for μ ECM process to identify indicators and metrics

5.3.1 Energy consumption

Energy consumption is the first dimension to be investigated. In general, and in terms of energy, the assumption is that new technologies will use less energy and should be more productive but at industrial environment it is not easy to judge without enough data and measurements. Although there is possibility to use less energy at production level for micro-scale machining, it is important to consider the need for ventilation, filtering and maintaining the clean room which would increase the cost of the energy.

Electrical energy consumption: electrical energy consumption can be used as an indicator to assess the energy consumption of the μ ECM process. Current energy related indicators are time based. Also, in the machining process, machining time predominates in terms of the energy demand. Therefore, time is very important variable to be considered in energy consumption assessment. However, a time-based energy indicator in machining process assessment is not enough without considering MRR. Thus, this indicator should be at least a two-dimensional function of time and material removal rate (MRR). A high MRR without having a precise finished product, would hinder the operation. The complex nature of the μ ECM process makes the MRR to change in respond to any other changes in the machining setup and subsequently to provide different outcomes.

Having a high MRR rate without having precise finished product, would not benefit the process and operation. Therefore, to have more knowledgeable indicator, it may be useful to add the precision percentage as third dimension to this function. Therefore:

$$\textit{Electrical energy consumption} = f(\textit{time}, \textit{MRR}, \% \textit{precision}) \quad (5-1)$$

Energy consumption indicator should capture the sum of used electrical energy by the μ ECM process and within the workshop. The general areas of power consumptions can be considered as a function of time and production, but the machining energy consumption should be a function of three dimensions. Table 1 summarises the effective aspects of this indicator.

Function	Process / activity	Detailed
F1	Logistics	Lighting, heating, cooling, cooking, IT
F2	PC and peripherals	PC, printers, monitoring unit...
F3	Machine cooling unit	Cooling unit to maintain the electrolyte temperature
F4	Clean room	In case of using clean room for special activities
F5	Power supply unit	Current/Voltage pulses
F6	Machine control unit	Digital and analogue control unit
F7	Spindle motors	Tool spindle
F8	Axis drivers' motors	Axis movement in three dimensions

Table 5-1: Effective factors in energy consumption indicator

And finally, sum of the mentioned functions will be calculated using the equation below.

$$\text{Energy consumption} = \left\{ \sum_1^4 f_i(\text{time, production unit}) + \sum_5^8 f_j(\text{time, MRR, \%percision}) \right\} \quad (5-2)$$

Water consumption: μ ECM is based on anodic dissolution which uses aqua solutions. The electrolyte is continuously flowing while the process is taking place. The volume of the used water in the process should be measured as a function of time and MRR (f_1) but there is general water usage in the workshop as well which can be measured as a function of time and production level.

$$\text{Water consumption} = f_1(\text{time, MRR}) + f_2(\text{time, production unit}) \quad (5-3)$$

If other forms of energy are consumed during the production (machining), they need to be assessed as well.

Other point to consider is the different modes of machine states: idle, standby, start up, busy and so on. The energy consumption functions can be adapted to each different state.

Machin tools are the most dominant element in the energy consumption in the machining operation. (Priarone, 2018). Hence, one of the core concerns in research is to minimise the tools energy consumption. This will technically lead to a reduction in energy consumption and consequently positive environmental impact and reduction in the process cost.

In addition to the direct energy usage, there are other measures to consider such as the percentage of the consumed energy from renewal and green energy resources. Such indicators can be considered in a bigger frame for the factory performance rather than the process sustainability assessment.

5.3.2 Waste management

Proposed indicators to be used in waste assessment in μ ECM process can be divided in a few categories:

Material waste: in terms of material waste, the volume of defects should be considered. In addition to this, μ ECM process usually produces very high value-added products for specific applications; and in most cases required materials have significant commercial value. Therefore, any defect or waste can lead to a significant unnecessary raw material costs (Mortazavi and Ivanov, 2017)

On the other hand, μ ECM process is known for burr free products with no thermal and physical effects. This indicates that there are decreased defects in the production line, which creates less waste and thus, will increase the sustainability of the method if compared with other non-conventional manufacturing methods.

To sum up all the positive and negative outcomes, the proposed indicator to present this quantity (material waste) should be a function of produced defects in relation to the total production of finished products and unit material consumption.

$$\mathbf{material\ waste = f(defects\ per\ production, raw\ material\ consumption)} \quad (5-4)$$

Tool wear: tool wear is one of the critical aspects of the machining. However, μ ECM has proven to have no or minimum tool wear as there is no direct contact between the workpiece and the tool. So, it is expected that to have no material waste due to the tool wear and tear. But tool design and its preparation are very cost effective in micro machining industry. By identifying the most suitable tool material and tool shape, the energy and material waste will be decreased, because this will positively affect the MRR, accuracy and efficiency of the process. However, in spite of the obvious advantages of μ ECM in terms of tool wear compared with other machining processes, it is still necessary to introduce an indicator to assess the material waste due to the tool deficiency as a function of tool material usage and tool damage rate per production unit.

$$\text{tool material waste} = f(\text{tool damage rate, tool material usage}) \quad (5-5)$$

Chemical waste: μ ECM requires electrolytes to activate the reaction and create the current path between the tool electrode and the workpiece. Also, the flow of the electrolyte is the way to remove sludge and by-products from the gap. The electrolyte should continuously flow through the gap and be filtered or renewed to be free of the sludge and by-products.

Chemical waste is the rate of discarded electrolyte during the machining process. Hence, the relevant criterion should include electrolyte lifetime and the production rate.

$$\text{chemical waste} = f(\text{discarded electrolyte, electrolyte lifetime, production rate}) \quad (5-6)$$

Finally, the waste assessment indicator should be the sum of all above wastes but should be a weighted algebraic sum.

$$\text{waste indicator} = A * \text{Material waste} + B * \text{tool material waste} + C * \text{chemical waste} \quad (5-7)$$

Waste assessment is closely associated with the process environmental impact which shows the interrelation between sustainability dimensions. This will be discussed later in this chapter.

5.3.3 Environment impact

As it was mentioned earlier, lifecycle assessment framework is the approach that evaluate environmental impact of product life cycle and this evaluation involves all other areas of the sustainability. But in this proposed approach, sustainability assessment of the μ ECM operation takes place for every dimensions of the sustainability independently. So, in terms of the environment impact, the concerns are related to the natural resources, raw materials, hazardous materials and chemicals, return of discarded materials and liquids to the nature. Therefore, the environment impact of the μ ECM can have qualitative and quantitative assessment.

Natural resources: this indicator pertains to assess the rate of the consumed energy per production unit from natural resources. With much more renewable energy being used in the system, in addition to improving the energy efficiency, the impact on natural resources will decrease and the carbon footprint level will be lessened too. Hence, this indicator can be used in two ways to produce data for saving resources and producing less carbon.

Raw material: this can be introduced to evaluate the rate of the raw materials' consumption per unit of the production which should include any defects as well. The type of input materials plays an important role in the performance of the machining and its sustainability assessment, given some materials need more energy to be modified, are harder to extract from nature or have limited resources. μ ECM has provided the opportunities to machine hard materials and semiconductors, which may have been too hard to be machined with conventional machining methods. This is an advantage and that have a positive impact on the sustainability of the process. However, it is important to have clear perception of the impact of these materials on the environment.

Another important criterion is how successful is the recycling of the defects and unwanted finished products and how long is needed for this process to take place. Also, the cost of recycling process should be measured. This is problematic, for whilst μ ECM may not generate a lot of defects, the process of recycling may be too intricate. The less

the recycle rate and the longer the return period to the nature is, the more negative the impact on the environment will be.

$$EI \text{ of material waste} = f(\text{recycling rate, recycling period, unit of production})$$

(5-8)

CO₂ emission: This is a very critical and important indicator; with various standards having been published regarding the acceptable level for CO₂ emissions for different industries. Recently, it has been reported that the global energy-related CO₂ emissions grew by 1.4% in 2017, an increase of 460 million tonnes, thereby reaching a historic high of 32.5 giga tons. However, in a few countries including United Kingdom, the level of emission declined. In the UK, due to the shift from coal to gas and renewable energy, a drop of 3.8% (15 M tons) emissions was observed (IEA, 2018).

Chemical pollution: the impact of the chemical substances and generated gases can be crucial and should be addressed thoroughly when the performance of the μ ECM is assessed. μ ECM requires electrolyte to activate the process and create the current path between tool electrode and workpiece. According to Bhattacharyya (2005), two main categories of electrolytes are being used in μ ECM: “passive electrolytes” which contain oxidising anions and they are known for better machining precision and “non-passive electrolytes” which contain aggressive anions and have less effect on electrode due to the formation of soluble products, as they can be completely swept from the IEG area.

However, μ ECM electrolyte considered to be nontoxic. This is an advantage in measuring the sustainability of μ ECM regarding the environment impact, but it should be considered that the performance of the machining is affected by the remaining sludge if the sludge accumulated in the gap by generating sparks. Therefore, it is very important to assure that any sludge and gases will be flushed away from IEG and electrolyte will be continuously filtered or renewed.

A useful indicator suitable for assessing the environmental impact of the chemical waste should present the level of hazard in relation to the unit of the production and precision percentage. Therefore, whilst the same indicator as chemical waste can be used to assess the environmental impact (EI) of the electrolyte waste in the nature, the toxic level should also be added to the function.

$$EI \text{ of chemical waste} = f(\text{discarded electrolyte, toxic level, electrolyte lifetime, production rate}) \text{ (5-9)}$$

In addition to the above indicators, environmental standards are a useful guide towards investigation and improvement of the machining performance in terms of environmental impact. ISO standards need to be followed when relevant to the nature of the operation.

5.3.4 Health and safety

Health and safety of the operators at workplace is a very important consideration and it is the primary right of the workers and key responsibility of the employer to provide it. There is a range of standards and regulations regarding health and safety requirements at work floor. In the manufacturing environment, there are various health threatening and hazardous areas that need to be investigated appropriately and necessary steps should be introduced. Vibration level, noise level, chemical gases, liquid and solid scatters are examples of what may be a danger to the health and safety of workers.

Topics such as exposure to toxic chemicals, high voltage energy as well as solid and chemical scatters can be investigated as safety indicators whilst level of the chemical contaminations, noise and vibration are related to the health indicators.

General speaking, there are standards out there to be followed by employers to minimise the hazard and dangers in workplace. However, it is important to know what risks and hazards μ ECM operation can have for workers' health and safety and whether the operation can meet the standards and measures required.

Table 5-2 shows different identified hazards and relevant indicators for the μ ECM process. Each indicator is a function of multi variables, and they have been mentioned in this table, too.

These indicators, individually and in combination should fall in a risk-free category. Although some of these parameters may lessen if the final product quality or production time sacrifice but this is not the right way to manage them. Therefore, quality and production rate have not been considered as effective parameters in these functions; Overlooking the production rate and the final product accuracy, the standardised limit for any hazardous parameter should be maintained.

Function	Indication	variables
F1	Noise level	Noise level, working hours
F2	Vibration level	Vibration level, working hours
F3	Electromagnet waves	Wave exposure level, working hours
F4	Toxic chemical	Volume, toxic level, exposure period
F5	High power risk	Risk probability, working hours
F6	Solid scatters	Volume, tool rotation speed, dimension of scatter, working hours
F7	Chemical scatters	Volume, dimension of scatter, tool rotation speed, electrolyte flow velocity, working hours

Table 5-2: Health and Safety indicators in μ ECM operation

There are other areas of personnel health that formally should be considered when health and safety is the concern, including staff well-being and work satisfaction, but their relevant indicators should be defined as part of the general assessment for the firm or factory.

5.3.5 Cost management

Cost of the process is as of a great deal in any manufacturing process; the cost of the process is very important not only from a sustainability dimension perspective, but the fact that the process needs to be financially attractive for the organisation/investors. There is no doubt that, currently, μ ECM is an expensive machining method but it has potential to be expanded industrially and to be commercialised through further research. μ ECM machining as with any other manufacturing process requires various types of expenditure, such as the cost of operation, maintenance and labour.

The cost of operation is a relative parameter and not an absolute value. The higher level of the cost does not necessarily mean a too expensive operation, for it may make

the whole process more effective through improving the quality of the final products and increasing the efficiency of the operation.

In a way cost of the machining process is under the effect of all other sustainability dimensions, so development of any cost management indicators is in fact developing indicators with interrelationship. The cost indicator should include the following areas.

Cost of labour: this indicator will pertain to assess any labour expenses, which will include, rates of pay, working hours and number of workers involved in the workflow. In addition, this indicator can be used as a more general form to include the assessment of the company in a bigger frame; it can present any extra action has been taken in order to provide a better work environment for the workers, especially in terms of the employees' well-being and work satisfaction.

Cost of energy consumption: this indicator refers to a different approach for considering the energy efficiency in the process. The most important parameter is the source of the energy, where renewable and green energies would cost less than using coal and electricity. Regardless the source of the energy, the cost of the consumed energies can be divided in two main categories, as follows:

There is a general cost of energy, which covers heating, cooling, cooking and lighting of the workshop or factory.

Then, there is the cost of energy consumed by the machinery equipment, such as spindle motors, DC axis motors, machine's pump as well as, control and power supply unit. This category needs detailed analysis as the expenses vary according to the machining quality and machining setup. Hence, in this assessment the quality of the final product and precision percentage should be considered. So, this indicator is a relative variable depending on the quality of the final product and clearly, improved quality comes with a price.

Cost of maintenance: maintenance fee includes any repair and expenses to maintain the production machinery equipment. It is a sum of expenses which paid for regular inspection, breakdown recovery, part exchange and regular cleaning. The maintenance cost will be a function of working hours of the machine.

Cost of consumable which includes materials and electrolyte, tool materials and preparation. The cost of the tool preparation is quite high but assessment of this cost in terms of production unit will make it efficient as there is no tool wear in the μ ECM process.

This indicator, in a way presents the cost of intermediate parts which involve a high share of the process resources and activities.

Cost of by-products disposal: disposal of by-products should be actioned according the standards and regulations. By-products of the μ ECM operation are in the form of sludge, chemical liquid which has a strict disposal process to follow and should be actioned by trained workers. The cost needs to be considered per unit of production.

All other costs: Any other expenses which do not fit in the above categories but are necessary for running the operation and production line should be taken into the account as well.

As above descriptions and explanations present, the cost management can be considered as an overseen factor in sustainability, which uses all other indicators and metrics under its cover to assess and evaluate the cost of each and all aspects of the process. This criterion is a great help when it is the time to restructure the process and reinvest in order to improve or expand the machining process.

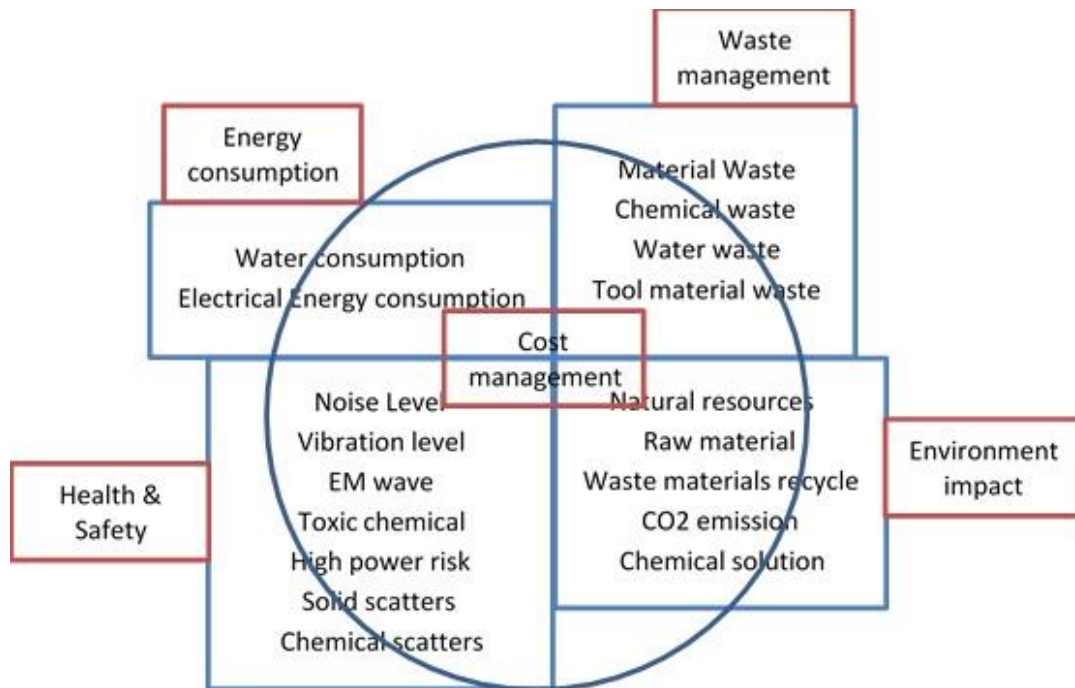


Figure 5-4: Brief presentation of μ ECM sustainability indicators and their dependency

Whilst the relation between the cost dimension and all other dimensions of the sustainability is very clear, but it does not make the assessment any easier as the price can change with a slight shift in the operation, quality and precision of the process. Similar relations are observed among all other dimensions as well; for example, improved impact on the environment comes from energy consumption efficiency, lower material usage stems from fewer defects, improved health and safety comes from improved chemical disposal and so on.

As figure 5-4 shows, there is not any solid boundary between the five dimensions of sustainability, but rather, there is a shared space between them, which symbolically presents their interrelation. Understanding this complex interrelation is crucial and should be investigated carefully as it will affect the substantially assessment outcomes.

5.4 Discussion

μ ECM machining method is an expensive technology and needs a higher initial investment in comparison with other non-conventional micro machining methods. This feature from one side, and the complex nature of the μ ECM process from the other side, are the key reasons why it has not been able to attract enough interest to be commercialised in an industrial environment. Hence, introducing indicators and measures for the evaluation and investigation of the sustainability of this process will help to expand the use of this method and perhaps to make it more interesting for investors.

For special types of material, including hard materials to machine, fragile ones and superconductors, μ ECM could be the only method which can provide maximum accuracy and minimum damage. There are other materials that could be machined using μ ECM and other alternative methods. Sustainability measures can help to identify the most optimum method for machining this group of materials. And of course, sustainability measurement can prevent the waste of resources, if μ ECM is not the best method to be used.

Table 5-3 summarises the introduced metrics in the dimensional sustainability assessment for the μ ECM process. Whilst these cover all dimensions of the sustainability assessment, but this is not enough, for in addition to the results and acquired data, their accurate interpretation is just as important as obtaining the data through the indicators in the first place.

Dimensions of Sustainability	Energy consumption	Water consumption
		Machine usage of power electricity
		Operation usage power electricity
		Any other energy usage
	Waste management	material
		energy
		Gaseous waste
		chemical
		hazardous
		Liquid waste
		Water waste
	Environment impact	Polluted Water release
		Renewal energy usage
		Chemical disposal rate
		liquid waste disposal
		CO2 emission
	Health & safety	Liquid scatter
		Material (solid) scatter
		Exposure to toxic
		Exposure to high temperature
		Exposure to high voltage
		Noise level
		Vibration level
		Other hazardous exposure
	Cost management	Raw Material Cost
		Water recycle cost
		Power electricity cost
		By-products treatment cost
Labor cost		
Operation cost		
Water cost		
Scrap recycle cost		

Table 5-3: μ ECM sustainability metrics and indicators

As the μ ECM process is a very complicated process and a slight change in machining parameters can change the result significantly, clearly understanding how these metrics work is crucial. In addition to the machining parameters, precision and accuracy of the final product will affect the interpretation of the metrics and indicators. Also, should not be forgotten that the interrelation between indicators can change the sustainability assessment results substantially. Therefore, it is very important to be alert to these matters and be able to respond appropriately when necessary.

A brief review on the table 5-3 and figure 5-4 confirms that the interrelation between the dimensions of the sustainability exist almost between all metrics. Also, this review confirms that most of these metrics are at least dependent on one of the units of production, quality of the finished work or precision percentage.

Although, the above proposed approach for the sustainability assessment of the μ ECM is the unique approach in this field and thus there is not any other approach to be analytically compared with this research, there are examples of recent researches in the field of machining sustainability assessment which can help to present the possible advantages of the proposed work for the future.

Mia et al (2018) investigated the machining performance of hardened AISI1060 steel under different cooling lubrication conditions and presented the results in terms of cutting temperature and surface roughness, and finally used the Pugh matrix environmental approach to assess the sustainability of the process among studied conditions.

The similarity between above mentioned example and proposed approach is that the machining outcome can differ based on initial machining setup; therefore, the aim is to find the optimum machining outcomes and assess the sustainability of the optimised approach.

One of the features of the μ ECM technology is the high share of intermediate parts (stages) which cannot be seen at the final product but are very significant towards the performance of the process. By introducing various indicators for all dimensions of the sustainability, it has been tried to cover all these intermediate parts and stages to have a more accurate picture of the process sustainability, specially knowing that these intermediate parts have impact on all five dimensions. Therefore, in addition to considering the dependency of the assessment to the process output features (like machining

accuracy and MRR), the effect of the intermediate parts and stages have been considered, too.

The second difference and in fact one of the aims of the proposed approach is to be able to find optimised machining parameters not only for a better machining output but to have a more sustainable approach. Therefore, the risk of optimisation with sacrificing the nature, environment or energy resources will be eliminated and a balance between optimised machining setup and sustainable performance can be achieved.

Figure 5-5 illustrates the proposed assessment's flowchart which presents the sustainability assessment of the μ ECM process and the important role it can play in optimisation of the process.

μ ECM is a complicated and multidisciplinary method based on a mysterious electrochemical phenomenon which yet to be fully explored; machining parameters are in a very complex correlation and any changes in one parameter can affect the whole process and the machining outcomes.

Ikkala et al (2015) showed that by increasing MRR, machine tool energy efficiency can be improved. MRR can be varied by changing the machining parameters including pulse supply features, electrolyte type and features, feed rate, tool rotational speed and the IEG size. Therefore, energy efficiency depends on all these parameters. In addition to this, the quality of the final part will improve by changing any of these parameters.

Increasing energy efficiency by sacrificing the quality is not a sustainable approach and wise decision to take; finding the balance between process efficiency and quality of the finished product is a challenge yet to overcome. Having a set of accurate, detailed and reliable machining parameters for μ ECM would improve sustainability assessment of the process. Furthermore, this can lead to creation of a comprehensive setup that can help in delivering a productive and economic method for desired machining.

And finally, the aim is that by presenting the advantages and enormous potential of the μ ECM process in terms of the technology, environment friendliness and operator safety, be able to justify its initial high cost and promote it to the industrial level.

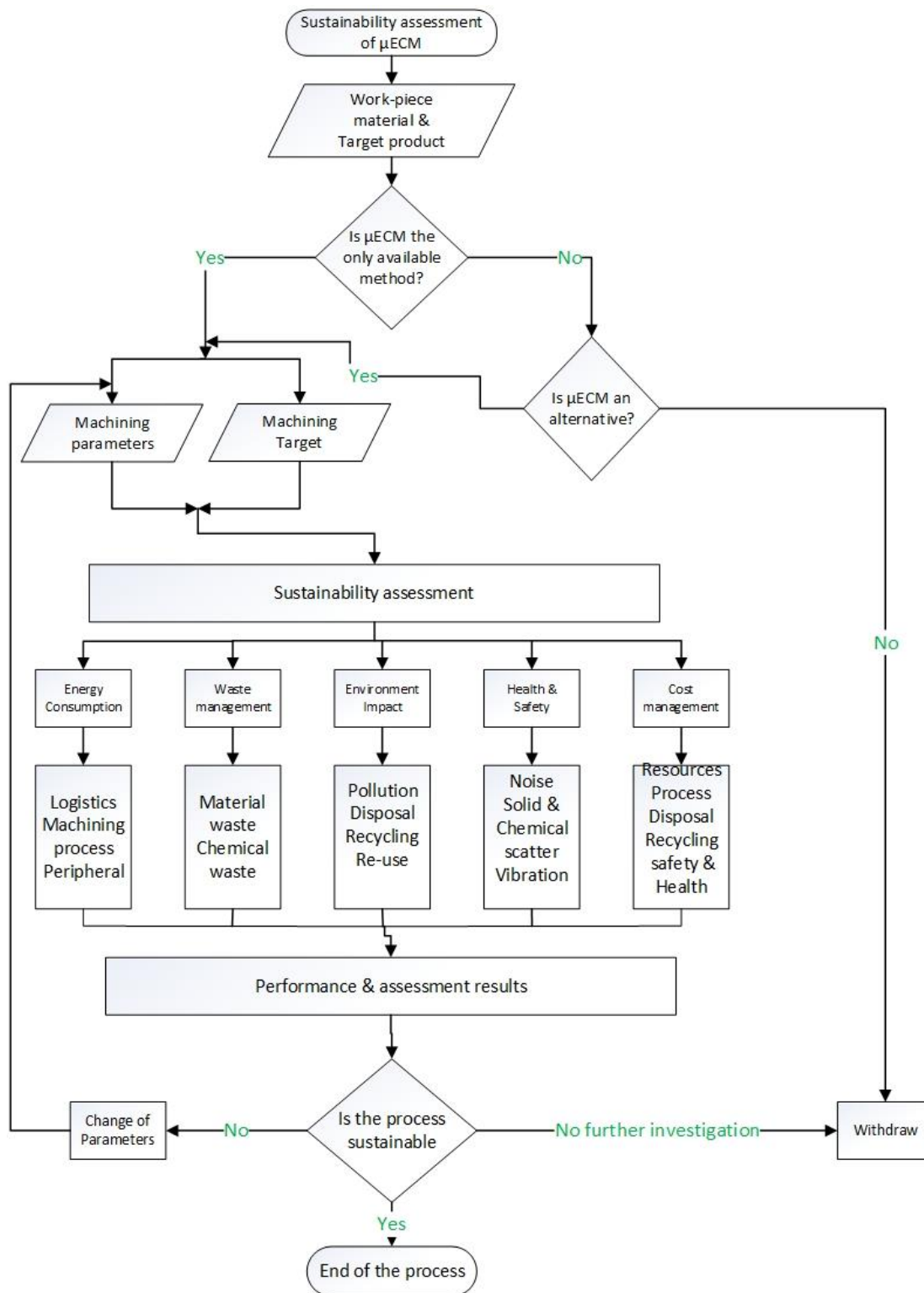


Figure 5-5: μ ECM sustainability assessment flowchart

5.5 Conclusion

Sustainability assessment and sustainable development are the key issues between the current manufacturing challenges that likely to increase in importance more rapidly. Currently, assessment for sustainable systems and processes are widely neglected, with the most efforts being concentrated on the product and supply chain. In addition to this, in the micro manufacturing field, non-traditional micro manufacturing methods have received less attention compared with the conventional methods despite increasing demand to be used. In this work, the aim is to promote the importance of the μ ECM process as a non-traditional micro machining process based on its sustainability assessment as of it is being the best option for machining special types of materials including but not limited to hard materials to cut, conductors and superconductors.

As aforementioned, despite the valuable advantages of the μ ECM over other machining processes, this technology is still at the research level and to become a commercial technology. The main reasons behind this are the expensive structure, uncertain and complex nature of the electrochemical process and process dependency on operator experiences.

Currently, there is a disconnection between data collectors (scientists and researchers) and operators who can practically influence sustainability of the manufacturing in the most of manufacturing processes and remarkably in μ ECM process. Hence, there is still a huge gap between practices at the research and commercial levels. However, sustainability assessment may help in addressing this by proving the process values and profitability despite the high investment cost.

In this research it has been tried to identify and introduce indicators and measures to assess the sustainability of the μ ECM process considering the five dimensions of the sustainable development. Additionally, introduced indicators and assessment approach and refining the interpretation of the assessment results can help to develop new ground to investigate optimised machining parameters in order to achieve higher accuracy and precision within a sustainable frame.

At present and based on the μ ECM process features, the assessment results should be interpreted based on general guidelines and manufacturer expectations but by implementing the introduced assessment and gathering more data it is possible to prepare a benchmark for all measures and indicators to make the results comparable.

The suggestion for the future work is to advance the research by developing an assessment model based on artificial intelligence or neural networks using the above indicators and metrics in order to have a uniform investigation methodology for all materials and products.

CHAPTER 6

Conclusions and Future Works

Over last two decades, μ ECM technique has been developed enormously and has been showing an astonishing progress. μ ECM technique has been successfully tested for different applications and has shown amazing outcomes. But its progress to the industrial environment has been delayed due to its complex nature, expensive structure and timing process setup. This research aimed to demonstrate an analytical review on available researches and published works to identify the knowledge gaps in the field of the μ ECM machining process and propose a new approach towards process investigation and development.

6.1 Conclusion:

In this work, μ ECM machining process was investigated considering three different aspects as follows:

- Identifying the effective machining parameters and the interrelation between these parameters and their effects on machining performance by applying a critical review on previous researches and published works.
- Exploring anodic reaction at electrode-electrolyte interface and the role of EDL behaviour in a successful μ ECM machining process.
- Reviewing current state of the sustainability assessment and exploring the position of the μ ECM machining with respect to sustainability assessment

This approach was resulted in identifying the following knowledge gaps within this technology:

- Setting the initial values for machining parameters is a challenge due to complex nature of the process and complex interrelation between parameters. Currently, initial values for machining parameters are selected based on trial and error approach which is dependent on operator experience or they are selected through mathematical calculations which is based on several assumptions. This issue has been identified as one of the knowledge gaps

which has been addressed by designing a laboratory experimental approach and mathematical analysis of the obtained results.

- Throughout the literature review, EDL behaviour was identified as the key element in μ ECM machining performance; the success of the machining is very much dependent on the reaction which takes place at electrode-electrolyte interface. To understand the details of this reaction, it is necessary to explore the EDL structure and its behaviour. Currently, there is not enough publications with the focus on EDL, as a result, lack of the knowledge and investigation regarding the EDL was identified as second knowledge gap. This issue was addressed by proposing a laboratory experimental work using viumstat and based on impedance spectroscopy techniques to estimate the EDL equivalent RC network. Also, electrical features of the achieved equivalent network were analysed using Matlab Simulink.
- Sustainability assessment of the μ ECM process was identified as the third knowledge gap which needed further investigation. Currently, there are limited number of academic and industrial publication about sustainability assessment of the non-traditional machining process; this is more crucial when the process is applied at micro and nano level. This applies to the μ ECM sustainability assessment as well; therefore, the lack of recognised approach in sustainability assessment of the μ ECM was addressed by introducing several indicators and measures based on the five dimensions of the sustainability.

The achieved results and outcomes through this research demonstrate that μ ECM is a valuable process which can be used at industrial environment and for variety of applications but it requires cooperation between researchers and technology developers to establish a general framework and follow similar rules and approaches to build a valid and reliable database for different combination of electrodes' materials and electrolyte solutions to save the time by preventing repetitive experiences.

6.2 Key contribution and publications

The development of this research work is associated with the following outcomes and contribution to knowledge:

- Proposed experimental work using iviumstat and mathematical analysis using Matlab successfully helped to reach a narrow range for the predominant parameters' initial values. The suggested methodology resulted in setting voltage level, electrolyte concentration and IEG within a narrow range to achieves the best machining performances including maximum MRR and minimum OC.
- EIS is a valuable technique in order to have better understanding of the μ ECM process with emphasis on electrochemical reaction which takes place at electrode-electrolyte interface. Proposed experimental works using iviumstat can save the time and the cost of current rial and error approach when new materials are machined using μ ECM technology.
- EDL equivalent RC circuit simulation, presented the relation between EDL capacitor time constant and pulse-on time, duty cycle and faradic and charging currents. The simulation results suggested that pulse on time should be equal or greater than EDL capacitor time constant to achieve maximum faraday current and current density.
- Sustainability assessment of the μ ECM machining can facilitate the development of the process at industrial levels as manufacturing industries are under tremendous pressure to improve their performance considering dimension of sustainability. The proposed indicators and measures can help μ ECM technology developers to assess the sustainability of the process. This assessment can subsequently be used to optimise the machining process by reviewing the results continuously and improving the results. Additionally, sustainability assessment of the process can help to justify the high initial cost of the process and validate its advantages for the micro and nano manufacturing over other machining techniques.

The following publications have demonstrated the above efforts and contributions:

❖ **Sustainable μ ECM machining process: indicators and assessment**

Mina Mortazavi, Atanas Ivanov- Journal of cleaner production, 2019, Volume 235,

1580-1590

DOI: 10.1016/j.jclepro.2019.06.313

❖ **μECM process investigation considering pulse signal features and EDL capacitance**

Mina Mortazavi, Atanas Ivanov- The International Journal of Advanced Manufacturing Technology, 2019

DOI: 10.1007/s00170-019-03864-2

❖ **Sustainability of micro electrochemical machining: Discussion**

Mina Mortazavi, Atanas Ivanov- Sustainable design and manufacturing 2017, selected papers on sustainable design and manufacturing, 2017, 203-2010

DOI: 10.1007/978-3-319-57078-5

❖ **Advanced applications of micro ECM technology**

Atanas Ivanov, Mina Mortazavi- The 5th International Conference on Nanomanufacturing (nanoMan2016) 15 – 17August, 2016, Macau

6.3 Recommendation for the future work

μECM process is a valuable technology full of potential in micro and nano manufacturing applications. This process is complex and requires a multidisciplinary approach towards its investigation and development. Therefore, investing on generating a comprehensive database consisting of the simulation and experimental results would ease the development and the progress of this technology to the industrial level.

Based on this research and experiences and knowledge gained through this work the following suggestions for the future work are recommended:

- EDL features and behaviour as key elements in a successful μECM machining process need to be explored in more depth. It is beneficial if EDL equivalent electric circuit could be modelled using variable resistors and capacitors to present the dynamic behaviour of the process as a time variable function to demonstrate on-line changes of the process.
- Electrochemical impedance spectroscopy is a very useful and powerful tool to model the electrode- electrolyte interface equivalent circuit. It is a huge help if an open access database can be generated for any combination of tool and workpiece materials and developers and researchers be able to update the database with their finding and experiments results.

- Evaluation of the faradic and non-faradic currents using the equivalent electric circuit can be used to optimise the pulse signal features in order to maximise the share of the faradic current and subsequently to increase the current density
- One of the critical challenges in μ ECM process using ultra-thin tool electrodes when creating deep shapes on workpiece, is the removal of sludge from IEG; it is worth to invest on further investigation to find the most efficient electrolyte inlet design. This challenge has not been addressed practically in current research and development activities.
- Sustainability assessment of the μ ECM process is a forward-thinking approach due to importance of sustainable manufacturing and pressure on manufacturer to improve their production in terms of technology, operation and product. Enriching the proposed approach in this research can speed up the application of μ ECM at industrial level and expand its application in various micro and nano industries. This can happen by applying the proposed charts in real experiments and improving the assessment by introducing an intelligent model using artificial intelligence or neural networks.

APPENDIX A

Details of the resources used for Table 2-3

	IEG	MRR	Overcut (side gap)	stray current	Localisation	Current	Electrolyte resistance	improved Surface Roughness	machining precision
IEG	[16]					[5]	[2],[13]	[16]	
Electrolyte Concentration	[1],[5],[15]	[1],[5],[6],[12],[19]	[1],[12],[21]	[1],[21]	[12],[21]	[21]		[10],[11]	
Pulse Voltage Amp.	[1],[7],[8],[10],[14]	[3],[6],[12],[15],[19]	[1],[3],[4],[11],[12],[14],[15],[19]	[15],[21]	[13],[21]	[9],[21]		[9]	
Pulse on-time (duty ratio)	[17]	[1],[3],[5],[6],[9],[20]	[11],[21]		[13],[21],[20]	[1]		[9]	[16]
Current		[3],[21]	[1]		[1]				[15]
Pulse period (frequency)		[5],[6],[19]	[3],[4],[5],[11]						[10],[18]
Feed rate	[14]	[19]	[14]						

1	Bhattacharyya & Munda, 2003
2	Skoczypiec, 2016
3	Reddy, 2013
4	Kozak, et al., 2004
5	Kurita, et al., 2006
6	Sarvanan, et al., 2012
7	zhang & Zhu, 2008
8	Zhang, et al., 2007
9	Lee, et al., 2007
10	Rajurkar, et al., 2006
11	Ghoshal & Bhattacharyya, 2013
12	Govindan, et al., 2013
13	Skoczypiec, 2016
14	Kozak, et al., 2004
15	Bhattacharyya, et al., 2005
16	Bhattacharyya, et al., 2004
17	Jo, et al., 2009
18	Kim, Jung, & Park, 2013
19	Rao & Padmanabhan, 2013
20	Mithu, et al., 2014
21	Munda & Bhattacharyya, 2008

Table 2-3 in chapter 2, presents the qualitative interrelation between machining parameters and machining criteria. The gathered data has been obtained through different researches and publications which has been mentioned in above table. Also the table on left hand side in this page shows the references for the gathered information.

APPENDIX B

IVIUMSTAT specification

Product description:

Wide application range:

The IviumStat.h is well suited for applications requiring a wide dynamic range, such as battery testing, corrosion measurements and electrochemical research applications. It has a high power of $\pm 5A$ and low current ranges, down to 1pA full scale.

Complete solution:

The IviumStat.h offers a complete package, all the standard electrochemical techniques are included. The IviumStat.h also has an integrated high-performance Frequency Response Analyser for EIS measurements from 10 μ Hz to 8MHz. All measurement and dataprocessing software is included (for Windows based PCs).

Safety:

The compliance (maximum current or potential) of the instrument can be defined by the operator. Thus valuable samples may be protected, and unsafe situations prevented.

Automation:

Multiple analog and digital input & output ports are available for monitoring & control of peripheral equipment. This functionality is fully integrated in the software.

Expandability:

The IviumStat.h can be expanded with a wide variety of options and modules, including a Bipotentiostat, True Linear Scan generator, various power boosters, multiplexer and FastScan.

Hardware:

- Automatic current range selection: 1pA to 10A/1mV to 10V (50V)
- Automatic variable noise filter and potentiostat/galvanostat stability settings
- Simultaneous acquisition of current/potential and up to 8 peripheral analog signals
- Real time data display up to 500 pnts/s. Acquisition up to 100,000 pnts/s is stored in instrument memory

- Applicable scanrates: 1 μ V/s to 10,000V/s
- Minimum interval time/resolution: 10 μ s
- Result optimisation by automated tuned filters, gain amplifiers and DC-subtraction

Software:

The IviumStat.h is controlled via Ivium's own IviumSoft. This versatile, yet intuitive software, allows instrument control, data management and analysis, peripheral instrument control, etc. IviumSoft can also interface with and be controlled from LabVIEWTM, C++, Delphi, etc. A full suite of IviumSoft is included as standard with each instrument.

Specifications

System performance

Current compliance	$\pm 5A$
Maximum output voltage	$\pm 10V$ below 1A, and $\pm 8V$ up to 5A
Electrode connections	4; WE, CE, RE, S (and GND) with 4mm banana plugs
Potentiostat bandwidth	8MHz for small signals, 300kHz for large signals
Stability settings	High Speed, Standard and High Stability
Programmable response filter	1MHz, 100kHz, 10kHz, 1kHz, 10Hz
Signal acquisition	Dual channel 24bit ADC, 100,000 samples/s

Potentiostat

Applied potential range	$\pm 10V$, 0.02mV res. (20bit)
Applied potential accuracy	0.2% or 1mV
Current ranges	$\pm 10nA$ to $\pm 10A$ in 10 decades
High sensitivity current ranges	$\pm 1pA$, $\pm 10pA$, $\pm 100pA$, $\pm 1nA$
Measured current resolution	0.00001% of current range, minimum 0.6aA
Measured current accuracy	0.2%

Galvanostat

Applied current resolution	0.00013% of applied current range
Applied current accuracy	0.2%
Potential ranges	$\pm 1mV$, $\pm 10mV$, $\pm 100mV$, $\pm 1V$, $\pm 10V$
Measured potential resolution	0.00001% of potential range, minimum 0.15nV
Measured potential accuracy	0.2% or 1mV

Impedance Analyser

Frequency range	10 μ Hz to 8MHz
Amplitude	0.015mV to 1.0V, or 0.03% to 100% of current range
DC offset	16bit DC offset subtraction and 2 DC-decoupling filters
Dynamic range	0.05nV to 10V, and 0.2aA to 5A

Electrometer

Input impedance	>1000Gohm //<8pF
Input bias current	<10pA
Bandwidth	>16MHz

Special functions

Ohmic drop compensation	2V/current range, 16bit resolution
Safety features	Automatic disconnect on internal/external limits

Peripheral connections

Analog in/out	8/2 (0 to +4V, 16bit resolution)
Digital input/output	2/3 (0 to +5V)
I-out/E-out	Analog monitor for cell current and potential
AC-out	\pm 0.5V sinewave 10 μ Hz-8MHz with variable attenuation
Channel-X input, Channel-Y input+4V:	to record impedance from peripheral devices

Environment

Power requirements	100-240V, 47-63Hz, 150VA
Interfacing	USB
Size (w x d x h)	26 x 33 x 12cm
Weight	4.2kg
PC requirements	Windows 7/8/10, with free USB port

www.ivium.com/product/iviumstat-h-standard - Accessed on 21.05.2019

APPENDIX C

A few useful tips to consider when using potentiostat (in this research iviumstat)

One of the common reasons for inaccuracy in EIS measurements is drift in the system under the investigation.

The second reason could be the instability and variation in cell characteristics including temperature, oxide layer thickness, adsorption of solution impurities and reaction products.

To improve the achieved results and information, it has been advised by manufacturer to increase the frequency range and include more frequencies per decade.

Due to possible unexpected reaction, it is important to clean the instrument before and after experiments (using pure water and sterilised materials) which would help to achieve more accurate results.

External electric fields can significantly affect the impedance measurement by increasing the noise level. Using Faraday cage can eliminate the possible influences of the electrical fields.

Polarisation curves should be determined only after the open-circuit electrode potential of the tested metal has attained a steady-state value. The length of time required to reach the steady state depends upon the nature of the system.

For a more reliable data analysis, it is helpful to run Kramers-Kronig transform, and find out whether Warburg impedance exists and to use the simplest model and fit it and finally extract the data.

APPENDIX D

Lacomit specification

Physical and chemical properties:

Appearance	Clear liquid.
Colour	Pink to Red.
Odour	Organic solvents.
Solubility	Slightly soluble in water.
Initial boiling point and boiling range	> 100 °C @ 760 mm Hg

Reactivity:

Stable under normal temperature conditions and recommended use.

Chemical stability:

Stable under normal temperature conditions and recommended use.

Possibility of hazardous reactions:

Flammable/combustible - Keep away from oxidisers, heat and flames. Avoid contact with acids and oxidising substances. Reacts violently with strong oxidising substances. Reacts violently with strong acids. Hazardous Polymerisation Will not polymerise.

Conditions to avoid:

Avoid heat, flames and other sources of ignition. The product is flammable, and heating may generate vapours which may form explosive vapour/air mixtures.

Materials to Avoid:

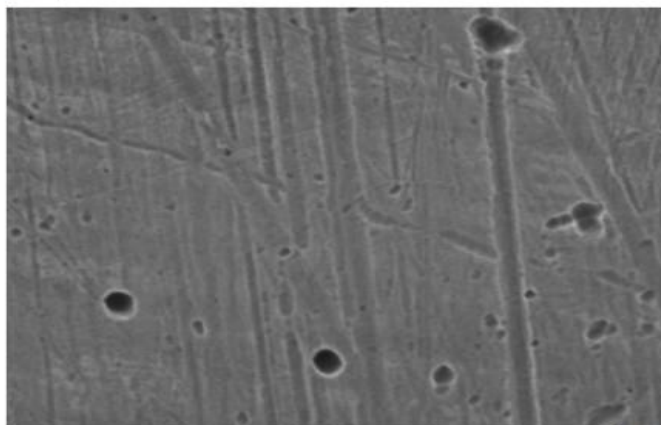
Strong oxidizing substances. Strong acids.

APPENDIX E

Chapter 3 detailed results

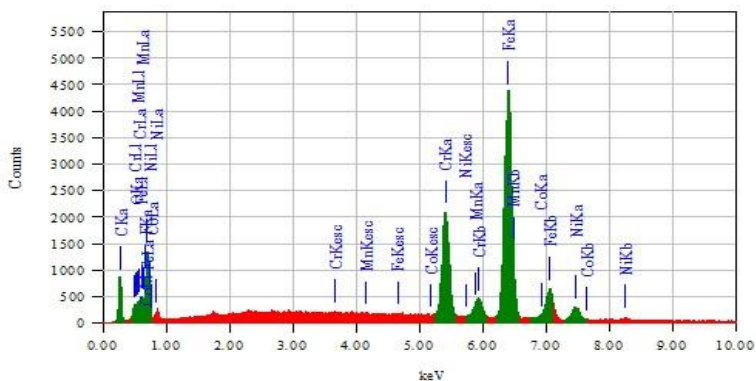
Workpiece surface (EDS report):

View000



JEOL 1/1

Title : IMG1
 Instrument : JCM-6000
 Volt : 15.00 kV
 Mag. : x 2,000
 Date : 2019/06/13
 Pixel : 512 x 384



Acquisition Parameter
 Instrument : JCM-6000
 Acc. Voltage : 15.0 kV
 Probe Current: 1.00000 nA
 PHA mode : T3
 Real Time : 52.45 sec
 Live Time : 50.00 sec
 Dead Time : 4 %
 Counting Rate: 4950 cps
 Energy Range : 0 - 20 keV

ZAF Method Standardless Quantitative Analysis
 Fitting Coefficient : 0.7517

Element	(keV)	Mass%	Sigma	Atom%	Compound	Mass%	Cation	K
C K*	0.277	0.74	0.00	2.22				0.8589
O K*								
F K*	0.677	25.36	0.54	48.17				21.7562
Cr K*	5.411	50.39	0.34	34.97				53.7965
Mn K*	5.894	4.49	0.17	2.95				4.7351
Co K*								
Ni K*	7.471	19.03	0.34	11.70				18.8533
Total		100.00		100.00				

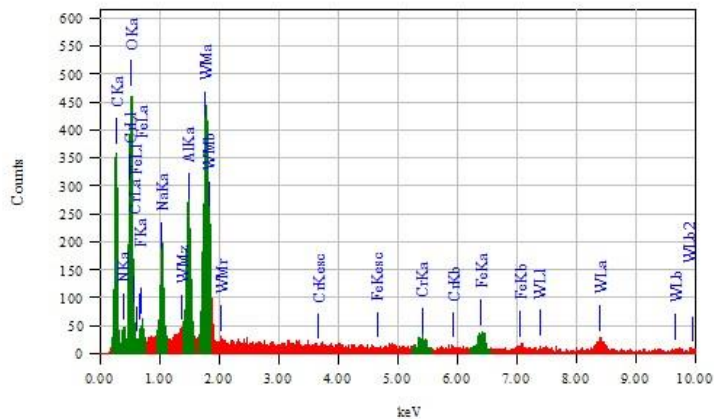
Tungsten tool surface (EDS report):

View000



JEOL 1/1

Title : IMG1
 Instrument : JCM-6000
 Volt : 15.00 kV
 Mag. : x 130
 Date : 2019/06/24



Acquisition Parameter
 Instrument : JCM-6000
 Acc. Voltage : 15.0 kV
 Probe Current : 1.00000 nA
 PHA mode : T3
 Real Time : 50.81 sec
 Live Time : 50.00 sec
 Dead Time : 1 %
 Counting Rate : 541 cps
 Energy Range : 0 - 20 keV

ZAF Method Standardless Quantitative Analysis

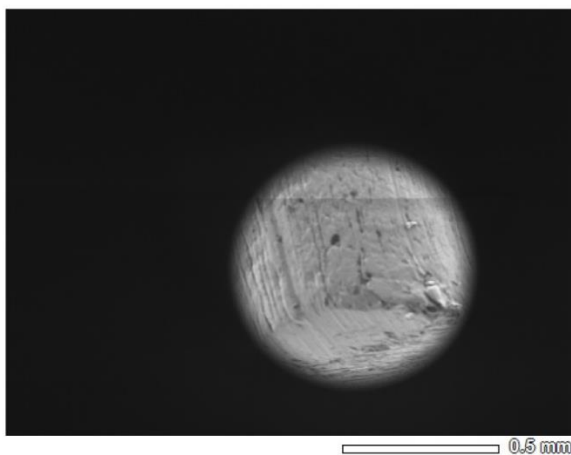
Fitting Coefficient : 0.0908

Element	(keV)	Mass%	Sigma	Atom%	Compound	Mass%	Cation	K
C	0.277	0.80	0.01	1.49				0.9858
N	0.392	13.61	0.47	21.73				32.4866
O	0.525	44.61	0.68	62.34				33.9431
F								
Na	1.041	5.71	0.19	5.55				3.7299
Al	1.486	4.72	0.13	3.91				4.4930
Cr	5.411	1.23	0.10	0.53				1.3259
Fe	6.398	3.15	0.17	1.26				3.4372
W	1.774	26.17	0.58	3.18				19.5984

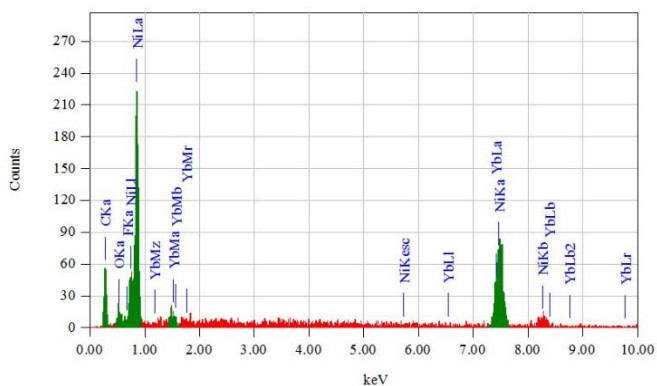
Nickel tool surface (EDS report):

View000

JEOL 1/1



Title : IMG1
 Instrument : JCM-6000
 Volt : 15.00 kV
 Mag. : x 65
 Date : 2019/07/05
 Pixel : 512 x 384



Acquisition Parameter
 Instrument : JCM-6000
 Acc. Voltage : 15.0 kV
 Probe Current : 1.00000 nA
 PHA mode : T3
 Real Time : 50.55 sec
 Live Time : 50.00 sec
 Dead Time : 1 %
 Counting Rate : 151 cps
 Energy Range : 0 - 20 keV

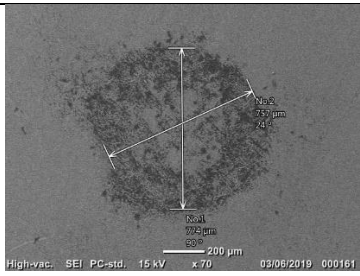
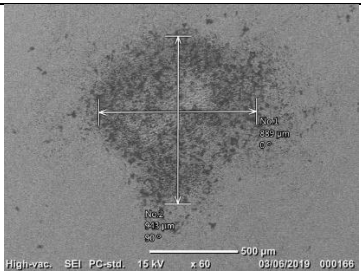
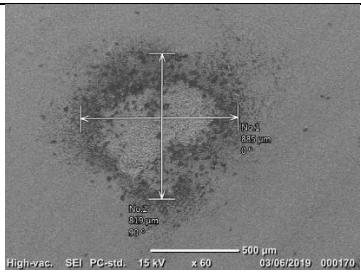
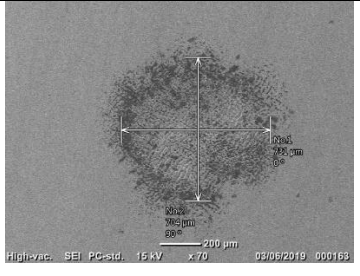
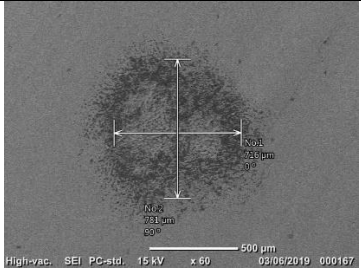

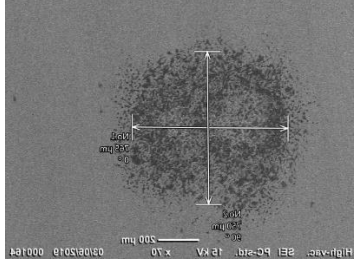
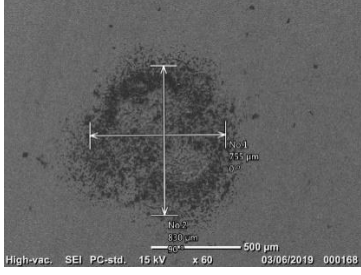
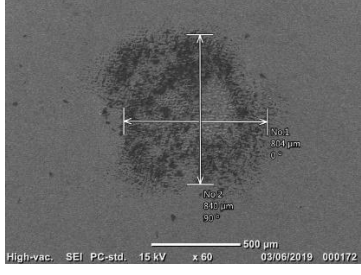
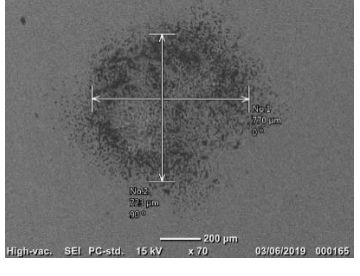

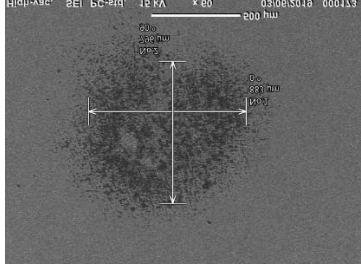
ZAF Method Standardless Quantitative Analysis
 Fitting Coefficient : 0.1755

Element	(keV)	Mass%	Sigma	Atom%	Compound	Mass%	Cation	K
C K*	0.277	1.14	0.03	4.94				0.9224
O K*	0.525	5.08	0.51	16.54				5.6777
F K*								
Ne K*								
Ni K*	7.471	85.69	2.61	76.08				91.5279
Yb M*	1.521	8.09	2.59	2.44				1.8720
Total		100.00		100.00				

APPENDIX F

Chapter 4 detailed results:

SEM images for the Impedance investigation using iviumstat (Tungsten tool electrode)

Gap	6.5 Volt- 0.5 mole/L	7 Volt- 0.5 mole/L	7.5 Volt- 0.5 mole/L
22 μm			
24 μm			
25 μm			
26 μm			

SEM images for the Impedance investigation using iviumstat (Tungsten tool electrode)

Ga p	6.5 Volt- 0.6 mole/L	7 Volt- 0.6 mole/L	7.5 Volt- 0.6 mole/L
22 μm			
24 μm			
25 μm			
26 μm			

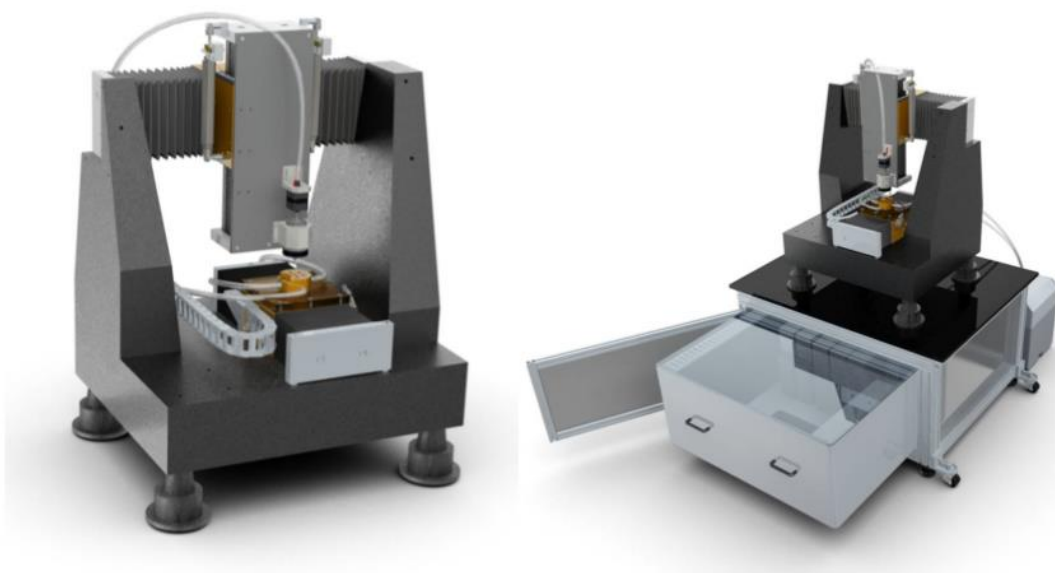
Matlab simulation measurements for 50% and 75% pulse duty cycle

Time constant	Pulse on time	Duty Cycle	Pulse width	Max voltage EDL Capacito	Max current EDL Capacitor	Max current Charge transfer R.	Current Flat time Charge transfer R.	Current Flat time Electrolyte R.
	μs	%	μs	V	A	A	μs	μs
τ	2.335	50%	4.67	3.069	0.5097	0.2549	0.096	0.522
2τ	4.67	50%	9.34	3.421	0.581	0.2842	0.576	0.605
3τ	7.01	50%	14.02	3.475	0.577	0.2886	1.766	1.842
4τ	9.34	50%	18.68	3.481	0.582	0.2892	4.167	3.482
5τ	11.68	50%	23.36	3.482	0.578	0.2892	6.346	5.818
6τ	14.01	50%	28.02	3.482	0.578	0.2892	8.432	8.177
τ	2.335	75%	3.11	3.238	0.3031	0.269	0.153	0.38
2τ	4.67	75%	6.23	3.437	0.4287	0.2854	0.576	0.593
3τ	7.01	75%	9.35	3.475	0.501	0.2887	2.684	2.84
4τ	9.34	75%	12.45	3.481	0.583	0.2892	4.359	3.939
5τ	11.68	75%	15.57	3.482	0.579	0.2892	6.731	6.369
6τ	14.01	75%	18.68	3.482	0.568	0.2892	9.175	8.437

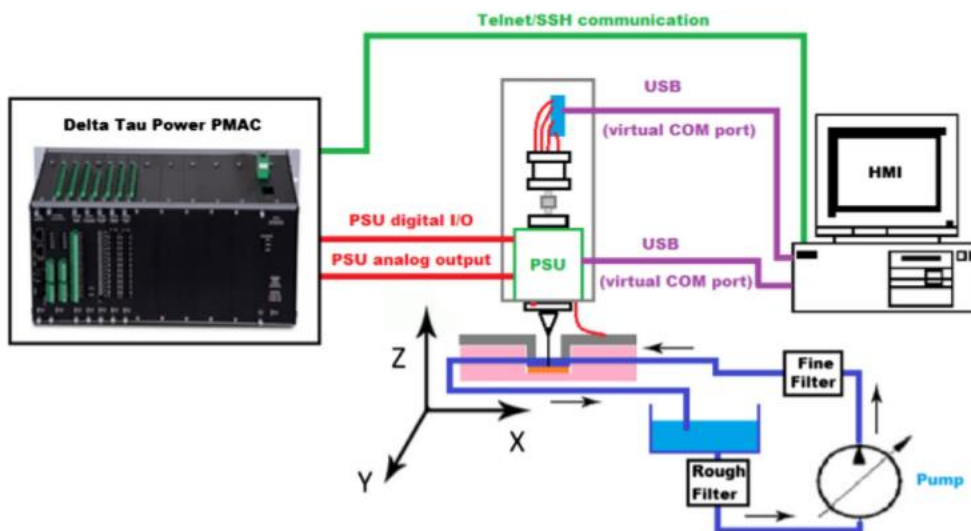
APPENDIX G

In-house built μ ECM machine

3D-Cad models of the In-house built μ ECM machine (Spieser & Ivanov, 2015)



Schematic diagram of the In-house built μ ECM machine (Spieser & Ivanov, 2015)



REFERENCES

- Anon., n.d. [Online]
 Available at: <https://www.ivium.com/product/iviumstat/>
 [Accessed 14 Aug 2018].
- Asokan, P., Ravi Kumar, R., Jeyapaul, R. & Santhi, M., 2008. Development of multi-objective optimization models for electrochemical machining process. *International journal of manufacturing technology*, Volume 39, pp. 55-63.
- Bai, J. et al., 2019. Feasibility study of manufacturing microgrooves on beryllium with electrochemical machining. *International journal of advanced manufacturing technology*, Volume 103, pp. 4553-4562.
- Bard, A. & Faulkner, L., 2001. *Electrochemical methods*. Second ed. s.l.:JohnWiley & Sons.
- Bhattacharyya, B., 2015. *Electrochemical micromachining for nanofabrication, MEMS and nanotechnology*. Oxford: Elsevier.
- Bhattacharyya, B., Malapati, M. & Munda, J., 2005. Experimental study on electrochemical micromachining. *Journal of Materials Processing Technology*, 169(3), pp. 485-492.
- Bhattacharyya, B., Malpati, M. & Munda, J., 2005. Experimental study on electrochemical micromachining. *Journal of materials processing technology*, Volume 169, pp. 485-492.
- Bhattacharyya, B. & Munda, J., 2003. Experimental investigation on the influence of electrochemical machining parameters on machining rate and accuracy in micromachining domain. *International Journal of Machine Tools and Manufacture*, 43(13), pp. 1301-1310.

- Bhattacharyya, B., Munda, J. & Malapati, M., 2004. Advancement in electrochemical micr-machining. *International journal of machining tools & manufacturere*, 44(15), pp. 1577-1589.
- Bignon, C., Bedrin, C. & Weill, R., 1982. Application of Eddy Currents to the In-Process Measurement of the Gap in E.C.M.. *CIRP Annals Manufacturing Technologies*, 31(1), pp. 115-118.
- Cakir, O., Yardimeden , A. & Ozben, T., 2007. Chemical machining. *International Scientific Journal as the organ of the Committee of Materials Science of the Polish Academy of Sciences*, 28(8), pp. 499-502.
- Chourasia, A., Singh, S. & Angrawal, P., 2014. Ultraprecision high rate anodic dissolution processes in ECM. *International Journal of Application or Innovation in Engineering & Management* , 3(10), pp. 347-353.
- Clifton, D., Mouni, A., Alder, G. & Jardine, D., 2002. Ultrasonic measurement of the inter electrode gap in electrochemical machining. *International journal of machine tools and manufacturing*, 42(11), pp. 1259-1267.
- De Grave, A., Olsen, S., Hansen, H. & Arentoft, M., 2010. Sustainability of Micro-Manufacturing Technologies. In: Y. Qin, ed. *Micromanufacturing Engineering and Technology*. s.l.:William Andrew, pp. 394-405.
- De Grave, A. & Oslen, S. I., 2006. *Challenging the sustainability of micro products development*. Grenoble, Elsevier Science, pp. 285-288.
- Fan, Z., Hourng, L. & Wang, C., 2010. Fabrication of tungsten microelectrodes using pulsed electrochemical machining. *Precision Engineering*, 34(3), pp. 489-496.

- Feng, S. C. & Joung, C. B., 2009. *An Overview of a Proposed Measurement Infrastructure for Sustainable Manufacturing*. Chennai, s.n.
- Gamage, J. R. & DESilva, A. K. M., 2015. Assessment of Research Needs for Sustainability of Unconventional Machining Processes. *Procedia CIRP*, Volume 26, pp. 385-390.
- Ghoshal, B. & Bhattacharyya, B., 2013. Micro electrochemical sinking and milling method for generation of micro features. *Journal of Engineering Manufacture*, 227(11), pp. 1651-1663.
- Gongadze, E., Peterson, S., Beck, U. & Rienen, U. V., 2009. *Classical Models of the Interface between an Electrode and an Electrolyte*. Milan, COMSOL.
- Goswami, D. & Chakraborty, S., 2014. Differential search algorithm-based parametric optimization of electrochemical micromachining processes. *International journal of industrial engineering computations*, 5(1), pp. 41-54.
- Govindan, P., Arjun, M., Arjun, M. & Akshay, S., 2013. Analysis of electrochemical micromachining. *International Journal of Management, Information Technology and Engineering*, 1(1), pp. 5-14.
- Guodong, L., Yong, L., Quancun, K. & Hao, T., 2016. *Selection and Optimization of Electrolyte for Micro Electrochemical Machining on Stainless Steel 304*. Tokyo, Elsevier, pp. 412-417.
- Hackert-Oschatzchen, M., Jahn, S. & Schubert, A., 2011. *Design of Electrochemical Machining Processes by Multiphysics Simulation*. Stuttgart, COMSUL.

- Hackert-Oschatzchen, M., Kowalick, M., Meichsner, G. & Schubert, A., 2012. *Multiphysics Simulation of the Electrochemical Finishing of Micro Bores*. Milan, COMSUL.
- Harrington, D. A. & Van, D. D., 2011. Mechanism and equivalent circuits in electrochemical impedance spectroscopy. *Electrochimica Acta*, 56(23), pp. 8005-8013.
- Harris, J., Wise, T., Gallagher, K. & Goodwin, N., 2001. *Survey of Sustainable Development: Social And Economic Dimensions*. Washington: Islandpress.
- Hegab, H. A., Darras, B. & Kishawy, H. A., 2018. Towards sustainability assessment of machining processes. *Journal of Cleaner Production*, Volume 170, pp. 694-703.
- Hegab, H., Darras, B. & Kishawy, H. A., 2018. Sustainability Assessment of Machining with Nano-Cutting Fluids H. Hegab a,*, B. Darrasb, H A. Kishawya. *Procedia Manufacturing*, 26(1), pp. 245-254.
- Heilala, J. et al., 2015. *The concept for sustainability performance indicators, reporting and improvement*, Tampere: FIMECC Ltd.
- Hotoiu, E. L. et al., 2013. Simulation of nano-second pulsed phenomena in electrochemical micromachining processes- Effects of the signal and double layer properties. *Electrochimica Acta*, Volume 93, pp. 8-16.
- Hotoiu, E. L. & Deconinck, J., 2014. A novel pulse shortcut strategy for simulating nano-second pulse electrochemical micro-machining. *Journal of applied electrochemistry*, 44(11), pp. 1225-1238.
- Hotoiu, L. & Deconinck, J., 2013. Time-efficient simulations of nano-pulsed electrochemical micromachining. *Procedia CIRP*, Volume 6, pp. 469-474.

Huang, V. M. et al., 2011. Local electrochemical impedance spectroscopy: A review and some recent. *Electrochimica Acta*, 56(23), pp. 8048-8057.

IEA, 2018. *Global Energy & CO2 Status Report 2017*, s.l.: OECD/IEA.

Ikkala, K., Lanz, M., Kivio, J. & Coatanea, E., 2015. *Energy efficiency evaluation method for machine tools*. Wolverhampton, The Choir Press, pp. 58-65.

Ivanov, A. & Mortazavi, M., 2016. *Advanced applications of micro ECM technology*. Macau: s.n.

J. Ross Macdonald, 1987. *Impedance spectroscopy emphasizing solid materials and systems*. New York: Joh Wiley & sons.

Jayal, A. D., Badurdeen, F., Dillon, O. W. & Jawahir, I. S., 2010. Sustainable manufacturing: Modeling and optimization challenges at the product, process and system levels. *CIRP Journal of Manufacturing Science and Technology*, 2(3), pp. 144-152.

Jo, C. H., Kim, B. H. & Chu, C., 2009. Micro electrochemical machining for complex internal micro features. *CIRP annals- Manufacturing technologies*, 58(1), pp. 181-184.

Kamaraj, A. B. & Sundaram, M. M., 2013. Mathematical modeling and verification of pulse electrochemical micromachining of microtools. *International journal of manufacturing technology*, 68(5), pp. 1055-1061.

Kellens, K. et al., 2013. Environmental Impact Reduction in Discrete Manufacturing: Examples for Non-Conventional Processes. *Procedia CIRP*, Volume 6, pp. 27-34.

- Kenney, J. A. & Hwang, G., 2005. Electrochemical machining with ultrashort voltage pulses: modelling of charging dynamics and. *Nanotechnology*, November, 16(7), pp. 309-313.
- Kim, B. et al., 2005. Micro Electrochemical Machining of 3D Micro Structure Using Dilute Sulfuric Acid. *CIRP Annals manufacturing technology*, 54(1), pp. 191-194.
- Kim, D. B., Leong, S. & Chen, C., 2012. *An Overview of Sustainability Indicators and Metrics for Discrete Part Manufacturing*. Chicago, ASME, pp. 1173-1181.
- Kim, U., Jung, Y. & Park, J., 2013. Vibration Electrochemical Micromachining Based on Coulostatic Analysis. *International journal of applied physics and mathematics*, 3(2), pp. 123-126.
- Klocke, F. et al., 2013. Modeling and Simulation of the Electrochemical Machining (ECM) Material Removal Process for the Manufacture of Aero Engine Components. *Procedia CIRP*, Volume 8, pp. 265-270.
- Kozak, J., 2004. Thermal models of pulse electrochemical machining. *BULLETIN OF THE POLISH ACADEMY OF SCIENCES*, 52(4), pp. 313-320.
- Kozak, J., Gulbinowicz, D. & Gulbinowicz, Z., 2009. *The Mathematical Modeling and Computer Simulation of Electrochemical Micromachining Using Ultrashort Pulses*. s.l., IAENG, pp. 174-185.
- Kozak, J., Gulbinowicz, D. & Gulbinowicz, Z., 2008. The Mathematical Modeling and Computer Simulation of Pulse Electrochemical Micromachining. *Engineering Letters*, 16(4), pp. 556-561.

- Kozak, J., Rajurkar, K. & Makkar, Y., 2004. Selected problems of micro-electrochemical machining. *Journal of Materials Processing Technology*, Volume 149, pp. 426-431.
- Kozak, J., Rajurkar, K. & Makkar, Y., 2004. Study of Pulse Electrochemical Micromachining. *Journal of manufacturing processes*, 6(1), pp. 7-14.
- Kozak, J., Rajurkar, K. P. & Wei, B., 1994. Modelling and analysis of pulse electrochemical. *Engineering for industry*, Volume 116, pp. 316-323.
- Krolczyk, G. M. et al., 2019. Ecological trends in machining as a key factor in sustainable machining- A review. *Journal of cleaner production*, Volume 218, pp. 601-615.
- Kumar, M., Mahto, P., Kushwaha, D. & Singh, N., 2016. Electrochemical machining: Review of historical and recent developments. *International Journal of Advance Research in Science and Engineering*, 5(3), pp. 217-227.
- Kurita, T., Chikamori, K., Kubota, S. & Hattori, M., 2006. A study of three-dimensional shape machining with an ECM system. *International journal of machine tools and manufacturer*, 45(12-13), pp. 1311-1318.
- Lee, E., Baek, S. & Cho, C., 2007. A Study of the characteristics for electrochemical micromachining with ultrashort voltage pulses. *International journal of advanced manufacturing technologies*, 31(7-8), pp. 762-769.
- Lee, E., Park, J. & Moon, Y., 2002. A study on electrochemical micromachining for fabrication of microgrooves in an air-lubricated hydrodynamic bearing. *International journal of Advanced Manufacturing Technologies*, 20(10), pp. 720-726.
- Liu, W. et al., 2017. Modeling and fabrication of microhole by electrochemical micromachining using retracted tip tool. *Precision engineering*, Volume 55, pp. 77-84.

- Li, Z. & Niu, Z., 2008. *System Design and Low-speed Characteristic Analysis of Electrochemical Micro-machining Set-up for Micro-holes*. Sanya, China, IEEE, pp. 146-150.
- Macdonald, D. D., 2006. Reflections on the history of electrochemical impedance spectroscopy. *Electrochimica Acta*, Volume 51, pp. 1376-1388.
- Macdonal, J. R., 1992. Impedance spectroscopy. *Annals of Biomedical Engineering*, Volume 20, pp. 289-305.
- Mani, M. et al., 2013. *Review on Sustainability Characterization for Manufacturing Processes*, s.l.: National Institute of Standards and Technology- U.S Department of Commerce .
- Ma, N., Xu, W., Wang, X. & Tao, B., 2010. Pulse electrochemical finishing: Modeling and experiment. *Journal of materials processing technologies*, 210(6-7), pp. 852-857.
- Marla, D., Joshi, S. S. & Mitra, S. K., 20018. Modeling of electrochemical micromachining: comparison to experiments. *Modeling of electrochemical micromachining: comparison to experiments*, 7(3), pp. 033015-1-033015-7.
- Mathew, R. & Sundaram, M. M., 2012. Modeling and fabrication of micro tools by pulsed electrochemical machining. *Journal of material processing technologies*, 212(7), pp. 1567-1572.
- Mia, M. et al., 2018. An approach to cleaner production for machining hardened steel using different cooling-lubrication conditions. *Journal of cleaner production*, Volume 187, pp. 1069-1081.

- MI, D. & Natsu, W., 2016. *Simulation of Micro ECM for Complex-shaped Holes*. Tokyo, Elsevier, pp. 345-349.
- Mithu, M., Fantoni, G. & Ciampi, J., 2014. How microtool dimension influences electrochemical micromachining. *International journal of advanced manufacturing technologies*, 70(5-8), pp. 1303-1312.
- Mithu, M., Fantoni, G., Ciampi, J. & Santochi, M., 2012. On how tool geometry, applied frequency and machining parameters influence electrochemical microdrilling. *CIRP Journal of Manufacturing Science and Technology*, 5(3), pp. 202-2013.
- Modica, F., Marrocco, V., Copani, G. & Fassi, I., 2011. Sustainable Micro-Manufacturing of Micro-Components via Micro Electrical Discharge Machining. *Sustainability*, Volume 3, pp. 2456-2469.
- Mortazavi, M. & Ivanov, A., 2017. Sustainability of Micro Electrochemical Machining: Discussion. *Sustainable Design and manufacturing 2017- Smart Innovation, Systems and Technologies 68*, pp. 203-210.
- Munda, M., Malapati, M. & Bhattacharyya, B., 2007. Control of micro-spark and stray-current effect during EMM process. *Journal of materials processing technology*, 194(1-3), pp. 151-158.
- Munda, J. & Bhattacharyya, B., 2008. Investigation into electrochemical micromachining (EMM) through response surface methodology based approach. *International journal of advanced manufacturing technologies*, 35(7-8), pp. 821-832.
- Natsu, W., 2018. Micro Electrochemical Machining. In: J. Yan, ed. *Micro and Nano Fabrication Technology*. s.l.:Springer, Singapore, pp. 807-855.

- Orazem, M. E. & Tribollet, B., 2007. An integrated approach to electrochemical impedance spectroscopy. *Electrochimica*, 53(25), pp. 7360-7366.
- Pajkossy, T. & Jurczakowski, R., 2017. Electrochemical Impedance Spectroscopy in Interfacial Studies. *Current opinion in electrochemistry*, 1(1), pp. 53-58.
- Park, B., Kim, B. & Chu, C., 2006. The Effects of Tool Electrode Size on Characteristics of Micro Electrochemical Machining. *CIRP Annals Manufacturing Technology*, 55(1), pp. 197-200.
- Peralta, M. E., Barcena, M. M. & Gonzalez, F. A., 2017. On the sustainability of machining processes. Proposal for a unified framework through the triple bottom-line from an understanding review. *Journal of Cleaner Production*, Volume 142, pp. 3890-3904.
- Pratheesh Kumar, M. R., Prakasan, K. & Kalaichelvan, K., 2016. Experimental Investigation and Multiphysics Simulation on the Influence of Micro Tools with Various End Profiles on Diametrical Overcut of Holes Machined Using Electrochemical Micromachining for a Predetermined Optimum Combination of Process Parameters¹. *Russian Journal of Electrochemistry*, 52(10), pp. 1059-1072.
- Priarone, P. C., Robiglio, M. & Settineri, L., 2018. On the concurrent optimization of environmental and economic targets for machining. *Journal of Cleaner Production*, Volume 190, pp. 630-644.
- Purcar, M., Bortels, L., Bossche, B. & Deconineck, J., 2004. 3D electrochemical machining computer simulations. *Journal of materials processing technology*, 149(1-3), pp. 472-478.
- Qin, Y., 2015. *Micromanufacturing Engineering and Technology, A volume in Micro and Nano Technologies*. 2nd ed. s.l.:Elsevier.

- Rahdari, A. & Anvary Rostamy, A. A., 2015. Designing a general set of sustainability indicators at the corporate. *Cleaner production*, Volume 108, pp. 757-771.
- Rajurkar, K. et al., 2006. Micro and Nano Machining by Electro-Physical and Chemical Processes. *CIRP Annals - Manufacturing Technology*, 55(2), pp. 643-666.
- Rajurkar, K. P., Wei, B., Kozak, J. & McGeough, J. A., 1995. Modelling and Monitoring Interelectrode Gap in Pulse Electrochemical Machining. *CIRP Annals*, 44(1), pp. 177-180.
- Rajurkar, K., Sundaram, M. & Malshe, A., 2013. *Review of Electrochemical and Electrodischarge Machining*. Leuven, Elsevier, pp. 13-26.
- Rao, S. & Padmanabhan, G., 2013. Linear Modeling of the Electrochemical Machining Process Using Full Factorial Design of Experiments. *Journal of Advanced Mechanical Engineering* , 1(1), pp. 13-23.
- Reddy, M. M. K., 2013. Influence of pulse period and duty ratio on electrochemical micro machining (EMM) characteristics. *International Journal of Mechanical Engineering and Applications* , 1(4), pp. 78-86.
- Riemer, D. P. & Orazem, M. E., 2014. Impedance Based Characterization of Raw Materials Used in Electrochemical Manufacturing. *The electrochem Society interface*, 23(13), pp. 63-67.
- Sarvanan, D., Arularasu, M. & Ganesan, K., 2012. A study on electrochemical micromachining of super duplex stainless steel for biomedical filters. *ARPJ Journal of Engineering and Applied Sciences* , 7(5), pp. 517-523.

- Skoczypiec, S., 2016. Discussion of ultrashort voltage pulses electrochemical micromachining: a review. *International journal of Advanced Manufacturing Technologies*, 87(1-4), pp. 177-187.
- Spieser, A. & Ivanov, A., 2015. Design of an electrochemical micromachining machine. *The international journal of advanced manufacturing technology*, 75(5-8), pp. 737-752.
- Stojek, Z., 2002. Thermodynamics of Electrochemical Reactions. In: F. Scholz, ed. *Electroanalytical Methods. Guide to Experiments and Applications*. s.l.:Springer, pp. 3-8.
- Sueptitz, R. et al., 2013. Electrochemical micromachining of passive electrodes. *Electrochimica*, Volume 109, pp. 562-569.
- Tristo, G., Bissacco, G., Lebar, A. & Valentincic, J., 2015. Real time power consumption monitoring for energy efficiency analysis in micro EDM milling. *Int J Adv Manuf Technol*, Volume 78, pp. 1511-1521.
- Volgin, V. et al., 2016. Effect of Current Efficiency on Electrochemical Micromachining by Moving Electrode. *Procedia CIRP-- 5th CIRP Global Web Conference Research and Innovation for Future Production*, Volume 55, pp. 65-70.
- Volgin, V. M., Lyubimov, V. V. & Davydov, A. D., 2016. Modeling and numerical simulation of electrochemical micromachining. *Chemical Engineering Science*, Volume 140, pp. 252-260.
- Wang, H. & Pilon, L., 2011. Accurate Simulations of Electric Double Layer Capacitance of Ultramicroelectrodes. *Journal of physical chemistry*, 115(33), pp. 16711-16719.

- Wang, Y., Zeng, Y. & Zhang, W., 2019. Improving the machining efficiency of electrochemical micromachining with oscillating workpiece. *International journal of advanced manufacturing technology*, pp. 1-14.
- Weber, O., Natter, H. & Bahre, D., 2015. Pulse electrochemical machining of cast iron: a layer-based approach for modeling the steady-state dissolution current. *Journal of Solid State Electrochemistry*, 19(5), pp. 1265-1276.
- Weber, O., Rebschlager, A., Steuer, P. & Bahre, D., 2013. *Modeling of the Material/Electrolyte Interface and the Electrical Current Generated during the pulse electrochemical machining of Grey Cast Iron*. Rotterdam, COMSOL.
- Zemann, R., Bleicher, F. & Zisser-Pfeifer, R., 2012. Electrochemical micromachining with ultra short voltage pulses. *The archive of Mechanical Engineering*, 59(3), pp. 313-327.
- Zhang, Z., Wang, Y., Chen, F. & Mao, W., 2011. *RUSSIAN JOURNAL OF ELECTROCHEMISTRY*, 47(7), pp. 819-824.
- Zhang, Z. & Zhu, D., 2008. Experimental research on the localized Electrochemical Micromachining. *Russian journal of Electrochemistry*, 44(8), pp. 998-1003.
- Zhang, Z., Zhu, D., Qu, N. & Wang, M., 2007. Theoretical and experimental investigation on electrochemical micromachining. *Microsystem technologies*, 13(7), pp. 607-612.
- Zhu, B. & Wang, Z., 2006. Fabrication of microelectrode by current density control. *Material science forum*, December, Volume 532-533, pp. 221-224.